



**HAL**  
open science

# Development and valorization of a membrane emulsification process for the production of nanoemulsions

Océane Alliod

► **To cite this version:**

Océane Alliod. Development and valorization of a membrane emulsification process for the production of nanoemulsions. Pharmaceutical sciences. Université de Lyon, 2018. English. NNT : 2018LYSE1264 . tel-02064194

**HAL Id: tel-02064194**

**<https://theses.hal.science/tel-02064194>**

Submitted on 11 Mar 2019

**HAL** is a multi-disciplinary open access archive for the deposit and dissemination of scientific research documents, whether they are published or not. The documents may come from teaching and research institutions in France or abroad, or from public or private research centers.

L'archive ouverte pluridisciplinaire **HAL**, est destinée au dépôt et à la diffusion de documents scientifiques de niveau recherche, publiés ou non, émanant des établissements d'enseignement et de recherche français ou étrangers, des laboratoires publics ou privés.



N° d'ordre NNT : 2018LYSE1264

**THÈSE DE DOCTORAT DE L'UNIVERSITÉ DE LYON**

opérée au sein de  
**l'Université Claude Bernard Lyon 1**

**École Doctorale ED206**  
**Ecole Doctorale de Chimie de Lyon**

**Discipline : Génie pharmaceutique**

Soutenue publiquement le 20/11/2018, par :

**Océane Alliod**

---

**Development and valorization of a  
membrane emulsification process for the  
production of nanoemulsions**

---

Devant le jury composé de :

Li Huai-Zhi, Professeur, Université de Lorraine  
Vladislavljević Goran, Senior Lecturer, Loughborough University  
Dupin Damien, Responsable de laboratoire, CIDETEC  
Briançon Stéphanie, Professeure, Université Lyon 1

Rapporteur  
Rapporteur  
Examinateur  
Président(e)

Charcosset Catherine, Directrice de recherche, Université Lyon 1  
Fessi Hatem, Professeur, Université Lyon 1

Directrice de thèse  
Co-directeur de thèse



## Résumé

Les nanoémulsions sont des formulations intéressantes pour des applications telles que les cosmétiques, les produits pharmaceutiques et les produits alimentaires. Elles peuvent être produites par des techniques à basse ou haute énergie. Dans ce travail, un procédé impliquant une pression modérée, l'émulsification membranaire par prémix a été proposée comme alternative. Des nanoémulsions huile-dans-eau (H/E) et eau-dans-huile (E/H) ont été produites avec une installation à l'échelle pilote composée d'un pousse-seringue à haute pression et d'une membrane Shirasu Porous Glass (SPG). Tout d'abord, l'influence de nombreux paramètres du procédé et de la composition sur la taille des gouttelettes et la pression résultante a été étudiée avec des compositions modèles. Ainsi, des nanoémulsions H/E d'environ 260 nm et E/H d'environ 600 nm ont été produites avec succès. Puis, le montage a été utilisé pour produire des nanoémulsions de compositions spécifiques, des nanoémulsions H/E et E/H stabilisées avec des tensioactifs polypeptidiques et une nanoémulsion H/E adaptée à l'injection. Enfin, le procédé développé a été comparé à deux procédés à haute énergie traditionnels, le microfluidiseur et les ultrasons en termes de taille des gouttelettes et de conservation d'actifs. Aucune différence entre les procédés n'a été observée en ce qui concerne la préservation de l'acif choisi. Cependant, en ce qui concerne la taille, les nanoémulsions produites par les membranes ont présenté des gouttelettes monodisperses de 335 nm par rapport aux autres procédés qui ont produit des nanoémulsions d'environ 150 nm de taille moyenne mais contenant aussi des gouttelettes de taille micrométrique détectées par diffraction laser et microscopie optique et instables à 3 mois en vieillissement accéléré pour le microfluidizer. Pour cette raison, les nanoémulsions produites par procédé membranaire conviennent pour des applications parentérales avec l'avantage de ne nécessiter aucune étape de filtration. De manière générale, le procédé développé présente par rapport aux autres procédés existants les avantages d'un meilleur contrôle de la taille finale de l'émulsion, d'un procédé industrialisable et stérilisable, et d'une diminution de l'énergie requise.

## **Abstract**

Nanoemulsions are interesting carriers for applications such as cosmetics, pharmaceutical and food. They are produced usually by low or high energy techniques. In this work, a process involving moderate pressure, premix membrane emulsification (PME) was proposed as an alternative. Oil-in-water (O/W) and water-in-oil (W/O) nanoemulsions were produced with a pilot scale set-up composed of a controlled high pressure syringe pump and Shirasu Porous Glass (SPG) membrane. First, the influence of process and composition parameters on droplet sizes and pressures was extensively studied with model compositions to optimize the production. Thus, nanoemulsions down to 260 nm for O/W and around 600 nm for W/O were successfully produced. Then, the set-up was used to produce nanoemulsions of specific compositions: O/W and W/O nanoemulsions stabilized with polypeptidic surfactants and O/W nanoemulsions suitable for injection. Finally, the set-up developed was compared to two traditional high energy processes, microfluidizer and ultrasound in terms of droplet size and active preservation. No real difference between the three processes was seen on active preservation with the model active chosen. However, regarding droplet size, PME produced monodispersed droplets of 335 nm compared to the other processes which produced nanoemulsions of around 150 nm but with the presence of micron size droplets detected by laser diffraction and optical microscopy and unstable at 3 months under stress conditions for microfluidizer. Therefore, PME nanoemulsions are also suitable for parenterals applications with no additional filtration step required. In general, the process developed present several advantages over existing process: a better control of the final droplet size, a lower amount of required energy together with high stability and scalability potential.

## Aknowledgement

Je souhaite remercier toutes les personnes qui m'ont accompagnée et soutenue durant ces trois années de thèse.

Je veux remercier en premier lieu Catherine Charcosset, ma directrice de thèse pour son encadrement. Je la remercie pour sa présence tout au long de ma thèse. J'ai apprécié nos discussions régulières et sa gentillesse. Je souhaite aussi remercier Hatem Fessi, mon co-directeur de thèse. Il m'a fait profiter de ses grandes connaissances et de son expérience tant scientifique qu'humaine. Je remercie aussi Stéphanie Briançon, directrice du Lagepp pour son accueil au sein du laboratoire. Ainsi que tous les membres permanents et non-permanents de l'équipe Gepfarm. Merci d'avoir enrichi mon travail de vos remarques et de vos idées.

En particulier, je souhaiterais remercier Eyad Almouazen pour l'intérêt qu'il a montré envers mon sujet et pour avoir accepté de collaborer avec moi sur la dernière partie de ma thèse. Merci pour ton investissement scientifique et humain dans ce travail.

Je remercie aussi Célia et Georgio qui ont accepté de réaliser leur stage sous ma direction et qui ont obtenus de très bons résultats.

Par ailleurs, merci à Damien Dupin d'avoir monté et dirigé le projet Européen Pepticaps et d'y avoir associé le LAGEPP ce qui a permis de financer ma thèse. Merci Damien pour nos échanges très enrichissants et d'avoir accepté d'être membre de mon jury de thèse.

Merci aussi à tous les membres du projet pour leur gentillesse et leur professionnalisme. Travailler en collaboration avec eux durant 3 ans a été très enrichissant.

Je tiens à remercier tout le personnel du LAGEPP.

Pour leur aide précieuse et leurs excellentes idées : Jean-Pierre et Sébastien, du service ingénierie sans qui je n'aurais jamais monté mon pilote.

Merci aussi à Géraldine et Quentin du service analytique pour leurs connaissances et leur disponibilité.

Merci aussi à Nadia, secrétaire de LAGEPP pour son sourire et sa bienveillance.

Je souhaite remercier aussi Pierre-Yves Dugas du C2P2 pour m'avoir aidée dans mes tentatives de photos cryo-TEM.

Merci à mes 4 Mousquetaires, Camille, Joëlle, Joris et Romain pour avoir illuminé ma thèse de leur humour flamboyant.

Merci mille fois à mes co-bureaux, Romain du début à la fin, les anciens Alexis et Loulou, La Greta et ses accueils toujours chaleureux, les petites nouvelles Laura et Maya. Merci à Aline et Pierre pour leur bonne humeur quotidienne et leur amour des autres.

Merci à Maité pour nos déjeuners en tête-à-tête.

Merci à tous les Lagepiens pour cette belle ambiance pendant 3 ans.

Merci à tous ceux qui ont fait que ma vie en dehors de la thèse fût si belle pendant 3 ans : les Incroyables Comestibles, mes potes du lycée, mes ami.e.s, ma Gagou et mon Titou, mes parents et mon Pichou.

## General Preamble

The work described in this Thesis was carried out at the laboratory LAGEPP (Laboratoire d'automatique, de génie des procédés et de génie pharmaceutique) which is part of Université Claude Bernard Lyon 1. This work was supported by PeptiCaps project. This project has received funding from the European Union's Horizon 2020 Research and Innovation program under Grant Agreement no. 686141.

The manuscript is based on three publications, which form chapters 3, 4 and 6, and chapter 5 is a summary of reports written for the PeptiCaps European project. Each publication is introduced in the Thesis by a preamble but the contents of the publications are unchanged except for the section, figure, table and equation numbers and the numbering of references (the numbering was adapted to follow the manuscript format). For chapter 6, the article is followed by complementary data.

The publication references are the following:

1. O. Alliod, J.-P. Valour, S. Urbaniak, H. Fessi, D. Dupin, C. Charcosset, Preparation of oil-in-water nanoemulsions at large-scale using premix membrane emulsification and Shirasu Porous Glass (SPG) membranes, *Colloids and Surfaces A*, published online, 2018
2. O. Alliod, L. Messenger, H. Fessi, D. Dupin, C. Charcosset, Influence of viscosity for oil-in-water and water-in-oil nanoemulsions production by SPG premix membrane emulsification, *Chemical Engineering Research and Design*, submitted, 2018
3. O. Alliod, E. Almouazen, G.Nemer, H. Fessi, C. Charcosset, Comparison of three processes for parenteral nanoemulsion production: ultrasounds, microfluidizer and premix membrane emulsification, *Journal of Pharmaceutical Sciences*, submitted, 2018

This work was also presented during oral presentations or posters at three international conferences:

- 7th International Workshop on Bubble and Drop Interfaces 2017, June 26-30th 2017, Lyon, France. Océane Alliod, Hatem Fessi, Catherine Charcosset « Innovative process for precise size control of emulsion production at pilot scale »
- 31st Conference of the European Colloid & Interface Society, ECIS 2018, September 3-8th, 2017, Madrid, Spain. Océane Alliod, Léa Messenger, Hatem Fessi, Catherine Charcosset “Production of controlled and reliable novel emulsions for skin care applications with membrane processes”
- 4th Annual meeting SFNano 2017 (Société Française Nanomédecine), December 5th-7th 2017, Bordeaux, France. Océane Alliod, Léa Messenger, Hatem Fessi, Catherine Charcosset “Production of controlled and reliable novel nanoemulsions for skin care applications with membrane processes”

# Contents

<b>Abstract (English and French)</b>	<b>i</b>
<b>Aknowledgement</b>	<b>i</b>
<b>General Preamble</b>	<b>i</b>
<b>Contents</b>	<b>iii</b>
<b>Nomenclature</b>	<b>v</b>
<b>List of Figures</b>	<b>xi</b>
<b>List of Tables</b>	<b>xv</b>
<b>Introduction</b>	<b>1</b>
<b>1 Literature review</b>	<b>5</b>
1.1 Nanoemulsions: Generalities and Processes . . . . .	6
1.1.1 Definition and physico-chemistry of nanoemulsions . . . . .	6
1.1.2 Emulsifiers . . . . .	12
1.1.3 Processes for nanoemulsions production . . . . .	16
1.1.4 Some applications of nanoemulsions . . . . .	24
1.1.5 Conclusion . . . . .	28
1.2 Membrane emulsification . . . . .	29
1.2.1 Type of emulsification . . . . .	29
1.2.2 Set-ups for membrane emulsification . . . . .	31
1.2.3 Forces involved and parameters of influence . . . . .	38
1.2.4 Applications of premix membrane emulsification . . . . .	47
1.2.5 Conclusion . . . . .	51
1.3 General conclusion and aim of the work . . . . .	52
1.3.1 Literature review conclusion . . . . .	52
1.3.2 Aim of the work . . . . .	52
<b>2 Materials and methods</b>	<b>55</b>
2.1 PME set-ups developed . . . . .	56
2.1.1 Intermediate set-ups . . . . .	56
2.1.2 High pressure pump set-up . . . . .	57
2.2 Method of nanoemulsion production . . . . .	61
2.2.1 Premix composition and preparation . . . . .	61
2.2.2 Production of nanoemulsions with the final set-up . . . . .	64
2.2.3 Production of nanoemulsions by other processes . . . . .	67
2.3 Characterization of emulsions . . . . .	68
2.3.1 Droplet Size . . . . .	68
2.3.2 Viscosity . . . . .	70
2.3.3 Interfacial tension . . . . .	71
2.3.4 Stability . . . . .	71

<b>3 Preparation of oil-in-water nanoemulsions at large-scale using premix membrane emulsification and Shirasu Porous Glass (SPG) membranes</b>	<b>73</b>
3.1 Abstract . . . . .	75
3.2 Introduction . . . . .	75
3.3 Materials and methods . . . . .	77
3.3.1 Materials . . . . .	77
3.3.2 Experimental set-up . . . . .	77
3.3.3 Membranes . . . . .	78
3.3.4 Formulation of nanoemulsions . . . . .	78
3.3.5 Preparation of nanoemulsions . . . . .	78
3.3.6 Membrane cleaning . . . . .	78
3.3.7 Particle size distribution measurements . . . . .	79
3.3.8 Viscosity measurement . . . . .	79
3.4 Results and discussion . . . . .	79
3.4.1 Process parameters . . . . .	79
3.4.2 Composition parameters . . . . .	84
3.4.3 Stability . . . . .	87
3.5 Conclusion . . . . .	88
<b>4 Influence of viscosity for oil-in-water and water-in-oil nanoemulsions production by SPG premix membrane emulsification</b>	<b>91</b>
4.1 Abstract . . . . .	93
4.2 Introduction . . . . .	93
4.3 Materials and methods . . . . .	95
4.3.1 Materials . . . . .	95
4.3.2 Experimental set-up . . . . .	95
4.3.3 Membranes . . . . .	95
4.3.4 Formulation of nanoemulsions . . . . .	96
4.3.5 Preparation of nanoemulsions . . . . .	96
4.3.6 Membrane cleaning . . . . .	97
4.3.7 Particle size distribution measurements by laser diffraction . . . . .	97
4.3.8 Viscosity measurements . . . . .	97
4.4 Results and discussion . . . . .	98
4.4.1 Influence of viscosity on $\Delta P_{pipe}$ . . . . .	98
4.4.2 O/W nanoemulsions . . . . .	98
4.4.3 W/O nanoemulsions . . . . .	104
4.5 Conclusion . . . . .	108
<b>5 Production of O/W and W/O PeptiCaps nanoemulsions</b>	<b>111</b>
5.1 Introduction . . . . .	112
5.2 Materials and methods . . . . .	112
5.3 Results for O/W emulsions production . . . . .	113
5.3.1 Influence of copolypeptide percentage . . . . .	113
5.3.2 Influence of flowrate . . . . .	113
5.3.3 Stability . . . . .	115
5.4 Results for W/O emulsions production . . . . .	116
5.4.1 Model composition with PGPR . . . . .	116
5.4.2 PeptiCaps composition with PP2 . . . . .	117
5.5 Conclusion . . . . .	119
<b>6 Comparison of three processes for parenteral nanoemulsion production: ultrasounds, microfluidizer and premix membrane emulsification</b>	<b>121</b>
6.1 Abstract . . . . .	123
6.2 Introduction . . . . .	123
6.3 Experimental Section . . . . .	125

6.3.1	Materials . . . . .	125
6.3.2	Preparation of the premix . . . . .	125
6.3.3	Production of nanoemulsions . . . . .	126
6.3.4	Particle size distribution measurements . . . . .	127
6.3.5	Optical microscopy . . . . .	127
6.3.6	High Performance Liquid Chromatography . . . . .	128
6.3.7	Stability . . . . .	128
6.4	Results . . . . .	128
6.4.1	Determination of optimal formulation . . . . .	128
6.4.2	Effect of the process on the resulting droplet size of the nanoemulsions . . . .	128
6.4.3	Effect of the process on API degradation . . . . .	133
6.5	Discussion . . . . .	137
6.6	Conclusion . . . . .	137
	<b>Conclusion</b>	<b>143</b>
	<b>A Appendixes</b>	<b>147</b>
A.1	"Proof of concept" set-up results . . . . .	147
A.1.1	Model composition . . . . .	147
A.1.2	PeptiCaps composition . . . . .	148
A.2	Preliminary results with a 1.1 $\mu\text{m}$ pore size membrane . . . . .	149
	<b>References</b>	<b>152</b>
	<b>French abstract (Résumé en Français)</b>	<b>166</b>



# Nomenclature

## Acronyms

AFM	Atomic Force Microscopy
API	Active Pharmaceutical Ingredient
atRA	All-trans retinoic acid
CA	Cellulose acetate
CMC	Critical micellar concentration
CTAB	Cetrimonium bromide
DLS	Dynamic light scattering
DLVO	Derjaguin, Landau, Verwey, Overbeek
DME	Direct membrane emulsification
E/H	Eau-dans-huile
E/V	Energy input per unit volume
EHP	Ethylhexyl palmitate
EMA	European Medicines Agency
FDA	Food and Drug Administration
FKM	Fluorocarbon elastomer
H/E	Huile-dans-eau
HLB	Hydrophilic lipophilic Balance
HPH	High pressure homogenizer
HPLC	High pressure liquid chromatography
LCT	Long-chain triglycerides
LD	Laser diffraction
M	Manometer
M52	Marcol 52
M82	Marcol 82
MCT	Medium-chain triglycerides

## CONTENTS

---

MF	Microfluidizer
NCA	Alpha-amino acid N-carboxyanhydrides
O/W	Oil-in-water
O/W/O	Oil-in-water-in-oil
PC	Polycarbonate
PDI	Polydispersity index
PE	Polyester
PEG	Polyethylenoxide
PES	Polyethersulfone
PGA	Polyglutamic acid
PGPE	Propyleneglycol propylether
PGPR	Polyglycerol polyricinoleate
PIC	Phase Inversion Composition
PIT	Phase Inversion Temperature
PME	Premix membrane emulsification
PP1	Polypeptide 1
PP2	Polypeptide 2
PPO	Polypropyleneoxyde
PS	Polysulfone
PTFE	Polyetrafluoroethylene
PVDF	Polyvinylidene fluoride
RHLB	Required hydrophilic lipophilic Balance
ROP	Ring opening polymerisation
rpm	Rotation per min
SDS	Sodium dodecyl sulfate
SEM	Scanning electron microscopy
SLN	Solid lipid nanoparticles
SPG	Shirassu porous glass
TEM	Transmission Electron Microscopy
US	Ultrasounds
W/O	Water-in-oil
W/O/W	Water-in-oil-in-water

WMO White Mineral Oil

**Symbols**

$\Delta\rho$	Difference in volumetric weight between the dispersed and the continuous phase
$\Delta P$	Laplace pressure
$\Delta P_{disr}$	Disruption pressure
$\Delta P_{flow}$	Flow pressure
$\Delta P_{tm}$	Transmembrane pressure
$\delta A$	Surface unit
$\delta G$	Gibbs surface free energy
$\eta$	Dynamic viscosity
$\gamma$	Interfacial tension
$\gamma_{MO}$	Wetting of the oil phase on the membrane
$\gamma_{MW}$	Wetting of the water phase on the membrane
$\gamma_{WO}$	Interfacial tension between water and oil
$\omega$	Velocity of sedimentation
$\rho$	Volumetric weight
$\sigma_{w,p}$	Wall shear stress
$\theta$	Contact angle
$\varepsilon$	Porosity
$\varphi$	Volume fraction of dispersed phase
$\varphi$	Volume fraction
$\xi$	Tortuosity
$\zeta$	Zeta potential
$g$	Gravitational constant
$m$	Mass
$r$	Droplet radius
$R_1$	Hydrophobic side chain
$R_2$	Hydrophilic side chain
$u$	Velocity
$B_M$	Brownian motion
$C$	a constant
$Ca$	Capillary number

## CONTENTS

---

d	Diameter
$D_{10}$	Droplet diameter for which 10% of droplets in volume are below this size
$D_{50}$	Droplet diameter for which 50% of droplets in volume are below this size
$D_{90}$	Droplet diameter for which 90% of droplets in volume are below this size
E	Energy
$F_{\gamma}$	Interfacial force
$F_B$	Buoyancy force
$F_D$	Drag force
$F_G$	Gravitational force
$F_L$	Dynamic lift force
$F_{SP}$	Force due to the static pressure difference
J	Transmembrane flux
L	Characteristic length
n	Unit number of monomer
$P_E$	Emulsification pressure
$R_h$	Hydraulic membrane resistance
$R_m$	Membrane resistance
Re	Reynolds number
S	Surface
Span	Sample dispersity
$V_o$	Volume of oil
We	Weber number
$x_{S80}$	Span 80 concentration
$x_{T20}$	Tween 20 concentration
$x_{TS}$	Total surfactant concentration

### **Subscripts**

d	Droplet
m	Membrane
o	Oil
p	Pore
pm	Premix
w	Water

# List of Figures

1.1	Different types of emulsions from left to right, W/O, O/W and W/O/W . . . . .	6
1.2	Oil/Water/Solid Interface and contact angle ( $\theta$ ) . . . . .	8
1.3	Forces on an oil droplet dispersed in water . . . . .	9
1.4	Electrical double layer of a charged emulsion . . . . .	9
1.5	Droplet stabilization by steric hindrance . . . . .	10
1.6	O/W emulsions destabilization processes . . . . .	11
1.7	Schematic representation of an amphiphilic surfactant . . . . .	12
1.8	Evolution of the interfacial tension with emulsifier concentration and oil, water and emulsifier interactions . . . . .	13
1.9	Different types of molecules showing a surface activity and stabilizing emulsions . .	14
1.10	Schematic representation of the synthesis of an amphiphilic copolypeptide . . . . .	16
1.11	Schematic representation of phase inversion methods . . . . .	17
1.12	Schematic representation of nanoprecipitation set-up . . . . .	18
1.13	Schematic microemulsion domain in a phase diagram from Malik et al. [30] . . . . .	19
1.14	Principle of rotor stator systems . . . . .	20
1.15	Schematic representation of a microfluidic device . . . . .	21
1.16	Schematic representation of a high pressure homogenizer . . . . .	22
1.17	Schematic representation of a microfluidizer and principle of the interaction chamber	22
1.18	Energy consumption with droplet size range for high energy processes . . . . .	24
1.19	Patents and publications containing the word or concept "nanoemulsion" from Sci- finder . . . . .	25
1.20	Schematic overview of the skin layers and pH and temperature variation adapted from Jepps et al. [43] . . . . .	25
1.21	Schematic figure of direct membrane process principle . . . . .	29
1.22	Different type of formulation that can be produced with DME . . . . .	30
1.23	Different types of utilization of PME . . . . .	31
1.24	SEM photography of a SPG membrane with 200 nm pore size . . . . .	32
1.25	SEM and AFM photographs of seven different types of polymeric membranes [53] PC: polycarbonate; PES: polyethersulfone; CA: cellulose acetate; PE: polyester; PS: polysulfone; PVDF: polyvinylidene fluoride . . . . .	33
1.26	Optical microscopy photography of a 30 $\mu\text{m}$ regular pore size micro-engineered metallic membrane (Micropore Technologies Ltd)[54] . . . . .	34
1.27	Optical microscopy photography of a silicon micro-engineered membrane with an uniform 5 $\mu\text{m}$ pore size and a porosity of 30% [55] . . . . .	34
1.28	External pressure type microkit available at SPG Technology Co., Ltd, schematic view from the supplier brochure . . . . .	36
1.29	Typical experimental set-up for the cross-flow membrane emulsification process; M:manometer [64] . . . . .	36
1.30	Dead-end stirred cell for membrane emulsification commercialised by Micropore Technologies [65] . . . . .	37
1.31	Schematic representation of an extruder device for liposomes homogenization or nanoemulsion production [59] . . . . .	38
1.32	Large scale set-up for liposomes production [71] . . . . .	39

1.33 Forces exerted at membrane, oil and water interface for an O/W emulsion and an hydrophilic membrane . . . . .	40
1.34 Droplet break-up in PME from [62] (a) Droplet retention under a critical pressure, (b) Moderate break-up at moderate shear stress, (c) Intensive break-up at high shear stress . . . . .	45
2.1 Schematic representation of the proof of concept set-up . . . . .	56
2.2 Schematic representation of the experimental set-up . . . . .	57
2.3 Connection of the cross-flow tubular module to the high pressure syringe pump . . . . .	58
2.4 Photography of the high pressure syringe pump . . . . .	59
2.5 Details of the control panel . . . . .	59
2.6 Details of the control panel and the two different modes, constant pressure and constant flow . . . . .	60
2.7 Note file containing data acquired by the pump software . . . . .	60
2.8 Chemical structure of Polysorbate 20 . . . . .	61
2.9 Chemical structure of Sorbitan monooleate . . . . .	61
2.10 Chemical structure of ethylhexyl palmitate . . . . .	61
2.11 Chemical structure of caprylic and capric acids . . . . .	63
2.12 Chemical structure of all-trans retinoic acid . . . . .	63
2.13 Resulting pressure for pure water through the pipe connecting the pump to the membrane module . . . . .	64
2.14 Examples of different $R_m$ measured a) 125 mm long membrane with 0.5 $\mu\text{m}$ pore size b) 20 mm long membrane with 0.3 $\mu\text{m}$ pore size c) 125 mm long membrane with 0.1 $\mu\text{m}$ pore size . . . . .	65
2.15 $R_h$ variation with pore radius; $R_h$ (measured) is the mean value of membranes of different length at this pore size with standard deviation . . . . .	65
2.16 Pressure variation with injected volume . . . . .	66
2.17 Photography of an UP400S Ultrasonic Processor . . . . .	67
2.18 Photography of the Microfluidizer processor . . . . .	68
2.19 Photography of the Mastersizer 3000 . . . . .	69
3.1 Experimental set-up of the high syringe pump with membrane holder and SPG membrane . . . . .	77
3.2 Resulting pressure and droplet size variation with scaling up from 40 mL to 500 mL with 125 mm length and 0.5 $\mu\text{m}$ pore size membrane at 200 mL/min at a composition of 10% EHP and 5% overall surfactant concentration . . . . .	80
3.3 Pressure profiles at different flowrates with a 125 mm length and 0.5 $\mu\text{m}$ pore size membrane at a composition of 10% EHP and 5% overall surfactant concentration . . . . .	81
3.4 Droplet size as function of flow rate with a 125 mm length and 0.5 $\mu\text{m}$ pore size membrane at a composition of 10% EHP and 5% overall surfactant concentration . . . . .	82
3.5 Droplet size distribution of the premix and nanoemulsions obtained at different pore sizes (at 200 mL/min, except for 0.3 $\mu\text{m}$ pore size membrane at 100 mL/min and 0.2 $\mu\text{m}$ pore size membrane at 5 mL/min) and resulting pressure except for 0.2 $\mu\text{m}$ and 0.3 $\mu\text{m}$ pore size membrane as flowrate was changed, at a composition of 10% EHP and 5% overall surfactant concentration . . . . .	83
3.6 Droplet size as a function of resulting pressure for different membrane length and different flowrates with a 0.5 $\mu\text{m}$ pore size membrane at a composition of 10% EHP and 5% overall surfactant concentration . . . . .	84
3.7 Droplet size and pressure variation with cycle number with 125 mm length and 0.5 $\mu\text{m}$ pore size membrane at 200 mL/min at a composition of 10% EHP and 5% overall surfactant concentration . . . . .	85
3.8 Droplet size and pressure variation as a function of oil weight percentage in the formulation with 125 mm length and 0.5 $\mu\text{m}$ pore size membrane at 150 mL/min . . . . .	86
3.9 Dynamic viscosity variation as a function of oil weight percentage in the formulation . . . . .	86

3.10	Evolution of droplet size and resulting pressure with total surfactant concentration with 125 mm length and 0.5 $\mu\text{m}$ pore size membrane at 200 mL/min at 10% EHP concentration . . . . .	87
3.11	Example of nanoemulsion stability observed at 9 months for nanoemulsion obtained with a 125 mm length and 0.2 $\mu\text{m}$ pore size membrane at 5 mL/min . . . . .	88
4.1	Experimental set-up of the high syringe pump with membrane holder and SPG membrane . . . . .	95
4.2	Resulting pressure, $\Delta P_{pipe}$ , without membrane module for different O/W emulsions at flowrate from 10 to 100 mL/min . . . . .	99
4.3	Slope of the resulting pressure, $\Delta P_{pipe}$ with flow rate as a function of viscosity for O/W and W/O emulsions of different composition . . . . .	99
4.4	Membrane pressure variation with flowrate from 10 to 100 mL/min at four different concentrations in glycerol in the water phase and at 10 % of Marcol 82 and 5% surfactant . . . . .	100
4.5	Droplet size and viscosity of the emulsion versus the viscosity of the continuous phase at 10 % of Marcol 82 and 5% surfactant and a flowrate of 100 mL/min . . . . .	101
4.6	Membrane pressure and droplet size at different flowrates with different oils or oil mix at 10% and 5% overall surfactant concentration . . . . .	101
4.7	Membrane pressure and droplet size as a function of dynamic emulsion viscosity for different oil contents at 100 mL/min . . . . .	103
4.8	Membrane pressure as a function of cycle number for different Marcol 82 contents at a flowrate of 100 mL/min . . . . .	103
4.9	Influence of dynamic emulsion viscosity on $\Delta P_{flow}$ and $\Delta P_{dis}$ . . . . .	104
4.10	Membrane pressure variation with flowrate for oils of different viscosities as continuous phases with oil and surfactant content kept constant at 10% and 5% respectively . . . . .	105
4.11	Membrane resistance variation with flowrate and dynamic viscosity of the emulsion as a function of continuous phase viscosity . . . . .	105
4.12	Variation of membrane pressure for different amounts of glycerol in the dispersed phase, with oil and surfactant content kept constant at 10% and 5% respectively . . . . .	106
4.13	Variation of droplet size and membrane pressure with water content at 50 mL/min . . . . .	107
4.14	Effect of cycle number on membrane pressure at a composition of 10% water, 5% surfactant and 85% Marcol 82 at a flowrate of 50 mL/min . . . . .	107
4.15	Droplet size distribution of W/O nanoemulsions with different oils obtained at 50 mL/min except for WMO at 40 mL/min . . . . .	108
5.1	PeptiCaps logo . . . . .	112
5.2	Size distribution in volume at different polypeptide concentrations and 10% oil with the 0.8 $\mu\text{m}$ membrane . . . . .	113
5.3	Size distribution in volume of emulsion with the smallest droplet size at two polypeptide concentrations and two different pore sizes . . . . .	114
5.4	Size distribution in volume for different flowrates with the 1.1 $\mu\text{m}$ membrane at 10% oil and 2% PP1 . . . . .	114
5.5	Size distributions for the smallest emulsion obtained with PP2 at 2% , 0.8 $\mu\text{m}$ membrane and 10% oil just after production, (t0) and after 9 months at room temperature (t+9 months) . . . . .	115
5.6	Variation of the resulting pressure as function of flowrate for W/O emulsions with different water contents . . . . .	116
5.7	Variation of the resulting pressure with water phase content at various flowrates . . . . .	117
5.8	Size distribution comparison of the emulsions obtained with or without PP2 after passing through a 0.5 $\mu\text{m}$ pore size membrane at a flowrate of 30 mL/min. Composition: dispersed phase 10 % of a 30/70 citrate buffer /glycerol mixture with or without 1 % PP2; continuous phase: 90 % of 20 % Ewocream in MCT oil . . . . .	118

5.9	Composition: dispersed phase 10 % of a 30/70 citrate buffer /glycerol mixture with or without 1 % PP2; continuous phase: 90 % of 20 % Ewocream in MCT oil . . . . .	118
5.10	Variation of the average droplet diameter as a function of flowrate for emulsions with or without PP2. Emulsification conditions: membrane pore size 0.5 $\mu\text{m}$ . . . . .	119
6.1	Experimental set-up of the high syringe pump with membrane holder and SPG membrane . . . . .	126
6.2	Effect of cycles number on particle size distribution in intensity a); Z-average and PDI b) by DLS for PME at cycles 1 to 4 . . . . .	129
6.3	Effect of cycle numbers on particle size distribution in intensity a); Z-average and PDI b) by DLS for MF at a pressure of 1000 bars and cycles 1 to 5 . . . . .	130
6.4	Effect of US duration from 1 min to 5 min on particle size distribution in intensity by DLS a) and effect of US duration and intensity on Z-average and PDI b) . . . . .	131
6.5	Comparison of size distribution in intensity by DLS a) and in volume by LD b) for the three different processes PME, MF and US for selected conditions . . . . .	132
6.6	Optical microscopy photographs at x40 of three emulsions a) first cycle of MF at 1000 bars; b) fifth cycle of MF at 1000 bars; c) 5 min at 60% intensity US; and one at x 100, d) fourth cycle of PME . . . . .	133
6.7	Comparison of size distributions in intensity (DLS) at t0, t+2 weeks and t+3months under accelerated stability at (40°C) for nanoemulsions prepared by PME, MF and US with selected conditions . . . . .	134
6.8	Stability of atRA nanoemulsions during 2 weeks: remained atRA was determined and expressed as percentage of post-production content . . . . .	135
6.9	Peak areas at different retention times after 2 weeks in stability at day light exposure and 40°C . . . . .	136
6.10	Comparison of size distributions in volume (LD) at t0, t+2 weeks and t+3months accelerated stability at 40°C for the three different processes PME, MF and US for selected conditions . . . . .	139
6.11	Comparison of size distributions in intensity (DLS) at t0 and t+3months accelerated stability at 40°C for the different cycle number in MF . . . . .	140
6.12	Comparison of size distributions in intensity (DLS) at t0, t+2 weeks and t+3months for different stability conditions, ambient temperature and 40°C for MF sample at cycle 5 . . . . .	140
A.1	Size distribution in volume with different membranes with a composition of 10% EHP and 5% Span 80 and Tween 20 mix . . . . .	147
A.2	Size distribution in volume with membranes of different pore size with 10% EHP and 1% PP1 in citrate buffer at pH 5.5 . . . . .	148
A.3	Size distribution in volume for 10% EHP and 5% PP1 concentration and with the 0.8 $\mu\text{m}$ membrane in citrate buffer at pH 5.5 . . . . .	149
A.4	Size distribution in volume for different membrane pore sizes at 200 mL/min, 10% EHP and 5% surfactants . . . . .	150
A.5	Influence of membrane length on resulting pressure and size with 1.1 $\mu\text{m}$ membrane at 10% EHP and 5% surfactants . . . . .	150
A.6	Size distribution in volume for different flowrates with 1.1 $\mu\text{m}$ membrane 10% EHP and 5% surfactant . . . . .	151
A.7	Resulting pressure variation with oil concentration at a surfactant/oil ratio of 10% with 1.1 $\mu\text{m}$ membrane . . . . .	151

# List of Tables

1.1	HLB ranges and applications . . . . .	14
1.2	Summary of advantages and disadvantages of processes for nanoemulsions production . . . . .	23
1.3	Examples of commonly used oils for parenteral emulsions and recommended concentrations from A.G. Floyd [45] . . . . .	27
1.4	Properties of commercial SPG membranes from Vladisavljević et al. [46] with data from [47, 48, 49, 50] . . . . .	32
1.5	Summary of types of commercial available membranes, adapted set-up and pore sizes available . . . . .	39
1.6	Effect of each parameter on droplet size in DME, IFT: interfacial tension . . . . .	43
1.7	Effect of each factor on droplet size in PME . . . . .	47
1.8	O/W emulsions produced by PME, n is the number of cycle equal to 1 if not mentioned; BSA: bovine serum albumin; PGPR: Polyglycerol polyricinoleate; PGPE: Propylene glycol propylether; SDS: Sodium dodecyl sulfate . . . . .	48
1.9	W/O emulsions produced by PME . . . . .	49
1.10	W/O/W emulsions produced by PME . . . . .	50
1.11	O/W nanoemulsions produced by PME . . . . .	50
4.1	Composition and dynamic viscosities of oils used to study the influence of dispersed phase viscosity . . . . .	96
5.1	Variation of the Z-average, PDI and mean value at various flowrates from 1 to 15 mL/min . . . . .	117
6.1	Composition of the atRA emulsions formulation . . . . .	128
6.2	Summary of size results for the three different processes PME, MF and US for selected conditions . . . . .	132



# Introduction

### Context

This work was part of the European H2020 project: PeptiCaps. The global aim of the project was the design of emulsifiers to produce safe, controlled and reliable novel stimuli-responsive nanocapsules for skin care applications. The aim of LAGEPP was to produce O/W and W/O nanoemulsions with a membrane process with specific project compositions first at lab scale and then at pilot scale. The interest of this process over conventional processes is its low energy consumption, its mild conditions which can be better for sensitives actives, its selectivity and the monodispersity of emulsions produced.

Membrane processes have been investigated for more than 20 years for emulsion production. However, only very few studies reported production of O/W emulsions at large scale. It can be explained by the fact that in direct membrane emulsification (DME) the droplet generation flowrate has to be very low in order to get monodispersed droplets. This characteristic can be an issue for large scale production. However, with an other membrane process, premix membrane emulsification (PME), the higher the flowrate is the smaller the droplets are. Thanks to these properties, this process has been extensively studied over the past decades, however only a few studies reported the production of nanoemulsions. The first study was published in 2012 and all other results reporting the production of nanoemulsions with PME were published by one group who studied mainly polymeric membranes and at small scale.

Moreover, regarding W/O only two groups reported the production of emulsions with PME. To our knowledge, the production of W/O nanoemulsions with PME has never been reported.

### Research questions

From these observations, we see that no set-up allows the production of O/W and W/O nanoemulsion production with membrane processes at pilot scale. Thus, some questions were raised:

- Is it possible to develop a membrane process at pilot scale to produce O/W and W/O nanoemulsions?
- Which parameters have the main impact on final nanoemulsion droplet size and feasibility of the process?
- Is it possible to produce nanoemulsions with specific compositions (viscous emulsions, polypeptidic surfactants or suitable for injection)?
- What are the advantages and drawbacks of PME over a traditional industrial process, microfluidizer, and a laboratory process, ultrasounds, for nanoemulsions production?

In this work, we tried to answer to these questions.

### Organization of the work

First, a literature review was done and summarized in Chapter 1. The first part presents general backgrounds on nanoemulsions and their production processes. The second part concerns membrane processes for emulsification and the parameters of influence end forces involved.

In Chapter 2, the set-ups developed to answer the questions raised above are presented in details. Analytical techniques used to characterize the premix emulsions, the different phases and the nanoemulsions are also presented.

In Chapter 3 and 4, we answered to the first and second questions by reporting results obtained for nanoemulsion production with the high pressure syringe pump set-up. In Chapter 3, the O/W nanoemulsions production with a model composition is described, and in Chapter 4, the production of W/O nanoemulsions with a model composition. In these chapters, the effect of process and composition parameters on the nanoemulsions production were investigated.

The production of O/W and W/O nanoemulsions with the specific PeptiCaps composition are reported in Chapter 5.

Finally, in the last result chapter, Chapter 6, three processes Microfluidizer, ultrasounds and PME are compared for the production of injectable nanoemulsions. The evaluation of the different processes was analyzed mainly in terms of nanoemulsion characterization, active preservation and stability. This last study allows to answer to the last question by understanding if the process developed has significant advantages over conventional processes.

In Appendix A.1, results obtained during the set-up development are presented. Finally, in Appendix A.2 preliminary results obtained with the set-up for the preparation of micron scale emulsions are presented.



# **Chapter 1**

## **Literature review**

## 1.1 Nanoemulsions: Generalities and Processes

### 1.1.1 Definition and physico-chemistry of nanoemulsions

#### 1.1.1.1 Definition

An emulsion is a system of two immiscible phases with one dispersed in the other. One phase consists of droplets, the dispersed phase in suspension in an other phase, the continuous phase. Emulsions are thermodynamically unstable but can show long term kinetic stability [1]. Emulsion are present in nature for example in milk products and latexes. They are also of interest in many industries as final products:

- Cosmetics industry : hand creams, conditioners, sunscreens... [2]
- Pharmaceutical industry: dermatology, nutrition and vaccines
- Food industry : salads sauces, desserts... [3]
- Paints : emulsions of alkyd resins, latex emulsions
- Agrochemicals: self-emulsifiable oils, emulsion concentrates

Emulsions are also involved in the first step of emulsion polymerization [4] for applications such as production of synthetic rubbers, plastics and polymers in dispersion. Also emulsions have to be removed in processes like petroleum extraction where water-in-oil (W/O) emulsions are created and required to be demulsified [5].

The term emulsion often describes systems with droplet diameter higher than 1  $\mu\text{m}$ . Nanoemulsions are emulsions with a droplets diameter under 1  $\mu\text{m}$ , 500 nm, 200 nm or 100 nm depending of the definition used and the field of application. The terms mini-emulsions and sub-micron emulsions can also be used for emulsions with droplets size between 200 nm and 1  $\mu\text{m}$ . In this work, all emulsions within the nano-range, below 1  $\mu\text{m}$ , will be called nanoemulsions.

Emulsions are classified in different types, the main one is called oil-in-water emulsions (O/W) (Figure 1.1) where the dispersed phase is the organic phase or oil phase and the continuous phase is the aqueous phase. The other type is water-in-oil (W/O) emulsion where the dispersed phase is the aqueous phase and the continuous phase the oil or organic phase.

Double emulsions are also commonly used, they can be water-in-oil-in-water (W/O/W) (Figure 1.1) or oil-in-water-in-oil (O/W/O), the first one having more applications than the second one [6].

Different types of other specific emulsions exist such as concentrated emulsions, W/W emulsions or O/O emulsions, when a polar oil is dispersed in a non-polar oil, these emulsions will not be discussed in this work.

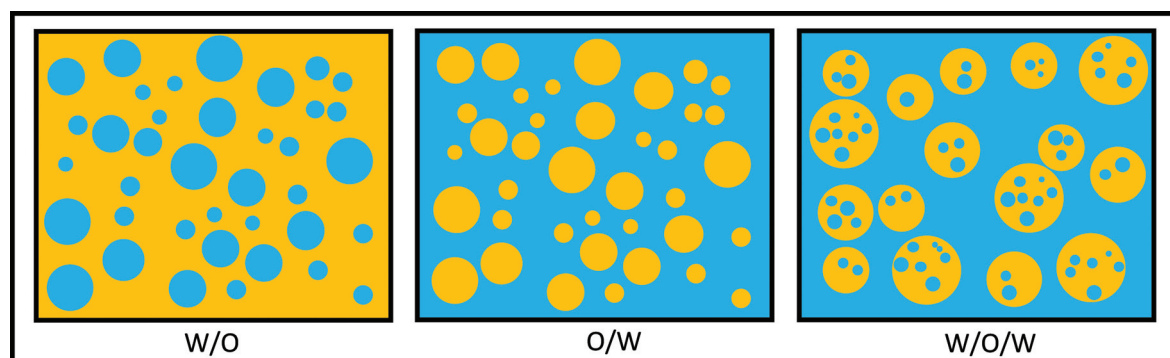


Figure 1.1: Different types of emulsions from left to right, W/O, O/W and W/O/W

### 1.1.1.2 Physico-chemical principles

Nanoemulsions do not form by themselves, to produce stable nanoemulsions, energy and surfactant are required. Understanding the phenomenon at the interface and between droplets is crucial to formulate emulsions for specific applications.

**The oil/water interface** Both phases, two non miscible liquids or gas and liquid, on each part of the interface have uniform thermodynamics properties. In addition the interface has specific properties. At the interface, water molecules can not satisfy all hydrogen bondings while Van der Waals bondings are nearly satisfied. Creating emulsions increases the interface area, one force is opposite to this creation, as the water loses hydrogen bondings in the process, and is called the surface (liquid/gas) or interfacial (liquid/liquid) tension.

The interfacial tension  $\gamma$ , is the force necessary to break the surface between two immiscible liquids. It is expressed by a force, Gibbs surface free energy,  $\delta G$  per surface unit,  $\delta A$  as it is the cohesion force of the liquid molecules that are attracted inside the droplet. At constant temperature, composition and volume [7]:

$$\gamma = \frac{\delta G}{\delta A} \quad (1.1)$$

$\gamma$  is energy per unit area ( $mJ.m^{-2}$ ), which is dimensionally equivalent to force per unit length ( $mN.m^{-1}$ ), the unit usually used to define surface or interfacial tension. Here  $\gamma$  is defined for a plan surface, but is very similar for a curved interface.

**Laplace pressure** The interfacial energy induces an important excess in pressure inside the droplets due to change in physical state inside the droplets compare to the droplet outside. This pressure is called Laplace pressure  $\Delta P$  and is proportional to the interfacial tension  $\gamma$  and inversely proportional to the radius  $r$  of the droplets.

$$\Delta P = \frac{2\gamma}{r} \quad (1.2)$$

For nanoemulsions,  $r$  is very low, so the Laplace pressure becomes higher and creates more resistance to the droplets disruption making more difficult to reduce their size. Moreover, as it will be seen in the next section, the Laplace pressure causes Ostwald ripening so it has a large impact on nanoemulsions stability [8].

**Energy requirement for interface creation** As emulsions require energy to be created, it is interesting to calculate the energy required for their creation.

To produce 1 L of nanoemulsion at 20% in volume of oil, so a volume  $V_o = 200$  ml with a mean droplet diameter of  $d_d = 200$  nm, even with no surfactant, and a very non-polar oil,  $\gamma = 50$   $mN.m^{-1}$ , the area of the water/oil interface created during this process would be:

$$S = \frac{6V_o}{D} = 1500 \text{ m}^2 \quad (1.3)$$

So, the energy required (E) is:

$$E = S \times \gamma = 75 \text{ J} \quad (1.4)$$

This is a very low value compared to the energy involved in classical processes used for emulsification, for example, a rotor-stator system dissipates a power of  $22 \text{ kJ}.s^{-1}$  [9] and a high-pressure homogenizer at least  $10 \text{ kJ}.L^{-1}$  [8], 99 % of the energy being dissipated as heat.

One explanation for such an energy loss, is the viscous energy dissipation in the continuous phase. Nanoemulsions can not be created by mechanical turbulences contrary to macroemulsions. The mixing device agitates the continuous fluid that creates a shear stress and reduces the size of the emulsion. It is not directly the contact between the droplet and the device that reduces the droplet size. Thus, much energy loss occurs when the fluid circulates, leading to heat increase.

**The oil/water/solid interface** Liquid/liquid and liquid/gas interfaces have similar behaviors with both low bonding between molecules and no defined shape. Interface with a solid is different because it has a definite shape. An emulsion in contact with a solid presents a triple point, where solid (S), oil (O) and water (W) are in contact and a specific contact angle ( $\theta$ ) at this point (Figure 1.2). A droplet on a surface spreads more or less according to the surface wettability. This contact angle is a balance between adhesive and cohesive forces. If the contact angle is low, the wetting is high or even perfect, that means that the solid-oil interaction are high and that the solid is lipophilic (hydrophobic). If the contact angle is high, the wettability is low, the interaction between the solid and the oil is weak and the surface is hydrophilic.

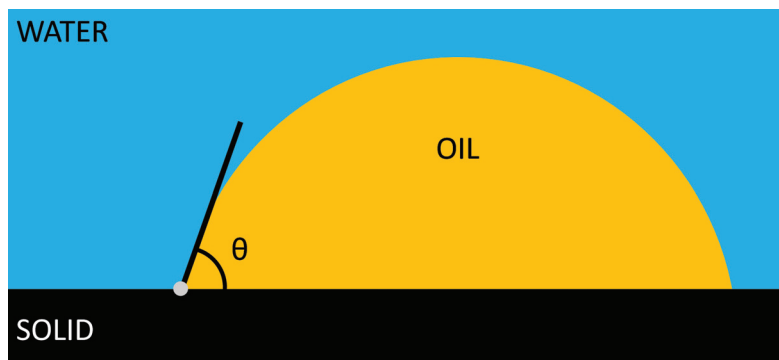


Figure 1.2: Oil/Water/Solid Interface and contact angle ( $\theta$ )

### 1.1.1.3 Stabilization: Forces involved between nanoemulsions droplets

The more important forces to consider to form emulsions is the interfacial tension and physico-chemical or mechanical forces required to overcome interfacial tension. Once the nanoemulsion is produced and the droplets are in suspension in the continuous phase, other forces are important to stabilize it and keep it at nanosize [10].

**Forces applied on one droplet** Oil droplets immersed in a water continuous phase undergo gravity ( $F_G$ ), buoyancy force ( $F_B$ ) and drag force ( $F_D$ ) (Figure 1.3). Buoyancy and drag forces depend on the density of the oil and the water phase but only gravity depends on the droplet weight so on its volume. As droplets are very small, they cause a large reduction in the gravity force compare to larger droplets.

Particles in a fluid move randomly due to the continuous phase molecules and micelles agitation, this phenomenon is called Brownian motion ( $B_M$ ). Brownian motion is even greater for continuous phase with low viscosity and with small particles. The emulsions with the smallest droplets size move faster due to Brownian motion. For nanoemulsions, Brownian motion may be sufficient for overcoming gravity.

**Van der Waals attraction force** Emulsions, like all other dispersed systems, undergo van der Waals forces that are attraction forces between molecules considered as independent and creating low energy bondings. These forces are highly dependent on the atomic structure of the molecules. They can be of three types, Keesom, Debye, and London forces. London forces are more important for emulsions because they are higher at low distance.

This force is always attractive for two molecules of same chemical nature. Van der Waals interaction between two particles is only within a few nanometers but can be a force of destabilization. To counterbalance this attractive force, repulsion forces have to be taken into consideration to produce stable nanoemulsions.

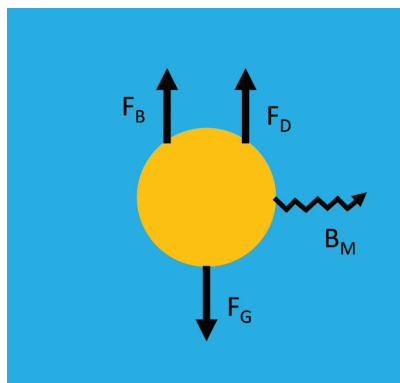


Figure 1.3: Forces on an oil droplet dispersed in water

**Electrostatic repulsion** The effect of attractive van der Waals forces and repulsive electrostatic forces has been studied in the DLVO (Derjaguin, Landau, Verwey, Overbeek) theory [11]. It explains and describes the forces that undergoes a charged particle dispersed in an aqueous medium. The particles are considered with their surrounding media and the charges in this medium that depend on the electrolyte in presence and temperature (Figure 1.4). The combination of the charged surface, the counter ions or Stern layer and the diffuse layer is called electrical double layer of the particle. The DLVO theory suggests that when two double layers of different charged particles overlap, a repulsive force is induced, that can stabilize the emulsions. For emulsion formulation, charged surfactants or polymers are used to improve the electrostatic repulsion effect. Usually the particle charge is measured at the level of the slipping plane, where two double layers overlap, to evaluate the effectiveness of the surface charge. This value is called,  $\zeta$ , the zeta potential. The DLVO theory indicates that there is a minimum charge to have repulsion between particles or droplets, it is usually considered that the zeta potential has to be higher than 30 mV either with a negative or positive charge to counterbalance the effect of van der Waals forces and to have stable nanoemulsions.

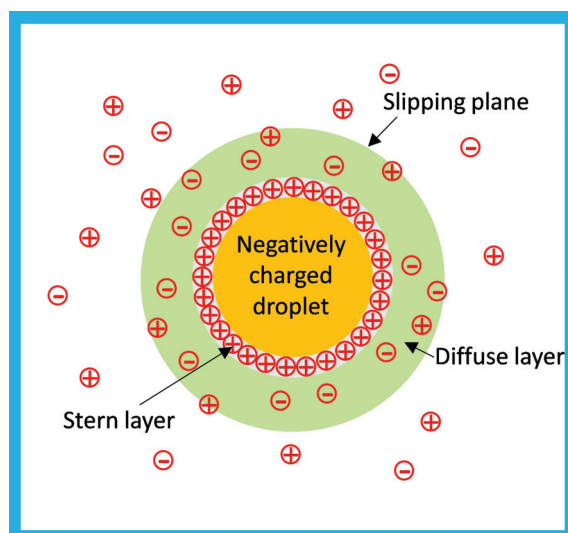


Figure 1.4: Electrical double layer of a charged emulsion

**Steric repulsion** A second repulsive effect can occur with the use of a non-ionic surfactant or a copolymer that has large chains in the continuous phase (Figure 1.5). The hydrophilic chains, the most used being polyethylenoxide (PEG) chains, show unfavorable mixing when they are in

a good solvent, which is the case of water, overlap is not favorable and the droplets repulse each other.

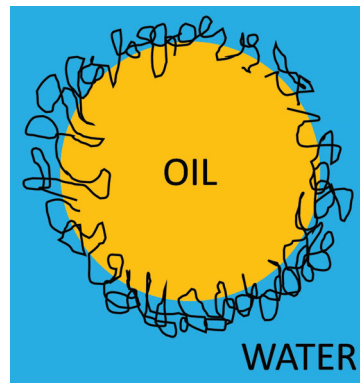


Figure 1.5: Droplet stabilization by steric hindrance

#### 1.1.1.4 Emulsion destabilization

The various destabilization mechanisms are illustrated in Figure 1.6. They are not simple phenomena, so a study of all the forces and parameters involved is required. Moreover, more than one phenomenon can occur simultaneously, increasing the difficulty of analysis. In addition, prediction of the breakdown of the emulsion usually takes into consideration a single droplet diameter or mass for the emulsion, assuming that the droplet size distribution is highly monodispersed. In reality, droplet distribution of emulsions are not monodispersed and the polydispersity increases the destabilization.

Understanding the phenomenon involved can help to prevent destabilization but they are difficult to predict exactly.

**Creaming and sedimentation** Creaming and sedimentation are both results of the same phenomenon gravity. If the density of the dispersed phase is greater than the density of the continuous phase, the droplet falls (sedimentation); in the opposite case, the droplet rises (creaming). This induces an heterogeneity in the emulsion if the emulsion is not agitated. The velocity of sedimentation or creaming  $\omega$ , of a droplet of radius  $r$  and mass  $m$  immersed in a continuous phase of viscosity  $\eta$  is mainly a competition between gravity and drag forces due to the continuous phase viscosity :

$$\omega = \frac{mg}{6\pi\eta r} = \frac{2\Delta\rho gr^2}{9\eta} \quad (1.5)$$

with  $\Delta\rho$  the difference in volumetric weight between the dispersed and the continuous phase and  $g$  the gravity acceleration. To limit these phenomena it is possible to modify the density difference but the scope of action is limited, or to increase the viscosity of the continuous phase by adding a viscosifier or to decrease the droplet size of the emulsion which can have a strong impact. Moreover, as the Brownian motion is more important for small droplet size and limits creaming/sedimentation by a random movement, nanoemulsions are much more stable to creaming and sedimentation than classical emulsions.

Creaming and sedimentation are reversible by shaking. However, as the concentration of the dispersed phase increases locally droplets are more likely to affect with each other and to undergo coalescence.

**Flocculation** When the particles aggregate without change in the droplet size because van der Waals forces overcome the repulsion forces, it is called flocculation. Flocculation can be reversible

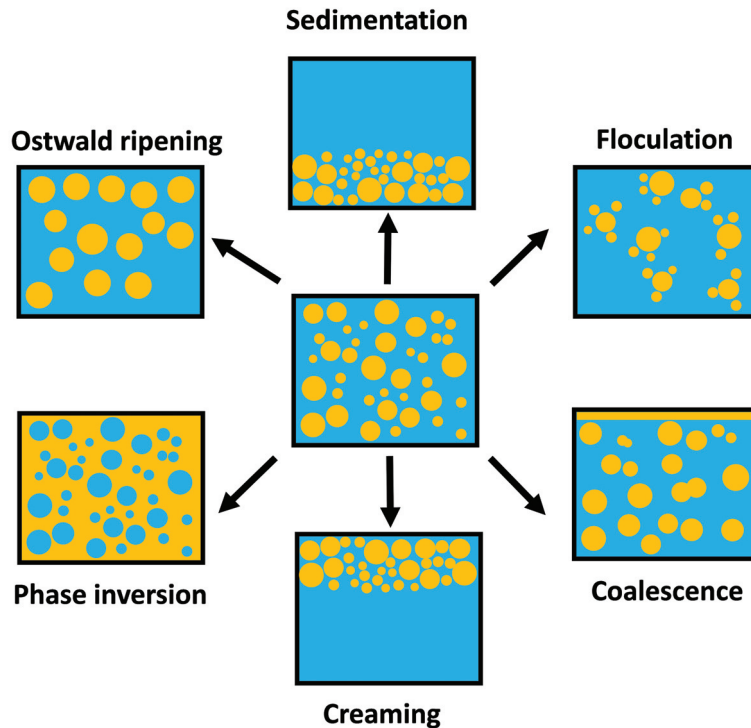


Figure 1.6: O/W emulsions destabilization processes

by shaking in case of "weak" flocculation due to van der Waals forces or difficult to redisperse, in case of "strong" flocculation.

**Phase inversion** This process is an exchange between the continuous and the dispersed phases. For example, an O/W emulsion can become a W/O emulsion. It can happen with time or with a change of conditions such as temperature, but is very rarely observed during storage and may be a wanted consequence due to a change in temperature or composition.

**Coalescence** Coalescence refers to a phenomenon of thinning and finally disruption of the film between two droplets. Contrary to the phenomena presented above, coalescence is non-reversible, the droplets are disrupted and can not go back to their original size. Eventually, the two phases are separated completely one above the other.

The driving force of this phenomenon is still under discussion and the scientific community does not agree on one major driving force, but the general scenario is admitted. First, as the distance between droplets narrows the film becomes more and more thinner due to a suction effect. The film between the two droplets finally breaks down.

The first step of coalescence is collision that can be induced by creaming, sedimentation, flocculation or a consequence of Brownian motion. The tendency of the film to break down or not is governed by different properties such as elasticity of the film, double layer repulsion, Marangoni forces, etc. . .

**Ostwald ripening** The destabilization paths presented above, creaming and coalescence, are minimized with smaller droplet size such as nanoemulsions. Ostwald ripening becomes the major phenomenon for nanosize emulsions [12]. It is also the less understood of all phenomena of emulsion destabilization. It depends on Laplace pressure (part 1.1.1.2), that depends on droplet size and interfacial tension. For smaller droplets, the pressure is higher than for larger ones. This induces a higher chemical potential in smaller droplets and so a mass transfer from the small

droplets to the larger ones through the continuous phase in order to establish a thermodynamic equilibrium [13].

Small droplets vanish while the larger ones grow and change in an irreversible way the droplet size distribution of the emulsion. As the Laplace pressure is higher for smaller droplet size emulsions, this phenomenon is more likely to happen in nanoemulsions.

## 1.1.2 Emulsifiers

### 1.1.2.1 Molecular characterization and principles

**Characterization and behavior in water** As mentioned in the previous part, in order to produce and stabilize emulsions, emulsifiers are used. Emulsifier molecules are present at the oil/water interface and reduce the interfacial tension. In order to do that, emulsifier molecules present two chemically different parts, one is oil soluble and the other is water soluble. They are amphiphilic molecules (Figure 1.7) and usually composed of [14]:

- An hydrophilic head made of polar molecules, able to share H bonding with water molecules. They are either cationic, anionic, zwitterionic (both charges) or uncharged.
- An hydrophobic tail, that has a strong affinity with the oil phase mainly hydrocarbonated chains (aliphatic or aromatic compounds).

This is schematic and other configurations are possible, for example the emulsifier molecule can have several hydrophilic and hydrophobic parts instead of two distinct parts.

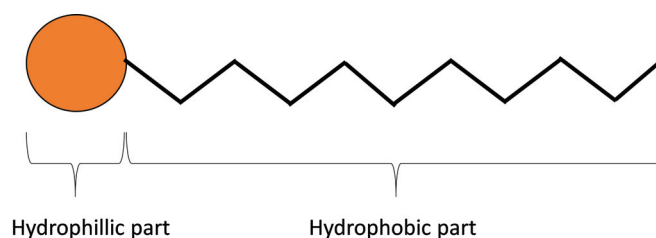


Figure 1.7: Schematic representation of an amphiphilic surfactant

In an aqueous medium, emulsifier molecules take a specific conformation that minimizes their hydrophobic part interaction with water and maximizes the interaction between their hydrophilic part and water, these systems are called micelles. They are very small aggregates of emulsifier molecules with mean size between 1 and 100 nm that organize differently (cylinder, sphere ...) according to the concentration, pH, ionic strength, temperature and to the relative length of their hydrophilic and hydrophobic parts.

**CMC** The emulsifier concentration has a great impact on the emulsion production and final characteristics. In order to optimize emulsifier concentration it is useful to determine the critical micellar concentration (CMC).

CMC characterizes the shift between free emulsifier molecules state to the apparition of the first micelles. Above this concentration, all the emulsifier added to the system directly form micelles, which explains the term CMC.

The easiest way to determine CMC is to measure the interfacial tension variation with emulsifier concentration (Figure 1.8).

At low concentrations, the interfacial tension depends highly on the emulsifier concentration. First, added emulsifier molecules adsorb at the interface or stay in the continuous phase as free molecules. Then, the oil/water interface is saturated with emulsifier molecules but interfacial tension continues to decrease linearly with emulsifier addition, with added molecules as free emulsifier. At the CMC, micelles start to form in the continuous phase with the additional emulsifier and

interfacial tension stays constant. For one single phase, CMC is determined from surface tension measurement. It can also be defined for an emulsion and is determined from interfacial tension measurement.

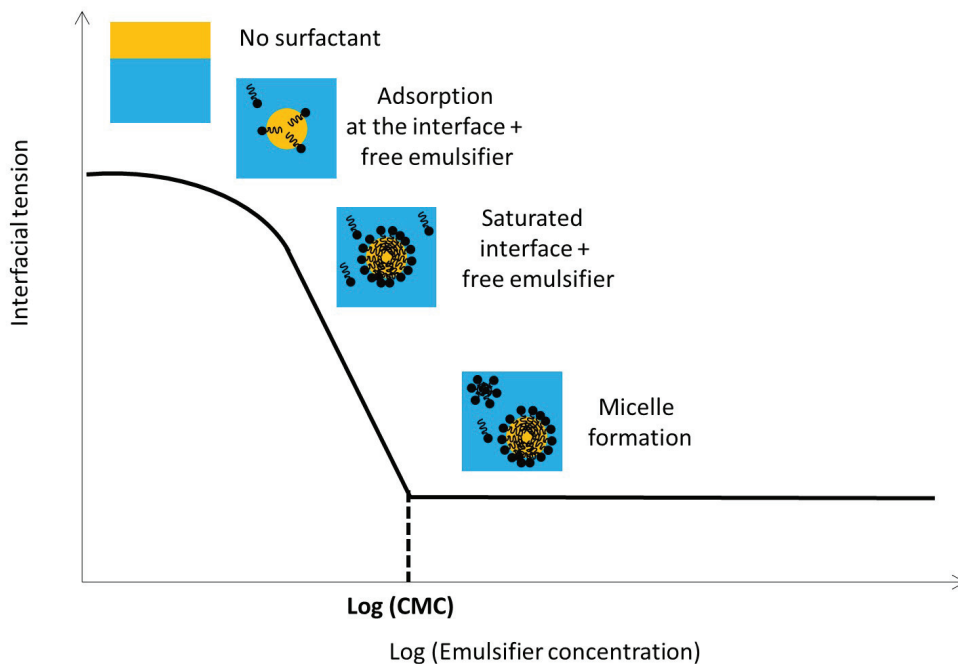


Figure 1.8: Evolution of the interfacial tension with emulsifier concentration and oil, water and emulsifier interactions

**HLB** Griffin has introduced the Hydrophilic Lipophilic Balance (HLB) method, 60 years ago, as a rational and simple way of formulating emulsions [15]. The aim of this method is to determine the optimal emulsifier blend theoretically in order to avoid empirical formulations. The HLB scale is based on the relative percentage in molecular mass of hydrophilic to lipophilic (hydrophobic) groups of the emulsifier molecule.

In the original formula for non-ionic emulsifiers, this relative percentage was divided by 5 so takes a value from 0 to 20 for all molecules but from 3 to 18 for emulsifiers having an interface activity (Table 1.1). An other scale has been proposed by Davies three years later, taking into account the effect of stronger and weaker hydrophilic groups, that was more adapted for ionic surfactants and is between 0 and 40 [16].

The HLB value of an emulsifier blend is obtained by addition of the HLB of each emulsifier regarding their weight content in the blend.

Similar to the HLB definition for emulsifiers, the critical or required HLB (RHLB) has been defined for the oil phase. Each oil has its own polarity and does not require the same HLB. The RHLB is the HLB value of the surfactant or surfactant blend required to obtain the more stable emulsion with this oil. An oil has two RHLB values one for W/O emulsions between 3 and 6 and one for O/W emulsions between 8-18.

Usually RHLB values are measured by preparing emulsions at each different HLB and choosing the more stable one. This method is not very precise and the standard deviation for an RHLB value is usually more than 1. However it can be of great help for formulators.

### 1.1.2.2 Classical types of emulsifiers

**Surfactants** Surfactants (Figure 1.9 b) are classified according to their charge:

HLB range	Surfactant function
3–6	W/O emulsifier
7–9	Wetting agent
8–18	O/W emulsifier
13–15	Detergent
15–18	Solubilizer

Table 1.1: HLB ranges and applications

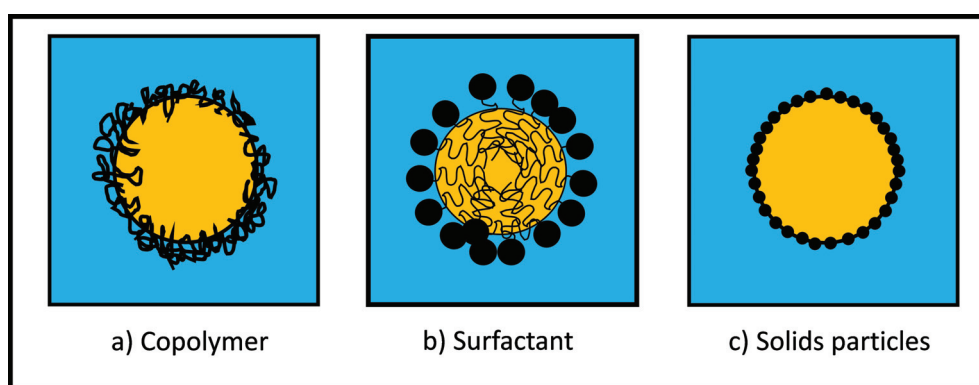


Figure 1.9: Different types of molecules showing a surface activity and stabilizing emulsions

- Anionic surfactants: have a negative charge on the hydrophilic head. It is the oldest kind of surfactant synthesised in soap production. They usually have very high HLB values so are good detergents.
- Cationic surfactants: present a positive charge, they are good emulsifiers and are used in applications such as conditioners or fabric softeners after the use of anionic surfactants to neutralize the charge.
- Zwitterionic surfactants: present two charges on their hydrophilic head, one positive and one negative. They are known to be mild detergents with good emulsifying properties but without irritation issues.
- Non-ionic surfactants: present no charge and are like zwitterionic surfactants mild detergents.

Charged surfactants are usually very effective and as seen previously, their charges create an electrical double layer which prevents droplets coalescence by electrostatic repulsion.

**Polymeric emulsifiers** Polymers used as emulsifiers are copolymers of two or more blocks with at least one being hydrophilic and at least one being hydrophobic (Figure 1.9 a) [17]. The most used polymeric emulsifiers are three block polymers of PEG-PPO-PEG (PPO: polypropyleneoxyde). PEG is hydrophilic and PPO hydrophobic. By tuning the chain length and ratio of PEG/PPO, a wide range of O/W and W/O emulsifiers with different HLB are achievable.

As seen previously concerning the stability, polymers create steric hindrance between droplets stabilizing the emulsion. For O/W emulsions, the hydrophilic chain has to be long enough in order to create steric repulsion in the aqueous continuous phase. For W/O emulsions, on the

contrary, it is the hydrophobic part of the polymer that creates the repulsion in the continuous phase.

However, if the chain is too long, polymers can create bridges between droplets in concentrated emulsions that are very difficult to redisperse. An optimum chain length has to be determined to avoid such phenomenon.

Both charged surfactants and long hydrophilic chains can be used to optimize long term stability thanks to both electrostatic and steric repulsion.

**Proteins as emulsifiers** Proteins are amphiphilic molecules containing both hydrophilic and hydrophobic amino acids. Proteins are natural surfactants found in nature such as milk caseins. In water,  $\alpha$ ,  $\beta$  and  $\kappa$  caseins form micelles and stabilize fatty globules. Thanks to their biocompatibility, they are often used in food industry [18]. Proteins have interesting properties because they are zwitterionic, present an isoelectric point and can change their hydrophobic/hydrophilic character by changing pH. This explains the phenomenon of coagulation when milk is acidified.

However, proteins because of their very complex composition and amino-acids sequences do not usually present long enough hydrophobic tails to be good emulsifiers. They are often associated with phospholipids that are the most common natural surfactants. Phospholipids consist of two hydrophobic protein long "tails" and one hydrophilic "head" with a phosphate group and are the major component of bi-layer cell membranes. They are also used to form vectors for topical, oral or parenteral administration, called liposomes. Liposomes can improve drug bio-availability, reduced toxicity and increased permeability across membranes [19].

**Solid particles** Pickering discovered that solid particles can also stabilize emulsions [20] (Figure 1.9). The ability of a droplet to be stabilized depends on the wetting properties of the two liquids, oil and water on the particles surface, so on its hydrophobicity.

### 1.1.2.3 Polypeptidic surfactants

Polypeptides are proteins with only few small amino acid units, between 10 and 100. Naturally, polypeptides are used for proteins synthesis but can also be produced and used for their unique properties, secondary structure and better bio-compatibility compared to polymers. Synthesized polypeptides are usually analogue to polymers with the monomer units being amino-acids instead of other molecules.

To be good emulsifiers, copolypeptides are usually composed of at least two blocks, one hydrophilic and one hydrophobic. The advantages over natural proteins is that amino acids can be chosen according to their hydrophilicity and so create long hydrophobic or hydrophilic chains that are good stabilizers.

**Synthesis** Copolypeptides can be synthesized by ring opening polymerisation (ROP) starting with NCA (alpha-amino acid N-carboxyanhydrides) material [21]. NCA has the advantages to present an activated CO group and a protected amine group. Primary amines usually generate an "amine mechanism" and for secondary and tertiary amines two mechanisms coexist. Figure 1.10 shows the schematic representation of the synthesis of an amphiphilic copolypeptide. Block 1 is composed of  $m$  units of peptide with  $R^1$  an hydrophilic side chain for example, glutamic acid or lysine. Block 2 is composed of  $n$  units of peptide with  $R^2$  an hydrophobic side chain, for example valine or leucine.

Copolypeptides can only be composed of peptides as shown on Figure 1.10 however one of the polymeric chains can also be a polymer such as PEG for the hydrophilic part. Copolypeptides can also have more than two blocks.

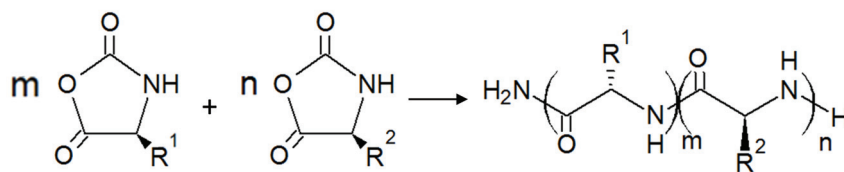


Figure 1.10: Schematic representation of the synthesis of an amphiphilic copolypeptide

**Self-assembling in water** In order to reduce the interaction between the hydrophobic part of the peptide and water, between blocks and between copolymers, amphiphilic polymers tend to organize themselves in micelles like structure in water. As CMC exists for surfactant micelles it exists for polymeric micelles. CMC depends on temperature, pH, nature of blocks and chain length.

Moreover, as phospholipids can form liposomes, some types of copolymers, with an appropriate chain length form vesicles called polymersomes [22]. Polymersomes have the advantage over liposomes to be 10 times less permeable to water.

**Interaction with surrounding medium** Copolypeptides are composed of amino-acids which make them very sensitive to their surrounding medium, especially temperature, pH and presence of enzymes. For example, polyglutamic acid (PGA) [23] is protonated in an acidic environment. This molecule takes an helical  $\alpha$  rod conformation and is less soluble in water. By tuning pH, the polymer is either hydrophobic or hydrophilic which can be an interesting property for emulsifiers.

**Application at the oil/water interface** The design of amphiphilic copolymers showed the capacity of copolypeptide diblocks to stabilize silicon oil nanoemulsions [24]. In this case, the hydrophilicity is provided by poly (L-lysine.HBr) which is highly charged at neutral pH and provides a high solubility in water. It also presents many amine groups that are easily functionalizable. Poly (L-leucine) is hydrophobic and has an  $\alpha$  helix conformation which confers very large interchain associations and poor solubility in organic solvents. As a result, the block copolymer associates strongly in water and forms vesicles due to the aggregation of the hydrophobic groups.

### 1.1.3 Processes for nanoemulsions production

As seen previously, the production of nanoemulsions requires much energy. It can be provided to the system by two ways, energy of physico-chemical origins or mechanical energy. These processes are called respectively low and high energy methods. Low energy processes are based on physico-chemical properties of the ingredients in the formulation, only a low amount of mechanical energy is required. High energy processes are based on mechanical energy creating a shear rate that reduces the droplet size of the emulsion.

#### 1.1.3.1 Physico-chemical processes

A method of producing nanoemulsions is to use physico-chemical properties of a surfactant or a co-surfactant/solvent to create a chemical energy that exceeds the interfacial tension, leading to the creation of nanodroplets. In this category, there exists mainly three processes [25]:

- Phase Inversion Temperature (PIT)
- Phase Inversion Composition (PIC)
- Nanoprecipitation

An other process presented in this section is based on physico-chemical properties to obtain microemulsion. They are often mistaken for nanoemulsions but they are fundamentally different as they are thermodynamically stable systems.

**Nanoemulsions by phase inversion methods** These methods are based on chemical energy from microemulsions phase transition during emulsification. This transition can happen with two types of change: composition change, the method is called PIC or because of a change in temperature, the method is called PIT (Figure 1.11).

The PIC method is based on a sudden change in composition at constant temperature, when adding a great amount of water to a W/O emulsion or a great amount of oil to an O/W emulsion.

The PIT method is based on a change in temperature that induces a change in the HLB of the surfactant [26]. Only specific non-ionic surfactants that are sensitive to temperature change such as polyoxyethylene-type surfactants can be used with this technique. The change of phase happens at the HLB temperature of the surfactant where the HLB of the surfactant molecule changes from low value to high value or inversely. This temperature depends on the surfactant.

The physico-chemical mechanisms involved are the same for both PIC and PIT. The inversion phase occurs when the mean spontaneous curvature of the surfactant molecule is zero. At this stage, the interfacial tension is very low and nanoemulsions are formed. The structures having a surfactant film with an average zero curvature can be either bicontinuous microemulsions or lamellar liquid crystalline phases.

The advantages of this technique are that no mechanical energy is required, which is better for sensitive actives and energy consumption, and no additional components have to be added. However, only simple compositions can be used and with specific surfactants that are able to change the film curvature.

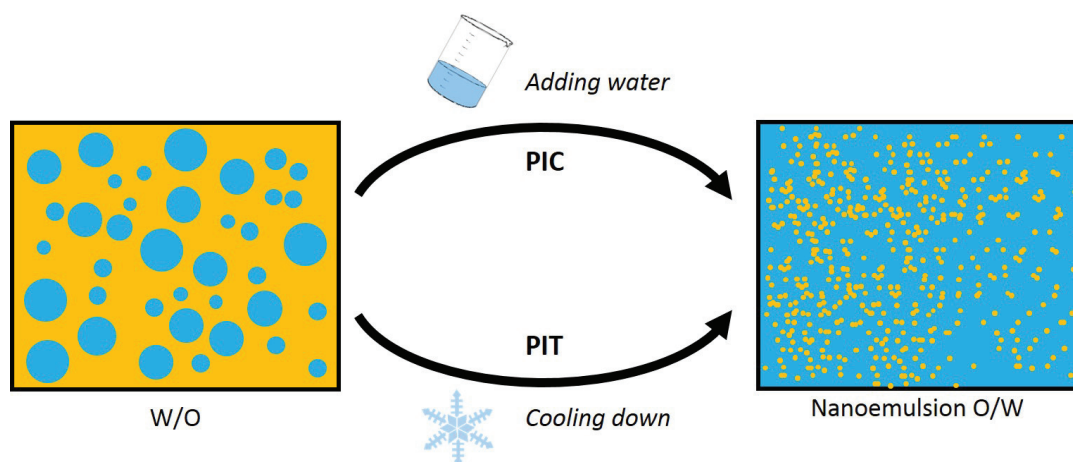


Figure 1.11: Schematic representation of phase inversion methods

**Nanoprecipitation** Nanoprecipitation also called solvent displacement method or spontaneous emulsification is a technique based on the addition of a water miscible solvent to an organic phase [27, 28]. The oil phase is dissolved in the water miscible solvent and then added to the water phase (Figure 1.12). When in contact, the solvent displaces in water generating turbulences and forming nanoemulsions.

This method is also called Ouzo effect from the observation that when water is added to this well known Greek alcoholic beverage, nanoemulsions of anise essential oils are created. The essential oil is solubilized in ethanol, once in contact with water the ethanol is displaced to the aqueous phase and the oil becomes insoluble and forms nanodroplets. No surfactant is required to obtain this type of nanoemulsions. However, for several applications surfactants are added in order to achieve long term stability.

The advantage of this technique is also very low mechanical energy consumption. One major drawback is that a very low amount of oil nanodroplets can be produced and large volumes of solvent and water are required. Moreover, an additional step is required to evaporate the solvent, and residues of solvent can be an issue for some applications such as injection.

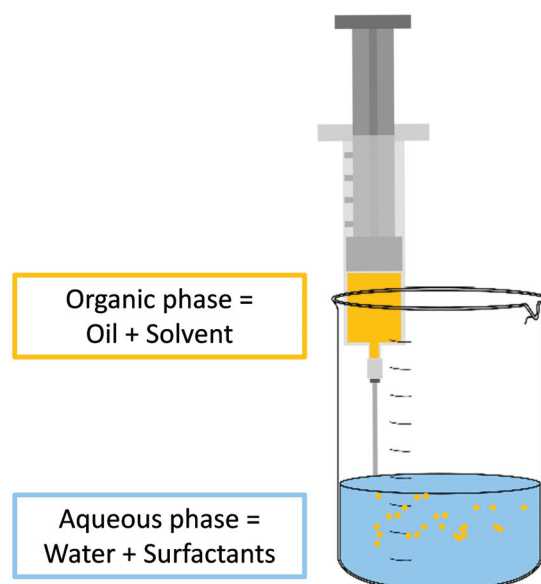


Figure 1.12: Schematic representation of nanoprecipitation set-up

**Exception of microemulsions** Microemulsions, like nanoemulsions are stable dispersions of two immiscible liquids. However, contrary to nanoemulsions, microemulsions are thermodynamically stable and formed spontaneously upon simple mixing. They are also homogenous and transparent [29]. The size range of the microemulsions vary from 1 to 100 nm and usually between 10 to 50 nm. The dispersions can be O/W or W/O droplets or present an interconnected structure (bicontinuous microemulsions).

They are composed of oil, water, surfactant and usually a co-surfactant. They are obtained only at certain specific conditions of composition called the "microemulsion domain" (Figure 1.13). Before forming a microemulsion, the microemulsion domain has to be determined usually by establishing a ternary phase diagram.

Nanoemulsions and microemulsions are fundamentally different and one should not mistake one for an other.

Microemulsions are advantageously very small and very stable. However, this type of formulation requires a large amount of surfactant and co-surfactant, and usually a low amount of dispersed phase, they are also sensitive to environmental parameters such as temperature and pH.

### 1.1.3.2 Mechanical processes

An other way of producing nanoemulsions is to give the system a mechanical energy that overcomes the interfacial tension. To form nanoemulsions, this energy has to be intense enough to reduce the droplet size at a nano range. A high energy process is the result of two phenomena. First, an intense mechanical force is given to the system that leads to deformation, rupture of droplets and increase of the interfacial oil/water area. Then, the adsorption of the surfactant at this new interface occurs. These two phenomena can occur simultaneously. Most of high-energy processes for the production of nanoemulsions are homogenization processes. It means that they require a pre-emulsification process that will produce micron size droplets prior to homogenization. Thus, four processes for production of emulsions with micron droplet size are presented below [31]:

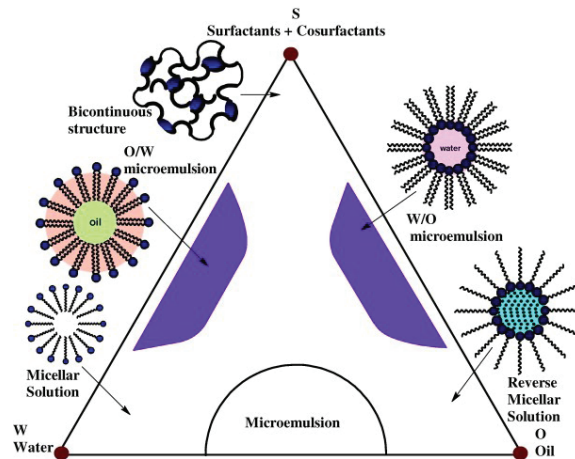


Figure 1.13: Schematic microemulsion domain in a phase diagram from Malik et al. [30]

- Mechanical stirrer
- Static mixers
- Rotor stators
- Microfluidic

and then two processes for the preparation of nanoemulsions:

- High Pressure Homogenizers
- Ultrasounds

**Mechanical stirrer** Mechanical stirring is the easiest and more classical way of mixing two fluids. Stirrers can be of different geometries and size and have to be chosen according to the application, scale, targeted size of the emulsions and fluids viscosity. The blade geometry and type (propeller, shaft, dispersion blades...) and the size of the tank have an impact on resulting droplet size. The droplet size reached is typically between dozen to hundred of microns so it can be used as a pre-emulsification process before nanoemulsion production.

The advantages of this process are that it requires low energy and it is very easy to perform. However it can only work in batches and create polydispersed emulsions with large droplets.

**Static mixers** Static mixers are continuous processes with the purpose of mixing fluids in a continuous way [32]. They are called static because they are motionless. The device is fixed and the fluid motion creates the shear stress leading to droplet size reduction.

In the plate type design, mixing is accomplished through intense turbulence and in the flow and housed-elements design, flow can be either laminar or turbulent. The resulting droplet size of the emulsions depends on the mixer geometry and dimensions, the velocity of the fluid and the emulsion properties such as viscosity, interfacial tension... This type of device creates emulsions with droplet size between 10 and 100  $\mu\text{m}$  and can be used to create pre-emulsions prior to nanoemulsions production.

The advantages are that they are cheap, they do not consume much energy, are resistant and work continuously. However, nanosize is not achievable with this process.

**Rotor stator systems** The rotor stator system is commonly used. It is composed of an immobile part, the stator with orifices or slits and a rotor rotating at high speed (Figure 1.14). This creates a vacuum and the emulsion is sucked into the head of the device, it is then expelled after going through the rotor and stator orifices. The emulsion undergoes a high shear stress by going through the gap between the rotor and the stator, this reduces the droplet size of the emulsion.

The parameters that influence droplet size and size distribution are for the process : the gap size between the rotor and stator, the speed of the rotor and the processing time. Different head geometries exist that should be chosen depending on the composition, volume of the emulsion and targeted droplet size [33]. Concerning the composition, the parameters of influence are : phase viscosities, volumes ratio of both phases and interfacial tension.

The advantages of this process are that size reduction is more effective than with mechanical stirrer or static mixers and it can be used at industrial scale (batch or continuous). The mean droplet size of the emulsion is often in a few micron range, a small part of the distribution can be of nano-range size. However if the targeted emulsion is a nanoemulsion, the rotor stator process can be the first step before homogenization.

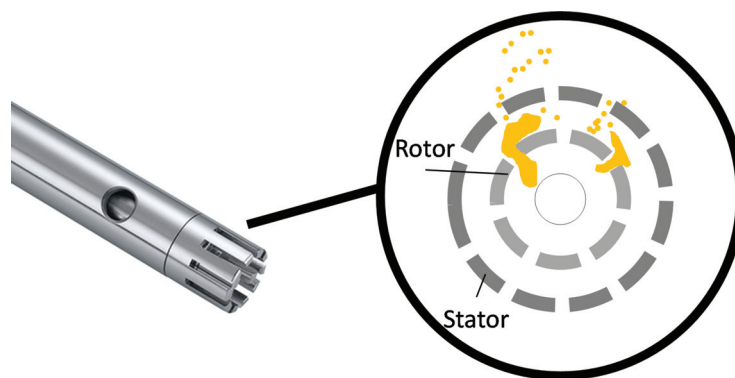


Figure 1.14: Principle of rotor stator systems

**Microfluidic** Microfluidics has emerged as a versatile tool for emulsification for less than 15 years. The definition of microfluidics is manipulating fluids with a dimension in the micrometer range. The principal characteristic is that laminar flows in micrometer capillaries are put in contact in order to produce emulsions (Figure 1.15) [34]. Three different types of geometry are used in microfluidics in order to produce droplets [35]. Co-flowing, where both phases flow in the same direction and detachment is obtained mainly by interfacial tension. Cross-flowing, for example in a T-junction, where phases flow perpendicular to each other and a higher shear stress is applied at the interface. The last geometry is flow focusing where the channel is narrowed to help forming the emulsion. The geometry represented in Figure 1.15 is considered as a specific case of a cross-flowing device.

Double or multiple emulsions can also be produced by this technique. Also spontaneous emulsification can be coupled with microfluidics for a very good control of the addition of the different phases to obtain a better monodispersity.

The main advantage of microfluidic devices is that the emulsions produced have very homogeneous droplet size. The droplet size can be tailored with the capillaries size and flowrate. However, the fact that emulsion is produced drop by drop makes this technique difficult to industrialize, even if many chips are put in parallel, the overall flowrate of production is still low. Furthermore, the droplets size depends on the capillary diameter. As nano-capillaries are not available, it is not possible to produce nanoemulsions with this technique.

**High pressure homogenizer (HPH)** The more classical type of HPH is called T-junction (Figure 1.16). A pre-emulsion is pushed at high pressure (between 200 and 2500 bars) to an impact ring perpendicular to the flow generating an emulsion with smaller droplets. The dispersion unit

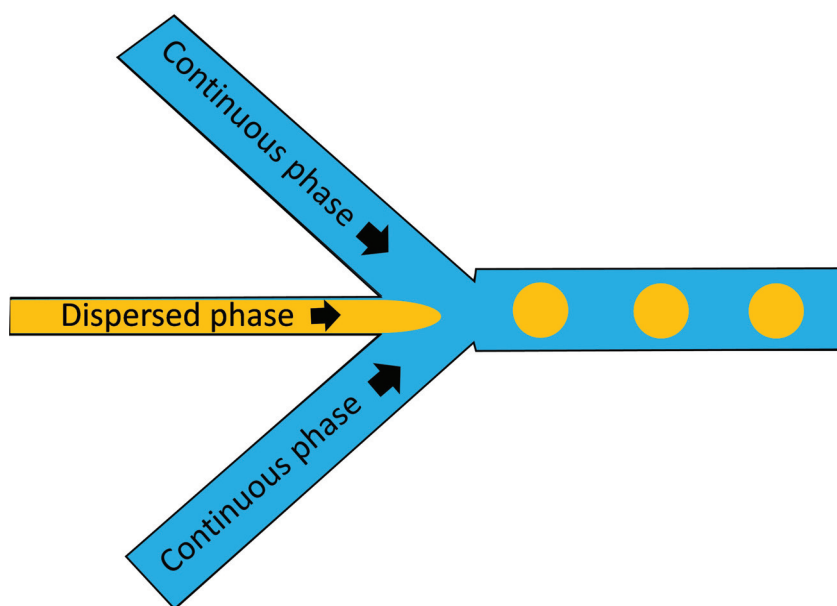


Figure 1.15: Schematic representation of a microfluidic device

is made up of a valve, valve seat and impact ring. The parameters that have an influence on the final emulsion are pressure, number of passes and formulation [36, 37].

The three main phenomena that participate to size reduction in this process are:

- Shear rate: Velocity difference between velocity close to zero at the wall and maximum velocity which is very high at the center creates an important shear rate
- Impact: The geometry is designed to create an impact zone, the emulsion is projected at high speed on a wall perpendicular to the flow creating droplet disruption.
- Cavitation: At the outlet of the device, a sudden relaxation causes a cavitation phenomenon causing the bursting of the droplets by the implosion of gas microbubbles.

The advantages of this process are that all kind of formulations can be reduced in droplet size, even viscous or concentrated and no specific composition is required. The droplet size reached, if the interfacial tension is low enough, is often around 200 nm or less. However, several passes are required to obtain a monodispersed emulsion, the droplet size depends on the composition and cannot be predicted. The energy consumption is also very high and there is a lot of energy loss in heat which can be an issue for sensitive actives. Moreover some recoalescence can happen leading to polydispersed droplet size distribution [38]. In a technical point of view, these apparatus often present clogging issues.

**Microfluidizer** A microfluidizer is a type of HPH sold by Microfluidics<sup>TM</sup>. The main difference compared to classical HPH is that the interaction chamber has a fixed geometry for the microfluidizer device [39]. In this process a very strongly compressed pre-emulsion is forced at very high speed through a tube of small size (Figure 1.17). The pre-emulsion is filled in the inlet reservoir. An intensifier pump compress the fluid up to 2000 bars creating a high velocity in the tube of the interaction chamber. Then the emulsion is collected in the outlet reservoir.

The interaction chamber has a fixed geometry but can be changed according to the application. It can be either a "Z" form as shown on Figure 1.15 or a "Y" form. Different dimensions are available according to the application and droplet size targeted, small internal dimensions creating higher shear stress. Compared to HPH, the same phenomena take place to reduce droplet size and the advantages and drawbacks are the same.

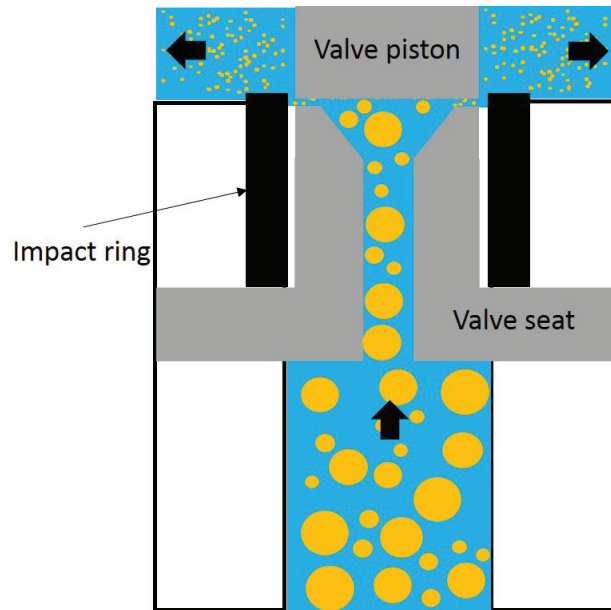


Figure 1.16: Schematic representation of a high pressure homogenizer

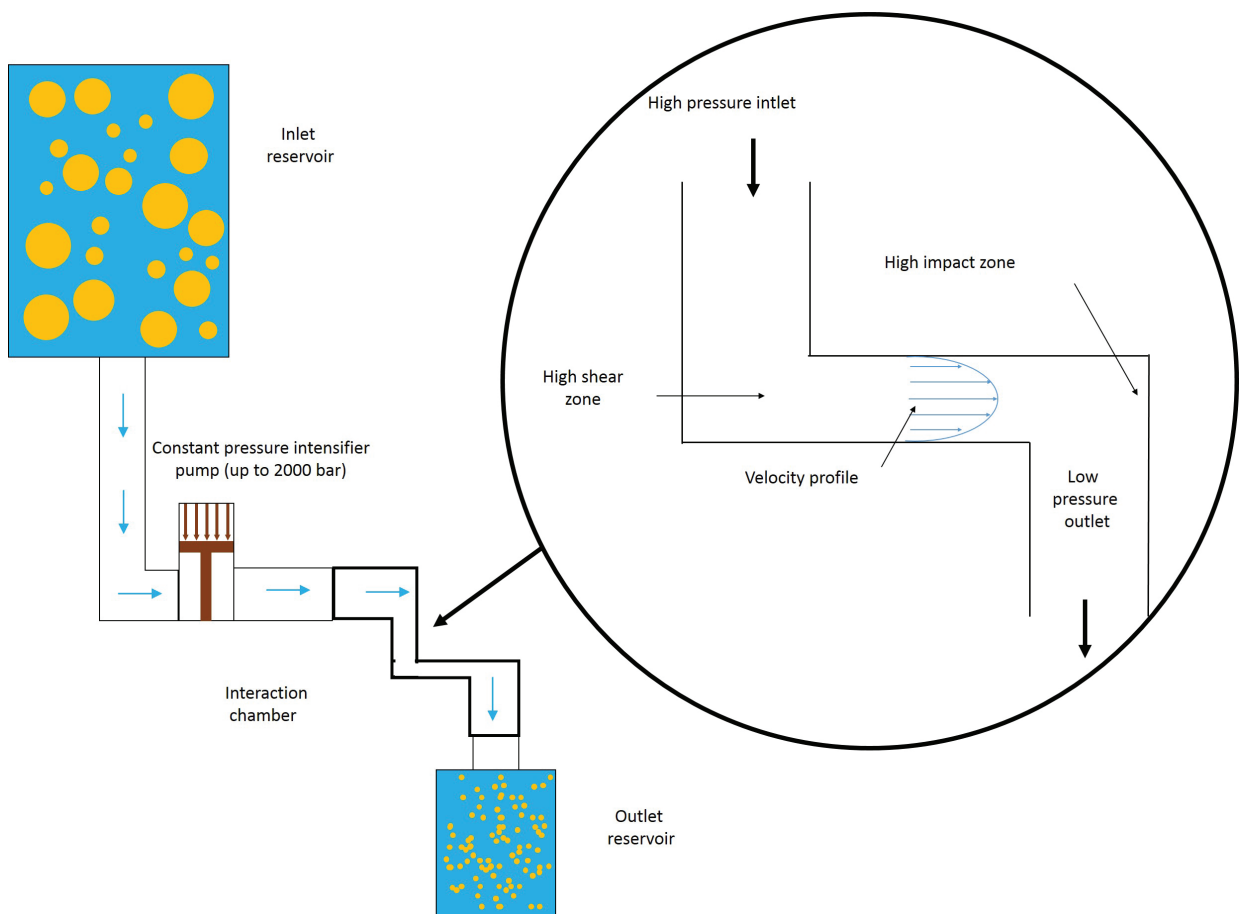


Figure 1.17: Schematic representation of a microfluidizer and principle of the interaction chamber

**Ultrasounds** Ultrasounds are waves with frequencies between 16 kHz and 1 MHz. Ultrasounds are applied to two separate phases or to coarse emulsions in order to produce an emulsion or reduce droplet size of the emulsion.

Ultrasound waves are propagating into the liquid medium creating cavitation bubbles which undergo dilatation and contraction. When the frequency is high there is a lot of dilatation ending with bubbles implosion disrupting the droplets close to them. The waves also create instabilities at the oil-water interface. However the first phenomenon seems to be predominant in ultrasound emulsification [31].

Emulsions produced with this method are very fine, around 100 nm droplets size depending on the process duration, process power, temperature, phase viscosities, phase volume ratio and interfacial tension. However, they are also often polydispersed and a lot of energy is required leading to a lot of energy loss in heat [40]. Moreover only small batches can be produced with this technique which is not scalable for industrial applications.

**Advantages and drawbacks of nanoemulsification processes** Nanoemulsions processes, their principle, advantages and drawbacks are summed up in Table 1.2.

Table 1.2: Summary of advantages and disadvantages of processes for nanoemulsions production

Process	Principle	Advantages	Disadvantages	References
HPH	Shear, impact and cavitation	Flexible on composition Low process time	High cost High energy consumption Not recommended for sensitive compounds	[37, 39, 41, 42]
Ultrasounds	Cavitation mechanism	Flexible on composition	Small batches Not recommended for thermosensitive compounds	[41, 42]
PIC	Changing of the interfacial film curvature	Low cost Easy to scale up Low energy consumption	Limitation on composition Long process time	[41, 42, 25]
PIT	Changing of the interfacial film curvature	Low cost Easy to scale up Low energy consumption	Limitation on composition Heating	[41, 42, 25]
Nano-precipitation	Solvent displacement	Low cost Easy to scale up Low energy consumption	Limitation on composition Limited amount of oil phase Presence of solvent	[41, 42, 25]

The main advantage of low energy processes is their low energy consumption which means that they are less expensive, smoother for the component and more sustainable. However, the formulation is very specific and has to be optimized for each applications. Also the use of certain solvent can be an issue if some residues are found in pharmaceutical or food products for example. Moreover, the droplet size and size distribution are difficult to control and to predict, with no tunability.

The main advantage of high energy processes is that they can be adapted to nearly every composition. However, they use a high amount of energy, which can be a problem in term of energy

consumption or for sensitive actives.

On Figure 1.18, the energy consumption (rough estimation) as a function of droplet size for high energy processes is represented. We see first that every process works in a narrow droplet size range. No process presented here can work for droplet size between nanometers and hundreds of microns. More importantly no process allows a precise size control for a specific application, except microfluidics but in very short range of droplet size and not at industrial scale.

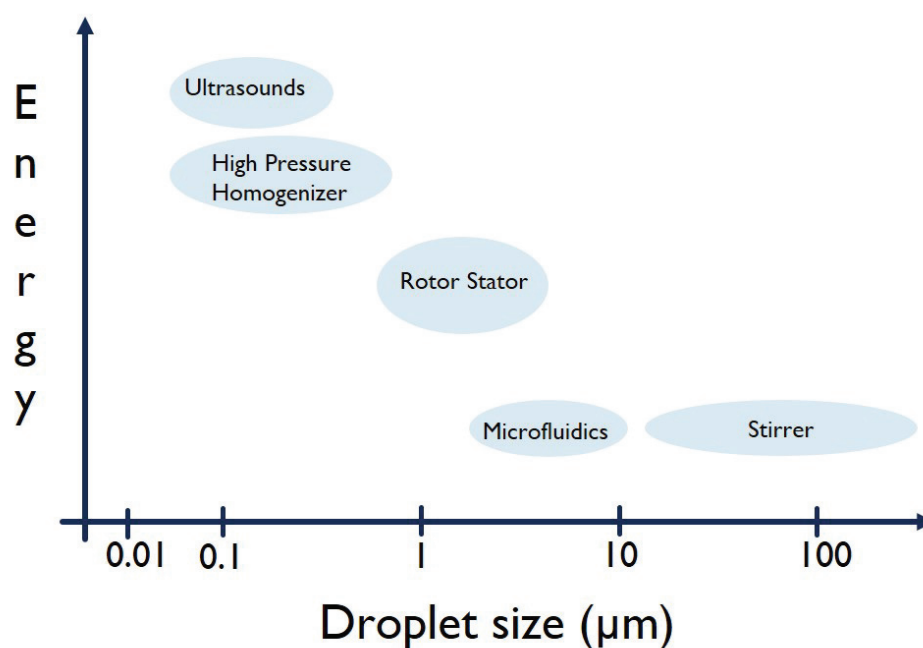


Figure 1.18: Energy consumption with droplet size range for high energy processes

### 1.1.4 Some applications of nanoemulsions

Nanoemulsions have known increasing interest for more than 20 years (Figure 1.19) for different applications, mainly in cosmetics and pharmaceutical industries.

#### 1.1.4.1 Skin applications

Skin is the largest human organ with a surface close to 2 m<sup>2</sup>. It has several functions such as protection from the external environment (UV radiation, dryness, physical, chemical and microbiological damages) and maintenance of body temperature.

It is mainly composed of two layers, the epidermis and the dermis (Figure 1.20). The epidermis is composed of several lipids and divided into several layers and its outermost layer, the stratum corneum, is responsible for the barrier function of the skin due to its lipophilicity. The dermis, on the contrary is hydrophilic and is the layer next to the subcutaneous tissue.

It is also worth mentioning that physical changes occur through the skin layer. The two main examples are temperature and pH. The temperature of the skin is at around 32 °C but increases after passing the layers to reach body temperature in the dermis layer at around 37 °C.

Similarly, the pH of the skin varies from its surface into deeper layers. pH of healthy skin is slightly acidic to fight against microbial contamination and is comprised between 4.5 < pH < 5.5. However, the intercellular pH after passing the stratum corneum is around 6.2-6.5. Then, pH reaches its physiological value (pH 7.4) in the deeper layer of the epidermis before reaching the dermis layer.

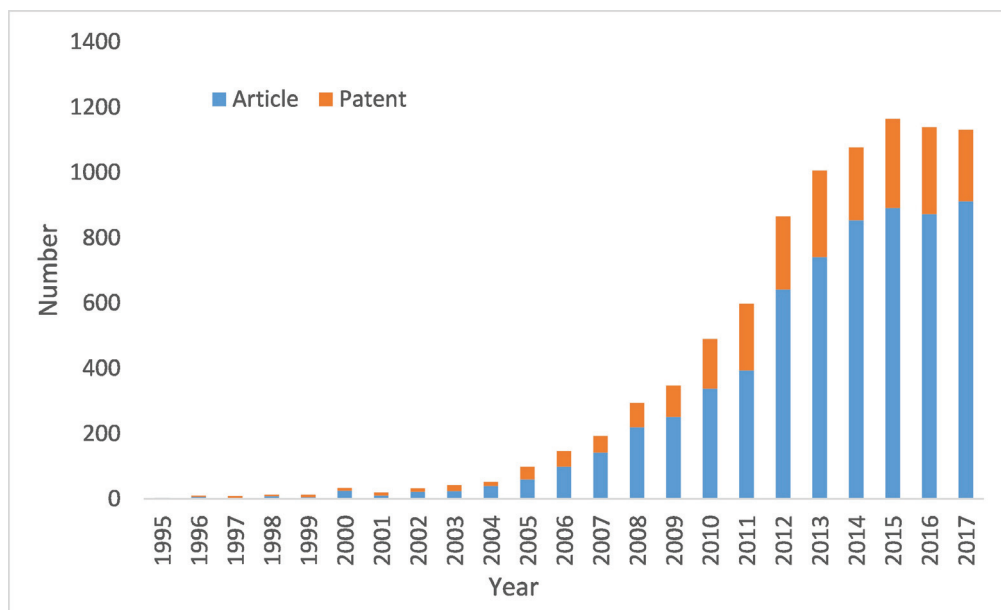


Figure 1.19: Patents and publications containing the word or concept "nanoemulsion" from Scifinder

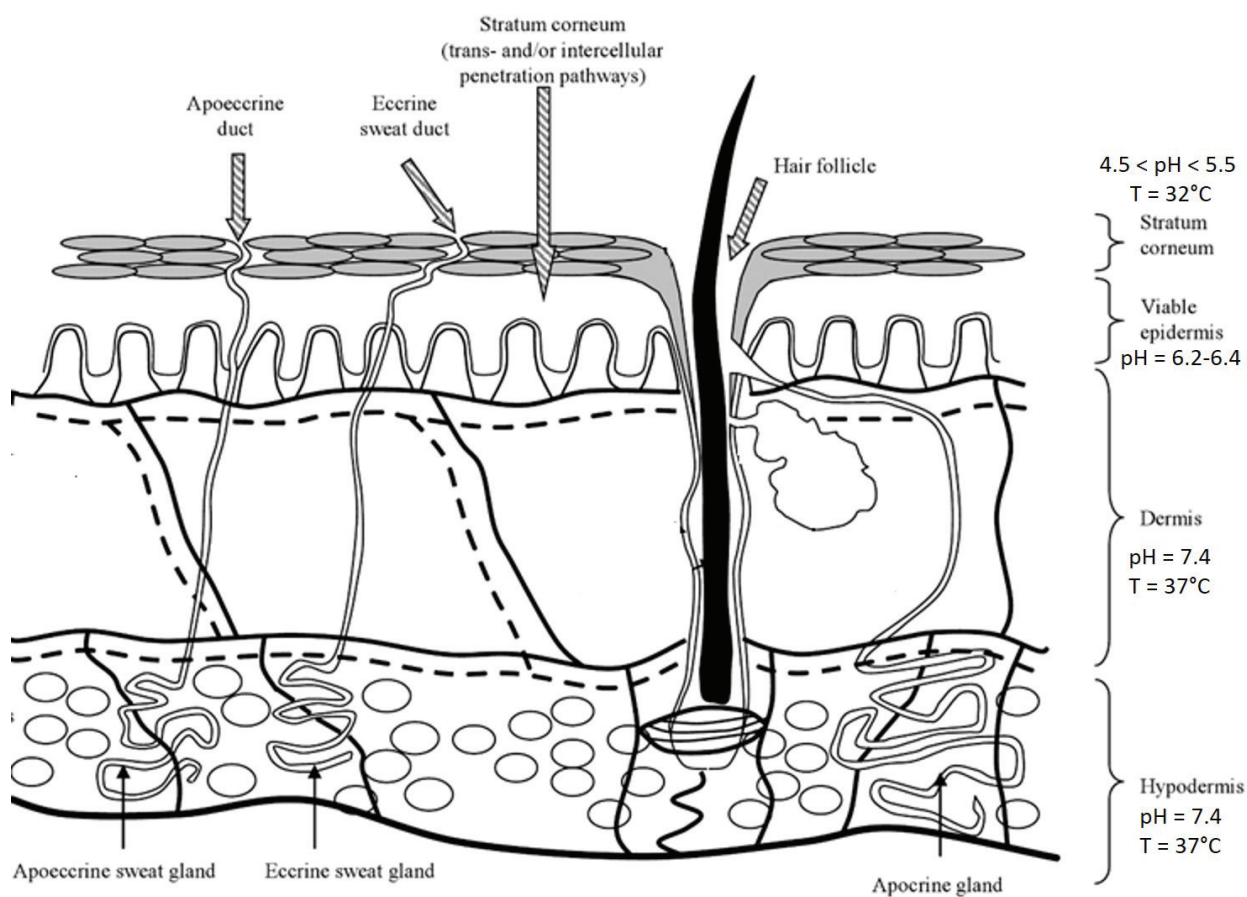


Figure 1.20: Schematic overview of the skin layers and pH and temperature variation adapted from Jepps et al. [43]

**Cosmetics** A cosmetic product is defined by the EU Cosmetics Regulation as:

*A "cosmetic product" shall mean any substance or mixture intended to be placed in contact with the various external parts of the human body (epidermis, hair system, nails, lips and external genital organs) or with the teeth and the mucous membranes of the oral cavity with a view exclusively or mainly to cleaning them, perfuming them, changing their appearance and/or correcting body odours and/or protecting them or keeping them in good condition.*

This means that cosmetics products for skin applications should have only an action on the upper part of the skin, the epidermis and mainly the stratum corneum. The formulations in skin care are mainly creams but than can be of other types also such as micellar solutions, oils, or gels.

Nanoemulsions, thanks to their droplet size, have several advantages for the cosmetic industry [44] :

- A high stability
- Uniform deposition on the skin with large surface area
- Modified release and active carrier properties,
- Better occlusiveness with film formation on the skin
- Unique texture : pleasant aesthetic character and skin feel
- Nanoemulsions are also the first step of numerous encapsulation techniques in order to create nanocolloids such as nanocapsules or nanospheres.

Moreover, some studies also report the advantages of nanoemulsions compared to liposomes as they are more stable, enabling even the formation of a lamellar liquid-crystalline phase around the droplets in some cases [28].

All types of actives can be encapsulated in O/W or W/O nanoemulsions or double nanoemulsions for all skin conditions, sensitive, damaged, irritated, dried and sunscreens.

**Dermatology** Dermatological products, on the contrary are formulated to treat a specific disease. They can be active on the upper layer of the skin but also deeper in the skin layers as the first layer is only composed of dead cells. An other topical route of administration is transdermal application where the active ingredient is administered onto the skin but is absorbed into the body to reach systemic distribution. In both cases, formulation may require nanosize droplets to reach their targeted site of administration. Moreover, nanoemulsions with their amphiphilic character can cross both hydrophilic and hydrophobic skin layers. Properties of interest are the same as for cosmetics, but with an other additional characteristic that is enhanced penetration thanks to large surface area and small droplet size [28].

#### 1.1.4.2 Injection applications

Some drugs are characterized by low aqueous solubility or propensity to be hydrolysed and are a real challenge during formulation. The use of an O/W emulsion can reduce or completely circumvent these risks. The drug is incorporated in the oily dispersed phase and is thus in a medium where its chemical and therapeutic integrity are preserved. These systems present a better therapeutic profile than the drug alone in an aqueous medium. Another advantage of parental emulsions is the potential to create a prolonged release of the active ingredient.

However, strict requirements for droplet size and surface charge are to be considered when formulating. The common feature of all injectable emulsions is the strict size of the droplets as it is directly related to toxicity and stability. Emulsions containing droplets ranging in size from 0.5 to 1.0  $\mu\text{m}$  are used more rapidly by the body than emulsions of size 3 - 5  $\mu\text{m}$ . Droplets wider than 4 - 6  $\mu\text{m}$  can increase the risk of embolism and can cause remarkable changes in blood pressure.

Although the debate about particle size persists, the formulator must minimize the size of the droplets and control the size distribution in the final forms to be administered. In general, the smallest droplets (usually between 100 and 500 nm) are the most stable.

For parenteral nanoemulsions authorized additives are on a very short list and all oils, surfactants or other additives have to be authorized by EMA (European Medicines Agency) or FDA (Food and Drug Administration) to be used. Most of the authorized oils are vegetable oils (see Table 1.3) or extracted from them such as long-chain triglycerides (LCT) and medium-chains triglycerides (MCT) which are the only oils with long-term commercial acceptability in parenteral emulsions and are found in several FDA approved products. MCT have usually better solubilizing capacities than LCT.

Excipient	Range
<i>General oils</i>	
Soybean oil	10–20% w/w
Safflower oil	10–20% w/w
Sesame oil	20–20%
Corn oil	10–20% w/w
Castor oil	20% w/w
Castor oil: soybean oil (1:1)	Up to 30%
Castor oil: MCT (1:1)	Up to 30%
Coconut oil	30%
<i>MCTs</i>	
MCT/LCT mixture	10–20% w/w Up to 30%
<i>Altered fatty acid patterns</i>	
Triolein	50%
Iodized ester of poppy seed oil	10% w/w
Purified fish oil	10% w/w
Ethyl oleate	Not available
Squalane	10%

Table 1.3: Examples of commonly used oils for parenteral emulsions and recommended concentrations from A.G. Floyd [45]

Parenteral emulsions also contain natural or synthetic surfactants. The most used natural emulsifier is lecithin. Natural lecithin is a phosphatide found in all living organisms and is either of animal origin (egg yolk) or vegetable (soya) origin. The synthetic emulsifiers of choice for parenteral emulsions are poloxamers, a triblock of PEG-POP-PEG with a wide range of HLB according to chain length and ratio.

Usually, the incorporation of osmotic agents, antioxidants, buffers and preservatives is necessary. For this, the isotonic adjustment (280 - 300 mOsm Kg<sup>-1</sup>) is important for parenteral emulsions. Glycerol or sorbitol are often used. Also, antimicrobial agents should be added to the aqueous phase as it is sensitive to contamination. The pH is adjusted using a small amount of NaOH as the optimum pH of a final emulsion is usually 6-7. Most of the classical buffers can not be used in parenteral administration.

### 1.1.5 Conclusion

Nanoemulsions are biphasic systems of nanometric size. One phase is dispersed into the other forming nanometric droplets. These systems find a lot of applications in different fields mainly because of the increased stability but also other characteristics that depend on the application.

In order to produce stable nanoemulsions which are thermodynamically unstable by nature, both formulation and process have to be optimized. The aim of adjusting formulation is first to decrease the interfacial tension between oil and water. For this purpose, the addition of an emulsifier to the system is required. This emulsifier can be either a surfactant (an amphiphilic molecule with different charges), a copolymer with blocks of different hydrophilicity or particles.

Copolymers are gaining interest because even if they are less effective than some surfactants, they are less irritant which is better for cosmetic or pharmaceutical applications. Also they can be composed of synthetic peptides blocks in order to mimic protein natural surfactants and have a great biocompatibility.

In order to produce emulsions the most used devices are mechanical stirrer and rotor-stator system. However, these techniques do not allow to obtain nanodroplets. To produce nanodroplets, two types of processes can be used: low energy and high energy processes. All these processes present advantages and drawbacks presented in table 1.2, among these processes, the most used at industrial scale is HPH systems.

The HPH process drawbacks are that it is expensive, consumes a lot of energy (with a lot of heat loss) and is not recommended for sensitive compounds. Moreover, the size range achievable with this technique, even by modifying the pressure, is very narrow, a few hundred of nanometers and depends on the composition. It is not possible to achieve a specific droplet size by modifying process parameters.

An other type of process, called membrane emulsification, overcomes these drawbacks and require low energy consumption, low cost and allow droplet size control. However, it is difficult to produce nanoemulsions with this process. Only some studies have succeeded in doing so and only at small scale.

In the following section, the main principles and applications of membrane emulsification are presented.

## 1.2 Membrane emulsification

As presented in the previous part, emulsions are usually prepared using high-pressure homogenizers, ultrasounds and rotor/stator systems. In the dispersing zone of these machines high shear stresses are applied to deform and disrupt large droplets creating a temperature increase. Therefore, temperature or shear-sensitive ingredients such as proteins or starches may lose functional properties.

On the other hand, this kind of processes usually suffers from a lack of precision in droplet size control and results in droplet polydispersity. The production of monodispersed emulsions has been investigated by several new techniques such as microfluidic devices. Scaling up to industrial volumes is a major limitation of these processes. Unlike these methods, membrane emulsification has the potential for scaling up while producing droplets of well-defined size.

Membrane emulsification has received increasing attention over the last 30 years as an alternative to other methods of emulsification. Different types of emulsification, membranes and set-ups have been developed in order to produce several types of formulation, each of them having their own advantages and drawbacks.

### 1.2.1 Type of emulsification

#### 1.2.1.1 Membranes to generate emulsions

When membranes are used to generate emulsions, the technique is called direct membrane emulsification (DME). In DME, a dispersed phase is injected through membrane pores in a continuous phase (Figure 1.21). Both phases are immiscible so droplets form at the interface of both liquids and the membrane. Droplets grow at pore openings until they detach when having reached a certain size. Emulsifier molecules in the continuous phase stabilize the newly formed interface immediately after formation in order to prevent droplet coalescence. The resulting droplet size is controlled primarily by the choice of the membrane which allows a precise size control. Usually a shear stress is applied on the membrane surface in order to facilitate the detachment of the droplets.

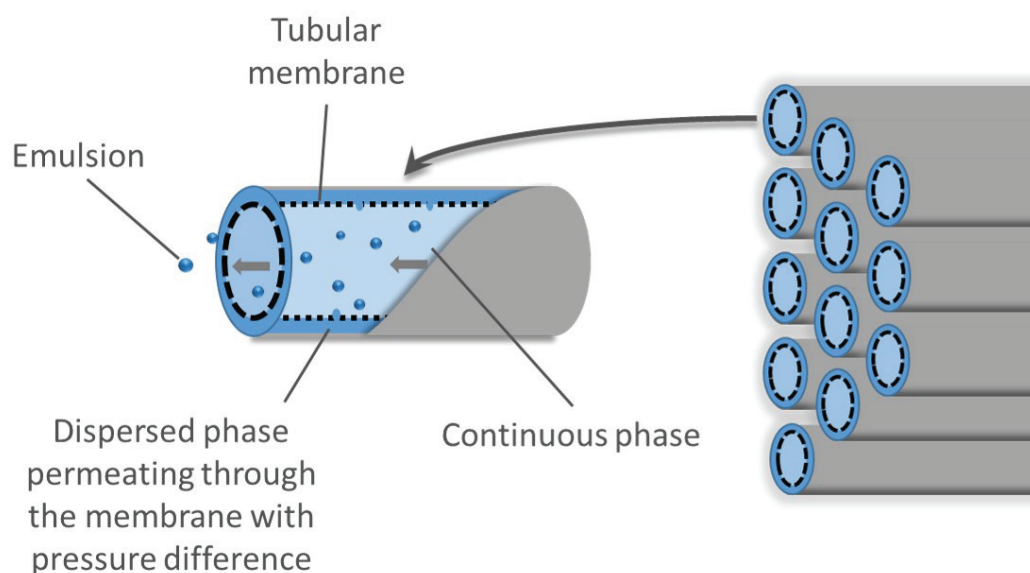


Figure 1.21: Schematic figure of direct membrane process principle

This technique can be used to form O/W, W/O, bubbles, double emulsions or can be the first step to form solid particles (Figure 1.22). It can also be coupled with spontaneous emulsifica-

tion or microemulsification techniques, this process is called membrane micromixing. In membrane micromixing, two phases one containing the oil and a water miscible solvent and water are put in contact through the injection of the first phase through the membrane pores into the second. When in contact, a solvent displacement occurs creating nanoemulsions, liposomes or microemulsions. The membrane is then not aimed at emulsifying but at controlling the addition of one phase into an other.

As the interface between the two liquids and the membrane is of great importance in DME the affinity of the membrane with both phases should be considered according to the formulation desired. O/W emulsions require hydrophilic membranes, so the oil having no affinity with the membrane can be pushed out of the pores to create the emulsions. W/O emulsions require hydrophobic membranes for the same reason.

Advantages of DME is that the emulsion is generated at low shear stress and low pressure without the requirement of an other process. The droplet size is controlled by the pore size and monodispersed droplets are created. Moreover, this process is easy to scale up by increasing membrane surface. Drawbacks are that the flux through the pores is extremely low, especially in the case of very small droplets and that membrane fouling can occur. Moreover, droplets size is 3-10 times larger than the pore size depending on composition and shear stress, which can be an issue to obtain very small droplets.

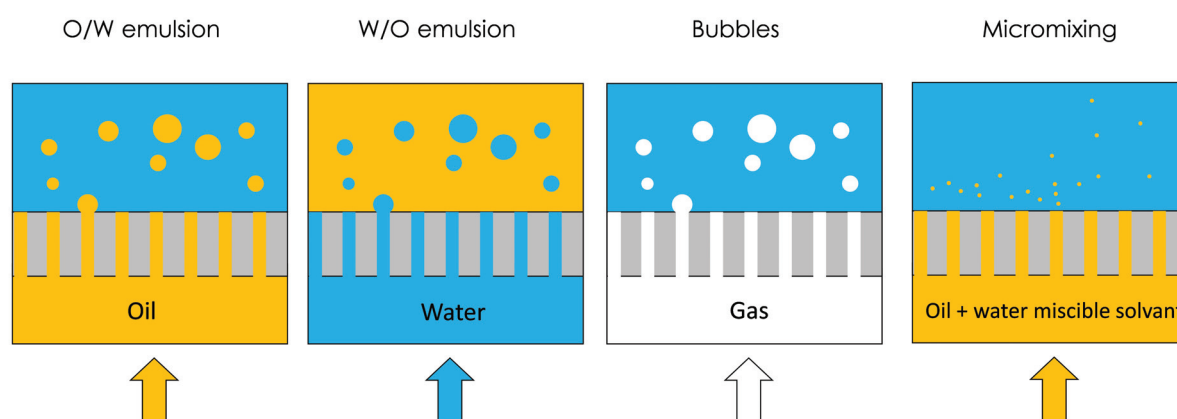


Figure 1.22: Different type of formulation that can be produced with DME

### 1.2.1.2 Membranes to modify emulsions

Membranes are also used to modify emulsions. In this process, a coarse emulsion is passed through the membrane pores in order to reduce the droplets sizes, change the emulsion sense or demulsify it (Figure 1.23). The most studied technique consists in reducing the size and homogenizing the emulsion and is called premix membrane emulsification (PME). In PME, a process to create the premix emulsion is first required. This coarse emulsion is usually obtained by magnetic stirrer or rotor stator systems but it can be prepared with any processes.

The chemical composition of the membrane has an important impact in this process. For PME, a membrane with affinity for the continuous phase should be used, hydrophilic for O/W emulsions and hydrophobic for W/O emulsions. If a membrane with affinity for the dispersed phase is used, two phenomenon can occurred depending of the concentration and the procedure used, phase inversion or demulsification.

Advantages of PME are the same as other membrane emulsification techniques: the emulsion is generated at low shear stress, the droplet size is controlled by the pore size and monodispersed

droplets are created and the process is easy to scale up by increasing the membrane surface. Additional advantages are that flux through the pores can be much higher than in DME and if the flux is high enough no fouling occurs. Drawbacks are that an additional step of premix emulsification is required and that a higher pressure than in DME is usually necessary depending of the pore size and composition.

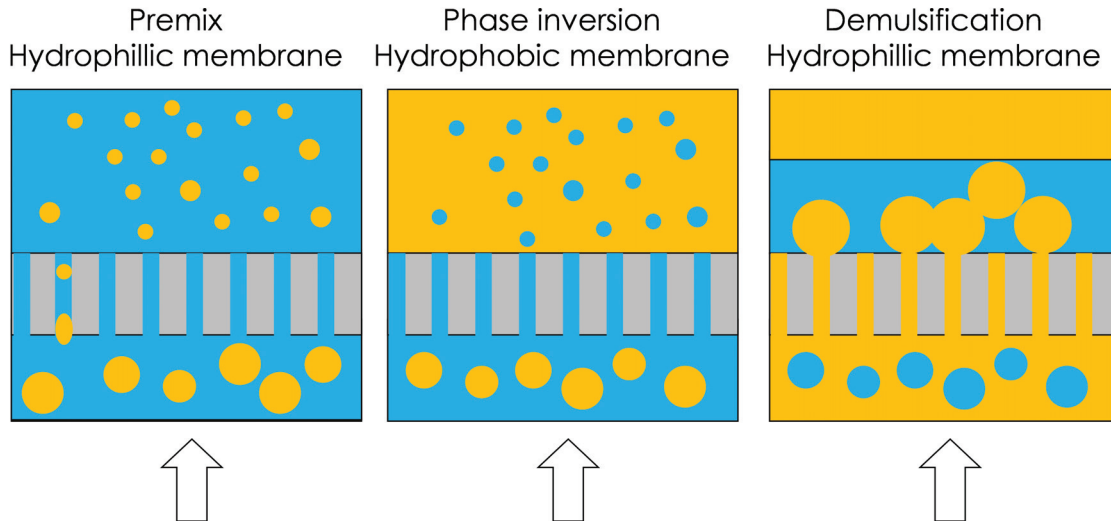


Figure 1.23: Different types of utilization of PME

## 1.2.2 Set-ups for membrane emulsification

### 1.2.2.1 Membrane types

A membrane is a selective barrier and the classical membrane uses are filtration processes (microfiltration, ultrafiltration, reverse osmosis...) requiring different types of membranes for each application. Only the most commonly used membranes for emulsification are presented here. Membranes used for emulsification should have certain properties: uniform pores, different pore sizes available, high mechanical strength and depending on the application resistance to temperature or organic solvent, possibility to modify the surface to change hydrophilicity or charge for example.

**Shirasu porous glass (SPG) membranes** SPG membrane is the most used type of membrane for emulsification. It is a glass composed mainly of  $SiO_2$  and  $Al_2O_3$  which is obtained by reaction of Shirasu (volcanic ash), boric acid and limestone. After several heat treatments, additives and acid leaching, the final membrane is produced. Final pore size depends, for the same composition, on the heating time and temperature. A large range of mean pore size is achievable by this process: from 40 nm to 40  $\mu m$ . The main properties of the SPG membranes available commercially are reported on Table 1.4. SPG membranes are available in tubes or flat discs. They are resistant to pressure and chemicals. As can be seen on Figure 1.24, the pores are cylindrical, tortuous and interconnected which is the specificity of SPG membranes.

SPG membranes are hydrophilic by nature, however they can be easily hydrophobized. Two main types of hydrophobization process are usually used: a physical coating with silicone resin [47] or a chemical reaction with organosilane [51].

A new type of asymmetric SPG membrane has been also investigated to increase flowrate through the membrane [52]. The authors proved that it allows to increase the flowrate 20 times without any change in droplet size distribution. However this membrane is more difficult to produce and not available commercially.

Shape	Tubes or flat discs
Thickness ( $\delta_m$ )	0.4–1 mm
Compressive strength	200–280 MPa
Pore diameter ( $d_p$ )	0.04–40 $\mu\text{m}$
Porosity ( $\varepsilon$ )	50–60%
True density	2000–2500 $\text{kg m}^{-3}$
Zeta potential at pH = 3–10 and $C_{\text{NaCl}} = 1\text{--}100 \text{ mol m}^{-3}$	–15 to –45 mV
Pore tortuosity ( $\xi$ )	1.25–1.4
Number of pores per unit cross-sectional area ( $N/A_m$ )	$10^9\text{--}10^{14} \text{ m}^{-2}$
Specific pore volume ( $V_p/m_m$ )	$0.5\text{--}0.6 \text{ dm}^3 \text{ kg}^{-1}$
Hydraulic resistance ( $R_{m,\text{sym}}$ )	$10^8\text{--}10^{12} \text{ m}^{-1}$

Table 1.4: Properties of commercial SPG membranes from Vladisavljević et al. [46] with data from [47, 48, 49, 50]

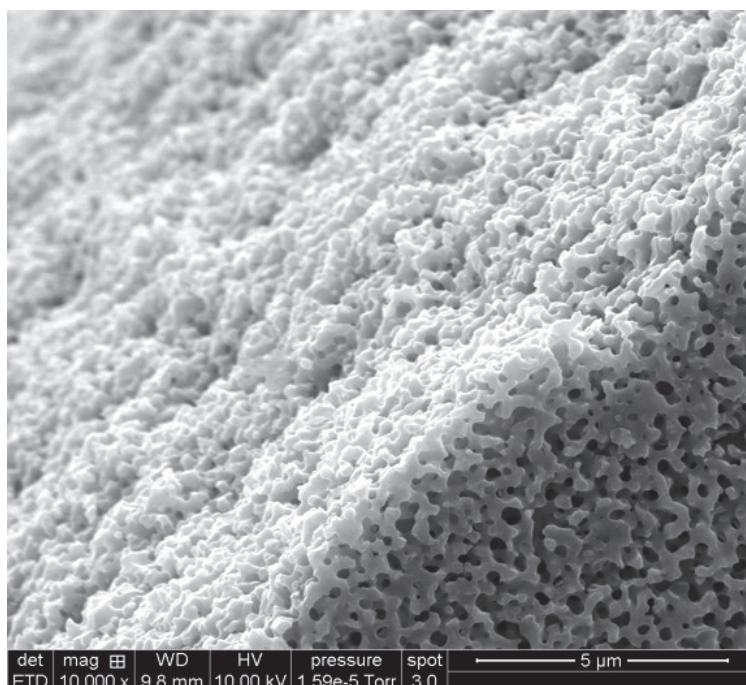


Figure 1.24: SEM photograph of a SPG membrane with 200 nm pore size

Advantages of SPG membranes are that a wide range of pore size is available as well as small modules for laboratory scale, they have a high porosity and are cheap. Disadvantages are mainly due to their tortuosity creating fouling and fragility but also decreasing the number of available pores for emulsification making it difficult to characterize exactly.

**Polymeric membranes** Polymeric membranes are traditionally used for liposomes extrusion or filtration at lab scale. Many different kinds of polymers can be chosen for this purpose depending of the chemical affinities between the membrane and the liquids: polycarbonate, polyether-sulfone, polypropylene, nylon, polyester, cellulose acetate. . .

All these membranes have their own properties. Bunjes et al. [53] investigated seven different polymeric membrane types by scanning electron microscopy (SEM), atomic force microscopy (AFM), and mercury porosimetry. Each polymeric membrane presents a specific geometry (poros-

ity, tortuosity, pore spacing...) as it can be seen on SEM and AFM images (Figure 1.25). For example, the polyester membrane is a track-etched membrane with highly defined straight-through pores and on the contrary nylon and cellulose acetate (CA) membranes are branched membranes. Thickness is also very different from one polymeric membrane to an other varying from 10 to 180  $\mu\text{m}$ .

It is hard to conclude on general advantages or disadvantages as this family of membranes is very diverse. Nonetheless, one advantage is that they are usually cheap and a lot of different chemical compositions are available for each application. The disadvantages are that they are quite fragile and not all of them are very effective for membrane emulsification.

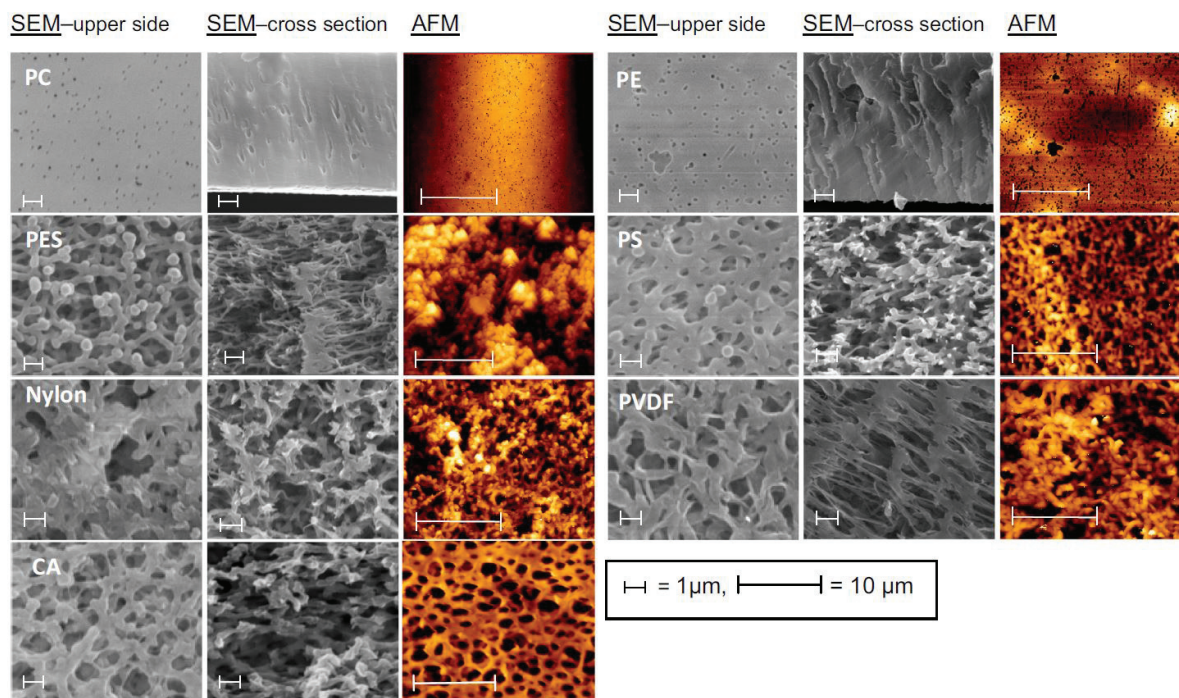


Figure 1.25: SEM and AFM photographs of seven different types of polymeric membranes [53] PC: polycarbonate; PES: polyethersulfone; CA: cellulose acetate; PE: polyester; PS: polysulfone; PVDF: polyvinylidene fluoride

**Metallic membranes** Metallic membranes are usually micro-engineered membranes with controlled pore geometry and pore spacing (Figure 1.26). The aim is to avoid fouling and to achieve high transmembrane flux by lowering membrane hydraulic resistance. At the same time, it lowers drastically the pores surface area for the same membrane area which can lead to lower flow rate than for SPG membranes [46]. Typical metallic membranes are made from nickel or stainless steel.

Advantages are that pores with controlled size produce more monodispersed droplets, they are resistant, there is less fouling as the pores are not tortuous. Disadvantages are that they are produced by technologies that are still expensive. The number of pores per membrane area is low so lower flowrates for the same membrane surface are obtained. Only few pore sizes are available and all in the micron range. Also chemical modification is not as easy as it is for SPG membranes.

**Silicon nitride micro-engineered membranes** An other type of micro-engineered membrane is also used: silicon nitride micro-engineered membranes (Figure 1.27) [55]. They are usu-

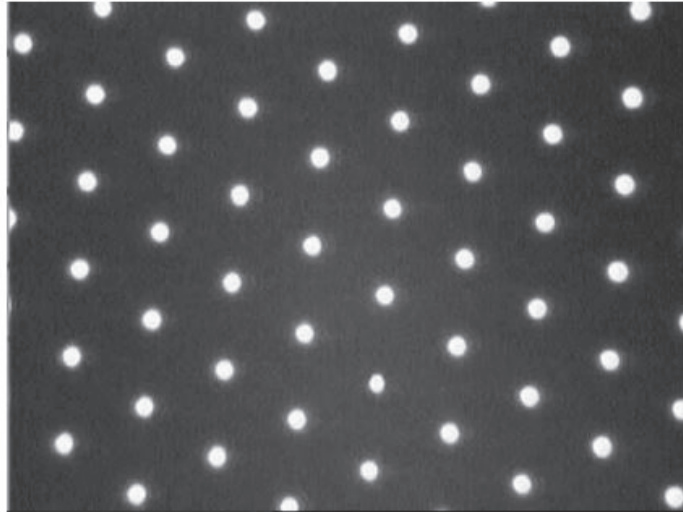


Figure 1.26: Optical microscopy photography of a 30  $\mu\text{m}$  regular pore size micro-engineered metallic membrane (Micropore Technologies Ltd)[54]

ally made with photolithographic techniques and treated with air plasma to obtain a hydrophilic surface.

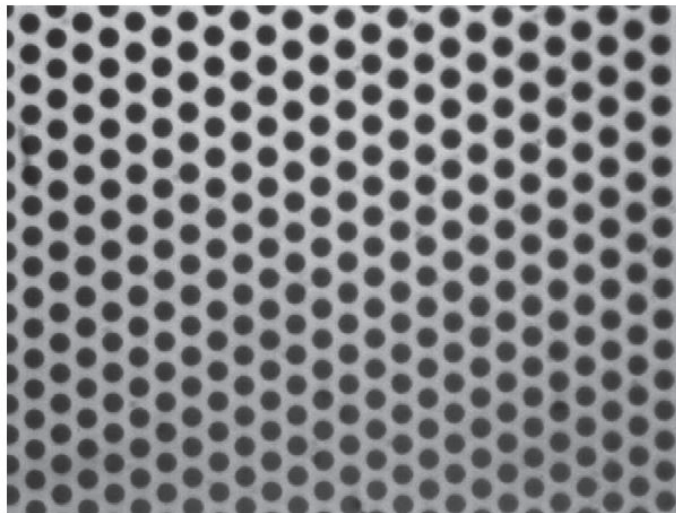


Figure 1.27: Optical microscopy photography of a silicon micro-engineered membrane with an uniform 5  $\mu\text{m}$  pore size and a porosity of 30% [55]

Their advantages and drawbacks are the same as the ones presented for micro-engineered metallic membranes.

**Ceramic membranes** Tubular ceramic membranes are typically used for ultrafiltration and microfiltration. They are composed of two layers; a thin filtration layer with a thickness of 20-30  $\mu\text{m}$  and pore size from 0.1 to 10  $\mu\text{m}$  for microfiltration and 2-50 nm for ultrafiltration, deposited on a macroporous layer with a thickness of some hundreds of microns.

These traditional ceramic membranes are less used than SPG membranes for emulsification may be because they produce more polydispersed emulsions in the same conditions as SPG membranes [56].

Their advantages and drawbacks are similar to SPG membranes, with the additional disadvantage that the interface between the two layers create a fragility and makes membranes less resistant to transmembrane pressure.

### 1.2.2.2 Membranes cleaning

Membrane cleaning is a key point in membrane processes as the membrane undergoes internal or external fouling in almost every applications. Every groups have their own procedures regarding membrane cleaning, depending on the membrane type and the molecules used in the process. The main strategy is usually chemical cleaning with highly reactive compounds or physico-chemical cleaning with surfactants. Regarding surfactant cleaning, Derquim + is considered as the best cleaning agent for membrane emulsification [57, 58]. Moreover, increasing temperature and number of cycles lead to better cleaning.

### 1.2.2.3 Set-up with tubular membrane

**Microkits** SPG Technology Co., Ltd. (Miyazaki, Japan) developed a special device to be used at lab scale with small SPG membranes of 20 mm length with effective length of 10 mm (Figure 1.28). This module exists with external pressure as shown on Figure 1.28 with the dispersed phase pushed from the tube outside to the inside, or internal pressure with the dispersed phase pushed from the tube inside to outside. The external pressure type microkit is known to be more effective for droplet size reduction than the internal one. It is also more resistant to transmembrane pressure.

The tank is filled with the to-be-dispersed phase of the emulsion or with a premix and pushed by  $N_2$  flux. It allows to pass only a few milliliters through the membrane as the tank capacity is typically 10 mL.

In DME, the device is immersed in the continuous phase within a beaker and the shear rate is generated by a magnetic stirrer. In order to facilitate flow through the pores, the membrane should be wetted by the continuous phase. In PME, the homogenized emulsion just fall by gravity into a beaker.

To our knowledge, most of the premix emulsions with SPG membranes were produced with this device [59, 60, 61, 62] except for the first study that used a cross-flow module which is presented in the next section [63].

Advantages of this device are that small volumes can be prepared with less than 1 mL of dead volume and both DME and PME can be performed without dilution. Disadvantages are that only small volumes batches can be prepared and that the set-up only resists up to 8 bars.

**Cross-flow** The cross-flow set-up is based on the ones used for microfiltration. A typical membrane emulsification set-up is shown in Figure 1.29. The system consists in a pressurized ( $N_2$ ) vessel filled with the dispersed phase that is pushed through a tubular membrane. Inside the membrane tube, the continuous phase circulates thanks to a pump. This configuration is a batch mode with recirculation of the emulsion that is created and concentrates. The emulsion obtained is kept under stirring in order to stay homogeneous. The flow of the dispersed phase is very low and usually the continuous phase flowrate is high to generate shear stress.

As seen previously, this set up can be used for premix emulsification as well but has the disadvantage of premix dilution [63].

Advantages of this device are that large volumes can be produced and the set-up is very simple. Disadvantages are that the minimum continuous phase volume is usually several hundred of milliliters and the process can not be proceeded in a continuous way unless a very small amount of dispersed phase is required or a very long membrane is used.

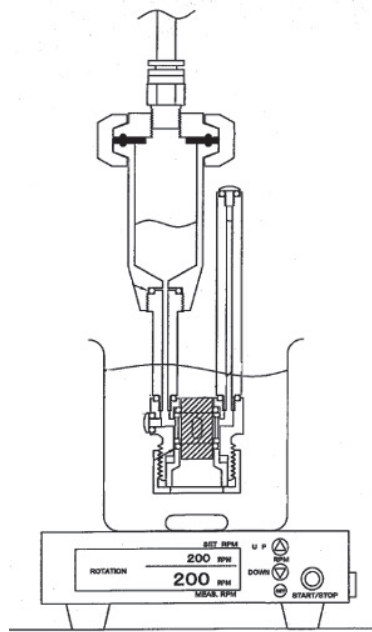


Figure 1.28: External pressure type microkit available at SPG Technology Co., Ltd, schematic view from the supplier brochure

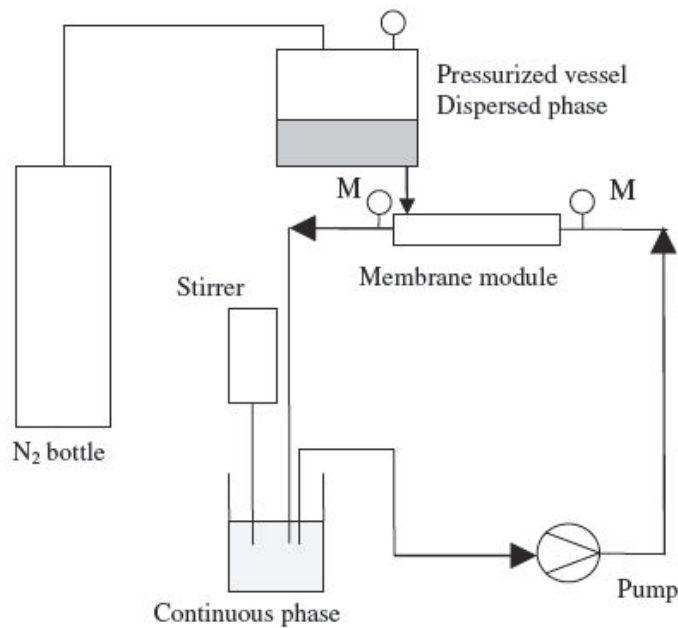


Figure 1.29: Typical experimental set-up for the cross-flow membrane emulsification process; M:manometer [64]

#### 1.2.2.4 Set-up with flat disc membrane

**Dead-end** Typically, flat disc membranes are assembled in a set-up with a dead-end configuration as represented in Figure 1.30 [64]. This set-up is used for micro-engineered membranes that are flat discs. The membrane is fixed in the device and the dispersed phase is pushed from the bottom of the set-up to the glass container above the membrane containing the continuous

phase. Inside the glass container, a mechanical stirrer generates the shear stress at the membrane/continuous phase interface. This shear stress detaches the droplets as a result of both centrifugal force and viscous shear force.

Advantages of this set-up are that it produces monodispersed droplets, small volumes can be produced at lab scale and no  $N_2$  is required. Disadvantages are that only small batches can be produced, the membrane surface is smaller than with tubular membranes, and the flowrate is low.



Figure 1.30: Dead-end stirred cell for membrane emulsification commercialised by Micropore Technologies [65]

**Extruder** Bunjes et al. investigated polymeric and alumina flat disc membranes in an extruder to create emulsions with PME (Figure 1.31) [59]. The membrane is held inside a specific device and with the help of two syringes the premix is pushed in and out until complete homogenization. This type of extruders is typically used to reduce size of liposomes. Several cycles are usually required. This technique is scalable to larger volumes with specific set-ups and a pump instead of syringes, however it works only in batches and several cycles are required.

Advantages are that small droplets can be created with this type of device as membranes are reinforced in the membrane support by different discs. Disadvantages are that processing times are long because cycle number can be typically 10 or 20. Moreover, a continuous process is not possible.

#### 1.2.2.5 Dynamic DME

In addition to static DME presented in the upper section, dynamic DME has also been developed. The aim of this characteristic is to improve detachment of the droplets.

**Rotational membranes** A dynamic membrane can be a rotating membrane, the membrane rotates on its axis in order to increase shear stress at the membrane continuous phase interface [66, 67, 68]. This is typically done with tubular SPG membranes. The parameters of importance

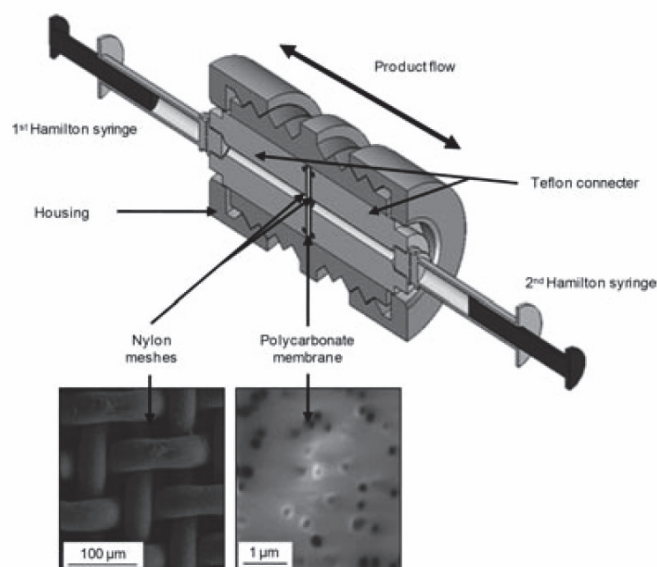


Figure 1.31: Schematic representation of an extruder device for liposomes homogenization or nanoemulsion production [59]

are the membrane diameter because the centrifuge force increases with the diameter of the tubes and the speed of rotation.

**Vibrating or oscillating membrane** Dynamic DME can also be performed by addition of vibrations to the membrane. This membrane vibrates to help droplet detachment from the pore openings. It can be done either on tubular or flat disc membranes. This idea was first investigated for filtration [69] and then applied to emulsification [70]. A piezoactuator system is assembled to the membrane in order to produce vibrations. It was found that smaller droplets could be produced by introducing low frequency (0–100 Hz) membrane vibrations without widening their droplet size distribution.

### 1.2.2.6 Industrial set-ups

Industrial set-ups of membrane emulsification are quite rare in literature. For example, Seebaly et al. for liposomes (Figure 1.32) [71] and Vladislavljević et al. [62] for emulsions with PME claimed production of large scales or high production rates.

Indeed, DME is not recommended for high flow rates because the transmembrane flux has to be very low in order to obtain monodispersed emulsions. Seebaly et al. produced liposomes with a micromixing technique, for which the flowrate has less influence than with DME. Vladislavljević et al. succeeded in working at high flowrate with PME, which does not present the same dispersity issues as DME.

### 1.2.2.7 Commercially available membranes

Typical commercially available membranes used for emulsification are presented in Table 1.5.

## 1.2.3 Forces involved and parameters of influence

### 1.2.3.1 Droplets generation in DME

In DME, droplets are generated at the oil/water/membrane interface. In this part, forces that are generated during the process and dimensionless numbers to characterize the relative effect of

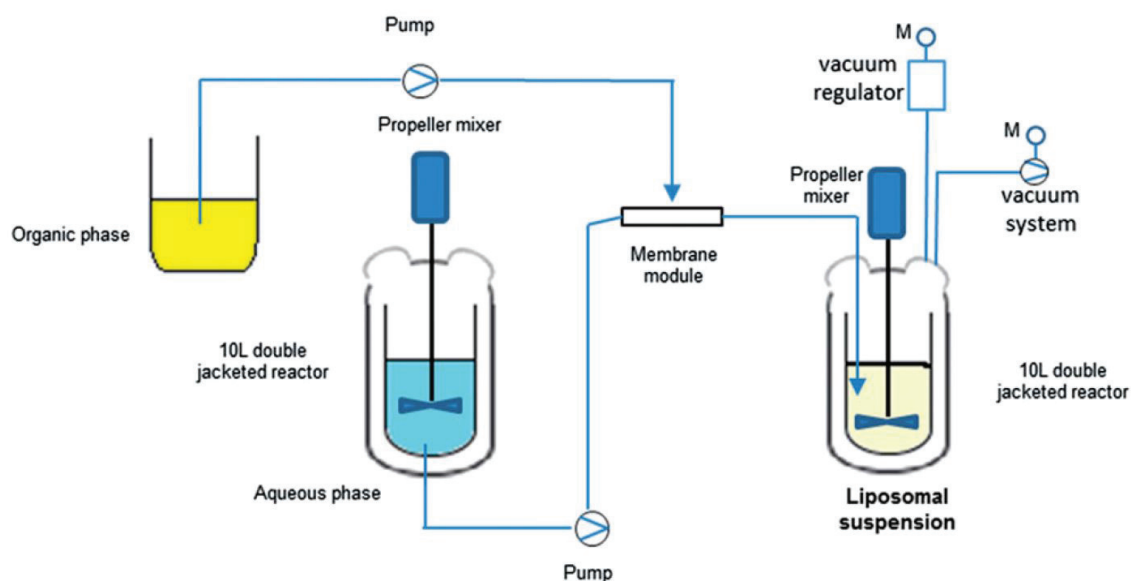


Figure 1.32: Large scale set-up for liposomes production [71]

Table 1.5: Summary of types of commercial available membranes, adapted set-up and pore sizes available

Type	Geometry	Set-up	Pore size	Material
SPG	Tubular: 20-500 mm Flat disc	Cross-flow Rotational Dead-end Vibrating	0.1-20 $\mu\text{m}$	Shirasu porous glass
Ceramic	Tubular: 250-1178 mm	Cross-flow	0.002-10 $\mu\text{m}$	Ceramic
Micropore	Flat disc	Dead-end Vibrating	5-20 $\mu\text{m}$	Metal
Aquamarjin	Flat disc	Dead-end Vibrating	0.1-100 $\mu\text{m}$	Silicon nitride
Polymeric filter	Flat disc	Dead-end Vibrating	0.1-100 $\mu\text{m}$	Different polymers

these forces are presented.

**Forces exercised during droplets generation** In DME, the droplets formed at the membrane surface, grow until a critical dimension and then are carried away with the continuous phase, flowing parallel to the membrane surface for cross-flow or not for other set-ups. The final droplet size of the emulsion is determined at the membrane, dispersed phase and continuous phase interface. This droplet size is the result of different forces (Figure 1.33):

Negligible forces:

- $F_B$ , the buoyancy force due to the density difference between the dispersed and continuous phases
- $F_G$ , the gravitational force

Force due to transmembrane pressure:

- $F_{SP}$ , due to the static pressure difference between the dispersed and continuous phases

Fluid forces due to shear stress:

- $F_L$ , the dynamic lift force due to the asymmetric shear stress profile at the membrane surface
- $F_D$ , Drag force, due to the continuous phase flow, parallel to the membrane surface

Interfacial forces:

- $\gamma_{WO}$ , Interfacial tension between water and oil
- $\gamma_{MO}$ , Wetting of the oil phase on the membrane
- $\gamma_{MW}$ , Wetting of the water phase on the membrane

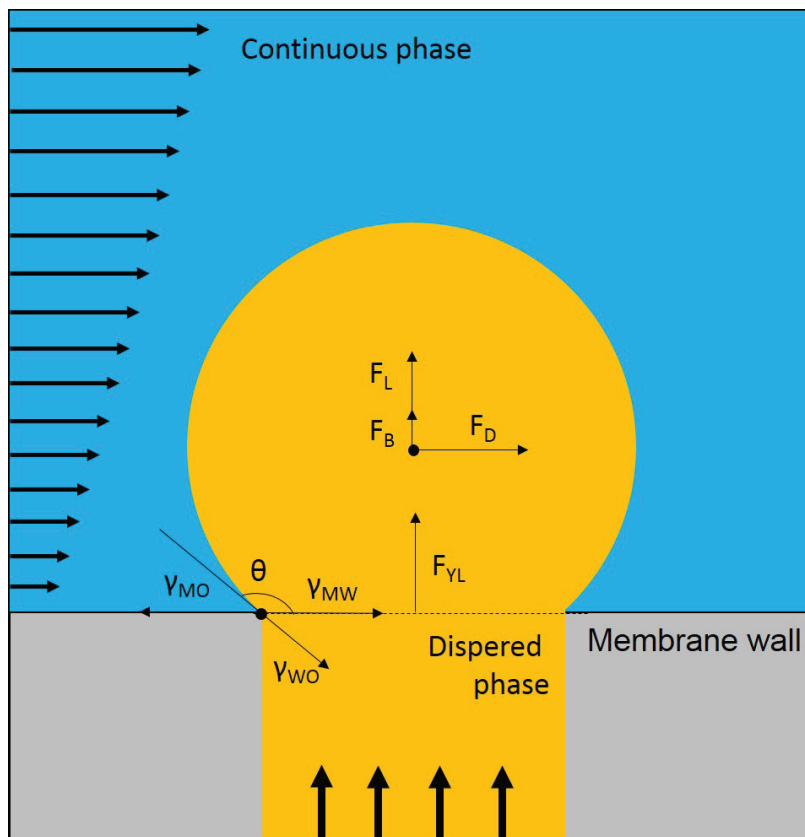


Figure 1.33: Forces exerted at membrane, oil and water interface for an O/W emulsion and an hydrophilic membrane

The resulting force of all interfacial contributions is called interfacial force  $F_\gamma$  or capillary force and is opposed to the static pressure difference.

**Instabilities** Instabilities are phenomena that lead to the breakup of liquid jets. However, in classical DME, the transmembrane velocity is usually low enough not to create this kind of instabilities. The different instabilities leading to droplet break-up are presented in the PME part, as they are much more important in this configuration.

**Dimensionless numbers** Dimensionless numbers are often used in fluid mechanics, the three more useful in our case are presented in the following section.

**Reynolds number** Reynolds number (Re) compares inertial and viscous forces:

$$Re = \frac{\rho u L}{\eta} \quad (1.6)$$

With  $u$ , the velocity of the flow,  $L$  a characteristic length (for a cylindrical pipe, the diameter of the pipe),  $\rho$  the density of the fluid and  $\eta$  the dynamic viscosity of the fluid. Usually  $Re$  is used to determine if a flow is laminar or turbulent. For a cylindrical pipe, flow is considered laminar for  $Re < 2000$  and turbulent for  $Re > 4000$ . In between, a transition regime occurs.

**Weber number** The ratio between inertial and capillary forces is illustrated by Weber number ( $We$ )

$$We = \frac{\rho u^2 L}{\gamma} \quad (1.7)$$

With  $u$ , the velocity of the flow,  $L$  a characteristic length (for a cylindrical pipe, the diameter of the pipe),  $\rho$  the density of the fluid and  $\gamma$  the interfacial tension between the two fluids.

**Capillary number** Capillary number ( $Ca$ ) compares viscous forces and capillary force.

$$Ca = \frac{\eta u}{\gamma} \quad (1.8)$$

With  $u$ , the velocity of the flow,  $\eta$  the dynamic viscosity of the fluid and  $\gamma$  the interfacial tension between the two fluids.

### 1.2.3.2 Parameters of influence in DME

Vladisavljević et al. differentiate two main categories of DME: shear-controlled emulsification, for circular rectilinear pores [72] or when interfacial tension is high and the shear stress is the main source of droplet detachment, and interfacial-tension-driven DME in tortuous pores such as SPG where droplets detachment is mainly a result of low interfacial tension. Some parameters do not have the same influence if DME is shear-controlled or interfacial-tension-driven, when it is the case, a difference is made.

## Membrane

**Wetting** As seen previously, membrane wetting is essential for effective emulsification. To prepare O/W emulsions, the membrane should be hydrophilic in order to avoid oil spreading onto the membrane surface and creating large polydispersed droplets. On the contrary, in order to produce W/O emulsions, membranes should be hydrophobic to avoid water spreading on the membrane.

Hydrophilicity can also be modified with time due to adsorption of molecules on the membrane. It can happen when cationic surfactants are used because SPG membranes are negatively charged. Cetyltrimethylammonium bromide (CTAB), for example can be adsorbed onto the surface which becomes more hydrophobic. This adsorption leads to polydispersed emulsions [73].

**Pore size** Pore size is the main parameter of influence regarding the final droplet size in membrane emulsification. Variation of droplet size with pore size is different if DME is shear stress or interfacial tension controlled [74].

For interfacial-tension-driven DME, droplet size varies linearly with pore size. For SPG membranes and microengineered membranes, the ratio between final droplet size and pore size is no less than 3, if the other parameters are optimized, transmembrane pressure and surfactant for example [52, 75].

In shear-controlled droplet DME, the mean droplet size is determined by a balance between the shear force exerted at the liquid–liquid interface by the continuous phase and the interfacial force  $F_\gamma$ . Increasing shear stress at the membrane interface decreases droplet size and typical droplet size to pore ratios are between 3 and 10 for SPG membranes and from 7 to 36 for silicon nitride membranes [76] depending on the composition of the emulsion.

**Activated pores** Due to their process of fabrication, SPG membranes present a high tortuosity (Figure 1.24 and Table 1.4). This high tortuosity implies that only a low proportion of pores are actually activated and available for emulsification. The proportion of activated pores does not change from one membrane to another, however it was found to vary with pressure, linearly [76] or exponentially [77].

**Pore spacing** If pore spacing is not large enough it can lead to coalescence of the droplets from adjacent pores before detachment. It is more eager to happen if the interfacial force is too low, meaning high wetting of the dispersed phase onto the membrane or high interfacial tension or at low shear stress.

However, in some cases, a push-off mechanism between droplets can occur leading to smaller droplet size with thinner pore spaces.

## Process

**Transmembrane flux** In DME, emulsification occurs only if the capillary pressure or emulsification pressure is reached.

$$P_E = \frac{4\gamma_{WO}\cos\theta}{d_p} \quad (1.9)$$

with  $\theta$  the contact angle between oil, water and membrane (Figure 1.33),  $\gamma_{WO}$  the interfacial tension between oil and water, and  $d_p$  the pores diameter.

For shear-controlled DME: the detachment is not spontaneous and requires a certain time. This time is constant so higher transmembrane flux produces larger droplets. At high fluxes, the push-off force as a result of droplet–droplet interaction on the membrane surface, facilitates the droplet detachment process, the droplet size becomes constant as the transmembrane flux increases [78]. For interfacial-tension-driven DME and low transmembrane pressure, droplets spontaneously detach from the membrane and their sizes do not change significantly with the flux. However, quite quickly, the regime changes from dripping to continuous outflow regime where droplets become a continuous jet. In this regime, the shear stress detaches the droplets. At these conditions, droplets are drastically larger at higher transmembrane flux and usually much more polydispersed due to random detachment from the membrane.

**Continuous phase flowrate** As described previously, in shear-controlled detachment the flow of continuous phase creates the shear and a higher shear lead to smaller droplets.

For interfacial-tension-driven DME, the flowrate of the continuous phase and shear have only a low impact as detachment is a spontaneous phenomenon. When the transition from dripping to outflow regime occurs, the continuous phase flowrate starts to have an impact. Droplets are getting smaller at higher flowrate but in a less controlled manner, meaning higher polydispersity.

Table 1.6: Effect of each parameter on droplet size in DME, IFT: interfacial tension

Parameter	Effect on droplet size	References
Membrane pores	Proportional to pore size (factor 3-10)	[52, 64, 75]
Membranes wet- tability	Good conditions = Same wettability as dispersed phase	[70, 75, 83]
Transmembrane pressure	IFT driven : plateau until a critical value then fast growing Cross-flow controlled: increasing with pressure then plateau phase	[74, 84, 85]
Continuous phase flowrate	Cross-flow controlled: higher flowrate given smaller droplets IFT driven: no effect	[77, 82, 86]
Surfactant	Lower IFT : smaller droplets Higher [surfactant] : smaller droplet Faster adsorption at the interface: smaller droplets	[79, 80, 81]
Viscosity of the continuous phase	Cross-flow controlled: Higher viscosity : smaller droplets IFT driven: Lower viscosity: larger droplets	[73, 82]

## Formulation

**Surfactants** Two characteristics are of importance regarding surfactants: their ability to low down the interfacial tension between oil and water and also their kinetics of adsorption to the newly created interface.

Locally, interfacial tension depends on the nature of surfactant but also on its concentration. Low interfacial tension is essential for an effective detachment of droplets but also to avoid coalescence and stabilize droplets.

The influence of surfactant adsorption kinetics on droplet stabilization has been investigated in several studies [79, 80, 81]. The faster the surfactant adsorbs at the interface, the smaller the droplets are. Fast adsorption allows faster detachment and avoid coalescence of newly created droplets from two close-by pores.

However, surfactants must be chosen carefully. Cationic surfactants can adsorb on the SPG membrane surface and change its hydrophilicity. Thus, oil spreads over the membrane and creates large and polydispersed droplets. Zwitterionic surfactants can also generate this kind of problem as they present a positive charge.

**Viscosity of the continuous phase** A few studies investigated the impact of phase viscosity in DME. The shear stress exerted on the droplets depends on viscosity, higher viscosity leading to higher shear stress. In shear-control emulsification, higher viscosity led to smaller droplets [82]. However, an other effect compete with this one, higher viscosity results in slower adsorption kinetics of the surfactant, and the droplets have more time to grow resulting in larger droplets [73]. Without shear stress, it was shown that an increase in dispersed phase viscosity leads to a decrease in droplet size [73].

**Sum-up of parameters of influence in DME** Effect of each parameters on droplet size in DME are presented in Table 1.6.

### 1.2.3.3 Break-up mechanisms in PME

In PME, membranes are used as homogenizers, mechanisms are different than the ones in DME. First, droplets break-up in PME occurs within the pores whereas in DME, break-up occurs at the membrane, continuous phase and dispersed phase interface. Moreover, in DME, the model geometry is a T-junction whereas in PME it is more complicated as disruption occurs within the pores of complex geometries (tortuosity, branching, dead-end... ). However, one major phenomenon, wall shear stress and four other phenomena have been identified as break-up mechanisms in PME [87].

**Wall shear stress** Droplet size reduction in PME is mainly due to wall shear stress. This shear stress is function of velocity of the premix emulsion within the pores as well as pore geometry (size, porosity and tortuosity). A formulation parameter, viscosity, has also an impact on shear stress. Overall, the wall shear stress  $\sigma_{w,p}$  is given by [62] :

$$\sigma_{w,p} = \frac{8\eta_e J \xi}{\epsilon d_p} \quad (1.10)$$

With  $\eta_e$  the premix emulsion viscosity,  $J$  the transmembrane flux,  $\xi$  the pores tortuosity,  $\epsilon$  the porosity and  $d_p$  the mean pore diameter.

At pressures below critical pressure, emulsions do not permeate through the membrane (Figure 1.34(a)). At moderate shear stress (Figure 1.34(b)), droplets are homogenized at the diameter of the pores or slightly higher due to droplets deformation. At high shear stress (Figure 1.34(c)), an oil jet phenomenon occurs generating impact of the droplets on the pore walls and leading to droplet size smaller than the pore size [62].

**Localized shear forces** Another shear stress is generated at the pores intersection due to localized shear forces [88, 89]. The difference in flux in the branches generates a shear stress that helps reducing the droplet size of the emulsion. However this effect is complicated to measure or predict. For example, Link et al. [89] studied a single T-junction showing that the critical capillary number for breaking depended on the diameter of the channel, the length of the elongated droplet within the channel, the viscosity ratio of both phases and the geometry of the channel. In a membrane composed of several complex branched pores, Y-branching, T-junction or in between, the effect of localized shear force on droplet disruption becomes impossible to predict. According to Van der Zwan et al. [88] this localized shear stress is more important at high flowrate because at low flowrate no branched pores are activated.

**Interfacial tension instabilities** Two types of instabilities can occur due to interfacial tension according to flow conditions. Laplace instabilities occur when a droplet is elongated at low flowrate, a difference in Laplace pressure is generated, creating dumbbell-shape and snap-off effects that disrupt the droplet. At high flowrate of the continuous phase, an other phenomenon takes place inside the channel, Rayleigh instabilities. The droplets remain elongated within the pores, which then may lead to break-up into polydispersed droplets [88].

**Steric hindrance between droplets** Nearby droplets can also have an impact on each other. If the interface is well stabilized, coalescence does not occur between droplets but steric hindrance can induce break-up. The more droplets accumulate within the pores the more likely steric hindrance occurs.

### 1.2.3.4 Parameters of influence in PME

**Membrane properties** As seen previously, membrane properties have a great influence on droplet disruption. Thus, porosity, tortuosity and pore size are determining properties regarding final droplet size. Moreover, like in DME, hydrophilic properties of the membrane have great influence on the PME process. As seen on Figure 1.23, the membrane should be hydrophilic if

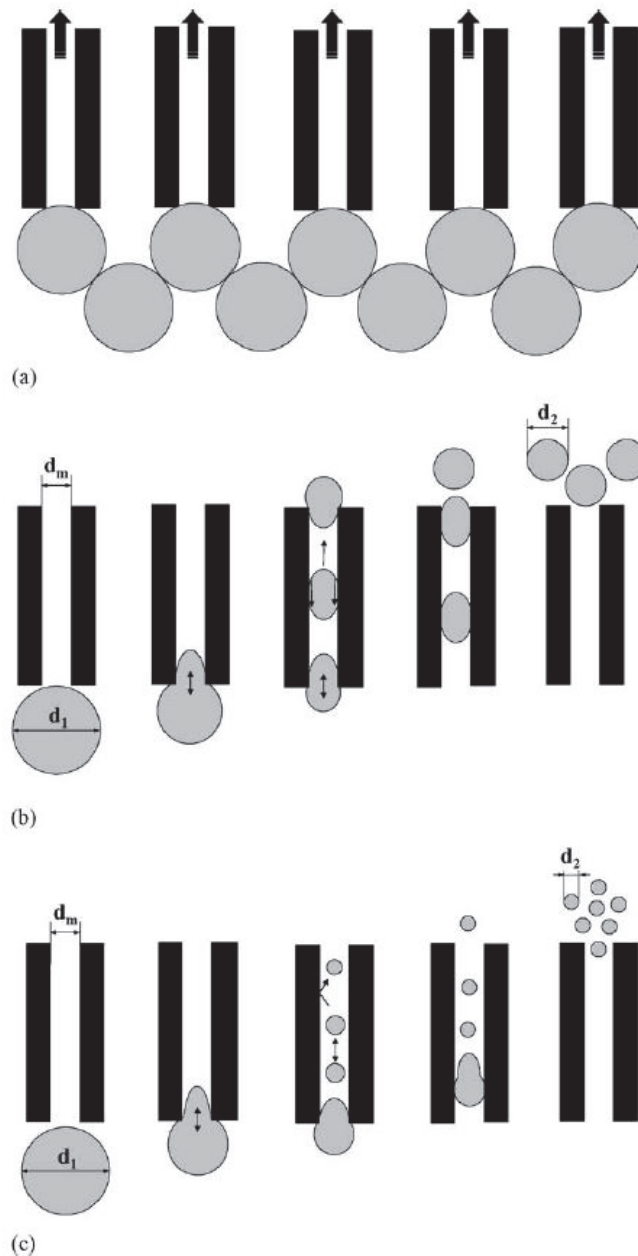


Figure 1.34: Droplet break-up in PME from [62] (a) Droplet retention under a critical pressure, (b) Moderate break-up at moderate shear stress, (c) Intensive break-up at high shear stress

the continuous phase is water and hydrophobic if the continuous phase is oil. If the dispersed phase has a high affinity with the membrane, demulsification occurs instead of PME.

**Pore size** Pore sizes have a direct influence on wall shear stress. Depending of the transmembrane pressure and pore size, the droplet to pore size ratio typically varies from 1 to 1.5 for SPG membranes [90].

**Pore geometry** Higher tortuosity increases the shear stress as seen on Equation 1.10. Moreover, membranes like SPG membranes present a lot of branching which can create more shear stress and more effective size reduction. On the contrary, in this type of geometry, a lot of pores are not active, typically only 1% [91], leading to higher pressure requirement for the same surface of membrane and same pore size.

**Transmembrane flux** As the premix emulsion is a mixture of hydrophobic and hydrophilic liquids, membrane pore walls have affinity with one of the two phases. Usually as mentioned previously for effective PME, the affinity is stronger with the continuous phase, so a minimum pressure is required to ensure that the premix emulsion goes through the membrane pores. Moreover, the minimum pressure for total premix emulsion to go through the pores is higher than in DME where only capillary pressure is present (Equation 1.9). In order to avoid filtration, with water permeating through the membrane pores as the chemical affinity is stronger, and oil fouling the membrane, a higher pressure is required to disrupt the droplets and having an homogeneous emulsion flowing through the pores.

Vladislavjević et al. [62] defined the transmembrane pressure ( $\Delta P_{tm}$ ) in membrane emulsification as the addition of two different pressures: the flow pressure required to overcome membrane resistance to the flow due to its pore sizes and geometry  $\Delta P_{flow}$  and also the disruption pressure required to overcome interfacial tension between oil and water in order to reduce the emulsion size and go through the membrane pores ( $\Delta P_{disr}$ ):

$$\Delta P_{tm} = \Delta P_{flow} + \Delta P_{disr} \quad (1.11)$$

$$\Delta P_{flow} = \eta_p R_m J \quad (1.12)$$

$$\Delta P_{disr} = C\phi\gamma_{ow}\left(\frac{1}{d_d} - \frac{1}{d_{pm}}\right) \quad (1.13)$$

with  $\eta_p$  the viscosity of the emulsion within the pores, which is equal to premix viscosity if the fluid is Newtonian,  $R_m$  the membrane hydraulic resistance, measured by pushing water at different pressures and analyzing resulting flowrate or calculated [47] and with  $J$  the transmembrane flux. For the disruption pressure,  $C$  is a constant,  $\phi$  the volume fraction of dispersed phase,  $\gamma_{ow}$  the interfacial tension between oil and water phase,  $d_d$  the final droplet diameter and  $d_{pm}$  the premix droplet diameter.

In PME, the optimal transmembrane pressure is in principle much higher than the minimum pressure required, 10-50 times [62]. Higher transmembrane pressure leads to higher flux within the membrane pores and thus higher shear stress and size reduction of the emulsion.

**Number of cycles** In HPH, several cycles are often required to reach targeted size or to reduce dispersity. In PME, the necessity of several cycles depends on the membrane type used. For tortuous and branched membranes like SPG membranes, shear stress is more important. Moreover they are thick membranes which explains why 1 extrusion cycle is required through SPG membranes [60, 90, 92], whereas polymeric membranes which are less tortuous and thinner, required up to 21 extrusion cycles [60, 92] to get droplets of a diameter close to pore size and monodispersed.

**Dispersed phase content and premix size distribution** In PME, the final droplet size does not depend of premix characteristics such as size distribution or oil content (if interfacial tension is constant). This is not the case for typical emulsification processes such as HPH where the final droplet size highly depends on dispersed phase content [93].

However, the transmembrane pressure depends highly on dispersed phase content due to increase in droplets number to be reduced in size and viscosity [62] (Equation 1.12 and 1.13) which can be a feasibility issue.

**Viscosities** As said in the previous paragraph, viscosity of the premix emulsion has a great impact on transmembrane pressure and flux, the permeate flux being inversely proportional to viscosity [62]. At the same time, the continuous phase viscosity increases the wall shear stress (Equation 1.9) leading to smaller droplets at higher viscosity [90].

**Surfactants** During PME, new oil/water interfaces are created. Surfactants should be in excess in the premix in order to stabilize the smaller droplets of the final emulsion. Moreover, like in DME, their ability to low down the interfacial tension and their kinetics of adsorption is important. Locally, interfacial tension depends on the nature of surfactant but also on its concentration. Low interfacial tension is essential for an effective stabilization of droplets and to avoid coalescence. Adsorption of the surfactant at the newly created interface, like in all other homogenization processes, such as HPH, has to be fast enough. In HPH, repeated cycles are used to counterbalance the fact that the new surface area cannot be covered fast enough by surfactants. In PME, the processing time is longer allowing more time for coverage of the new interface by the surfactant. However, this phenomenon is not negligible in PME.

**Sum-up of parameters of influence in PME** Effect of each parameters on droplet size in PME are presented in Table 1.7.

Table 1.7: Effect of each factor on droplet size in PME

Parameter	Effect on droplet size	References
Pore size	SPG: Proportional to pore size (factor 1-1.5) Others: less clear	[90]
Pore geometry	Tortuosity and branching = improve size reduction	[62, 88, 89]
Transmembrane pressure	Higher pressure or flux : More effective shear stress and size reduction	[62]
Number of cycle	SPG: Slight decrease after 1 cycle Others: 10 or 20 cycle required for monodispersity	[60, 90, 92]
Dispersed phase content	No important effect on size At same pressure decrease of transmembrane flux	[62]
Viscosity	Increase in continuous phase viscosity= Size decrease Increase in premix viscosity = Increase in transmembrane presure	[62, 90]
Surfactant	Higher concentration = smaller droplets Faster adsorption = smaller droplets	[87]

## 1.2.4 Applications of premix membrane emulsification

### 1.2.4.1 O/W emulsions

O/W, W/O and double emulsions presented here are emulsions finding a direct application in fields such as cosmetics, food or pharmaceutical industry. Typically, these emulsions are simple systems composed of an oil, emulsifier or emulsifier blend and a water phase. Applications of PME as a step of an encapsulation technique are not presented in this part but rapidly in a following part.

O/W emulsion is the most studied type of emulsions produced by PME (Table 1.8), starting in 1996 with Suzuki et al.[63] who produced corn oil emulsions with tubular SPG membrane. During 20 years, different formulations were tested for different applications with droplet size between 1 and 12  $\mu\text{m}$ . Polymeric membranes have been more studied than SPG membranes in PME (Table 1.8) contrary to DME. It can be explained as in PME, usually, several cycles are performed so the narrow size distribution of pores is less critical, emulsions being disrupted eventually by the smallest pore size [94].

Table 1.8: O/W emulsions produced by PME, n is the number of cycle equal to 1 if not mentioned; BSA: bovine serum albumin; PGPR: Polyglycerol polyricinoleate; PGPE: Propyleneglycol propylether; SDS: Sodium dodecyl sulfate

Membrane	Active, oil and surfactant	Droplet size	References
Tubular SPG 2.7 and 4.2 $\mu\text{m}$	Corn oil PGPR/PGPE	5-10 $\mu\text{m}$	[63]
Flat PTFE 1 $\mu\text{m}$	Corn oil ML-750 /CR-500	2-5 $\mu\text{m}$	[95]
Flat polycarbonate 0.33; 0.38; 0.47; 0.6; 1 $\mu\text{m}$	Kerosene SDS	1-4 $\mu\text{m}$	[96]
Flat PTFE 1 $\mu\text{m}$	No information	1-3 $\mu\text{m}$ n=3	[97]
Tubular SPG 1.1 $\mu\text{m}$	Modified insulin Soybean oil L-1695	1.1 $\mu\text{m}$ n=3	[98]
Tubular $\alpha$ -alumina 1.5 $\mu\text{m}$	Toluene SDS	1.75-3 $\mu\text{m}$	[99]
Tubular SPG 8 $\mu\text{m}$	Corn oil SDS, Tween 20 or $\beta$ -lactoglobulin	4-11 $\mu\text{m}$ n=7	[100]
Flat polymerics 0.8-1 $\mu\text{m}$	Sunflower oil Tween 20 or BSA	1-12 $\mu\text{m}$	[101]
Nitrocellulose mixed ester 13.2, 12.8, 11.6 and 10.6 $\mu\text{m}$	$\beta$ -carotene Sunflower oil BSA or whey protein and Tween 20	2-12 $\mu\text{m}$	[102]
Tubular SPG 10 $\mu\text{m}$	Sunflower oil whey protein and carboxymethyl cellulose	8.7-14.4 $\mu\text{m}$	[103]
Nickel membrane 10 and 20 $\mu\text{m}$	AMD-10 <sup>TM</sup> N,N-dimethyldecanamide and d-limonene PEG fatty acid ester	6 $\mu\text{m}$ n=6	[104]
Sintered glass ceramic spherical microbeads 10 to 100 $\mu\text{m}$	Rapeseed oil Tween 20 and Tween 80	<10 $\mu\text{m}$	[105]

#### 1.2.4.2 W/O emulsions

To our knowledge, only two teams reported the production of W/O emulsions with PME [61, 60, 106] (Table 1.9). W/O emulsions being more viscous than O/W emulsions and viscosity increasing transmembrane pressure, it is more difficult to produce W/O emulsions. Zhou et al. [61, 60, 106] produced W/O emulsions of minimum 5  $\mu\text{m}$  droplet size with low viscous oil between 2 and 10 mPa.s at 60°C. This temperature was chosen in order to lower the viscosity and succeed in producing W/O emulsion by PME. Liu et al. [106] performed PME with a premix of median size smaller than the pore size with the only purpose to homogenize the sample. This can explain why the

required pressure for W/O PME was achievable.

Table 1.9: W/O emulsions produced by PME

Membrane	Active, oil and Surfactant	Droplet size	References
Tubular SPG modified with silane 10.2 $\mu\text{m}$	Agarose Liquid paraffin or petroleum ether PO-500	5-7 $\mu\text{m}$	[61]
Tubular SPG (modified) Tubular Polyethylene 10.2; 11.8; 25.6 $\mu\text{m}$	Agarose Liquid paraffin or petroleum ether PO-500	5-100 $\mu\text{m}$	[60]
Tubular SPG 2.8 $\mu\text{m}$	Newcastle disease virus (NDV) Avian Influenza virus or BSA Mineral oil Tween 80	2.3 $\mu\text{m}$	[106]

#### 1.2.4.3 Double emulsions

Double emulsions produced by PME are all W/O/W (Table 1.10). PME is used at the end of the process to homogenize an already created W/O/W emulsion. The W/O primary emulsion is processed with a rotor/stator homogenizer in order to achieve small droplets of some microns. Then either the W/O/W is formed again by the use of a rotor/stator homogenizer [107, 108, 109] or by gentle mixing with a stirring bar [62, 90].

The final W/O/W is obtained by homogenization by PME. The main problem in producing W/O/W emulsions is to ensure that the inner and outer water phases do not mix during the rotor/stator or PME process. Shima et al. [107] revealed that the outer-phase solution was included into the oil phase during rotor/stator homogenization but that in certain conditions it could be externalized during PME.

#### 1.2.4.4 Nanoemulsions

The first article claiming the production of nanoemulsion by PME was published by Joseph et al. 6 years ago [59]. Since this first article, the same group published six articles relating the production of O/W nanoemulsions (Table 1.11). Membranes used are flat polycarbonate [59], multiple flat polymeric [53, 94, 110, 111], aluminium oxide [111] or SPG membranes [92].

In all these articles nanoemulsions of around 200 nm size were produced with the use of 200 nm pore size membranes.

For all polymeric and metal oxide membranes, 21 cycles were required in order to reach monodispersity and nano-size whereas only one cycle was required for production of nanoemulsion with SPG membranes.

In these studies, the authors reported the maximum production of 10 mL for SPG, polymeric and metal oxide membranes and 20 mL with polycarbonate membranes.

#### 1.2.4.5 Other applications of PME

PME can be used as a homogenization technique for many different types of formulation, either as a final product, such as Solid Lipid Nanoparticles (SLN) or as a step in an encapsulation technique.

Table 1.10: W/O/W emulsions produced by PME

Membrane	Active, oil and surfactant	Droplet size	References
Flat cellulose acetate 0.2, 0.45, 0.8 and 3.0 $\mu\text{m}$	Octanoic acid triacylglycerol decaglycerol monolaurate or hexaglyceryl ricinoleate	0.7-5 $\mu\text{m}$	[107]
Tubular SPG 10.7 $\mu\text{m}$	Glucose Soybean oil PGPR and Tween 80	4.4-13.2 $\mu\text{m}$ n=1-5	[62]
Tubular SPG 5.4, 7.6, 10.7, 14.8, and 20.3 $\mu\text{m}$	CaNa2-EDTA + glucose Soybean oil PGPR and Tween 80	3-25 $\mu\text{m}$ n=1-5	[90]
Glass bead 71 $\mu\text{m}$	Beetroot juice Sunflower oil PGPR and Whey protein	10-34 $\mu\text{m}$ n=5	[108]
Glass bead 71 $\mu\text{m}$	Beetroot juice Sunflower oil PGPR and Whey protein	20 $\mu\text{m}$ n=5	[109]

Table 1.11: O/W nanoemulsions produced by PME

Membrane	Active, oil and surfactant	Size	References
Flat polycarbonate membrane 50,100 and 200 nm	MCT or soybean oil SDS or Poloxamer 88 or polyglyceryl-10-laurate or sucrose laurate	100-200 nm n=21	[59]
Tubular SPG 0.1, 0.2, 0.3, 0.5, 1.1 $\mu\text{m}$	MCT or soybean oil SDS or Poloxamer 88 or polyglyceryl-10-laurate or sucrose laurate	100-200 nm	[92]
Multiple flat polymeric 200 nm	MCT SDS	150-200 nm n=21	[110]
Multiple flat polymeric 100 and 200 nm	MCT Phospholipids or Tween 80 or sucrose laurate	<500 nm n=21	[94]
Multiple flat polymeric and aluminium oxide 200 nm	MCT Poloxamer 88 or Tween 80 or sucrose laurate	150 nm n=21	[111]
Multiple flat polymeric 200 nm	MCT or peanut oil SDS or Poloxamer 88 Tween 80 or Tyloxapol or sucrose laurate	> 500 nm n=21	[53]

**Solid Lipid Nanoparticles** SLN are systems where the dispersed oil phase is solid at ambient temperature. For their production, the premix is heated above the melting temperature of the oil phase, the emulsion is homogenized through a membrane and then cooled down [59].

This technique is used to improve stability of the dispersed system.

**Emulsification as a step for encapsulation** Emulsification can be the first step to an encapsulation technique. These techniques are divided mainly into two categories: solvent evaporation technique and polymerization techniques.

In the first technique, a preformed polymer such as polylactide [112] is dissolved in a volatile water immiscible solvent (such as dichloromethane) without oil to create microspheres or with oil to create microcapsules. The solvent/polymer solution is mixed with water, homogenized by PME, finally the solvent is evaporated creating microspheres or microcapsules.

In the second technique, a polymerization or a cross-linking [113] is performed at the oil/ water interface. It results in creating a polymeric shell at the interface and thus a microcapsule. The capsule core can be either oil or water depending if the emulsion is O/W or W/O.

## 1.2.5 Conclusion

Membrane emulsification is a promising alternative to conventional emulsification processes. Its main advantages are very good control of the droplet size and narrow droplet size distribution but also low energy requirement and mild emulsification conditions. In DME, a dispersed phase is pushed through the membrane pores and droplets formed are detached either by interfacial tension or shear stress of the continuous phase flow. The main problem of this technique is that in order to have an effective control of droplet size a very low transmembrane flux is required, creating scalability issues.

An other membrane process, PME, can overcome this drawback. In PME, a coarse emulsion, the premix, is pushed through the membrane pores in order to reduce droplets size. The droplets size of the resulting emulsion is very well controlled by the membrane pore size and the size distribution is narrow. No excess energy is added to the system and the higher the flowrate is the smaller the droplets are. All these advantages make PME a good candidate to perform pilot scale production of emulsions.

The most common emulsification membranes are SPG membranes and microengineered membranes. SPG membranes are more used for DME and polymeric membranes for PME. Membranes can be either tubular or flat membranes. Regardless of the membrane type, membrane cleaning is a key point and should be considered during every membrane emulsification processes.

Different set-ups exist according to the membrane shape, the scale of production and other parameters. Oscillation or rotation can be added to traditional set-ups for better droplet detachment.

Parameters of influence and forces involved in DME and PME have been extensively studied during these last 25 years. In DME, the main parameters for a good size control are pore size, transmembrane flux, shear stress and interfacial tension between dispersed and continuous phases.

In PME, droplet size is mainly dependent on pore size with SPG membranes where only one cycle is required to have a precise size control and narrow size distribution. For polymeric membranes, several cycles are usually required, from five to twenty one, to produce monodispersed droplet size.

In the literature, PME is mainly used to homogenize O/W or double emulsion or as the first step for an encapsulation technique, while only two groups reported the production of W/O emulsions. Traditionally microemulsion are produced by PME but for 6 years a group reported the production of nanoemulsions at small-scale with SPG, polymeric and metal oxide membranes. Their studies focused on the production of nanoemulsions with polymeric membranes even if they showed that SPG membranes, thanks to their unique pore geometry was much more efficient in droplet size homogenization than other membranes.

## 1.3 General conclusion and aim of the work

### 1.3.1 Literature review conclusion

Nanoemulsions are ultra fine dispersed systems of two immiscible liquids with a droplet size below 1000 nm. They are kinetically stable systems but not thermodynamically stable, as they can be destabilized by some phenomena such as coalescence or Ostwald ripening. However their small droplet size confers a high stability.

Their droplet size confers them other interesting properties such as enhanced penetration, unique drug delivery properties but also for cosmetic applications, good aesthetic character and skin feel. They are also the first step of nanoencapsulation techniques to produce highly stable and functionalized drug delivery systems.

In order to create and stabilize these nanoemulsions, emulsifiers have to be chosen carefully, the more classical ones are surfactants which can be anionic, cationic, zwitterionic or non ionic. An other range of emulsifiers is diblock polymers. A lot of blocks can be used however polypeptidic blocks are interesting candidates for many applications due to their high biocompatibility.

Nanoemulsions are more difficult to produce than macroemulsions. High energy has to be provided to the system in order to overcome interfacial tension. Nanoemulsions are produced by two main types of processes, low and high energy processes. Low energy processes depend on the physicochemical properties and therefore require the use of specific surfactants and/or co-surfactants at high concentration and rely on the spontaneous formation of oil droplets. Techniques such as phase inversion composition, phase inversion temperature, emulsification in the micro-emulsification domain and nanoprecipitation are available.

High energy processes are the more common type of processes because they are suitable for a larger range of formulations. Nanoemulsions are generated using mechanical devices with intensive disruptive forces. They are generally formed by HPH at industrial scale or by sonication at lab scale. These techniques can both generate nanoemulsions with very small droplet size, but usually broad size distributions are obtained with sonication and several cycles are required with HPH to obtain monodispersed droplets.

Other processes that require less energy have been developed for emulsion production such as membrane emulsification. The advantages of membrane emulsification are low shear rate, a precise control of the droplets size and narrow particle size distribution.

The two main configurations are DME and PME. In DME, the dispersed phase is pushed through the membrane pores into a stirring or cross-flowing continuous phase. One of the main drawback is that for the preparation of nanomemulsions, DME leads to very low flowrates of the dispersed phase and may not be suitable for scale-up.

In PME, a coarse emulsion called pre-mix is pushed through the membrane pores, reducing the droplet size and size distribution. The flowrate of the product emulsion is generally much higher and higher droplet concentrations are obtained.

SPG, polymeric or microengineered membranes are the most commonly used membranes for emulsification. Typically, SPG membranes are used in DME and polymeric in PME. Many membrane set-ups exist depending on membrane shape, flat or tubular, membrane type and the production scale required.

PME has been reported for a lot of different compositions for food or pharmaceutical applications, mainly O/W and double emulsions and some for W/O. The droplet size was mostly higher than 1  $\mu\text{m}$ , except one group who has reported for 6 years the production of O/W nanoemulsions at small scale with a membrane process using mainly polymeric membranes.

### 1.3.2 Aim of the work

The starting point of this work is the requirement for the European Project PeptiCaps to produce O/W and W/O nanoemulsions with a membrane contactor at pilot scale with the polypeptidic surfactant developed in the frame of the project.

Moreover, some major drawbacks are encountered with industrial processes for nanoemulsions production such as high energy consumption, high polydispersity, and incompatibility with shear and temperature sensitive actives.

Membrane emulsification is a promising alternative, however O/W and W/O nanoemulsions production at large scale has never been reported before.

The first step was to develop a membrane process which would be able to produce model O/W and W/O nanoemulsions at pilot scale and understanding the parameters of influence of both composition and process on the nanoemulsion feasibility and droplet size.

First, the "proof of concept" set-up and the final set-up developed are presented in Material and Methods, as well as characterization methods especially size measurement as it is an important parameter in this study.

The first part of the result section is focused on the production of O/W nanoemulsions with the set-up developed. We ensured that scalability was achievable in any conditions and investigated process parameters, membrane pore size and length, flowrate and number of cycles. Regarding composition the oil and surfactant contents were studied as well as long term stability.

In the second part, we reported the production of W/O nanoemulsion with the set-up developed. We focused on understanding the effect of continuous phase and dispersed phase viscosities and oil content on the feasibility of the process. We succeeded in producing highly viscous nanoemulsions with the set-up and in understanding deeper the pressure increase generated by a viscosity increase.

Then, we reported the production of O/W and W/O nanoemulsions within the project frame. O/W and W/O emulsions were successfully produced with the diblock polypeptide developed by our partners in the European project and with the set-up developed in our laboratory.

The last part deals with the comparison of nanoemulsion production by several processes and active preservation. For that, a comparative study was realized between microfluidizer, ultrasound and PME for the production of injectable nanoemulsions of all-trans-retinoic acid.



# Chapter 2

## Materials and methods

### Contents

---

<b>1.1 Nanoemulsions: Generalities and Processes</b> . . . . .	<b>6</b>
1.1.1 Definition and physico-chemistry of nanoemulsions . . . . .	6
1.1.2 Emulsifiers . . . . .	12
1.1.3 Processes for nanoemulsions production . . . . .	16
1.1.4 Some applications of nanoemulsions . . . . .	24
1.1.5 Conclusion . . . . .	28
<b>1.2 Membrane emulsification</b> . . . . .	<b>29</b>
1.2.1 Type of emulsification . . . . .	29
1.2.2 Set-ups for membrane emulsification . . . . .	31
1.2.3 Forces involved and parameters of influence . . . . .	38
1.2.4 Applications of premix membrane emulsification . . . . .	47
1.2.5 Conclusion . . . . .	51
<b>1.3 General conclusion and aim of the work</b> . . . . .	<b>52</b>
1.3.1 Literature review conclusion . . . . .	52
1.3.2 Aim of the work . . . . .	52

---

## 2.1 PME set-ups developed

### 2.1.1 Intermediate set-ups

First, a classical microkit set-up, as described in the literature review, was investigated for nanoemulsion production with a SPG membrane [92]. In this set-up, a SPG external pressure microkit module was used with a maximum working pressure of 8 bars. The pressure was set by  $N_2$  pressurization. At 8 bars with the nanometric pore size membranes, only some microliters of emulsion were able to go through the membrane. Moreover, these few microliters were very diluted compared to the premix emulsion because at this pressure, filtration occurred.

An other set-up was developed to be able to increase the pressure safely in order to produce nanoemulsions by PME. The idea was first to test the ability of the SPG membrane to resist to higher pressures and to produce nanoemulsions. A "proof of concept" set-up was then developed (Figure 2.1).

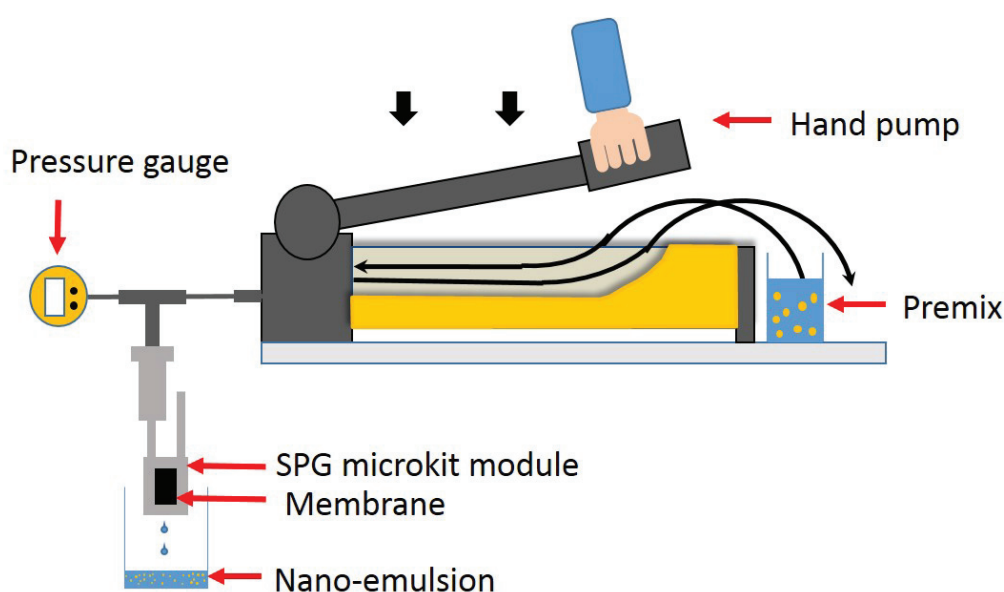


Figure 2.1: Schematic representation of the proof of concept set-up

The pump is a P-391 hydraulic hand pump from Enerpac (Wisconsin, USA). Maximum working pressure is 700 bars. This type of pump is traditionally used for elevation of heavy materials. The commercialized pump is filled with oil. First, the oil had to be removed and the pump cleaned. High pressure fittings (Swagelock, France) were connected at the outlet of the pump to the SPG microkit module. Plastic tubes were connected from the pump to a beaker containing the premix. A pressure gauge was added to read the working pressure at the inlet of the membrane module. The pressure was increased by pumping the premix with the hand pump. At the beginning of the experiment, the pressure did not increase as the pump and fittings were not filled with premix. Once they were filled the pressure increased suddenly. The flow was not constant and the manipulator had to regulate the pumping to maintain a constant pressure. Cleaning of the pump and membrane was made with several cycles of 1% Derquim + at room temperature or 70°C until a clear solution was recovered at the membrane outlet.

This set-up allowed us to prove that the membrane was able to resist to pressure up to around 80 bars and that nanoemulsions down to 260 nm were produced at such pressure (results in Appendix A.1). Moreover, this step-up confirmed that at low pressure mainly water was flowing through the membrane and a lot of resistance from the membrane is felt while pumping. But after a certain pressure was reached, the total emulsion flow through the membrane and no resistance to the flow was felt while pumping.

However, pressure and flowrate could not be kept constant and this set-up was not scalable. An other set-up was then developed in order to produce nanoemulsions with SPG membranes at pilot scale and in a controllable way.

## 2.1.2 High pressure pump set-up

### 2.1.2.1 Experimental set-up

The experimental set-up used for the preparation of nanoemulsions by PME is shown in Figure 2.2.

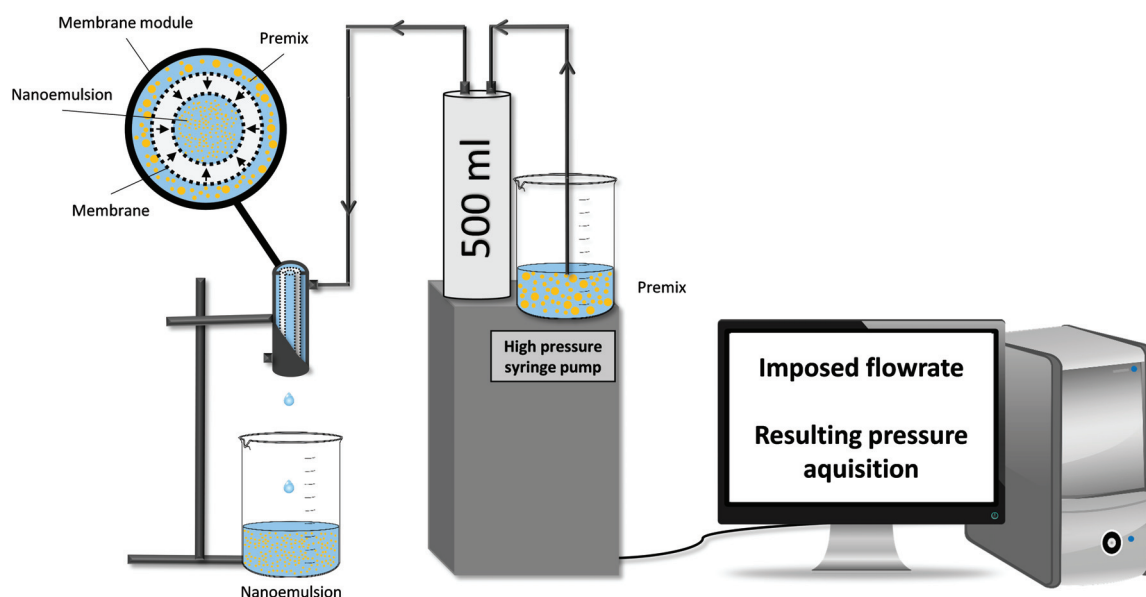


Figure 2.2: Schematic representation of the experimental set-up

### 2.1.2.2 Membranes and membrane modules

Hydrophilic and hydrophobic SPG membranes were provided by SPG Technology Co. Ltd (Miyazaki, Japan). These membranes are tubular with an inner diameter of 8.5 mm and thickness of 0.8 mm. Mean pore size varied from 0.2 to 1.1  $\mu\text{m}$ , the mean pore size data are given by the manufacturer. The pore size distributions, given by the span, were in the range 0.4 - 0.6 [47]. The membrane resistances were tested. The membranes were found to resist to transmembrane pressure up to a minimum of 65 bars.

Two different membrane modules have been adapted to be connected to the set-up.

First, the external pressure microkit module was connected to the pump with high pressure fittings (Swagelock, France). Sealing rings were placed at both ends of the membrane tube in order to maintain the membrane inside the module and the pressure difference. The membrane length was 20 mm with an effective length of 12 mm and effective membrane area of  $S = 3.20 \text{ cm}^2$ .

In order to increase the membrane area and to investigate scalability, a cross-flow tubular module of 125 mm length was adapted to be used in PME and connected to the pump (Figure 2.3). Sealing rings were placed at both ends of the membrane tube. Membranes used with this module were 125 mm length membranes with effective length of 115 mm and effective membrane area of  $S = 30.70 \text{ cm}^2$  which is about 10 times higher than the one of the 20 mm length membrane. The premix was pushed from the external part of the tube to the internal part in a similar way as in the external pressure microkit. The membrane module was connected to the pump with high pressure fittings (Swagelock, France).

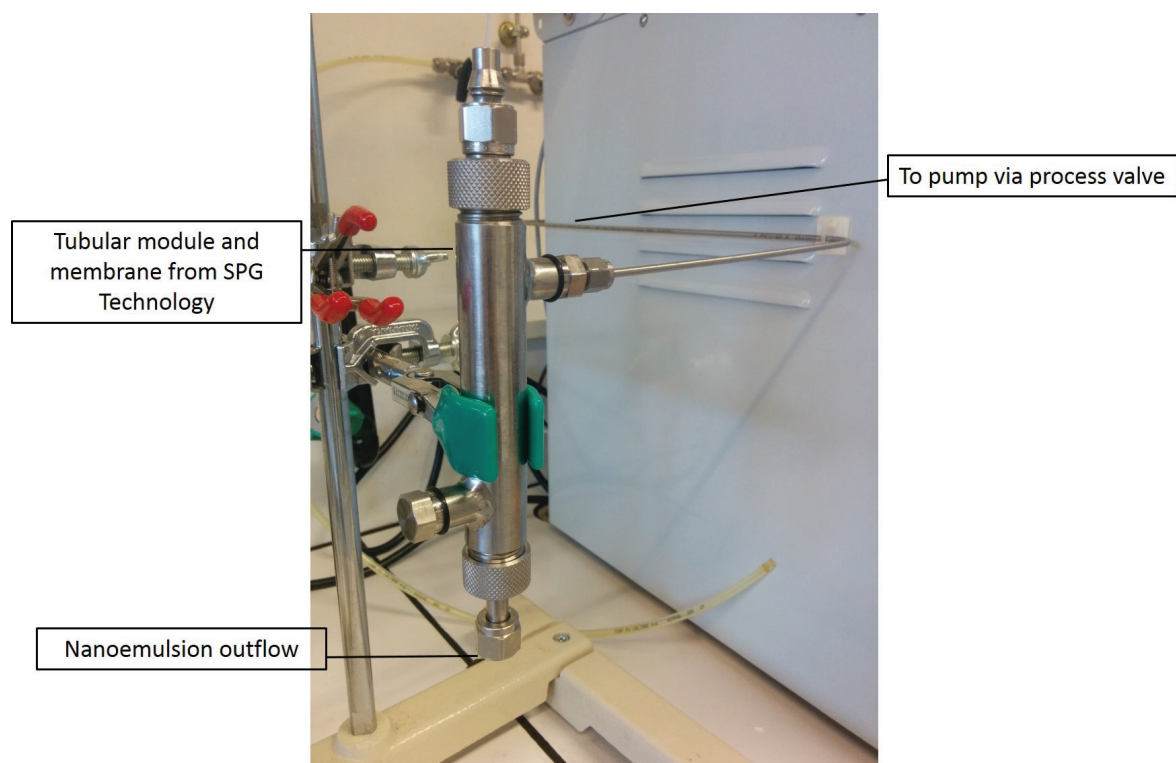


Figure 2.3: Connection of the cross-flow tubular module to the high pressure syringe pump

### 2.1.2.3 High pressure syringe pump

The pump was a high pressure benchtop single cylinder pump BTSP 500-5 (Floxlabs, Nanterre, France) ( Figure 2.4).

The parts of the pump in contact with the fluid are made of high grade stainless steel, the O-rings are made of fluorocarbon elastomer (FKM) and polytetrafluoroethylene (PTFE) for the backup rings, which give the pump a high chemical compatibility.

The pump is equipped with a 500 mL cylinder with a motor driven piston. The brushless motor is situated below the cylinder. The pump chamber is connected to two valves, a feeding valve connected to a feeding tank (inlet) and a process valve, going to the system being pressurized (outlet). These two valves are pneumatic valves and air supply is necessary for activation.

The pump is also equipped with a pressure sensor ( $\pm 0.1$  bar), the pressure being read on the control panel (Figure 2.5). On this panel, it can also be found the volume of fluid in the cylinder, given by the piston position,  $dV$  a counter of the volume of fluid injected. The counter can be reset at any time to zero.

### 2.1.2.4 Commands and acquisition

Commands can be made from the touch screen panel or from a computer connected to the pump. The touch screen panel and computer panel are exactly the same.

The command of the high pressure syringe pump is made by choosing first the working mode. There are four modes of operation (Figure 2.6):

- Constant Pressure
- Constant Flow
- Filling
- Emptying

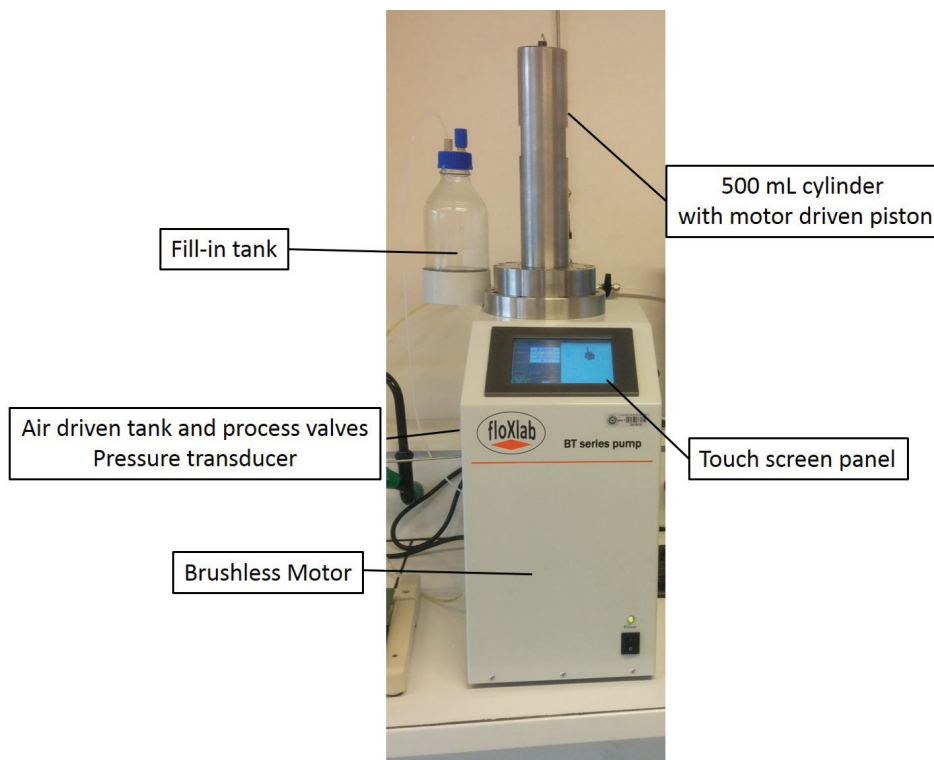


Figure 2.4: Photography of the high pressure syringe pump

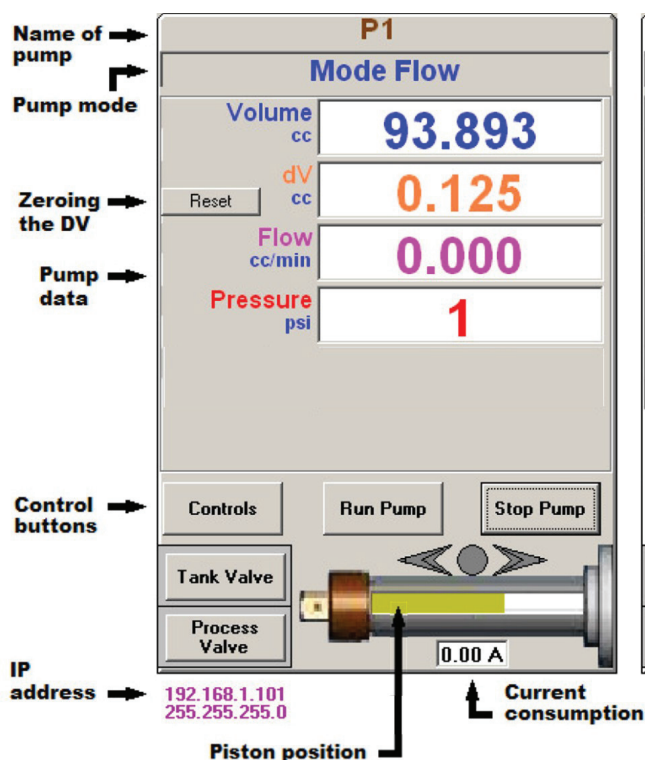


Figure 2.5: Details of the control panel

Filling and emptying are automatic commands that are performed manually with the constant flow mode, they are not presented here.

In the constant pressure mode, the working pressure, the pressure ramp, the maximum flowrate

and the volume injected are inputs. The maximum pressure delivered by the pump is 344 bars and the flowrate 200 mL/min. If no maximum flowrate value is entered, 200 mL/min is set automatically.

In the constant flow mode, inputs are: the working flowrate, the maximum pressure and the volume injected. Maximum pressure value should be entered at any time for safety reasons.

Once all these parameters are set, the pump can be started. Then, data can be read on the panel or acquired by the computer on a note file (Figure 2.7). Data acquisition frequency can be set, the minimum being every second. Data recorded are time, working mode (here always the constant flow mode, 2), flowrate (fixed parameter), pressure (result parameter) and volume of fluid in the pump.

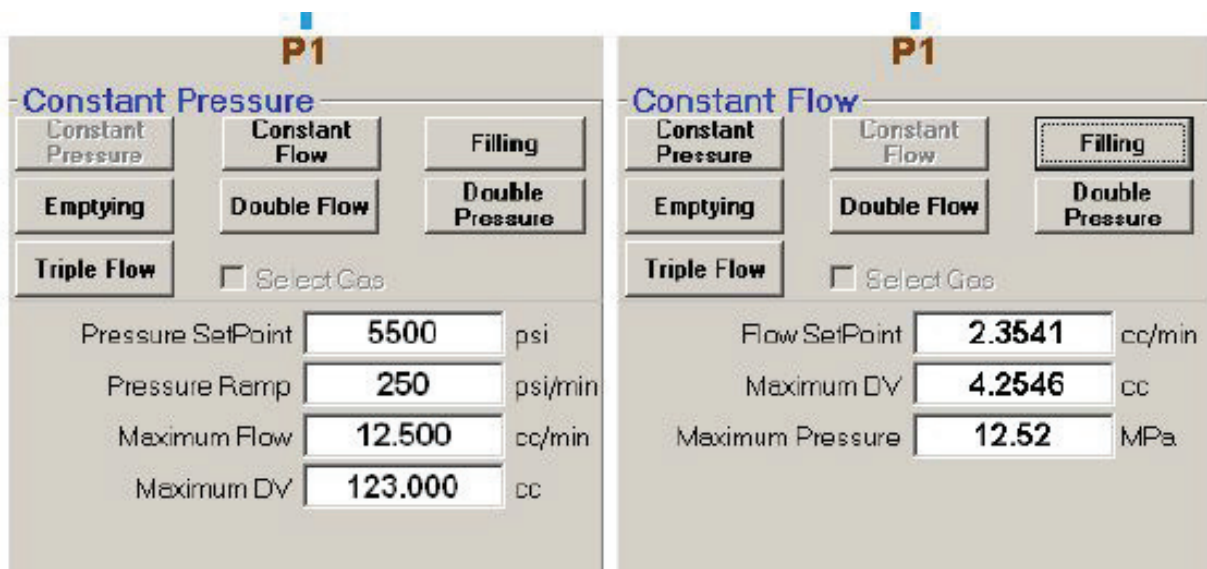


Figure 2.6: Details of the control panel and the two different modes, constant pressure and constant flow

Date/Time	P1A_MODE	P1A_P Pressure [bar]	P1A_Q Flowrate [mL/min]	P1A_V Volume [ml]
00:00:00	2	0.0	0.0000	75.7568
00:00:01	2	0.0	0.0000	75.7568
00:00:02	2	0.0	0.0000	75.7568
00:00:03	2	0.0	0.0000	75.7568
00:00:04	2	0.0	0.0000	75.7568
00:00:05	2	0.0	0.0000	75.7568
00:00:06	2	0.0	0.0000	75.7568
00:00:07	2	0.0	0.0000	75.7568
00:00:08	2	0.0	0.0000	75.7568
00:00:09	2	0.0	0.0000	75.7568
00:00:10	2	0.0	0.0000	75.7568
00:00:11	2	0.0	0.0000	75.7568
00:00:12	2	0.0	0.0000	75.7568
^^ ^^ ^^	~	~ ~	~ ~~~~~	~ ~~~~~

Figure 2.7: Note file containing data acquired by the pump software

## 2.2 Method of nanoemulsion production

### 2.2.1 Premix composition and preparation

#### 2.2.1.1 Model composition

A model composition was chosen to develop the process. First, the surfactant had to be a non-ionic surfactant to avoid electrostatic interactions with the membrane. Moreover, a blend of hydrophobic and hydrophilic surfactants are often used in order to facilitate formation of the emulsion and to improve its stability. Considering these considerations, Tween 20 (Polysorbate 20) (Figure 2.8) and Span 80 (Sorbitan monooleate) (Figure 2.9) from Sigma Aldrich (France) were chosen as they are classically used in many applications.

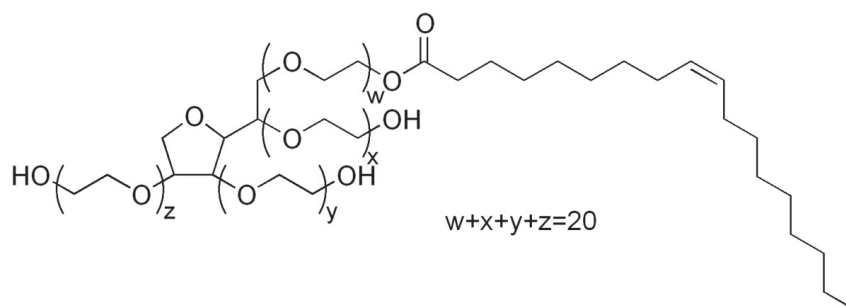


Figure 2.8: Chemical structure of Polysorbate 20

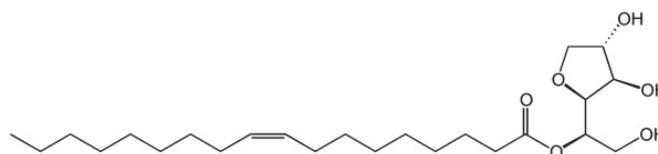


Figure 2.9: Chemical structure of Sorbitan monooleate

Tween 20 has an HLB = 16.7 and is an hydrophilic surfactant and Span 80, with an HLB of 4.3, is an hydrophobic surfactant.

Different cosmetic oils were investigated for model compositions. First, ethylhexyl palmitate (EHP) was chosen by our European partners because it showed the best size results (smaller and monodispersed droplet size distribution) and is a commonly used in cosmetic formulations. EHP (Figure 2.10), was purchased from Eigenmann & Veronelli (Spain). This oil has a RHLB of 9 for O/W emulsions (data given by the supplier and verified in the laboratory). For W/O emulsions the RHLB is 5.

EHP is the fatty acid ester derived from 2-ethylhexanol and palmitic acid. At room temperature it is a clear and colorless liquid. It has a viscosity of 13.15 mPa.s at 25°C, and thus is a low viscous oil.

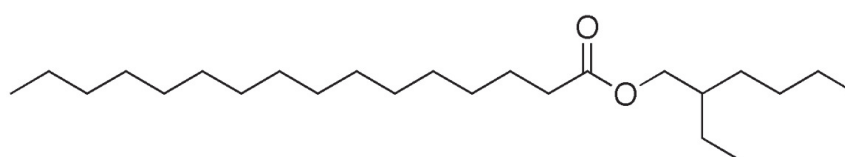


Figure 2.10: Chemical structure of ethylhexyl palmitate

Then, in order to investigate the viscosity influence, mineral oils were used. They are allowed and used in cosmetics. Mineral oil also called, white oil, paraffin oil, liquid paraffin, paraffinum liquidum (Latin), or liquid petroleum, is a by-product of refining crude oil composed mainly of alkanes and cycloalkanes. White Mineral Oil (WMO) was provided from Fisher (USA) with a viscosity of 44 mPa.s (at 25°C), Marcol 52 and Marcol 82 from Exxon mobil with viscosities of respectively 14.1 mPa.s and 24.1 mPa.s (at 25°C). These oils are transparent liquids with different viscosities obtained by changing alkanes and cycloalkanes chain length and ratio. The advantage is that the chemical compositions stay the same and also properties such as interfacial tension.

Water used in all formulations was obtained using a Synergy unit system (Millipore, France) delivering Ultrapure water with a resistivity of 18.2 MΩ at 25°C. Viscosity influence was investigated with glycerol which is a Newtonian viscous fluid and keeps its Newtonian behavior when mixed with water. Glycerol was supplied from Roth (Germany) and has a viscosity of 905.98 mPa.s at 25°C.

In most experiments, the overall surfactant concentration was fixed at 5 % in weight percentage of the total emulsion for 10% dispersed phase (oil or water) in order to ensure that the newly formed droplets were immediately covered with surfactants, hence preventing the increase in droplet size. Nanoemulsion creation requires much more surfactant than macroemulsions as the area of the oil/water interface to stabilize is much higher.

The total surfactant concentration  $x_{TS} = 5\%$ , is composed of a blend of Span 80 and Tween 20 whose HLB,  $HLB_b$  should reach the RHLB of the oil. HLB being an additive value:

$$HLB_b = x_{T20} \times HLB_{T20} + x_{S80} \times HLB_{S80} \quad (2.1)$$

$$x_{T20} + x_{S80} = x_{TS} \quad (2.2)$$

For the O/W emulsion, the concentrations were 2.3 % Tween 20 and 2.7 % Span 80 and for W/O emulsions, 0.28 % Tween 20 and 4.72 % Span 80.

Premixes were all prepared at room temperature. Both phases were first prepared separately. The water phase was obtained by dissolution of Tween 20 in water under magnetic stirring at 600 rpm and the oily phase by dissolution of Span 80 in oil using the same procedure. The two phases were then mixed under magnetic stirring for 10 min to produce the premix.

### 2.2.1.2 PeptiCaps composition

For O/W emulsions, as described in the previous part, EHP was used as the oil phase. The surfactant used was one of the polypeptides developed within the project and prepared at pilot scale by PTS (Polypeptide Therapeutic Solution) (Valencia, Spain). This surfactant was named PP1 (for polypeptide 1). The water phase was citrate buffer at pH 5.5.

PP1 was used at low concentration typically 10% or 20% of the oil content so respectively 1% to 2% of the total emulsion. Polypeptides are expensive and complex to produce, this is why the amount used has to be as low as possible.

For premix emulsion preparation, the first step was dissolution of PP1 in citrate buffer at pH 5.5. This step could necessitate the use of an ultrasonic bath which was proven to have no impact on the polypeptide structure. Then, the premix was obtained by mixing the aqueous and oil phases with an Ultra-Turrax T 50 basic (IKA) at 6,400 rpm during 2 min.

The composition for W/O emulsions was also chosen by our European partners. The oil phase was MCT oil and Ewocream (SINERGA) was used as a co-surfactant. For the water phase, citrate buffer at pH 5.5 or 30/70 % w/w citrate buffer glycerol was used with the second polypeptide (PP2) provided by PTS.

MCT oil was chosen for its compatibility for both cosmetic and pharmaceutical products and the better results (droplet size and stability) obtained at lab-scale by our partners when preparing nanoemulsions with ultrasounds. MCT oil was purchased at Gattefossé (commercial name Labrafac Lipophile WL 1349) and consists of saturated MCTs of around 50 to 80% caprylic (C8) and 20 to 50% capric (C10) acids (Figure 2.11). Its viscosity is 24.08 mPa.s at 25°C and it is a transparent oily liquid.

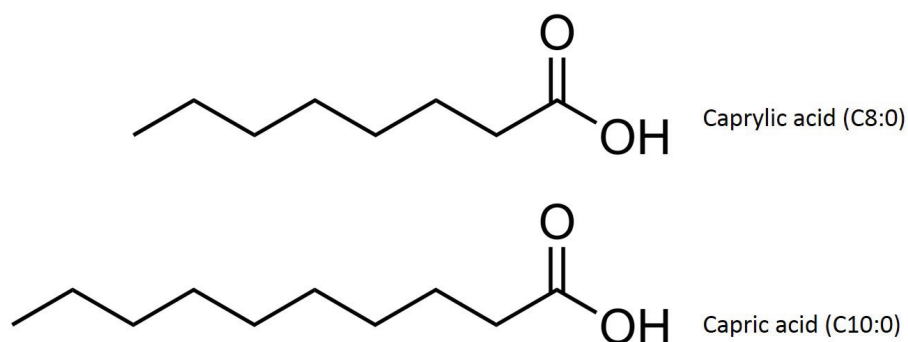


Figure 2.11: Chemical structure of caprylic and capric acids

Ewocream is a Polyglyceryl-3 sorbityl Linseedate sold as a W/O emulsifier of vegetable origin. It was used as an oil soluble co-emulsifier for the W/O formulation as PP2 is too hydrophilic to stabilize W/O emulsions when used alone in the formulation.

The premix was obtained by preparing both aqueous and oil phases separately. The oil phase was prepared by diluting Ewocream in MCT. The water phase was obtained by dissolving PP2 in citrate buffer at pH 5.5 or a mixture of citrate buffer/ glycerol.

### 2.2.1.3 Composition for injection

In order to produce O/W nanoemulsions for injection, the model composition was reformulated. MCT was used as it is the most extensively used FDA approved oil for parenteral formulations. Tween 20 and Span 80 were kept as emulsifiers as both are FDA approved for intravenous administration and innocuous in low quantities. The total emulsifier concentration was kept at 5% to keep potential toxicity at a minimum whilst simultaneously ensuring optimal emulsion stability. The RHLB of the oil was investigated and found to be 10 so the percentage of Span 80 was set at 2.7% and the percentage of Tween 20 at 2.3 %.

The active pharmaceutical ingredient (API) within the nanoemulsion was all-trans retinoic acid from Sigma-Aldrich (Figure 2.12). Its solubility in MCT was determined by UV spectroscopy and found to be 2 mg/mL in oil. A concentration of 10% in oil within the emulsion correspond to 0.2 mg/ ml of total emulsion which is sufficient to ensure a reasonable volume injected and the dose of active ingredient required.

Glycerol was added at 1.88% in order to increase osmolarity of the emulsion up to 0.307 osmol/kg which is close to the ideal osmolarity for intravenously administered galenic forms:  $0.300 \pm 10\%$  osmol/kg.

The oil phase was prepared by mixing together MCT, Span 80, BHT and API and the water phase was prepared by mixing water, glycerol and Tween 20. Then, both phases were mixed with a magnetic stirrer for 10 min.

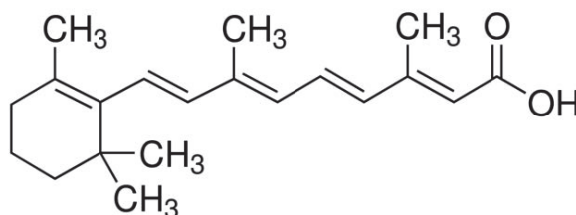


Figure 2.12: Chemical structure of all-trans retinoic acid

## 2.2.2 Production of nanoemulsions with the final set-up

### 2.2.2.1 Pipe resistance to water

The pressure generated by the water flow through the pipe was measured without the membrane module and reported on Figure 2.13. From 0 to 100 mL/min the resulting pressure increased linearly with flowrate. After 100 mL/min, a transition occurs which was explained as the transition between laminar and turbulent flow. At 100 mL/min the Reynolds number calculated at 25°C was 1570. The laminar flow to turbulent flow transition is known to be around 2000. In our case, it seems to be lower, but the critical Reynolds number depends on the pipe geometry.

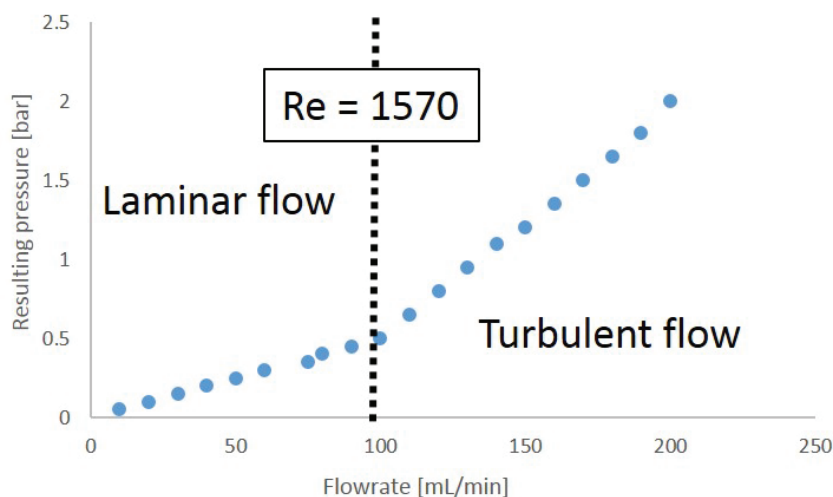


Figure 2.13: Resulting pressure for pure water through the pipe connecting the pump to the membrane module

### 2.2.2.2 Membrane resistance to water

Before each experiment with a hydrophillic membrane, the membrane resistance to water ( $R_m$ ) was measured in order to check that the membrane has been effectively cleaned. Pure water was injected to the system with the membrane module at different flowrates, typically from 10 to 200 mL/min. Membrane resistance ( $R_m$ ) was estimated from the slope of the pure water flowrate versus membrane pressure (Figure 2.14). It worth noting that for different unused membranes of same length and mean pore size significant differences were obtained.

In order to compare membranes of different length, the hydraulic membrane resistance ( $R_h$ ) can be expressed as a function of flux instead of flowrate (Equation 2.3):

$$R_h = R_m \times S \quad (2.3)$$

with  $S$  the effective membrane area of the membrane.  $R_h$  is function of the pore size as it can be seen on Figure 2.15. When fitting,  $R_h$  seem to be proportional to  $1/dp^2$  which is in agreement with Vladislavljević et al. [47].

A difference with the initial  $R_m$  below 20% was considered as acceptable for a clean membrane. Total recovery of  $R_m$  was possible in some conditions and sometimes not.

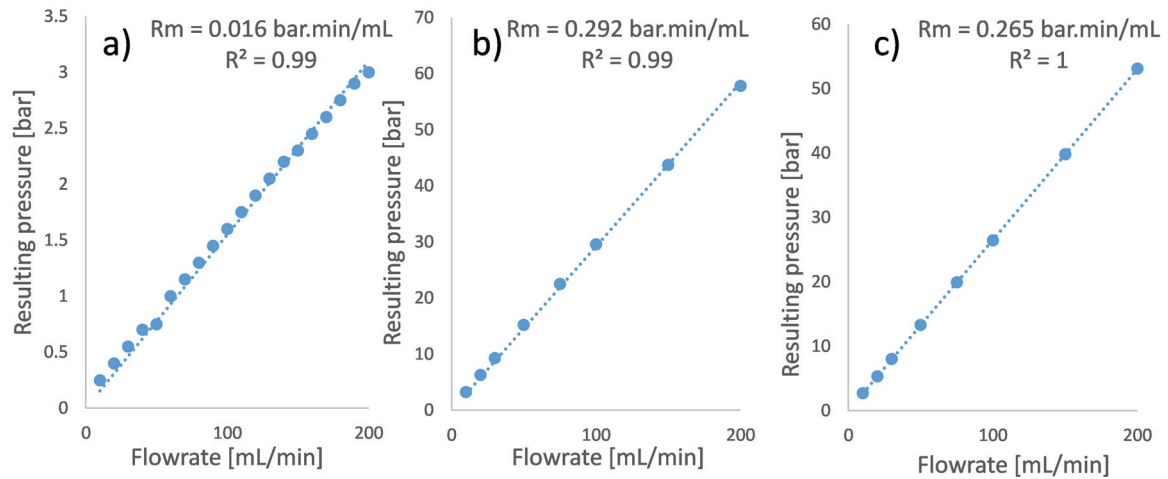


Figure 2.14: Examples of different  $R_m$  measured a) 125 mm long membrane with 0.5 μm pore size b) 20 mm long membrane with 0.3 μm pore size c) 125 mm long membrane with 0.1 μm pore size

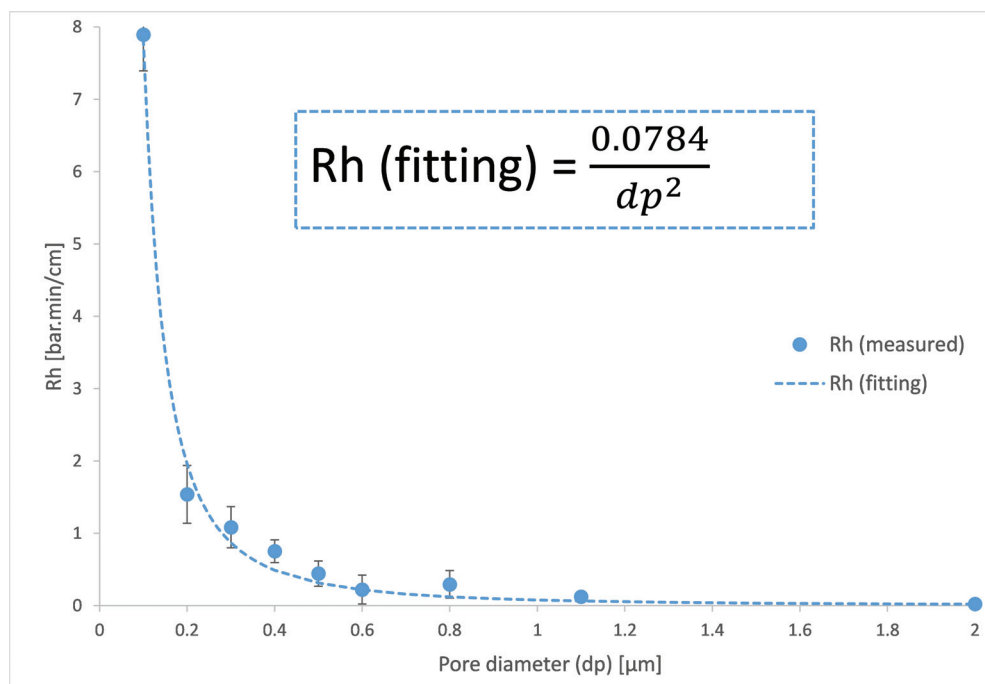


Figure 2.15:  $R_h$  variation with pore radius;  $R_h$  (measured) is the mean value of membranes of different length at this pore size with standard deviation

### 2.2.2.3 Pressure induced by the pipe

In order to understand the influence of all parameters of the set-up, before passing through the membrane, the premix was pushed through the set-up pipes without the membrane being connected. The procedure was similar as the one performed with water in the previous part. This allows the measurement of the pressure required to displace the premix within the pipe at different flowrates. Typically, the working flowrates were 10, 20, 50, 75, 100, 150 and 200 mL/min.

### 2.2.2.4 Nanoemulsion production

The premix was first pumped in the syringe pump from the feed tank at a speed from 5 to 40 mL/min depending on its viscosity, in order to ensure that no air was pumped into the system. Most of the experiments were then carried out with volume of injection of 40 mL to minimize time and material consumption. The nanoemulsion produced flew from the membrane tube under gravity and was collected in a beaker placed beneath the module.

Typically, when possible, flowrates of 10, 20, 50, 75, 100, 150 and 200 mL/min were investigated.

### 2.2.2.5 Data acquisition

As described previously, PME was performed in constant flow mode. The data of interest acquired during the process was pressure. A typical pressure variation with volume injected is drawn on Figure 2.16). Three distinct phases are observed:

- Phase 1: The membrane module is filled by the premix, and the fluid is compressed but does not pass through the membrane pores, as the pressure is below the emulsifying pressure.
- Phase 2: The emulsifying pressure is reached. The pressure is stable which means that no filtration occurs, the imposed flowrate and the flowrate through the membrane are equal. This is the phase where the emulsion is collected and characterized.
- Phase 3: The volume imposed is reached so the piston stops and the pressure decreases.

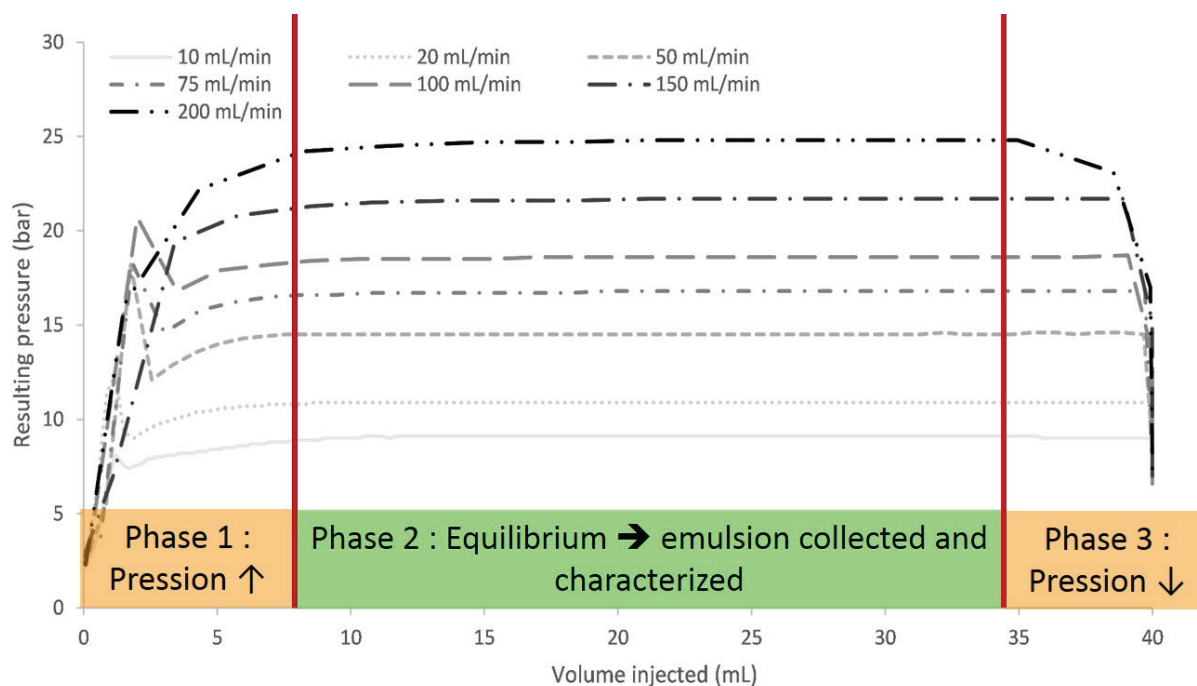


Figure 2.16: Pressure variation with injected volume

### 2.2.2.6 Cleaning procedure

**Water as the continuous phase** The cleaning procedure began by emptying and cleaning the pump. The membrane module was removed and the remaining premix in the pipe was discarded by pumping and injecting air pushing out the premix. Then a small amount (100 mL) of water was pumped and injected followed by emptying the pipes with air. This procedure was repeated until

the water outflowing from the high pressure syringe pump was clear; typically three cycles were needed.

Then, the membrane was carefully cleaned until recovery of its hydrodynamic resistance to water ( $R_m$ ). For that, the membrane module and the membrane were re-connected to the pump. The membrane cleaning procedure was three pumpings/injections through the membrane of 500 mL of a 1 % Derquim + solution at 70°C at 200 mL/min. A second step to remove the Derquim + solution from the membrane was required, and three injections of 500 mL of pure water at room temperature and 200 mL/min were performed. The membrane resistance to water was recovered after this treatment.

**Oil as the continuous phase** When using oil as the continuous phase the cleaning was not as easy as it was for O/W emulsions. Filling the pump and the membrane with detergent in an aqueous phase would not have any sense as the continuous phase is oil.

As for O/W emulsions, the pump was first cleaned by removing the membrane module and the membrane. The membrane was immersed in the continuous phase composed of oil and hydrophobic surfactant and placed in an ultrasonic bath at 85°C for 2 h in order to help removing the emulsion from the pores. The pump was cleaned by pumping and injecting small volumes of continuous phase (50 mL) until transparent oil was obtained, typically three cycles were needed. Then, the membrane was replaced inside the membrane module and the continuous phase was injected through the membrane pores until the liquid collected was transparent oil.

## 2.2.3 Production of nanoemulsions by other processes

### 2.2.3.1 Ultrasounds

An UP400S Ultrasonic Processor (Hielscher, Teltow, Germany) was used to create nanoemulsions (Figure 2.17). It is equipped with a 100 mm titanium cylindrical sonotrode (radius = 7 mm) and a sound protection box.



Figure 2.17: Photography of an UP400S Ultrasonic Processor

Its operating frequency is 24 kHz and its amplitude can be modulated from 0 to 100%. To obtain homogeneous size reduction, the emulsion was magnetically stirred during all the homogenization process. The beaker containing the sample was placed in an ice bath to limit temperature increase.

### 2.2.3.2 High pressure homogenizer

A LM20 series Microfluidizer processor (Microfluidics, Massachusetts, USA) (Figure 2.18) was used. Its reservoir capacity is 300 mL and it can operate at pressures up to 2068 bars.



Figure 2.18: Photography of the Microfluidizer processor

The procedure of operation was the following. First the premix was introduced into the microfluidizer tank. The motor of the machine was started and the pressure was selected from 500 to 2000 bars, created by the intensifying pump. The outflow is a jet of emulsions of around 7 mL. For safety reason the tank and pipes should never be emptied. Thus, the first three jets were not collected because it was a mix of the sample and the filling liquid (typically water). For the same reason, the tank pump was stopped before whole the sample is proceeded. If a second cycle was required the emulsion collected was filled in the tank for a second cycle.

If required, a cooling system can be added at the outlet of the microfluidizer.

## 2.3 Characterization of emulsions

The main methods of characterization are presented in this section. Specific characterization such as high pressure liquid chromatography (HPLC) methods are developed in Chapter 6.

### 2.3.1 Droplet Size

#### 2.3.1.1 Laser diffraction

The droplet size of nanoemulsions and premixes were measured systematically by Laser Diffraction (LD) particle size analysis with a Mastersizer 3000 (Malvern Instruments)(2.19). The technique is based on measurement of the intensity of light scattered as a laser beam passes through a dispersed particulate sample.

The apparatus is composed of an optical bench where a laser beam illuminates the particles and a series of detectors that measure the intensity of light scattered by the particles within the sample for both red and blue light wavelengths.

The sample is delivered in front of the laser beam by a sample dispersion unit. In our case, a wet dispersion unit where particles are in suspension in a dispersant was used, a dry dispersion unit



Figure 2.19: Photography of the Mastersizer 3000

where particles are injected in the measurement cell by gas pressure is also available. is controlled by a range of wet and dry dispersion units. The dispersion unit is under agitation; the speed of agitation and the intensity of ultrasound can be selected. In our case the agitation speed was set at 2000 rpm with no ultrasound.

In order to analyze the scattering data to calculate particle size distributions, the Mie scattering theory was used. This theory is more adapted for emulsions than Fraunhofer approximation because it takes into consideration the light absorption of the particles which is not negligible in case of emulsions.

For EHP and mineral oils, the refractive index was set at 1.47. The ultrapure water phase has a refractive index of 1.33. For all emulsions analyzed, the absorption index was set at 0.005. The emulsion was added until an obscuration value between 4-6% was reached.

In order to have good quality measurement, only results with good quality fitting are presented in this work. The residual and pondered residual values, which are quality factors, for acceptable quality, have to be below or close to 1% and values of both factors have to be nearly equal. It was always the case for the samples measured.

The software, for data treatment, offers different analytical models. Classically, the general purpose model was used. As the quality factors were good this model was selected for most of the samples. In Chapter 6, as samples were not as monodispersed, the narrow peak mode was used to improve quality factors.

The results were expressed either by the figure of the entire size distribution or by  $D_{50}$  the mean droplet diameter for which 50 % of droplets in volume are below this size, similarly 90 % lie below  $D_{90}$  and 10 % below  $D_{10}$ . The dispersity of the sample is given by the span value defined as  $span = \frac{D_{90} - D_{10}}{D_{50}}$ .

All measurements were done in triplicate, the values reported were the average of the three measurements.

### 2.3.1.2 Dynamic light scattering

Dynamic light scattering (DLS) essays have been performed to validate size results obtained by LD. Some samples of different sizes have been measured showing a good correlation between LD and DLS measurement. DLS was performed using a Zetasizer Nano Z (Malvern Instruments, France). Data processing of the DLS measurements were done with the Zetasizer software by both cumu-

lants and distribution analysis.

Results were z-average data which are the mean size and the size distribution in intensity. Before measurements, the nanoemulsions samples were diluted in ultrapure water if water was the continuous phase or oil if the continuous phase was oil (the dilution factor was adjusted to obtain an attenuation factor between 7 and 9). Viscosity of the dilution solution was changed according to the dilution solution used. The measurements were realized at 25°C and the values reported were the average of three repeated measurements.

For W/O, the results of Chapter a were obtained after the preparation of nanoemulsions with polypeptidic surfactant reported in Chapter 5. During size measurement of Chapter 5, we noticed that the viscosity of the emulsion could hinder an accurate size measurement by means of DLS. Indeed, Malvern website states that the maximum size which can be measured is related to the sample viscosity. As an example, the maximum size which can be measured for samples with a viscosity of 10 mPa.s and 100 mPa.s is less than 1 µm and 100 nm respectively. The continuous phase has a viscosity of at least 33 mPa.s (pure MCT), which means that droplet size which can be measured is around 300 nm.

For this reason we chose, in Chapter 4, to measure droplet size of W/O emulsions by LD instead of DLS even if LD measurement in oil are longer and more difficult to perform, as we expect LD to give more accurate data.

### 2.3.1.3 Microscopy

**Optical Microscopy** In order to validate the droplet size data obtained by other methods, samples were observed by optical microscopy. A Leica DM2000 LED optic microscope fitted with a high definition camera was used to observe droplets within the emulsion.

For nano-emulsions, the droplet size were not measurable, but the aim was to confirm or not the presence of micron size droplets.

**TEM and cryo-TEM** Some selected samples were imaged by Transmission Electron Microscopy (TEM) using a CM 120 TEM (Phillips) at the Centre Technologique des Microstructures (CTµ), a platform at Université Claude Bernard Lyon 1, Villeurbanne, France. TEM was operated at an accelerating voltage of 120 keV. An aliquot (10 µL) of the diluted nanoemulsion (dilution factor 10 times) was deposited onto a formvar/carbon coated copper grid for 2 min. Then, the excess liquid was blotted and the sample was further stained with sodium silicotungstate at 1% in water. Excess of staining solution was blotted and the sample was further dried at room temperature overnight. For the nanoemulsion stabilized by the polypeptide, the pH of the staining solution was adjusted to 5.5.

However, the TEM images obtained did not give convincing results with the oil used.

Then cryo-TEM was tested as it allows to see the emulsion in its native environment and as cryogenic temperature prevent the oil from radiation damage.

The same microscope was used for cryo-TEM but with a different sample preparation.

Thin liquid films of the suspensions were deposited onto 300 Mesh holey carbon films (AgarScientific, UK) and quench-frozen in liquid ethane using a cryo-plunge workstation. The specimens were then mounted on a precooled Gatan 626 specimen holder, transferred in the microscope and observed as described previously (at an accelerating voltage of 120 keV).

However, the film of emulsion in this technique has a thickness of 200 nm which was an issue to measure the droplet sizes of the nanoemulsion droplets as they were larger than this size.

### 2.3.2 Viscosity

When needed, the dynamic viscosity of the emulsions was measured using a rheometer MCR 302 equipped with the CP50 module and the software Rheocompass (Anton Paar, France).

For each measurement, we verify that within the shear rate range investigated from 0 to  $100\text{ s}^{-1}$ , the shear stress variation was linear which means that the emulsion is an ideal Newtonian fluid. Emulsions at high oil concentration showed a shear thinning effect, in this case, they were not selected for PME as this effect was not part of our study.

Measurements were made at  $25^{\circ}\text{C}$  in triplicate and average measurements are presented in Chapter 3 and Chapter 4.

### **2.3.3 Interfacial tension**

Interfacial tension was measured previous to this work in order to determine the best surfactants for the model composition.

The pendant drop method was used with a DSA10 Mk2 measurement system equipped with a CMOS camera (Krüss). An aqueous surfactant solution drop was formed with a 1.507 mm needle, immersed in a 10 mL quartz cell containing the oil. The image acquisition was realized with the camera and the interfacial tension was measured from drop shape analysis knowing the density of both liquids and by the mean of the Young-Laplace equation.

Measurement were made at  $25^{\circ}\text{C}$ .

### **2.3.4 Stability**

All samples were kept at room temperature around  $25^{\circ}\text{C}$  and without light. Some of the most interesting samples were measured in stability up to 12 months.



# Chapter 3

## Preparation of oil-in-water nanoemulsions at large-scale using premix membrane emulsification and Shirasu Porous Glass (SPG) membranes

### Contents

---

<b>2.1 PME set-ups developed</b> . . . . .	<b>56</b>
2.1.1 Intermediate set-ups . . . . .	56
2.1.2 High pressure pump set-up . . . . .	57
<b>2.2 Method of nanoemulsion production</b> . . . . .	<b>61</b>
2.2.1 Premix composition and preparation . . . . .	61
2.2.2 Production of nanoemulsions with the final set-up . . . . .	64
2.2.3 Production of nanoemulsions by other processes . . . . .	67
<b>2.3 Characterization of emulsions</b> . . . . .	<b>68</b>
2.3.1 Droplet Size . . . . .	68
2.3.2 Viscosity . . . . .	70
2.3.3 Interfacial tension . . . . .	71
2.3.4 Stability . . . . .	71

---

## Preamble

Nanoemulsions present a lot of different advantages over emulsions as detailed in section 1.1.1. This is why reaching nanometric size is a target in PeptiCaps European project. However, as exposed in the literature review in section 1.1.3, processes for nanoemulsions production present all some drawbacks especially at large scale.

As presented in section 1.2, some processes can overcome these drawbacks such as membrane emulsification. Membrane emulsification can be divided into two processes DME and PME as detailed in section 1.2.1. PME allows faster production and therefore is a better candidate for large scale production. However, as presented in section 1.2.4, only few studies reported nanometric size with membrane processes and none of them at volume larger than a few milliliters.

In order to reach the aim of the European project, i.e. producing nanoemulsions with a membrane process at pilot scale, a new set-up was developed. Steps of development and the set-up itself are described in Chapter 2. Moreover, this set-up allows a very good control and data acquisition of pressure, flowrate and volume, which is an important advantage for a better understanding of the process.

First the set-up was used to produce emulsions droplets at microscale with a 1.1  $\mu\text{m}$  membrane; the results obtained are presented in Appendix A.2 were in agreement with what is already reported in the literature.

The aim of the study presented in this chapter was to evaluate the influence of the same parameters but at nano-scale. These parameters are process parameters and composition parameters. The influence of volume, flowrate and membrane length are major process parameters that must be investigated in order to produce nanoemulsions at large scale. Then membrane pore size and number of cycles are known to have an influence on droplet size and smallest droplet size is one of the aim of the project. In this study, we worked with model compositions but the final objective is the PeptiCaps composition so oil and surfactant concentrations were investigated to understand the effect of composition on the process.

All these parameters were investigated in term of resulting pressure which is a crucial parameter. The pressure has to be minimized and not to be above 60 bars which is the limit of feasibility for the process.

Other important results in this study are the influence of process and composition on droplet sizes.

# Preparation of oil-in-water nanoemulsions at large-scale using premix membrane emulsification and Shirasu Porous Glass (SPG) membranes

*O. Alliod, J.-P. Valour, S. Urbaniak, H. Fessi, D. Dupin, C. Charcosset*

**Colloids and Surfaces A (published online, 2018)**

## 3.1 Abstract

Nanoemulsions are increasingly used in cosmetics, pharmaceuticals and food. They are produced usually by low or high energy techniques. In this study, a process involving moderate pressure in the range 10-60 bar was proposed as an alternative, in particular for the encapsulation of sensitive actives or applications that require a precise droplet size control. Oil-in-water (O/W) nanoemulsions were prepared by premix membrane emulsification (PME) using a set-up with a controlled high pressure syringe pump and 125 mm long SPG membrane. A coarse emulsion (premix) was injected through the membrane with pore size between 0.2 and 0.8  $\mu\text{m}$  in order to reduce and homogenize the droplet size. The effect of several parameters was investigated: process parameters (scalability, cycle number, membrane pore size, flowrate) or formulation (oil and surfactant concentrations). Nanoemulsions were prepared at large scale up to 500 mL at production rate up to 200 mL/min, pressure below 60 bar and one cycle. The droplet size was linearly related to the membrane pore size and highly monodisperse nanoemulsions of around 260 nm in diameter and stable for 9 months at room temperature were achieved with the smallest pore size membrane (0.2  $\mu\text{m}$ ). Moreover, the mechanisms involved in PME for nanoemulsions were discussed, such as flow through the membrane pores and droplet disruption by wall shear stress inside the membrane porous structure.

## 3.2 Introduction

Nanoemulsions find a wide range of applications in cosmetics [2], pharmaceuticals or food industry [3] and are defined by their droplet size which has to be smaller than 1000 nm, or 500 nm or 100 nm, depending on the definition used. Generally, nanoemulsions are oil-in-water emulsions (O/W) as the oil phase is dispersed into the water continuous phase, but can also be water-in-oil emulsions (W/O) when the water phase is dispersed into the oil continuous phase. Mini-emulsions, ultra-fine emulsions or sub-micron emulsions can also be used to name this type of emulsion. Small droplet size confers a high stability, unique texture and drug delivery properties [44]. In dermatology or cosmetics, these general characteristics are completed by specific properties such as uniform deposition on the skin, enhanced penetration thanks to large surface area and small droplet size, modified release and drug carrier properties, film formation on the skin, pleasant aesthetic character and skin feel [28]. Nanoemulsions are also the first step of numerous encapsulation techniques in order to create nanocolloids such as nanocapsules or nanospheres. Nanoemulsions are produced by two main types of processes, low and high energy processes. Low energy processes depends on the physicochemical properties and therefore require the use of specific surfactants and/or co-surfactants at high concentration and rely on the spontaneous formation of oil droplets. Several techniques are available such as phase inversion composition,

phase inversion temperature, emulsification in the micro-emulsification domain and nanoprecipitation, which involves a water soluble solvent [25]. These techniques require specific compositions which may not be suitable for cosmetics or pharmaceutical applications.

High energy processes are on the contrary suitable for a larger range of formulations as the nanoemulsions are generated using mechanical devices with intensive disruptive forces that breakup the oil and water phases[44]. Among these techniques, ultrasound or sonication is based on the cavitation mechanism. It requires high energy input and can only be applied at a very small scale. High-pressure homogenization (HPH) [37] needs also high energy input (pressure applied up to around 2000 bar). Unfortunately, only 0.1 % of the energy input is actually used for emulsification, while the remaining energy (99.9%) is dissipated as heat [8]. Both processes can generate nanoemulsions with very small droplet size, but usually broad size distribution are obtained with sonication and several cycles are needed with HPH to obtain monodisperse droplets. More recently, other processes, that require less energy like membrane emulsification, have been developed [64, 114]. The advantages of membrane emulsification are low energy requirement leading to no temperature increase during emulsification and low shear rate which gives better stability for shear sensitive actives. In addition, membrane emulsification allows a good control of the droplets size, which depends on the membrane pore size, and narrow particle size distribution. The two main configurations are direct membrane emulsification (DME) and premix membrane emulsification (PME). In DME, the dispersed phase is pushed through the membrane pores into a stirring or cross-flowing continuous phase and small droplets are formed at the membrane/continuous phase interface. For the preparation of nanomemulsions, membranes with very small pores have to be used, therefore DME leads to very low flowrates of the dispersed phase [92] and may not be suitable for scale-up.

In PME, a coarse emulsion called premix is pushed through the membrane pores, reducing the droplet size and size distribution. The mechanism of droplet formation in PME is related to the break-up of large droplets within the membrane due to wall shear stress inside the membrane pores. In general, higher flowrates are more effective for droplet disruption due to the higher stress applied on the droplets inside the pores, which leads to a decrease in particles size and size distribution. Also, to reduce the droplet size and make size distribution narrower, the emulsion can pass through the membrane several times (repeated PME). PME has several potential advantages compared to DME [87, 62]. The flowrate of the product emulsion is generally much higher, higher droplet concentrations are obtained, the mean droplet size are smaller than in DME, the experimental set-up is simpler and the process is easier to control and operate. Like in DME, the droplet size can be controlled by the membrane pore size. For the production of nanoemulsions, PME is particularly attractive as it can lead to higher flowrate than in DME. Bunjes et al. prepared nanoemulsions by PME with droplet size lower or around 200 nm with narrow size distribution [92, 110, 94]. Depending on the membrane material and thickness, up to 21 extrusion cycles through polymeric membranes [110, 94] were required or only 1 extrusion cycle through Shirasu Porous Glass (SPG) membranes [92, 60]. This result was explained by the high pore tortuosity and thickness of the SPG membranes.

SPG membranes are the most commonly used membranes for emulsification. They present the advantages of high porosity (50-60%), interconnected micropores, narrow pore size distribution, large range of pore sizes available (100 nm-50  $\mu\text{m}$ ) and low manufacturing cost [114, 87]. Oh et al. [60] reported the preparation of microemulsions by coupling microemulsification prior to the application of a SPG membrane process[115]. Bunjes and Joseph [92] described the production of few milliliters of nanoemulsions using PME with SPG membranes. Indeed, the production of nanoemulsions by membrane emulsification is challenging [56] especially for large volumes at high flowrates.

In general, scale-up production of nanocolloids is an issue [116]. Membrane emulsification which is known to be scaled-up can be a possible alternative to more classical processes. However, only some studies reported large-scale production of nanocolloids by membranes, for example for the production of liposomes [71, 117].

The aim of this study was to investigate the preparation at large-scale of O/W nanoemulsions using PME. For that, a set-up based on PME with SPG membranes was developed with a high pressure pump which allowed working pressure with SPG membranes up to 60 bar, flowrates up

to 200 mL/min and volumes of preparation up to 500 mL. In addition, to increase the flowrate of the nanoemulsions obtained, a membrane with length of 125 mm was used in most of the experiments. With this set-up, the effect of several parameters was investigated, including process parameters (volume of preparation, flowrate, membrane pore size and cycle number) and emulsion formulation (oil and surfactant concentrations). The emulsions obtained were characterized by their mean droplet size and/or size distribution.

### 3.3 Materials and methods

#### 3.3.1 Materials

Ultrapure water was obtained using a Synergy unit system (Millipore, France). Ethylhexyl palmitate (EHP) was purchased from Eigenmann & Veronelli (Spain), Tween 20 and Span 80 from Sigma Aldrich (France), and Derquim+ from Derquim (Spain).

#### 3.3.2 Experimental set-up

The experimental set-up used for the preparation of nanoemulsions by PME is shown in Figure 3.1. The set-up was composed of a high pressure benchtop single cylinder pump BTSP 500-5 (Floxab, Nanterre, France). The pump is made of high grade stainless steel and was equipped with a pressure sensor ( $\pm 0.1$  bar), two pneumatic valves for tank feeding and outlet delivery, a control panel and a storage tank of 500 mL. Pressurization was obtained via a motor-driven piston. A computer was connected to the pump for data acquisition. The flowrate, pressure and volume injected were recorded every second with the software. The maximum pressure delivered by the pump was 344 bar and flowrate 200 mL/min. The membrane module was connected to the pump with high pressure fittings (Swagelock, France).

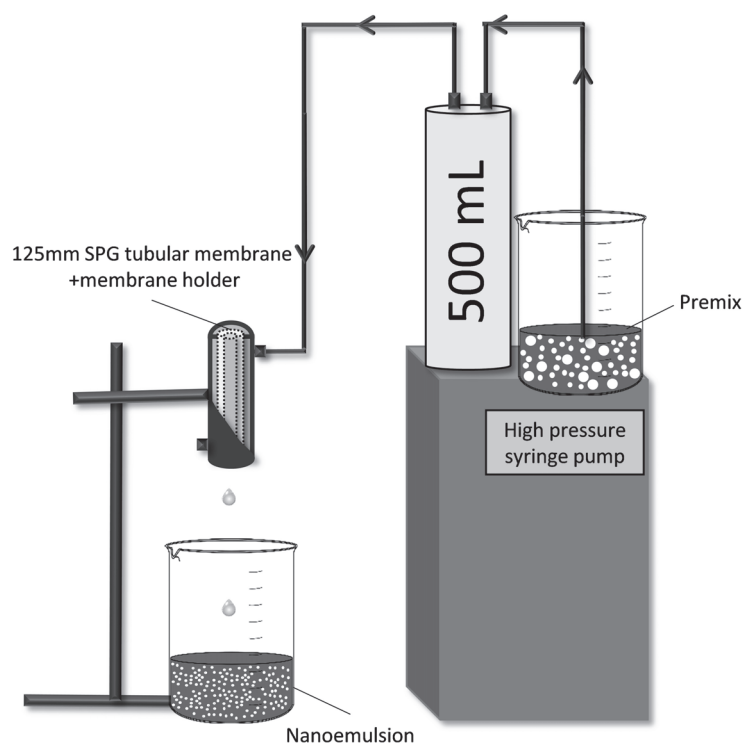


Figure 3.1: Experimental set-up of the high syringe pump with membrane holder and SPG membrane

### 3.3.3 Membranes

Hydrophilic SPG membranes were provided by SPG Technology Co. Ltd (Miyazaki, Japan). These membranes are tubular with an inner diameter of 8.5 mm and thickness of 0.8 mm. In most experiments, the membrane length was 125 mm, however, for some tests, membranes with length of 20 mm were used. Membranes with mean pore size of 0.2, 0.3, 0.4, 0.5, 0.6 and 0.8  $\mu\text{m}$  were investigated; the mean pore size data are given by the manufacturer. The membranes were able to resist to transmembrane pressure up to 60 bar.

The membrane modules used were respectively a tubular module and an external pressure microkit module [90] for membranes with length 125 mm and 20 mm. Both modules were supplied by SPG Technology. For the 125 mm membrane, the cross-flow tubular module was adapted to be used in PME. The premix was pushed from the external part of the tube to the internal part in a similar way as in the external pressure microkit. The effective length of the membranes was reduced due to sealing rings placed at both ends of the membrane tube. Therefore, the effective length was respectively 12 mm and 115 mm, for the 20 mm and 125 mm membranes. The effective membrane area of the 20 mm membrane (3.20  $\text{cm}^2$ ) was about 10 times the one of the 125 mm membrane (30.70  $\text{cm}^2$ ).

### 3.3.4 Formulation of nanoemulsions

Ultrapure water was used as the continuous phase and EHP as the dispersed phase. The required HLB (RHLB) of EHP was given by the supplier as RHLB=9. The surfactant system chosen to stabilize the emulsion was Tween 20, HLB= 16.7, as the hydrophilic surfactant and Span 80, HLB= 4.3, as the hydrophobic surfactant. In most experiments, the composition (in weight percentage of the total emulsion) was for the continuous phase, 1.9 % Tween 20 and 85 % water, and for the dispersed phase 3.1 % Span 80 and 10 % EHP. The overall surfactant concentration was then 5%. The surfactants and high concentrations were chosen to ensure that the newly formed droplets were immediately covered with surfactants, hence preventing the increase in droplet size.

The influence of oil concentration was investigated at 5, 10, 20, 30 and 40 %. The surfactant concentration to oil concentration ratio was kept constant at 0.5, so the total surfactant concentration in the formulation was respectively 2.5, 5, 10, 15 and 20 %. In addition, the influence of surfactant concentration was investigated at 2.5, 5, 10, 15 and 20 % while maintaining the oil percentage at 10 % so the oil concentration to surfactant concentration ratio was respectively 0.25, 0.5, 1, 1.5 and 2.

### 3.3.5 Preparation of nanoemulsions

Preparations were all performed at room temperature. Both phases were first prepared separately. The continuous phase was obtained by dissolution of Tween 20 in water under magnetic stirring at 600 rpm and the dispersed phase by dissolution of Span 80 in EHP using the same procedure. The two phases were then mixed under magnetic stirring for 10 min to produce the premix. This premix was then placed in the feed tank and pumped in the syringe pump. First 20 mL premix was injected in order to remove air from the experimental set-up and fill it with premix. Most of the experiments were then carried out with volumes of injection of 40 mL to minimize time and material consumption. The nanoemulsion produced flew from the membrane tube under gravity and was collected in a beaker placed beneath the module. Larger volumes of premix (100, 250 and 500 mL) were prepared to test the scalability of the technique. In most experiments, the flowrate was set to 200 mL/min. To investigate the effect of flowrate, the following flowrates were set: 5, 10, 20, 50, 75, 100 and 150 mL/min. The transmembrane flux is equal to the flowrate divided by the effective membrane area.

### 3.3.6 Membrane cleaning

Before each use, the membrane was carefully cleaned until recovery of its hydrodynamic resistance to water ( $R_m$ ). For hydrodynamic resistance measurements, water was permeated through

the membrane at different flowrates between 10 and 200 mL/min and the resulting pressure was measured.  $R_m$  was estimated from the slope of the pure water flowrate versus resulting pressure [47]. The cleaning procedure consists in three injections through the membrane of 500 mL of a 1 % Derquim + solution [57] at 70°C at 200 mL/min and then three injections of 500 mL of pure water at room temperature and 200 mL/min. The membrane resistance to water was recovered after this treatment.

### 3.3.7 Particle size distribution measurements

#### 3.3.7.1 Laser diffraction

The droplet size of nanoemulsions and premixes were measured by Laser Diffraction (LD) particle size analysis with a Mastersizer 3000 (Malvern Instruments, France). The technique is based on measurement of the intensity of light scattered as a laser beam passes through a dispersed particulate sample. The Mie scattering theory was used, with a refractive index and an absorption index set up at 1.47 and 0.005 for the dispersed phase, respectively. The continuous phase was ultrapure water with a refractive index 1.33. The results were expressed by  $D_{50}$  the mean droplet diameter for which 50 % of droplets in volume are below this size, similarly 90 % lie below  $D_{90}$  and 10 % below  $D_{10}$ . The dispersity of the sample is given by the span value defined as  $span = \frac{D_{90}-D_{10}}{D_{50}}$ . All measurements have been done in triplicate, the values reported were the average of the three measurements.

#### 3.3.7.2 Dynamic light scattering

The droplet size was also measured by means of dynamic light scattering (DLS) using a Zetasizer Nano Z (Malvern Instruments, France). Data processing of the DLS measurements were done with the Zetasizer software by both cumulants and distribution analysis. Results were z-average which is the mean size and the size distribution in intensity. Before measurements, the nanoemulsions samples were diluted in ultrapure water (the dilution factor was adjusted to obtain an attenuation factor between 7 and 9). The measurements were realized at 25°C and the values reported were the average of three repeated measurements.

### 3.3.8 Viscosity measurement

For the investigation of the effect of oil concentration, the dynamic viscosity of the emulsions was measured for each sample. The measurements were realized using a rheometer MCR 302 equipped with the CP50 module and the software Rheocompass (Anton Paar, France) at 25°C.

## 3.4 Results and discussion

### 3.4.1 Process parameters

All experiments in this section were performed at a composition of 10% EHP and 5% overall surfactant concentration. The premix was obtained by the same procedure for all experiments as described in Materials and Methods. The droplet size distribution of the premixes were similar for all experiments and are presented in section 3.1.3 and 3.1.5.

#### 3.4.1.1 Influence of volume for scalability

The volume of premix injected through the membrane was tested up to 500 mL (40, 100, 250 and 500 mL) with 125 mm length and 0.5  $\mu\text{m}$  pore size membrane at 200 mL/min, to investigate the scalability of the process (Figure 3.2). For all volumes injected, the resulting pressures were almost the same, 27.2 bar at 40 mL and 28.3 bar at 500 mL. As detailed below, the resulting pressure

was the sum of the pressure needed for droplet disruption, pressure due to flow of the premix through the membrane pores and pressure in the pipes from the pump to the membrane module. A constant pressure during injection of 500 mL of premix indicates very low membrane fouling as well as the absence of filtration. This is highly favorable to scaling-up and suggests that larger volumes of premix can be treated. Also, the droplet size was almost the same at the different volumes injected, with a mean droplet size of  $678 \pm 6$  nm from 40 mL to 500 mL. This also suggests that the process can be scaled-up and that large volumes of nanoemulsions can be obtained. Next experiments were performed at 40 mL, as it is expected that the results of the resulting pressure and droplet size should not be affected significantly by increasing volume.

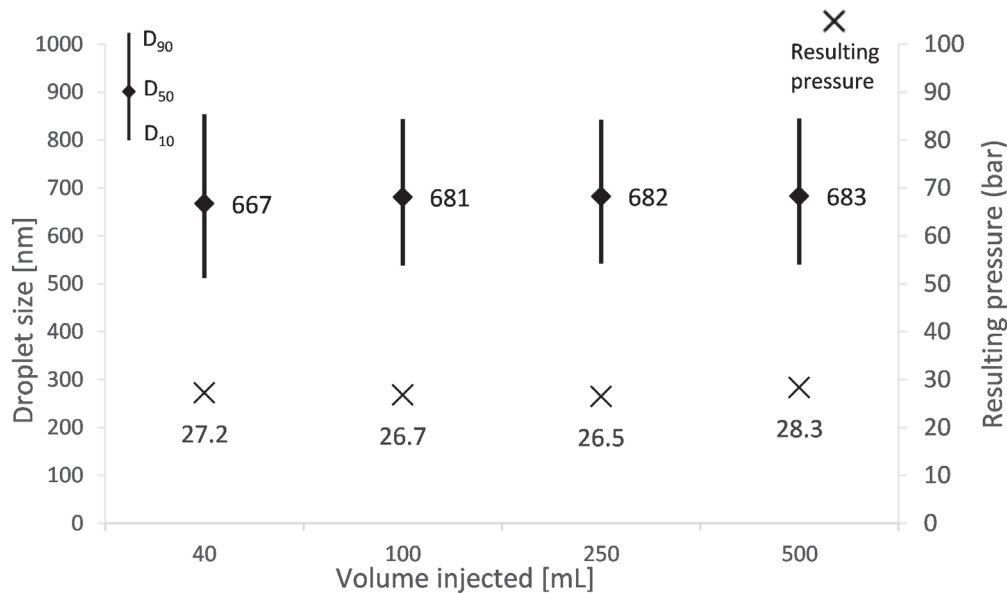


Figure 3.2: Resulting pressure and droplet size variation with scaling up from 40 mL to 500 mL with 125 mm length and  $0.5 \mu\text{m}$  pore size membrane at 200 mL/min at a composition of 10% EHP and 5% overall surfactant concentration

### 3.4.1.2 Influence of flowrate

The effect of flowrate was investigated from 10 to 200 mL/min on both nanoemulsion droplet size and resulting pressure with 125 mm length and  $0.5 \mu\text{m}$  pore size membrane. The pressure profiles were measured at various flowrates (Figure 3.3). A typical pressure profile was divided into three parts. The first part corresponded to the pressurization of the fluid inside the high pressure syringe pump, which led to a dramatic increase in pressure. Then, the pressure remained constant and this constant value obtained was termed “resulting pressure”, which was recorded for all experiments. Finally, the premix was almost totally injected (some last few mL remained in the high pressure syringe pump) and a decrease in pressure was observed. The fact that the resulting pressure remained constant during almost all the premix injection proved that no filtration occurred, no internal and/or external membrane fouling or change in the product nanoemulsion. This was observed at all flowrates. Indeed, in PME, larger droplets can be retained by the membrane surface if the shear stress through the membrane pores is too low, leading to a filtration phenomenon [56].

Moreover, the resulting pressure ( $\Delta P_r$ ) is equal to the sum of the flow pressure ( $\Delta P_{flow}$ ), the disruption pressure ( $\Delta P_{dis}$ ) and the pipe pressure ( $\Delta P_{pipe}$ ) (Equation 3.1). The flow pressure is the pressure necessary to pass through the very small membrane pores. The disruption pressure ( $\Delta P_{dis}$ ) is the pressure needed to break the premix emulsion into smaller droplets and therefore reducing the droplet size [62]. With our experimental set-up, high flowrates up to 200 mL/min

can be set, so the pressure along the pipes from the high pressure pump to the membrane module may not be negligible. This pressure is termed pipe pressure ( $\Delta P_{pipe}$ ), and is highly dependent on fluid viscosity. The resulting pressure is then expressed as:

$$\Delta P_r = \Delta P_{flow} + \Delta P_{dis} + \Delta P_{pipe} \quad (3.1)$$

When increasing the flowrate, the resulting pressure increased from  $9.06 \pm 0.08$  bar at 10 mL/min to  $24.7 \pm 0.20$  bar at 200 mL/min (Figure 3.3) mainly because  $\Delta P_{flow}$  increased.

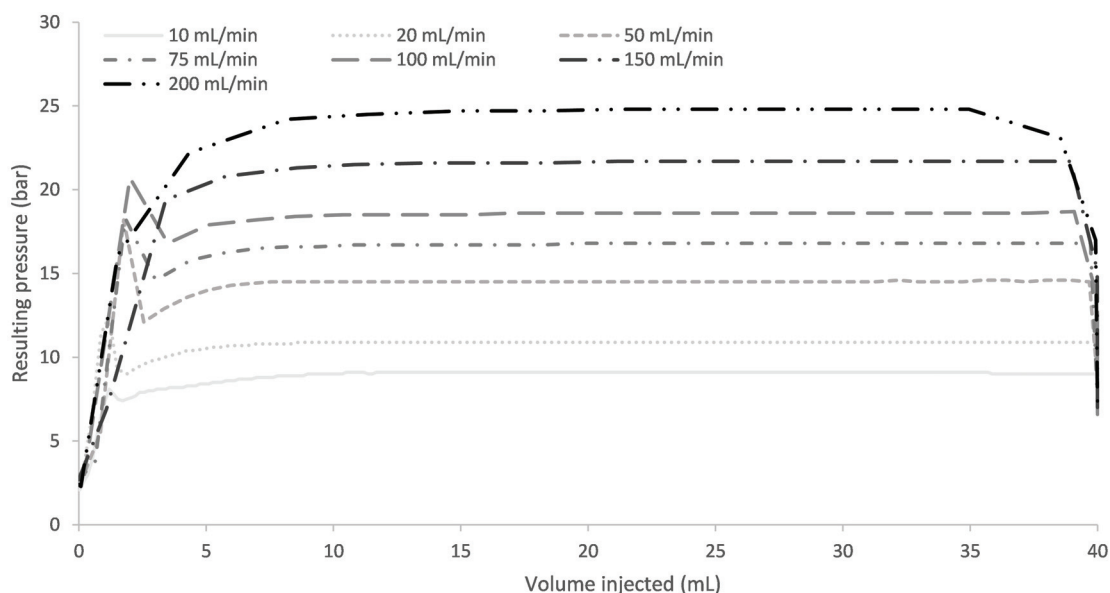


Figure 3.3: Pressure profiles at different flowrates with a 125 mm length and 0.5  $\mu\text{m}$  pore size membrane at a composition of 10% EHP and 5% overall surfactant concentration

The influence of flowrate on droplet size is presented in Figure 3.4. The droplet size decreased with flowrate while the span was higher (0.48) at the lowest flow rate of 10 mL/min and then stabilized (around 0.42). The ratio between droplet size and membrane pore size was 1.52 at 10 mL/min and 1.34 at 200 mL/min. Indeed, at higher flowrate the wall shear stress applied to the droplets inside the membrane porous microstructures is higher, so smaller and more monodisperse droplets are obtained. Previous studies on preparation of emulsions with droplet size of several microns also observed a decrease in droplet size when increasing the flowrate (or transmembrane pressure) [46].

### 3.4.1.3 Influence of membrane pore size

The influence of pore size on droplets sizes was tested for six membranes with pore sizes ranging from 0.2 to 0.8  $\mu\text{m}$  with a 125 mm length membrane at 200 mL/min except for smallest size. As expected, the membrane pore size greatly influenced the droplet size of the nanoemulsions product (Figure 3.5). The droplet size decreased linearly with pore size with a ratio between droplet and pore size equal to 1.26 and a regression coefficient  $R^2=0.99$ . Therefore, the droplet size can be controlled by changing the pore size. When preparing emulsions with droplet size of some few microns, Vladislajevic et al. [46], showed that the ratio between droplet and pore size was in the range from 1.51 to 0.98 as the mean pore size varied from 5.4 to 20.3  $\mu\text{m}$ . The droplet to pore size ratio obtained here for nanoemulsions was therefore in the same range as the ones previously obtained for emulsions. However, the mean droplet size was a linear function of the mean pore size, while a non-linear correlation was obtained at higher pore size. According to the membrane used, the droplet size of the premix was reduced by a factor from 15 to 58. The span was also reduced

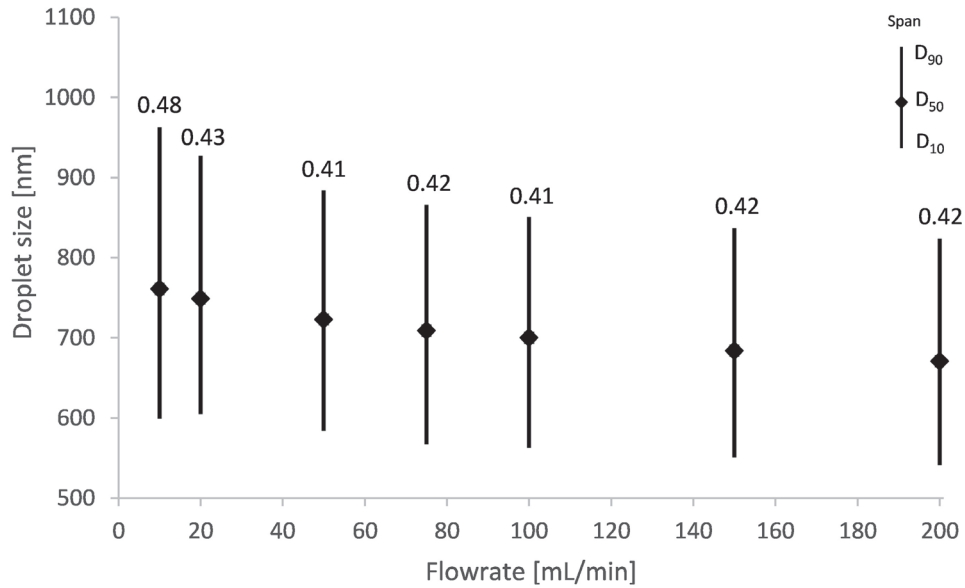


Figure 3.4: Droplet size as function of flow rate with a 125 mm length and 0.5  $\mu\text{m}$  pore size membrane at a composition of 10% EHP and 5% overall surfactant concentration

from 1.62 to a mean value of  $0.49 \pm 0.08$ . Vladislavljević et al. [47] showed that most SPG membranes have a relative span of pore size distribution in the range 0.4 - 0.6. Therefore, the span of the nanoemulsions obtained by PME was close to the typical spans of the SPG pore size distribution. A similar observation was reported for emulsions with droplet size of several microns obtained by DME [47].

For membranes with pore size larger than 0.3  $\mu\text{m}$ , nanoemulsions were prepared at 200 ml/min. For the 0.2  $\mu\text{m}$  and 0.3  $\mu\text{m}$  membranes, the flowrate was set at 5 ml/min and 100 ml/min respectively, to maintain the resulting pressure below 60 bar. As it can be seen on Figure 3.5, the resulting pressure increased with a decrease in membrane pore size due to the increase in  $\Delta P_{flow}$ . Moreover, at smaller pore size, the disruption had to be more intense to create smaller droplets so  $\Delta P_{dis}$  increased as well. As a result, the resulting pressure increased drastically with a decrease in membrane pore size. It was then impossible to prepare nanoemulsions through a 0.1  $\mu\text{m}$  pore size membrane for this nanoemulsion composition.

#### 3.4.1.4 Influence of membrane length

Usually in PME, SPG membranes with length of 20 mm have been used in a microkit module [90, 61]. Here, for all our experiments, a 125 mm length membrane was used, in addition with a 20 mm membrane to investigate the effect of membrane length both were 0.5  $\mu\text{m}$  pore size membrane investigated at different flowrates. The longest membrane required lower pressure but led to larger droplet size than the short membrane (Figure 3.6). Indeed, the droplet size decreased with an increase in pressure, independently of the membrane length. Nearly the same droplet size and resulting pressure were observed at 10 mL/min with the short membrane and 100 mL/min with the longest membrane. Indeed, in these two experiments, the transmembrane flux was almost identical. Thus, the wall shear stress in pores which governs droplets disruption was the same. In addition,  $\Delta P_{dis}$  and  $\Delta P_{pipe}$  did not change while changing membrane length. The 125 mm membrane was then used at a flowrate 10 times the one of the 20 mm membrane with no change in resulting pressure and droplet size.

Regarding droplet size, the shortest membrane led to smaller droplets. The droplet to pore size ratio even reached 1.05 at 200 mL/min for the short membrane. This means that nearly half of the droplet size distribution was below the pore size. This is explained by a phenomenon occurring at high shear stress induced by high flowrate within the pores called "snap-off" due to localized shear

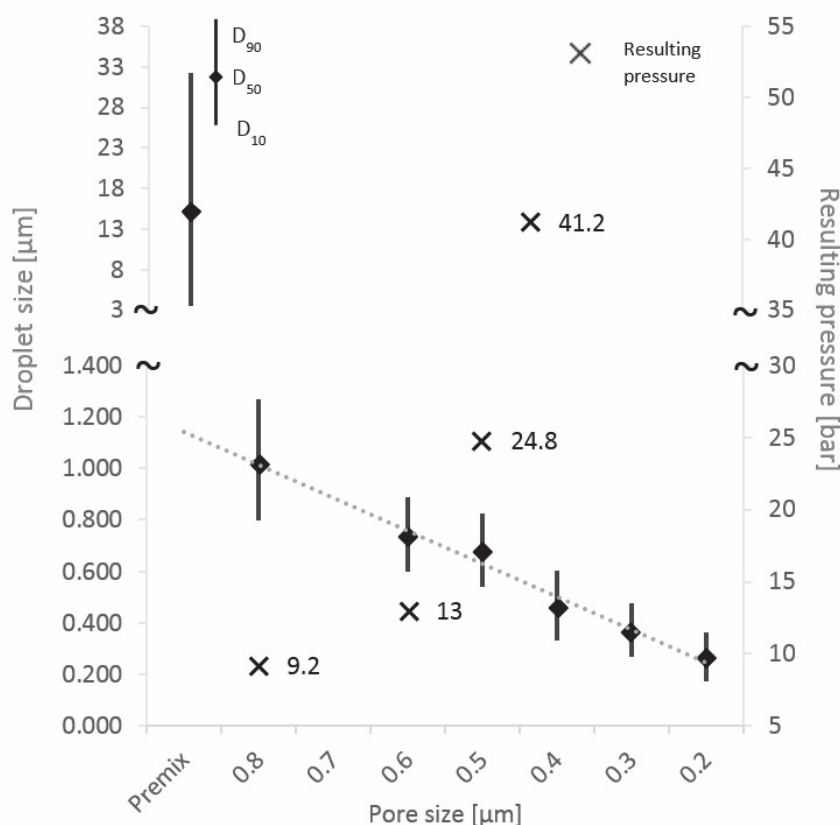


Figure 3.5: Droplet size distribution of the premix and nanoemulsions obtained at different pore sizes (at 200 mL/min, except for 0.3  $\mu\text{m}$  pore size membrane at 100 mL/min and 0.2  $\mu\text{m}$  pore size membrane at 5 mL/min) and resulting pressure except for 0.2  $\mu\text{m}$  and 0.3  $\mu\text{m}$  pore size membrane as flowrate was changed, at a composition of 10% EHP and 5% overall surfactant concentration

forces [88] which explains the creation of droplets smaller than the pore size. This phenomenon was only observed with the 20 mm membrane, because the transmembrane flux was then 10 times the one of 125 mm membrane. In this case, the premix droplets underwent a more intense snap-off whereas with the 125 mm membrane, droplet break-up mechanisms due to interfacial tension and steric hindrance between droplets were predominant.

### 3.4.1.5 Effect of cycle number

The effect of cycle number was investigated with 125 mm length and 0.5  $\mu\text{m}$  pore size membrane at 200 mL/min (Figure 3.7). After one cycle, the droplet size of the premix was reduced by a ratio of 22, 1.06 from the first to the second cycle, 1.03 from the second to the third cycle and 1.01 for all following cycles. The span of the premix equal to 1.89 decreased after one cycle to 0.43 (in the range of the span of the SPG pore size distribution) and was almost constant during the following cycles. Therefore, one cycle was sufficient to obtain nanoemulsions with droplet size around 630 nm. The following cycles did not significantly disrupt further the droplets. Previous studies on PME with SPG membranes have investigated the effect of cycle number for emulsions with droplets of several microns [62, 90, 100]. The cycle number required to reach a constant droplet size and span depended on a number of parameters such as membrane pore size, viscosity of the emulsions and pressure applied. Generally, more than three cycles were needed. In our study, only one cycle was sufficient to produce droplets with small size and span. This may be due to the highest pressure applied which means higher shear stress and more effective disruption.

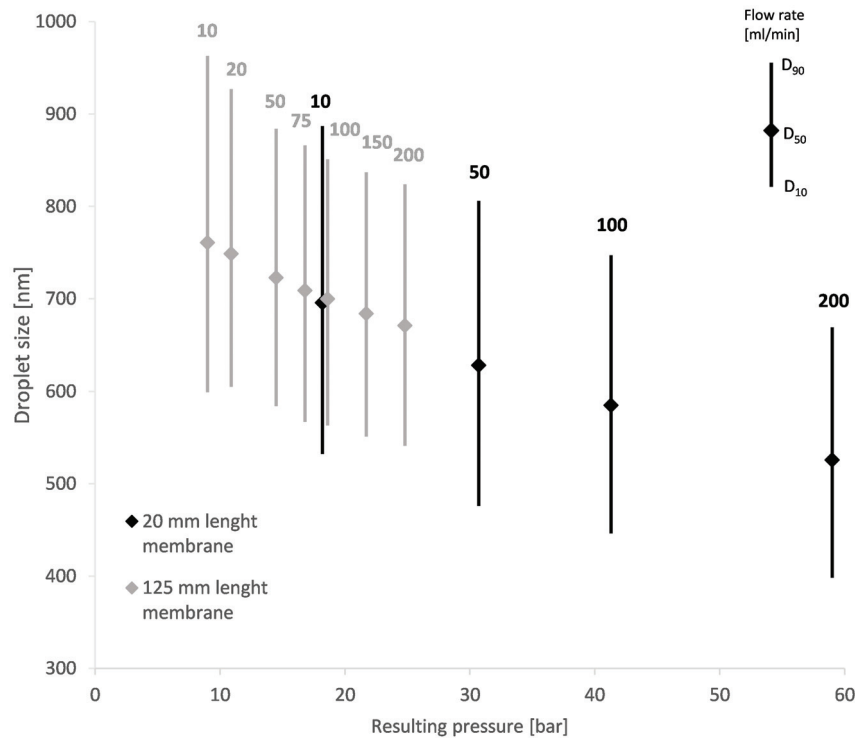


Figure 3.6: Droplet size as a function of resulting pressure for different membrane length and different flowrates with a  $0.5 \mu\text{m}$  pore size membrane at a composition of 10% EHP and 5% overall surfactant concentration

The resulting pressure shows the same trend: during the first cycle, it stabilized at 26.7 bar, at 10.2 bar during the second cycle and remained constant at  $8.45 \pm 0.4$  bar for all following cycles. The constant pressure obtained after the second cycle can be explained by the fact that no more droplet disruption occurred in the membrane pores, which means that  $\Delta P_{dis} = 0$  and therefore  $\Delta P_r = \Delta P_{flow} + \Delta P_{pipe}$  was constant. The effect of cycle number has been investigated previously with polymeric membranes for the preparation of nanoemulsions [8]. Polymeric membranes are very common in size reduction of liposomes with a technique called filter extrusion [118, 119], so their applications to the production of nanoemulsions is particularly attractive. In PME with polymeric membranes, several cycles were required to reach constant droplet size and dispersity. For polycarbonate membranes, about 10 cycles, depending on the flowrate, were needed and usually 21 extrusion cycles were performed with most polymeric membranes [110]. Our study confirms that SPG membranes decrease the cycle number needed compared to most polymeric membranes as previously reported [92]. This may be attributed to the higher tortuous pore structure and thickness of SPG membranes.

### 3.4.2 Composition parameters

All experiments in this section were performed with 125 mm length and  $0.5 \mu\text{m}$  pore size membrane. The premix was obtained by the same procedure for all experiments as described in Materials and Methods. The droplet size distribution of the premixes were similar for all experiments and are presented in section 3.1.3 and 3.1.5.

#### 3.4.2.1 Effect of oil concentration and viscosity

The effect of the dispersed phase concentration has been investigated at 6 concentrations from 1% to 40% and a flow rate of 150 mL/min. Flowrate of 200 mL/min could not be used at 40%

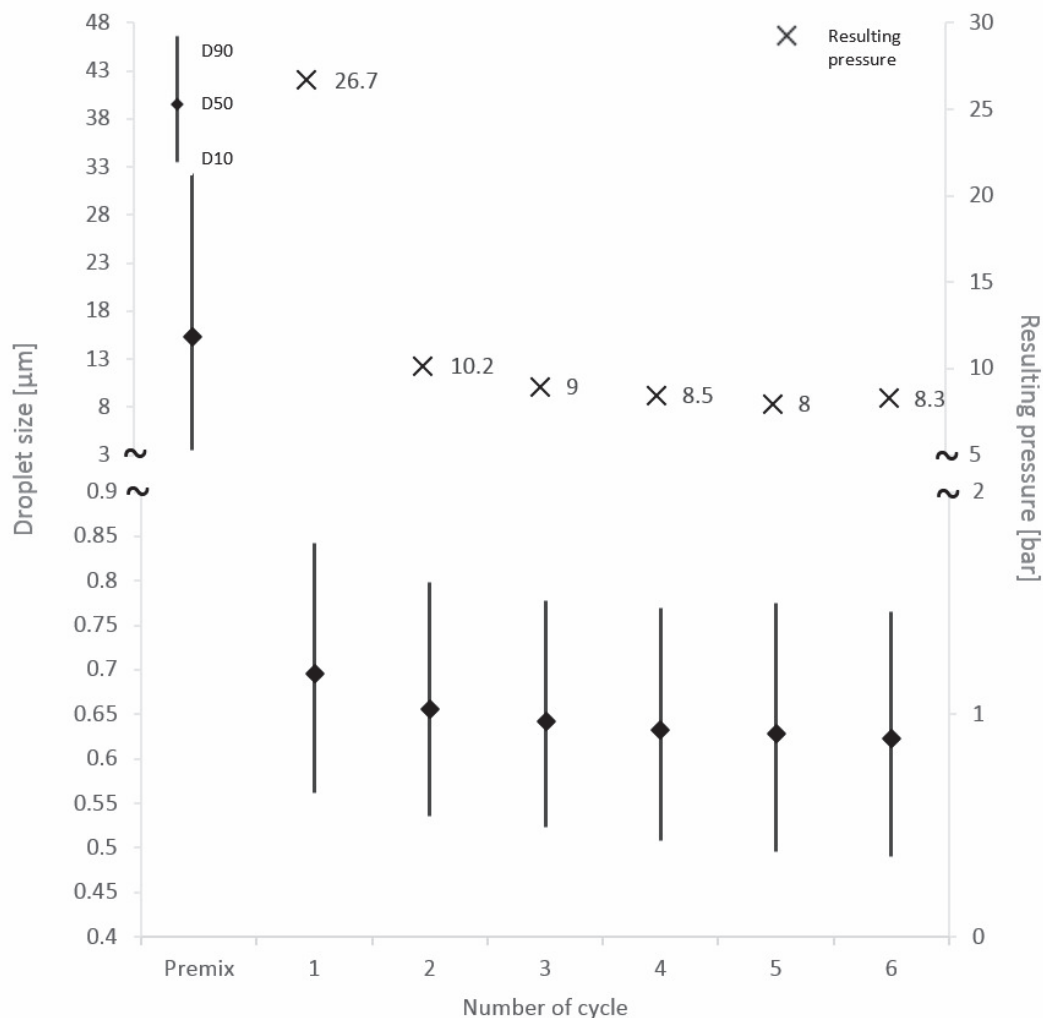


Figure 3.7: Droplet size and pressure variation with cycle number with 125 mm length and 0.5  $\mu\text{m}$  pore size membrane at 200 mL/min at a composition of 10% EHP and 5% overall surfactant concentration

of oil because the premix could not pass through the membrane at a pressure below 60 bar, so for all concentrations, the flow rate was set to 150 mL/min. In addition, for all preparations, the surfactant concentration to oil concentration ratio was 0.5 in order to have the same stabilization conditions. The effect on droplet size and resulting pressure is presented in Figure 3.8. The resulting pressure increased proportionally to the oil concentration with a regression coefficient  $R^2 = 0.96$ . On the other hand, the viscosity of the nanoemulsions also increased with oil content but at a much higher rate (Figure 3.9). The increase in pressure was multiplied by around 2 to from 20 % to 40 %, while the increase in dynamic viscosity was multiplied by around 4. Indeed, an increase in oil content led to an increase in  $\Delta P_{dis}$  as a result of the larger volume of droplets to be disrupted. Also,  $\Delta P_{flow}$  and  $\Delta P_{pipe}$  increased due to the higher viscosity of the nanoemulsion. Both phenomenon led to an overall increase of  $\Delta P_r$ . However, the viscosity may have less impact than oil concentration as  $\Delta P_r$  increased linearly with oil percentage and not exponentially like the viscosity.

In addition, droplet size were expected to remain constant as surfactant to oil ratio has been kept constant, but surprisingly droplet size decreased proportionally to the oil content. This can be explained as the overall concentration of surfactant increased with oil concentration even if the ratio was maintained constant. Break-up due to interfacial tension effects [88] might be more effective and so led to smaller droplets. It can be also explained as the increase of viscosity of emulsion in-

creases with increasing oil content, leading to increased shear stress inside the membrane pores and smaller droplet size[62]. Disruption at 40% oil concentration was very effective and resulted in droplet with droplet size around 502 nm close to membrane pore size.

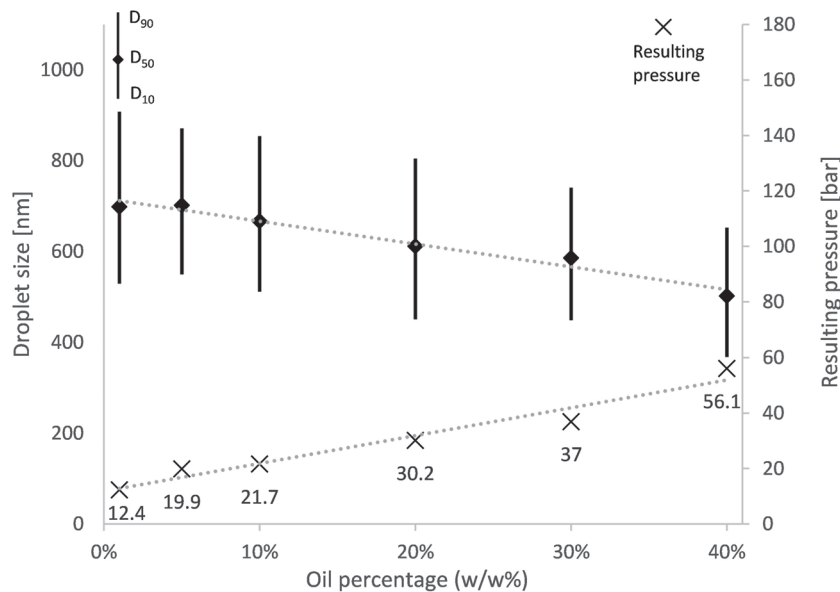


Figure 3.8: Droplet size and pressure variation as a function of oil weight percentage in the formulation with 125 mm length and 0.5  $\mu\text{m}$  pore size membrane at 150 mL/min

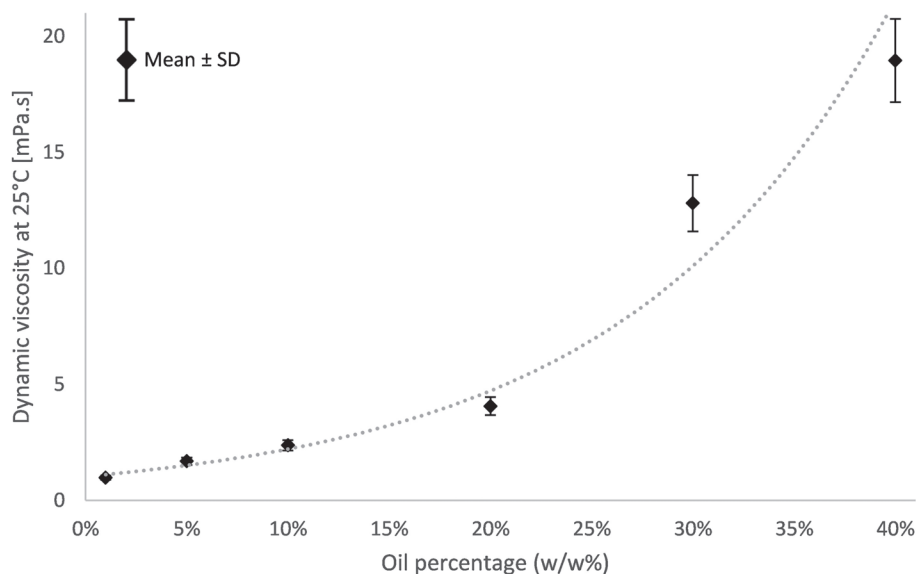


Figure 3.9: Dynamic viscosity variation as a function of oil weight percentage in the formulation

### 3.4.2.2 Effect of surfactant concentration

The effect of surfactant concentration has been tested from 2.5 % to 20 % maintaining EHP concentration at 10% and at 200 mL/min (Figure 3.10). Droplet size decreased with surfactant concentration, from 677 nm to 570 nm, respectively at 2.5 % and 20 %. The decrease in droplet size

can be explained by the fact that surfactant concentration governs two phenomena, first, the interfacial tension that induces break-up due to Rayleigh and Laplace instabilities [88] and secondly the adsorption kinetic of the surfactant at the interface [79]. Kinetic of adsorption of the surfactant at the newly created interfaces depends on the local concentration of surfactant in both phases. At high surfactant concentrations, the resulting droplets are stabilized faster than at low concentrations, so there is not sufficient time for droplet coalescence to occur and the resulting droplet size is smaller.

The resulting pressure decreased when increasing the surfactant concentration from 33.1 bar to 17.7 bar, respectively at 2.5 % and 20 % of total surfactant. However, dynamic viscosity of the premix emulsion increased significantly when increasing surfactant concentration as Tween 20 and Span 80 are viscous liquids. Similarly to the previous section, viscosity may not be a major parameter that can explain the  $\Delta P_{dis}$  variation. Indeed,  $\Delta P_{dis}$  decreased because disruption required less energy when more surfactants are used in the formulation. However, the pressure stabilized at about 15 bar at higher surfactant concentration. At the highest pressure of 33.1 bar, the 2.5 % surfactant concentration did not lead to smallest droplets compared to what was observed previously where the highest resulting pressure gave the smaller droplet size. This confirms that interfacial tension at equilibrium and dynamic interfacial tension are key factors that govern the resulting pressure and droplet size in PME for nanoemulsions production. This was already pointed out for the preparation of emulsions by PME [90, 100].

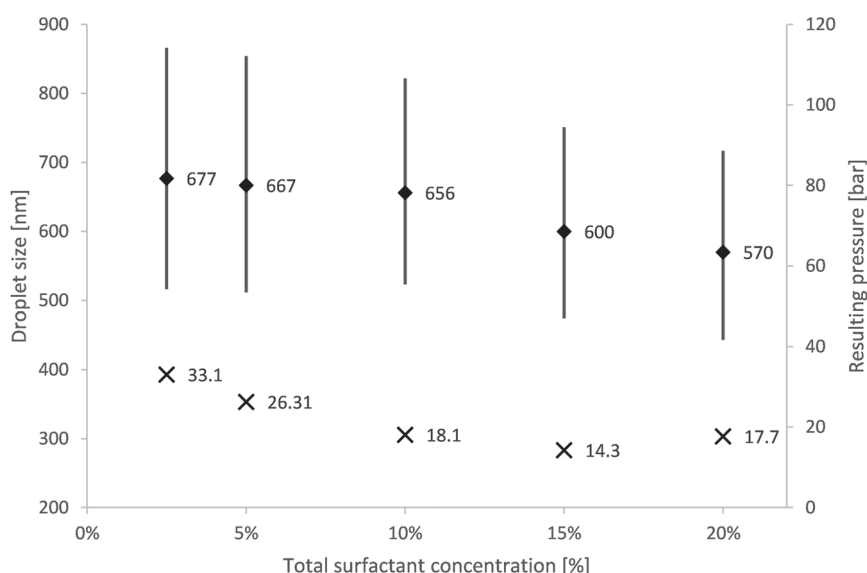


Figure 3.10: Evolution of droplet size and resulting pressure with total surfactant concentration with 125 mm length and 0.5  $\mu\text{m}$  pore size membrane at 200 mL/min at 10% EHP concentration

### 3.4.3 Stability

All nanoemulsions have been tested in stability at room temperature by measuring the droplet size distribution versus time by DLS and LD. Depending on droplet sizes, dispersions suffered reversible process of creaming, at different kinetics due to the difference in density between the dispersed and the continuous phases. However none of them showed irreversible coalescence leading to significant increase in droplets sizes within 9 months. On Figure 3.11, size distributions of nanoemulsion obtained with a 125 mm length and 0.2  $\mu\text{m}$  pore size membrane at 5 mL/min are presented as an example of all stability results obtained. It was observed that DLS measurements obtained with the distribution method and LD measurements did not give exactly the same size distribution and mean droplet size (Figure 3.11). The average size are not expressed by the same

parameters: Z-average measured by cumulant method by DLS and  $D_{50}$  by LD, derived from size distribution in intensity and volume respectively. The measurements are also based on different principles. Nevertheless, both methods suggest no significant increase in droplet size within 9 months at room temperature. This means that no irreversible phenomenon such as coalescence or Ostwald ripening occurred. Nanoemulsions formed were very stable because the amount of surfactant was sufficient for long term stability. Moreover, the energy input in PME was not sufficient enough to create new interfaces that are not well stabilized by surfactant. In addition, PME creates nanoemulsions with low polydispersity which are less sensitive to Ostwald ripening. This long term stability is sufficient for applications in cosmetics or pharmaceuticals.

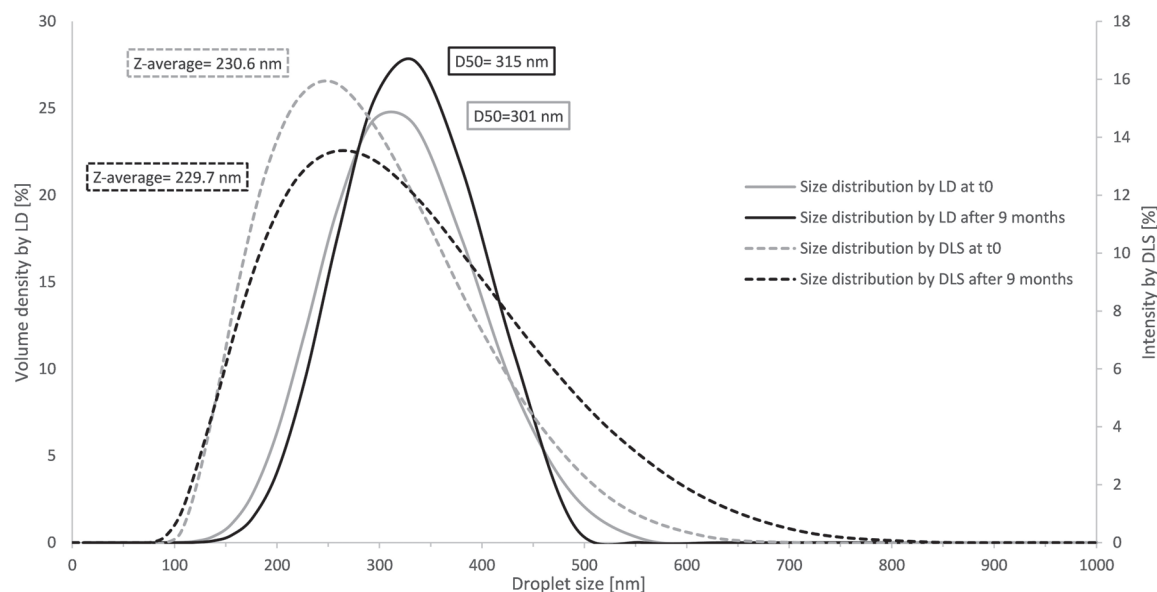


Figure 3.11: Example of nanoemulsion stability observed at 9 months for nanoemulsion obtained with a 125 mm length and 0.2  $\mu\text{m}$  pore size membrane at 5 mL/min

### 3.5 Conclusion

In this study, O/W nanoemulsions were prepared successfully by PME and SPG membranes at high flowrate. For that, a controlled set-up was developed including a high pressure syringe pump with data acquisition. Maximum values were respectively for the pressure, volume of premix treated and flowrate: 60 bar, 500 mL and 200 mL/min, except for the membranes with the smaller pores which were used at lower flowrates (respectively 10 mL/min and 5 mL/min with the 0.3  $\mu\text{m}$  and 0.2  $\mu\text{m}$  membrane) to keep the pressure below 60 bar. The effect of several parameters was investigated, related to the process: volume of premix, membrane pore size, flowrate, cycle number and formulation: oil and surfactant concentrations. The process was shown to be scalable up to 500 mL. Indeed, 500 mL of nanoemulsions produced had the same droplet size as 40 mL. In addition, the pressure was constant during injection of 500 mL which suggested no membrane filtration, no membrane fouling or change in the nanoemulsion obtained.

The resulting pressure was found to be a key parameter which governed the production of nanoemulsions by PME. First, it has to be minimized so the premix can pass through the membrane pores at moderate pressure. Then, pressure controlled transmembrane flux and therefore wall shear stress inside the micropores which allowed droplet disruption. In general, nanoemulsions with smaller droplets were obtained at higher pressures. The resulting pressure was the sum of  $\Delta P_{flow}$ ,  $\Delta P_{dis}$  and  $\Delta P_{pipe}$ . For each parameter investigated, the relative influence of these three terms was discussed.

In addition, the droplet size of the nanoemulsion product was highly dependent on other process parameters or formulation. In particular, a linear relationship was found between droplet size and pore size which suggests that the droplet size can be easily tuned. Parameters which influence the emulsion characteristics at micro-scale are also important at nano-scale. However, the formulation characteristics such as oil or surfactant concentrations appeared to have a greater effect than expected. As the oil/water interface increased with a decrease in droplet size, the effect of oil and surfactant concentration seems more important at nano-scale.

In conclusion, this study showed that PME with SPG membranes produced monodisperse nanoemulsions down to 260 nm with controlled size and very long stability over time. The nanoemulsions were produced in only one cycle at moderate pressure, which can be appropriate for encapsulation of sensitive actives. The technique is expected to be scalable to larger volumes and used as a continuous process with two high pressure syringe pumps in parallel.

## **Acknowledgment**

This work was supported by PeptiCaps project. This project has received funding from the European Union's Horizon 2020 Research and Innovation program under Grant Agreement n°686141.



# Chapter 4

## Influence of viscosity for oil-in-water and water-in-oil nanoemulsions production by SPG premix membrane emulsification

### Contents

---

<b>3.1 Abstract</b> . . . . .	<b>75</b>
<b>3.2 Introduction</b> . . . . .	<b>75</b>
<b>3.3 Materials and methods</b> . . . . .	<b>77</b>
3.3.1 Materials . . . . .	77
3.3.2 Experimental set-up . . . . .	77
3.3.3 Membranes . . . . .	78
3.3.4 Formulation of nanoemulsions . . . . .	78
3.3.5 Preparation of nanoemulsions . . . . .	78
3.3.6 Membrane cleaning . . . . .	78
3.3.7 Particle size distribution measurements . . . . .	79
3.3.8 Viscosity measurement . . . . .	79
<b>3.4 Results and discussion</b> . . . . .	<b>79</b>
3.4.1 Process parameters . . . . .	79
3.4.2 Composition parameters . . . . .	84
3.4.3 Stability . . . . .	87
<b>3.5 Conclusion</b> . . . . .	<b>88</b>

---

## Preamble

PeptiCaps European project also required the production of W/O nanoemulsions with a membrane process at pilot scale. As seen on section 3.4.2.1, the preparation of viscous O/W emulsions was already a challenge because of a drastic increase of pressure with viscosity increase.

This can explain why, in the literature, as seen on section 1.2.4, only a few authors reported the production of W/O emulsions with PME and none of them reported the production of nanoemulsions.

Moreover, to our knowledge, the influence of dispersed phase viscosity, has never been investigated in the literature.

In this study, the first aim was to produce W/O nanoemulsions with the set-up developed and presented in Chapter 2. However, the characterization of W/O nanoemulsions being a challenge, it was easier to investigate the viscosity parameters on O/W nanoemulsions production with PME than with W/O nanoemulsions. So, we first investigated the parameters of interest, the continuous and dispersed phase viscosities, the dispersed phase content for O/W nanoemulsion and then ensured that the same effect were observed with W/O nanoemulsions.

Moreover, in this study, the resulting pressure measured was analyzed in details. The resulting pressure was the sum of three different pressures:

- The pressure generated by the flow through the pipe,  $\Delta P_{pipe}$
- The pressure generated by the flow through the membrane,  $\Delta P_{flow}$
- The pressure required to break up the droplets inside the membrane pores,  $\Delta P_{dis}$

With this approach, it was expected to gain a better understanding on parameters influence on resulting pressure.

# Influence of viscosity for oil-in-water and water-in-oil nanoemulsions production by SPG premix membrane emulsification

*O. Alliod, L. Messenger, H. Fessi, D. Dupin, C. Charcosset*

**Chemical Engineering Research and Design (submitted, 2018)**

## 4.1 Abstract

Oil-in-water and water-in-oil nanoemulsions are interesting carriers for respectively oil soluble and water soluble actives. In this study, oil-in-water (O/W) and water-in-oil (W/O) nanoemulsions were prepared by premix membrane emulsification. A coarse emulsion (premix) was injected thanks to a high pressure pump through a Shirasu Porous Glass (SPG) membrane with pore size of 0.5  $\mu\text{m}$  in order to reduce and homogenize the droplet size. The effect of viscosities on the pressure and droplet size was investigated: the water phase viscosity by increasing glycerol concentration, the oil phase viscosity with mineral oils of different viscosities and the overall emulsion viscosity by increasing the dispersed phase content of the emulsion. The pressure required to break up the droplets inside the membrane pores  $\Delta P_{dis}$  did not depend on viscosities, while the pressures generated by the flows through the pipe  $\Delta P_{pipe}$  and the membrane  $\Delta P_{flow}$  were proportional to the viscosity of the overall emulsion. W/O nanoemulsions were more difficult to produce and to characterize but thanks to the original set-up working at pressures up to 65 bar and high flowrates, W/O mineral oil nanoemulsions were produced with mean droplets size around 600 nm and flow rate of 50 mL/min.

## 4.2 Introduction

Nanoemulsions, defined by their droplet size which has to be within the submicron range, show improved stability and delivery properties [3, 120, 121, 44]. They can be oil-in-water emulsions (O/W) with the oil phase dispersed into the water continuous phase, or water-in-oil emulsions (W/O) when the aqueous phase is dispersed into the oily continuous phase. W/O nanoemulsions can also be incorporated into a second water phase to create double water-in-oil-in-water emulsions (W/O/W) which have several applications in cosmetics or pharmaceuticals [122].

W/O and O/W nanoemulsions can be produced by different techniques [123]. For exemple, sonication and high pressure homogenization (HPH), are suitable for different types of formulations as intensive disruptive forces breakup the oil and water phases creating droplets [44]. However, sonication is not scalable and usually broad droplets size distributions are obtained, and HPH requires several cycles in order to obtain monodispersed droplets.

Membrane emulsification is a more recent process, that also uses mechanical forces but with less energy which give significant advantages over other processes [64, 114]. Membrane emulsification can be performed either by direct (DME) or premix emulsification (PME), that has several advantages for the production of nanoemulsions such as higher flowrates [124]. In PME, a coarse emulsion is pushed through the membrane pores, reducing the droplet size and size distribution. However, the production of nanoemulsions by membrane emulsification is challenging even with PME [56].

Bunjes et al. prepared nanoemulsions by PME with droplet size lower or around 200 nm with narrow size distribution with polymeric membranes and SPG membranes for volumes up to 10

mL. [92, 110, 94]. In a previous work, we reported the production of O/W nanoemulsions by PME and SPG membranes at high flowrate and relatively large volumes up to 500 mL [124].

In both DME and PME, the viscosities of the continuous and dispersed phase are important parameters, although their effect has been investigated by few authors. For example, Vladislavljević et al. studied the viscosity in PME by increasing the dispersed phase content which increased the overall emulsion viscosity [62] or the continuous phase viscosity [90]. Both studies were performed at constant pressure and showed that an increase in viscosity led to a decrease in trans-membrane flux and to smaller oil droplets due to increase of wall shear stress inside the membrane pores.

Also, in DME, only few studies reported the production of W/O emulsions, mainly micron size emulsions with kerosene as the continuous phase with different types of membranes or surface modifications [125, 126, 127] or with toluene [128]. A study reported the production of W/O emulsions suitable for cosmetics or dermatological applications with mineral oil as the continuous phase [129]. For double emulsion production, the first W/O emulsions has always been obtained by a high energy process [62, 56, 6]. To our knowledge, only a few studies reported the production of W/O emulsion by PME. It can be explained by the fact that viscous emulsions generate high pressure through the membrane pores [124]. Zhou et al. [61, 60, 106] produced W/O emulsions of minimum 5  $\mu\text{m}$  droplet size with low viscous oil between at higher temperature in order to lower the viscosity. Also, Liu et al. [106] performed PME with a premix of median size smaller than the pore size with the only purpose to homogenize the sample. This can explain why the required pressure for W/O PME was achievable.

In the present study, O/W and W/O nanoemulsions were produced by PME with a high pressure pump that pushed the premix through the SPG membrane. The resulting pressure  $\Delta P_r$  was equal to the sum of the flow pressure  $\Delta P_{flow}$ , the disruption pressure  $\Delta P_{dis}$  and the pipe pressure  $\Delta P_{pipe}$ :

$$\Delta P_r = \Delta P_{flow} + \Delta P_{dis} + \Delta P_{pipe} \quad (4.1)$$

The flow pressure was the pressure necessary to pass the premix emulsion through the very small membrane pores. The disruption pressure ( $\Delta P_{dis}$ ) was the pressure required to break the premix emulsion into smaller droplets and therefore reducing the droplet size [62]. Moreover, the pressure along the pipe from the high pressure pump to the membrane module was dependent on fluid viscosity and therefore had to be taken into account. This pressure was termed pipe pressure  $\Delta P_{pipe}$  and was measured without the membrane.  $\Delta P_{flow}$  and  $\Delta P_{dis}$  are pressures generated by the fluid circulating through the membrane  $\Delta P_{membrane}$ :

$$\Delta P_{membrane} = \Delta P_{flow} + \Delta P_{dis} \quad (4.2)$$

In this study, we investigated the effect of viscosity of the dispersed, continuous phase and overall emulsion, on the production of W/O and O/W nanoemulsions by PME. The final aim is to optimize the preparation of W/O nanoemulsions, which is challenging due to high viscosities involved. For that, O/W and W/O premixes with different viscosities were produced. The influence of viscosity was investigated by modifying the continuous phase viscosity, the dispersed phase viscosity, and the dispersed phase content, with all phases and final products being Newtonian fluids. The water phase viscosity was modified by adding glycerol and the oil phase viscosity was modified by using different mineral oils with similar interfacial tension with water. The premixes were pushed through the membrane pores using a high pressure pump in the set-up developed previously for O/W nanoemulsions production [124]. The influence of the formulation on the resulting pressure and on  $\Delta P_{flow}$ ,  $\Delta P_{dis}$  and  $\Delta P_{pipe}$  was investigated. The nanoemulsions obtained were characterized by their mean droplet size and/or size distribution.

## 4.3 Materials and methods

### 4.3.1 Materials

Ultrapure water was obtained using a Synergy unit system (Millipore, France). Mineral oil of different viscosities were given by different suppliers: White Mineral Oil (WMO) from Fisher (USA)  $\eta=44$  mPa.s (at 25°C), Marcol 52 and Marcol 82 from Exxon mobil (France) respectively  $\eta=14.1$  mPa.s and  $\eta=24.1$  mPa.s (at 25°C). Other products were glycerol from Roth (Germany), Tween 20 and Span 80 from Sigma Aldrich (France) and Derquim+ from Derquim (Spain).

### 4.3.2 Experimental set-up

The experimental set-up used for the preparation of nanoemulsions by PME is shown in Figure 4.1 and described in a previous work [124]. The set-up was composed of a high pressure benchtop single cylinder pump BTSP 500-5 (Floxlabs, Nanterre, France) and a membrane module from SPG Technology Co. Ltd (Miyazaki, Japan)

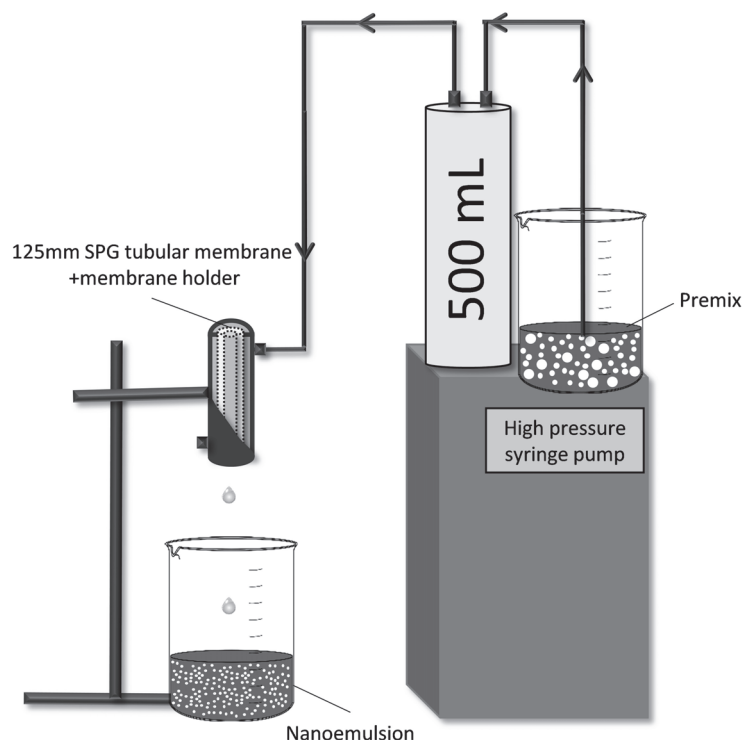


Figure 4.1: Experimental set-up of the high syringe pump with membrane holder and SPG membrane

For each premixes, the set-up resistance to the flow without the membrane module was tested at different flowrates between 10 and 200 mL/min and the resulting pressure,  $\Delta P_{pipe}$ , was measured.

### 4.3.3 Membranes

Hydrophilic and hydrophobic SPG membranes were provided by SPG Technology Co. Ltd (Miyazaki, Japan). Hydrophilic SPG membranes were used for O/W nanoemulsion production and hydrophobic for W/O nanoemulsions. Both membranes are first produced the same way, hydrophobic membranes are then obtained thanks to a special coating made by the supplier. The membranes are tubular with an inner diameter of 8.5 mm, thickness of 0.8 mm and length of 125 mm.

	Content in (w/w%)			Dynamic viscosity at 25°C
	WMO	Marcol 82	Marcol 52	
<b>WMO</b>	100%	X	X	44.1
<b>Marcol 82</b>	X	100%	X	24.1
<b>WMO+ M82</b>	50%	50%	X	30.6
<b>Marcol 52</b>	X	X	100%	9.87

Table 4.1: Composition and dynamic viscosities of oils used to study the influence of dispersed phase viscosity

In all experiments, the membrane length was 125 mm and the mean pore size 0.5  $\mu\text{m}$ . The membranes were able to resist to transmembrane pressure up to 65 bar.

The cross-flow tubular module was adapted to be used in PME. The effective length of the membranes was reduced due to sealing rings placed at both ends of the membrane tube. Therefore, the effective length was 115 mm and the effective membrane area was 30.70  $\text{cm}^2$ .

#### 4.3.4 Formulation of nanoemulsions

Oil phases compositions studied and viscosities measured with the method detailed in the following viscosity measurement part, are described in Table 4.1.

For O/W nanoemulsions, ultrapure water with or without glycerol was used as the continuous phase and mineral oils as the dispersed phase. The required HLB (RHLB) of mineral oils were all the same and given by the supplier as RHLB=10. The surfactant system chosen to stabilize the nanoemulsions was Tween 20, HLB= 16.7, as the hydrophilic surfactant and Span 80, HLB= 4.3, as the hydrophobic surfactant. In most experiments, the composition (in weight percentage of the total emulsion) was for the continuous phase, 2.3 % Tween 20 and 85 % water, and for the dispersed phase 2.7 % Span 80 and 10 % oil. The overall surfactant concentration was then 5%. The surfactants and high concentrations were chosen to ensure that the newly formed droplets were immediately covered with surfactants, hence preventing the increase in droplet size.

Three oils with different viscosities were investigated, WMO, Marcol 82 and Marcol 52 and a mixture of WMO and Marcol 82 (Table 4.1). The influence of oil concentration was investigated at 5, 10, 20, 25 and 30 % for Marcol 82. The surfactant concentration to oil concentration ratio was kept constant at 0.5, so the total surfactant concentration in the formulation was respectively 2.5, 5, 10, 12.5 and 15 %. In addition, the influence of glycerol concentration was investigated at 10, 25, 50 and 62.5 % of the aqueous phase completed with water up to 85% of the total formulation. For W/O nanoemulsions, mineral oils as supplied or mixtures of mineral oils were used as the continuous phase and ultrapure water with or without glycerol as the dispersed phase. RHLB of mineral oils were all the same and given by the supplier as RHLB=5. In most experiments, the composition (in weight percentage of the total emulsion) was for the continuous phase, 0.28 % Tween 20 and 85 % oil, and for the dispersed phase 4.72 % Span 80 and 10 % water. The overall surfactant concentration was then 5%. The oil phases investigated were pure WMO, Marcol 82 or Marcol 52 or a mixture of WMO and Marcol 82 (Table 4.1).

The influence of water concentration was investigated at 1, 5, 10 and 15 %. The surfactant concentration to oil concentration ratio was kept constant at 0.5, so the total surfactant concentration in the formulation was respectively 0.5, 2.5, 5 and 7.5 %. In addition, the influence of glycerol concentration was investigated at 25, 50, 75 and 100 % of the aqueous phase completed with water up to 10% of the total formulation.

#### 4.3.5 Preparation of nanoemulsions

Both phases were first prepared separately. For O/W nanoemulsions, the continuous phase was obtained by dissolution of Tween 20 in water or water with glycerol under magnetic stirring at

600 rpm and the dispersed phase by dissolution of Span 80 in the oil using the same procedure. For W/O nanoemulsions, the continuous phase was the oil mixed with Span 80 and the dispersed phase Tween 20 in water or water and glycerol.

In both cases, the two phases were then mixed with magnetic stirrer for 10 min to produce the premix. This premix was then placed in the feed tank and pumped in the syringe pump. First 20 mL premix was injected in order to remove air from the experimental set-up and fill it with premix. The experiment was then carried out with a volume of injection of 40 mL to minimize time and material consumption. The nanoemulsion produced flew from the membrane tube under gravity and was collected in a beaker placed beneath the module. All experiments were performed at room temperature and for each conditions five different flow rates were investigated depending of composition between 10 and 100 mL/min.

### 4.3.6 Membrane cleaning

For O/W nanoemulsions, before each use, the membrane was carefully cleaned until recovery of its hydrodynamic resistance to water ( $R_m$ ). For hydrodynamic resistance measurements, water was permeated through the membrane at different flowrates between 10 and 200 mL/min and the resulting pressure was measured.  $R_m$  was estimated from the slope of the ultrapure water flowrate versus resulting pressure [47]. The cleaning procedure consisted in three injections through the membrane of 500 mL of a 1 % Derquim + solution [57] at 70°C at 200 mL/min and then three injections of 500 mL of pure water at room temperature and 200 mL/min. The membrane resistance to water was recovered after this treatment.

For W/O nanoemulsions, membrane was carefully cleaned with Span 80 in Marcol 82 until a clear solution was recovered and pressure stabilized. Filling the membrane with oil allows a better flow of the emulsion through the membrane [129].

### 4.3.7 Particle size distribution measurements by laser diffraction

The droplet size of emulsions were measured by Laser Diffraction (LD) particle size analysis with a Mastersizer 3000 (Malvern Instruments, France). The technique is based on measurement of the intensity of light scattered as a laser beam passes through a dispersed particulate sample. The Mie scattering theory was used, with a refractive index and an absorption index set at 1.47 and 0.005 for the oil phase, respectively and 1.33 and 0.005 for the water phase. For O/W nanoemulsions, the continuous phase was ultrapure water and for O/W, Marcol 82. Before measuring the droplet size of W/O nanoemulsions the instrument, including injection line and measurement cell, was emptied, cleaned with surfactant, filled with ethanol, dried and fill with oil. The same procedure was used to clean the apparatus after measurement.

The results were expressed by  $D_{50}$  the mean droplet diameter for which 50 % of droplets in volume are below this size, similarly 90 % lie below  $D_{90}$  and 10 % below  $D_{10}$ .  $D_{90}$  and  $D_{10}$  giving information about the sample dispersity. The closest they are to the  $D_{50}$  the more monodisperse the distribution is.

All measurements were done in triplicate, the values reported were the average of the three measurements.

### 4.3.8 Viscosity measurements

For the investigation of the effect of oil concentration, the dynamic viscosity of the emulsions, continuous phase and dispersed phase were measured. The measurements were realized using a rheometer MCR 302 equipped with the CP50 module and the software Rheocompass (Anton Paar, France) at 25°C. Viscosity was measured with a shear rate from 0 to 100  $s^{-1}$ .

## 4.4 Results and discussion

In this section, we first measured the pressure generated through the pipe connecting the pump to the membrane module. This pressure is then substrated to the resulting pressure measured during the preparation of nanoemulsions to obtain the membrane pressure. Then, results obtained for O/W and W/O nanoemulsions are presented including the effect of continuous phase viscosity, dispersed phase viscosity and dispersed phase content, which determines the viscosity of the overall emulsion, on membrane pressure and droplet size. Also, for both O/W and W/O nanoemulsions, the disruption pressure and flow pressure were determined from the influence of the cycle number on the membrane pressure.

### 4.4.1 Influence of viscosity on $\Delta P_{pipe}$

The pressure generated by the pump through the pipe connecting the pump to the membrane module was measured for different premixes at flowrates from 10 to 100 mL/min. For that, the premix was injected through the pipe without the membrane module being connected. The resulting pressure measured was then equal to  $\Delta P_{pipe}$ . All premixes tested were Newtonian and the flows through the pipe were laminar. The hydraulic resistances measured were specific to pipe used (length, diameter, elbows).

Figure 4.2 shows the pressure variation with flowrate for different O/W premixes. Two types of premixes were prepared: premixes with water as the continuous phase (without glycerol) and different Marcol 82 content (from 10 to 30%) and premixes with 10% Marcol 82 and different contents of glycerol in the water phase (10 to 62.5% glycerol).  $\Delta P_{pipe}$  was found proportional to the flowrate, as predicted by the Poiseuille equation, with the hydraulic resistance dependent on the premix composition. Figure 4.3 shows the variation of the hydraulic resistance through the pipe versus the premix viscosity. As expected from Poiseuille's law, the hydraulic resistance was proportional to the premix viscosity. Figure 4.3 also includes hydraulic resistances obtained with W/O premixes in a similar way as O/W premixes.

For O/W premixes, the pressure generated through the pipe was in the range 0-3 bar, except for the higher content of glycerol (up to 6 bar). For W/O premixes, higher values were obtained, from 2 to 18.6 bar. In the following parts, to obtain the pressure generated through the membrane  $\Delta P_{membrane}$  during the preparation of nanoemulsions,  $\Delta P_{pipe}$  was subtracted from the resulting pressure  $\Delta P_r$ .

### 4.4.2 O/W nanoemulsions

In this section, we prepared O/W nanoemulsions with different compositions as described in Materials and Methods. The influence of the continuous phase viscosity, dispersed phase viscosity as well as the dispersed phase content on the droplet size and membrane pressure was investigated. Also,  $\Delta P_{dis}$  and  $\Delta P_{flow}$  were determined from the effect of the cycle number on the membrane pressure.

#### 4.4.2.1 Influence of the continuous phase viscosity

The effect of the continuous phase viscosity was investigated at four different glycerol concentrations in the continuous water phase, 10, 25, 50, 62,5 %, corresponding respectively to aqueous phase viscosities of 1.14, 1.79, 5.00 and 10.5 mPa.s. It was observed that at higher glycerol concentrations, the emulsion was non-Newtonian. The oil type, oil concentration and surfactant concentration were the same: 10% Marcol 82 and 5% total surfactant concentration. Figure 4.4 shows the membrane pressures measured at various flowrates.

The continuous phase viscosity had no influence on the membrane pressure at low flowrates (below 50 mL/min), and at higher flowrates and low continuous phase viscosity (below 1.79 mPa.s). In these conditions, the flow pressure was relatively low so the membrane pressure was mainly attributed to the disruption pressure. At higher flowrates and continuous phase viscosities, the

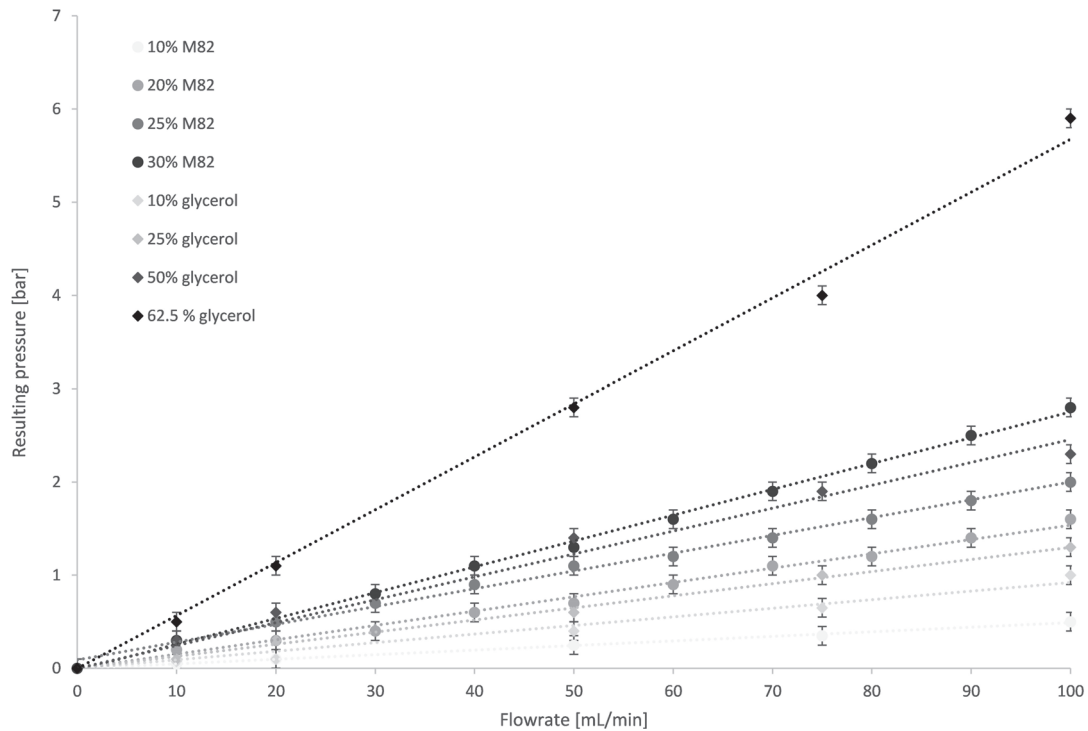


Figure 4.2: Resulting pressure,  $\Delta P_{pipe}$ , without membrane module for different O/W emulsions at flowrate from 10 to 100 mL/min

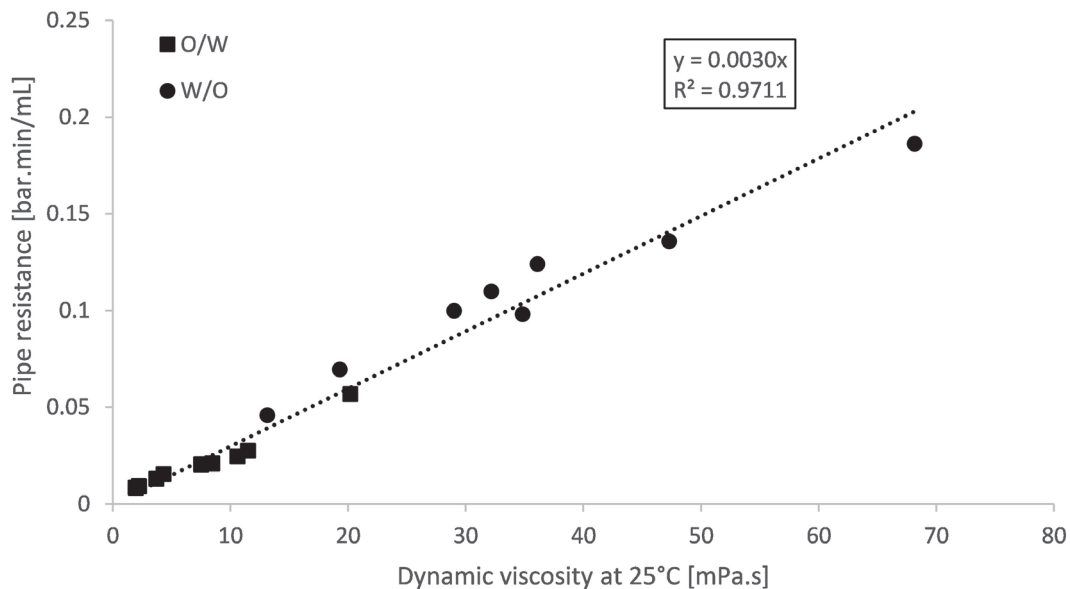


Figure 4.3: Slope of the resulting pressure,  $\Delta P_{pipe}$  with flow rate as a function of viscosity for O/W and W/O emulsions of different composition

membrane pressure increased when increasing the continuous phase viscosity. At 100 mL/min, the membrane pressure was 20.6 bar for a continuous phase viscosity of 10.5 mPa.s and around two times less 11.2 bar at 1.14 and 1.79 mPa.s. Indeed, the flow pressure  $\Delta P_{flow}$  is proportional to viscosity [62]. At higher viscosity of the continuous phase, the flow pressure was then much higher and might be in the same range as the disruption pressure.

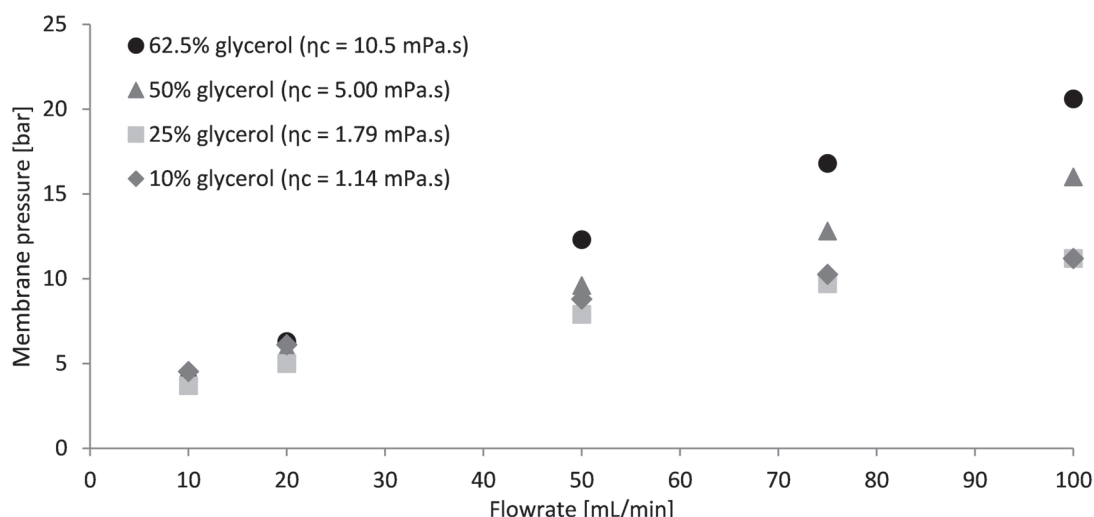


Figure 4.4: Membrane pressure variation with flowrate from 10 to 100 mL/min at four different concentrations in glycerol in the water phase and at 10 % of Marcol 82 and 5% surfactant

The influence of the continuous phase viscosity on the droplet size is presented in Figure 4.5. The mean droplet size decreased when increasing the viscosity of the continuous phase, as the shear stress within the pores increased, leading to a more significant size reduction [90]. At high viscosities, the shear stress obtained was very high, and very small droplets were obtained with  $D_{50}$  equal to 293 nm, which was 59% smaller than the membrane pore size. Figure 4.5 also shows that the viscosity of the overall emulsion increased proportionally to the continuous phase viscosity. It remains unclear whether the viscosity of the continuous phase, or the viscosity of the overall emulsion or both influence the membrane pressure and droplet size. This will be discussed in a following section.

#### 4.4.2.2 Influence of the dispersed phase viscosity

The influence of the dispersed phase viscosity on the membrane pressure and droplet size was investigated with four different oils: three mineral oils from different suppliers used as received: WMO, Marcol 82 and Marcol 52 and a mix of 50%/50% WMO and Marcol 82 (Table 4.1). The oil concentration and surfactant concentration were kept constant at 10% and 5%, respectively. The viscosities of the four emulsions were the same (4.3 mPa.s).

For the different oils, the membrane pressure and droplet size as a function of flowrate are presented in Figure 4.6. The membrane pressure did not change with the dispersed phase viscosity at low flowrates. However, at higher flowrates, from 75 mL/min, the membrane pressures were slightly higher for the more viscous oils. The difference between the less viscous oil Marcol 52 ( $\eta = 9.87$  mPa.s) and the more viscous WMO ( $\eta = 44.1$  mPa.s) which is more than four times more viscous, was of  $\Delta P_r, WMO - \Delta P_r, M52 = 20.5 - 18.6 = 1.9$  bar. This effect might be more important at higher flowrate or higher oil content.

The similar viscosities of the overall emulsions cannot be the reason of the increase in membrane pressure for the more viscous oils. This effect may be explained by the critical capillary number for breaking a drop in a T-junction (which is a simple model of a membrane pore) which is proportional to a dimensionless constant  $\alpha$ , function of the viscosity difference between the dispersed and continuous phases and the geometry of the channel [89]). As the oil viscosity increased, the viscosity difference between the two phases increased and so the capillary number. Droplet break-up became more difficult so the pressure needed for oil droplets disruption in the membrane pores  $\Delta P_{dis}$  became higher.

Moreover, the droplet size distribution did not change with the dispersed phase viscosity (Figure 4.6) at these experimental conditions. Figure 4.6 also shows a slight decrease in droplet size versus

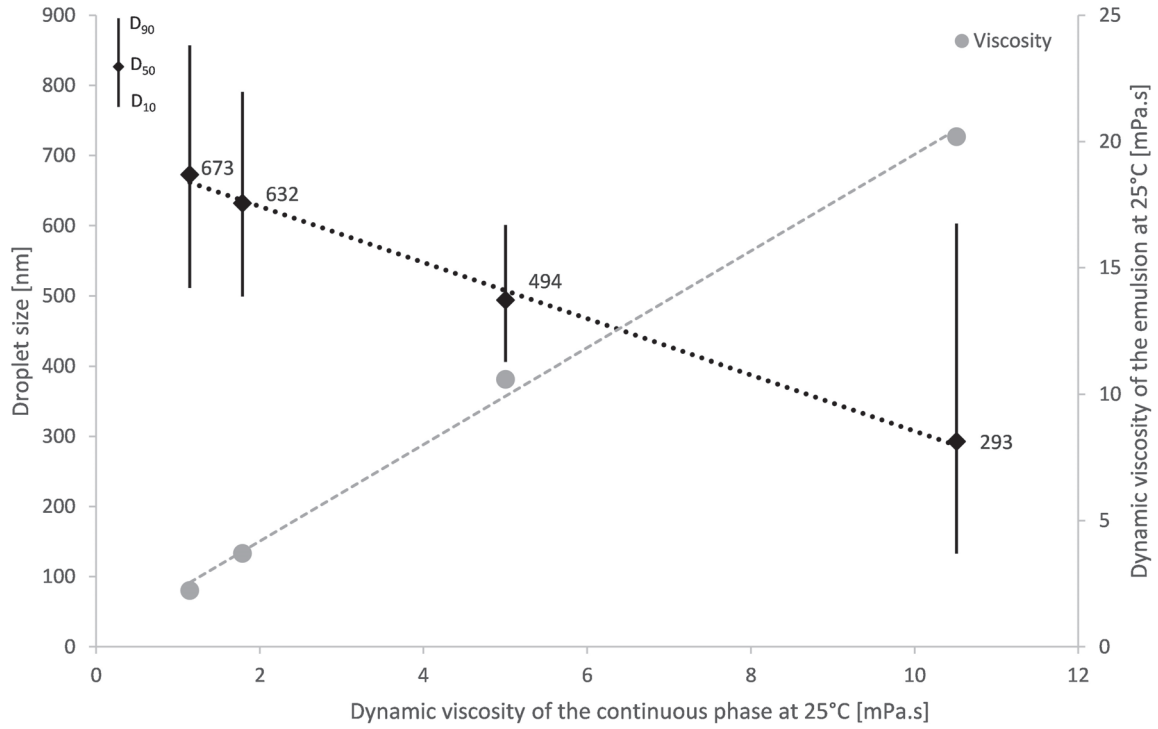


Figure 4.5: Droplet size and viscosity of the emulsion versus the viscosity of the continuous phase at 10 % of Marcol 82 and 5% surfactant and a flowrate of 100 mL/min

flowrate, as observed in our previous study with 10% ethylhexyl palmitate (EHP) as the dispersed phase and 5% total surfactant concentration [124].

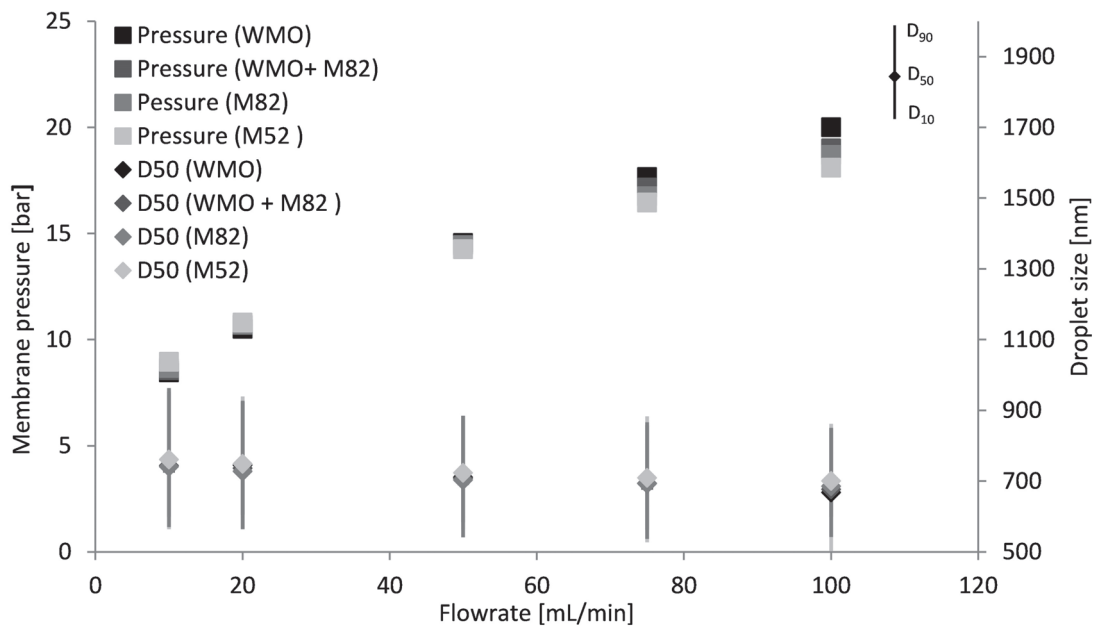


Figure 4.6: Membrane pressure and droplet size at different flowrates with different oils or oil mix at 10% and 5% overall surfactant concentration

#### 4.4.2.3 Influence of the dispersed phase content

The influence of the dispersed phase content on the membrane pressure and droplet size was investigated at four Marcol 82 concentrations 10, 20, 25 and 30% at 100 mL/min. Higher oil concentrations were not tested because of the non-Newtonian behavior of the emulsions. The viscosity of the overall emulsions increased with the amount of oil, 4.3, 7.05, 10.85 and 17.85 mPa.s for the 10, 20, 25, 30% oil concentrations, respectively.

As explained in Materials and Methods, the surfactant concentration based on the amount of oil was kept constant, corresponding to 2.3, 4.6, 5.75, and 6.9% Tween 20 in the continuous water phase, and 5, 10, 12.5, and 15 % total surfactant, for Marcol 82 concentrations of 10, 20, 25, 30%, respectively. Therefore, the continuous phases prepared at various oil contents had slightly different viscosities due to the different amounts of Tween 20 (1.03 mPa.s at lowest concentration of surfactant 2.3% and 1.39 mPa.s at highest concentration of surfactant, 6.9%). By varying the dispersed phase content, the viscosity of the overall emulsions changed, but the continuous phase viscosity remained constant.

Figure 4.7 shows the variation of the membrane pressure and droplet size versus the overall emulsion viscosity. As expected, the pressure through the membrane increased with the overall emulsion viscosity. The contribution of both  $\Delta P_{flow}$  and  $\Delta P_{dis}$  is presented in the next section.

Moreover, the droplet size decreased with the oil content and so with the emulsion viscosity (Figure 4.7). In Figure 4.5, the droplet size was proportional to the continuous phase viscosity and to the overall emulsion viscosity. In the present section, from a continuous phase viscosity of 1.95 mPa.s to 11.5 mPa.s (corresponding respectively to an oil content of 10 % and 30 %), the droplet size decrease was very small (687 nm to 586 nm). In addition, the continuous phase viscosity was nearly constant with the oil content. It might strongly indicate that the increase in shear stress suggested in section 3.2.2 is due to the continuous phase viscosity and not the overall emulsion viscosity.

It is also suggested that the droplet size decreased at higher oil concentrations due to the higher surfactant content present in the formulation. Indeed, an increase in surfactant percentage has three effects: a slight increase of the continuous phase viscosity which increases the shear stress within the pores, and also a decrease of the interfacial tension that induces break-up due to Rayleigh and Laplace instabilities [88] and an increase of the local concentration of surfactant, hence the adsorption kinetic at the newly created interfaces [79]. These two last effects could contribute to a decrease of the droplet size.

#### 4.4.2.4 Experimental determination of $\Delta P_{flow}$ and $\Delta P_{dis}$

To obtain the values of  $\Delta P_{flow}$  and  $\Delta P_{dis}$ , repeated cycles were realized. For that, the premix was passed first through the membrane, and then the nanoemulsions obtained was passed again during three cycles at 100 mL/min. The formulations investigated were those tested in the influence of the dispersed phase section : four Marcol 82 concentrations 10, 20, 25, 30%. The viscosity of the emulsions remained nearly constant with the number of cycles, with a slight decrease from the first pass to the second pass as the droplet size was reduced. The membrane pressures measured during each cycle are reported in Figure 4.8.

The membrane pressures were higher during the first cycles, but stabilized after first pass. For all cycles, the membrane pressure stabilized at a higher value for emulsions with a higher oil content. During the first cycle, the membrane pressure stabilized at 30.8 bar and 18.3 bar for emulsions containing 30% and 10% Marcol 82, respectively. During the fourth cycle, the membrane pressure stabilized at 14.5 bar and 3.7 bar for 30% and 10% Marcol 82, respectively. The membrane pressure remained constant after the first cycles as no more droplet disruption occurred in the membrane pores, which means that after the first cycles  $\Delta P_{dis}=0$  therefore  $\Delta P_m = \Delta P_{flow}$ .

The variations of  $\Delta P_{dis}$  and  $\Delta P_{flow}$  with the overall emulsion viscosity are presented in Figure 4.9.  $\Delta P_{m1}$  is the membrane pressure obtained during the first cycle. The stabilized pressure value  $\Delta P_{mf}$  was calculated as the average membrane pressure values of the two last cycles, cycles n°3 and n°4. As said previously, disruption occurs mainly during the first cycle, whereas most of the droplets do not undergo any droplet disruption for the following cycles. So,  $\Delta P_{dis} = \Delta P_{m1} - \Delta P_{mf}$

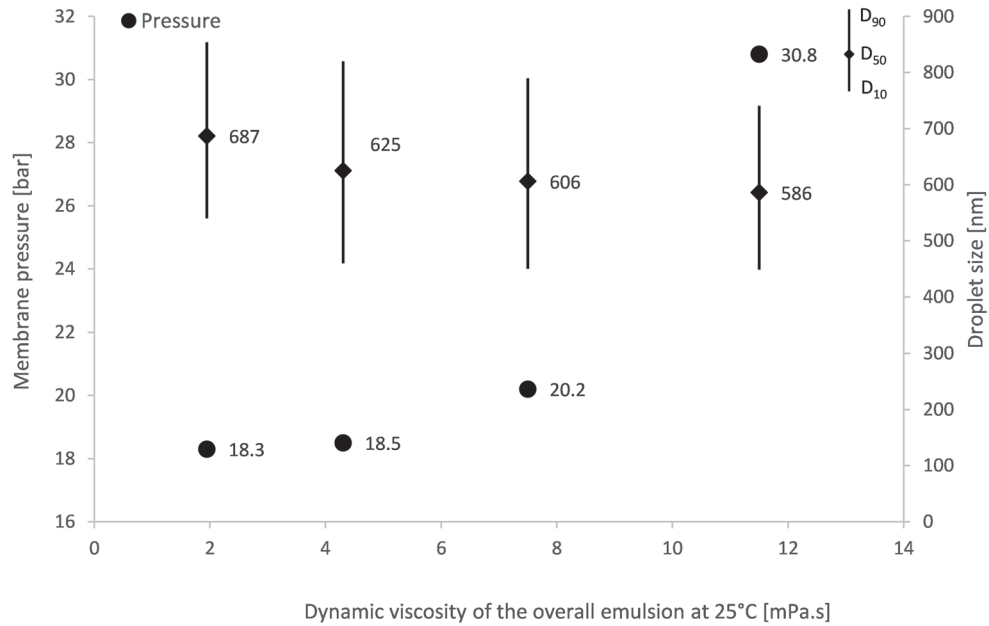


Figure 4.7: Membrane pressure and droplet size as a function of dynamic emulsion viscosity for different oil contents at 100 mL/min

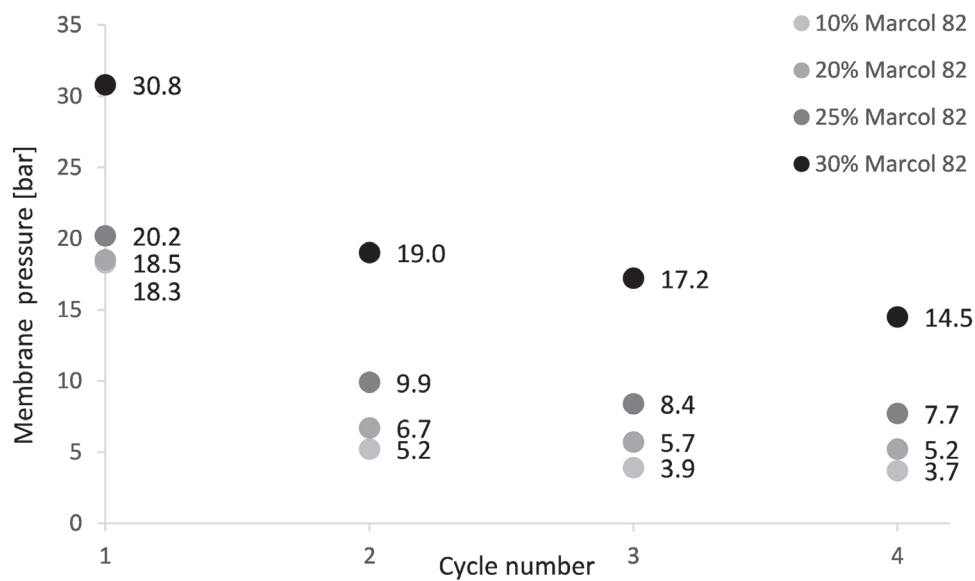


Figure 4.8: Membrane pressure as a function of cycle number for different Marcol 82 contents at a flowrate of 100 mL/min

and  $\Delta P_{flow} = \Delta P_{mf}$ .

Figure 4.9 shows that  $\Delta P_{dis}$  was independent of the overall emulsion viscosity. It means that the energy required for droplet disruption was the same for the various oil contents, if the oil to surfactant ratio was kept constant. As expected,  $\Delta P_{flow}$  was proportional to the emulsion viscosity [129].

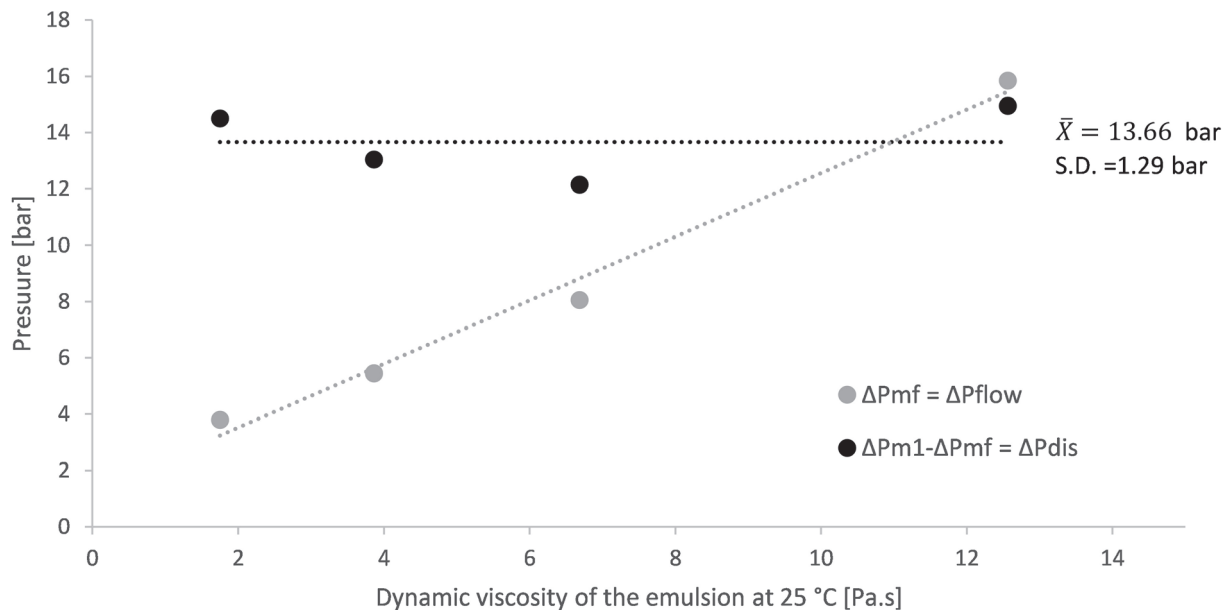


Figure 4.9: Influence of dynamic emulsion viscosity on  $\Delta P_{flow}$  and  $\Delta P_{dis}$

### 4.4.3 W/O nanoemulsions

In this section, W/O nanoemulsions were prepared at different compositions by varying the viscosity of the continuous phase, viscosity of the dispersed phase and water content, which modifies the overall emulsion viscosity as described in Materials and Methods. The membrane pressure was measured for all formulations, while the droplet size was reported only for formulations with different continuous phases.

#### 4.4.3.1 Influence of the continuous phase viscosity

The effect of the continuous phase viscosity was investigated with four different oils as described in Table 4.1: WMO, WMO + Marcol 82, Marcol 82 and Marcol 52. Water and total surfactant concentration were kept constant at 10% and 5%, respectively. Figure 4.10 shows the membrane pressures measured at various flowrates up to 50 mL/min except for the more viscous oil WMO where 40 mL/min was set to keep the resulting pressure below 65 bar. The membrane pressure was proportional to the flowrate for the four oils. At low flowrates, the membrane pressures were closed to each other except for the more viscous oil WMO, for which the pressure was higher. The differences between membrane pressures became higher when increasing the flowrate. The membrane pressures tended to the same value, around  $16.43 \pm 0.94$  bar, as the flowrate approached 0 mL/min. This value may represent the minimum pressure required for the emulsion to flow through the membrane, also called emulsifying pressure in DME [46]. On the contrary, the membrane resistance greatly increased when increasing the oil viscosity.

The membrane resistance and the overall emulsion viscosity are plotted versus the continuous phase viscosity in Figure 4.11. Both parameters are proportional to the continuous phase viscosity. Like for O/W emulsions, the overall emulsions viscosity was proportional to the continuous phase viscosity. The membrane resistance was also proportional to the viscosity.

As for O/W nanoemulsions, the viscosity of the continuous phase has a great influence on the feasibility of nanoemulsions production by PME. Indeed, the resulting pressure has to be lower than 65 bar, and the viscosity has a major impact on the membrane pressure. The viscosity is of greater importance for W/O nanoemulsions production as higher viscosities are involved.

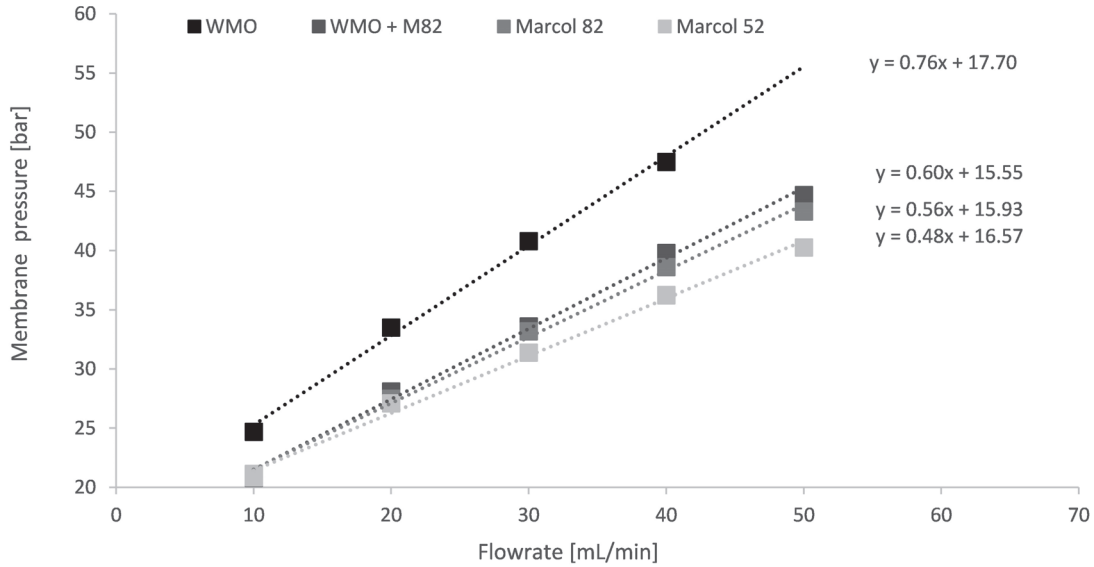


Figure 4.10: Membrane pressure variation with flowrate for oils of different viscosities as continuous phases with oil and surfactant content kept constant at 10% and 5% respectively

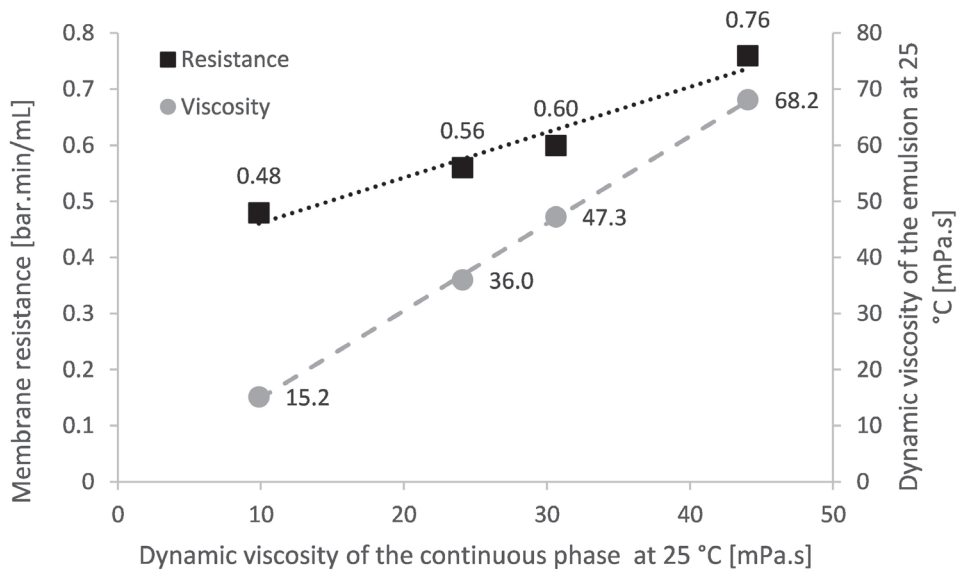


Figure 4.11: Membrane resistance variation with flowrate and dynamic viscosity of the emulsion as a function of continuous phase viscosity

#### 4.4.3.2 Influence of the dispersed phase viscosity

To investigate the influence of the dispersed phase viscosity, nanoemulsions with five different concentrations of glycerol in the dispersed phase (0, 25, 50, 75 and 100 %) were prepared. Figure 4.12 shows the membrane pressure as function of flowrate for a fixed composition of 10% dispersed phase, 5% surfactant and 85% Marcol 82 as the continuous phase. For concentrations up to 50% glycerol, the membrane pressure did not change, however, at higher amounts of glycerol 75 and 100%, the membrane pressure values were much lower. Indeed, at high glycerol concentrations, the density of the dispersed phase became higher and so the difference of density between the continuous and dispersed phases might induce sedimentation. It is likely that the premix un-

derwent sedimentation in the high pressure syringe pump and so the injected dispersed phase was less concentrated, which might result in a decrease of the membrane pressure. Indeed, the membrane pressure decreases when decreasing the amount of dispersed phase as seen previously with O/W nanoemulsions and observed below for W/O nanoemulsions.

In addition, when increasing the glycerol content, the viscosity of the dispersed phase increased to 27.8 mPa.s for 75% glycerol and 905.7 mPa.s for 100% glycerol. The difference in viscosities between the continuous and dispersed phases was lower for 75% glycerol than for lower concentrations and can explain the decrease in membrane pressure as seen for O/W results. However, this effect could not explain the decrease in membrane pressure for 100% glycerol, where the difference in viscosities was very high. So, it seems that this effect could not explain the difference in membrane pressure observed as it did with O/W nanoemulsions.

These results suggest that for both O/W and W/O nanomulsions the dispersed phase viscosity in PME has not a significant effect.

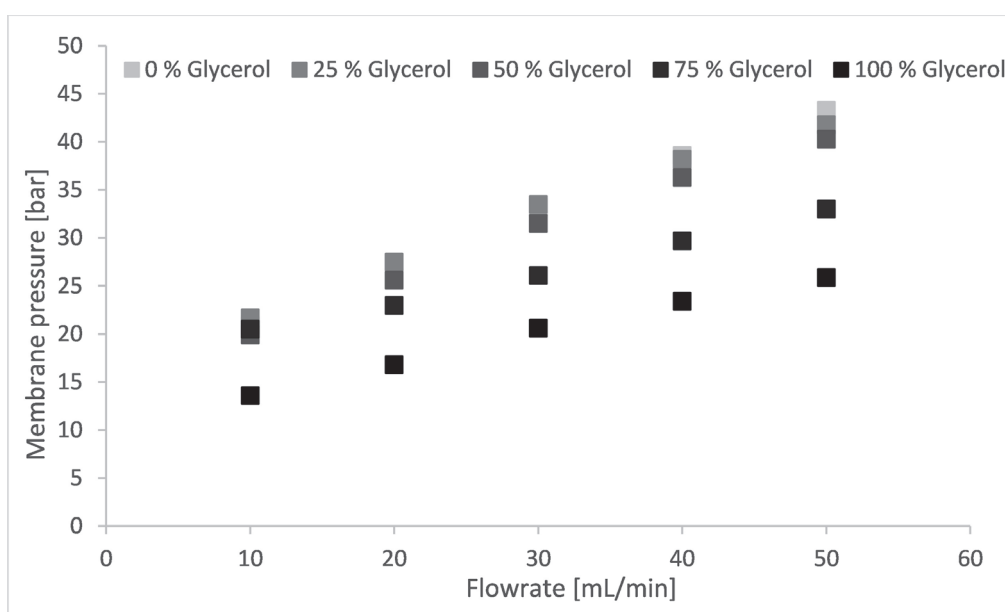


Figure 4.12: Variation of membrane pressure for different amounts of glycerol in the dispersed phase, with oil and surfactant content kept constant at 10% and 5% respectively

#### 4.4.3.3 Influence of the dispersed phase content

The influence of the dispersed phase content was tested for four water concentrations 1, 5, 10 and 15%. The surfactant to water ratio was kept constant at 0.5 corresponding to surfactant concentrations of respectively 0.5, 2.5, 5, 7.5%. The oil used was Marcol 82 for all experiments. Figure 4.13 shows the variation of the membrane pressure and emulsion viscosity with the dispersed phase content. The membrane pressure and the dynamic viscosity were a linear function of the water content, at this range of concentrations. However, as shown on Figure 4.9, for O/W nanoemulsions and at a larger range of dispersed phase concentrations,  $\Delta P_m$  was the addition of a parameter that was highly dependent on viscosity  $\Delta P_{flow}$  and one which was constant  $\Delta P_{dis}$ . At our experimental conditions, the membrane pressure increased linearly with the water content; it might be explained by the fact that in this dispersed phase range, viscosity increases linearly with water content. In this case, the membrane pressure is the addition of one term that increase linearly with the water content and one that does not depend on the water content, which explain its linearity.

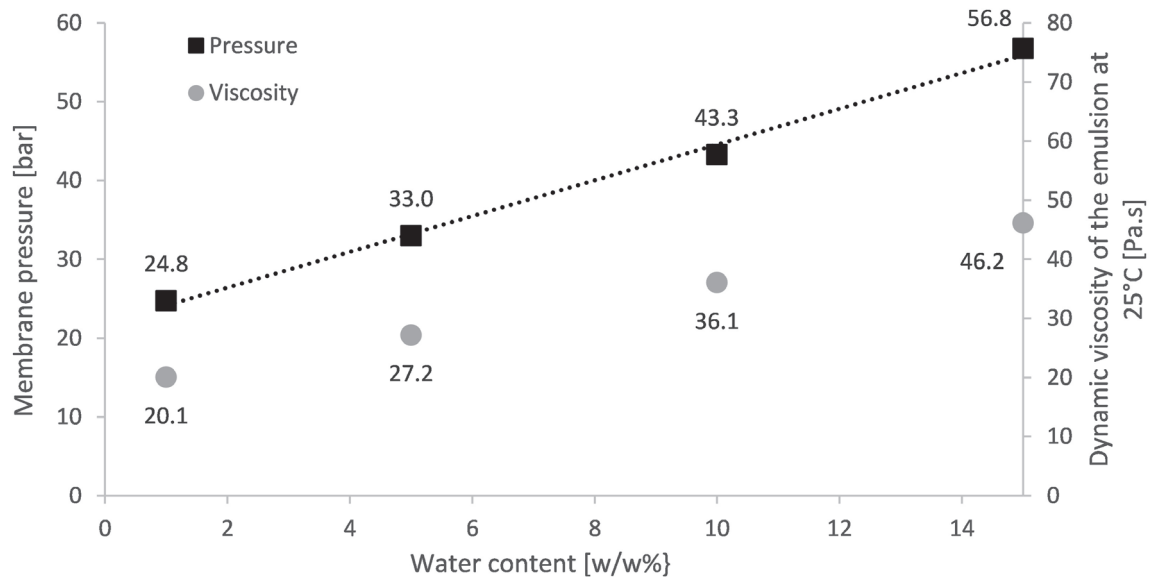


Figure 4.13: Variation of droplet size and membrane pressure with water content at 50 mL/min

#### 4.4.3.4 Determination of $\Delta P_{flow}$ and $\Delta P_{dis}$

As for O/W nanoemulsions,  $\Delta P_{flow}$  and  $\Delta P_{dis}$  were determined from the influence of the cycle number on the membrane pressure. For W/O, one composition was tested: 10% water, 5% surfactant and 85% Marcol 82, at 50 mL/min and the result is presented in Figure 4.14. At this composition and for these experimental conditions, the difference in pressure between the first cycle and the stabilized pressure was  $\Delta P_{dis} = \Delta P_{m1} - \Delta P_{mf} = 7.6$  bar and  $\Delta P_{flow} = \Delta P_{mf} = 35.7$  bar.  $\Delta P_{dis}$  was lower than for O/W nanoemulsions. Indeed, the flowrate was two times lower (50 mL/min for W/O and 100 mL/min for O/W nanoemulsions).  $\Delta P_{dis}$  should decrease when decreasing the flowrate, as suggested by Figure 4.6 where  $\Delta P_{membrane}$  was equal to 14.7 bar at 50 mL/min, suggesting a lower value of  $\Delta P_{dis}$  than that obtained at 100 mL/min (14.5 bar). Further investigations would be needed to investigate the effect of flowrate on  $\Delta P_{dis}$ .

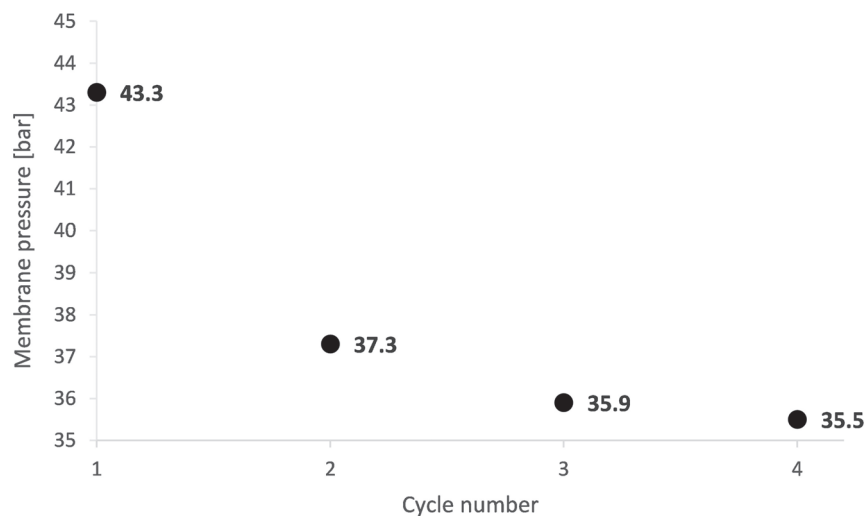


Figure 4.14: Effect of cycle number on membrane pressure at a composition of 10% water, 5% surfactant and 85% Marcol 82 at a flowrate of 50 mL/min

#### 4.4.3.5 Influence on droplet size distribution

For W/O nanoemulsions, the droplet size measurement with the oil as the continuous phase is much more difficult compared to O/W nanoemulsions with water as the continuous phase. Consequently, it was more difficult to see the variation of droplet size. However, droplets size around 550 to 660 nm were observed by laser diffraction (Figure 4.15). There was only a little effect of the continuous phase viscosity on the droplet size distribution. D50 decreased when increasing the continuous phase viscosity except for WMO but the nanoemulsions were obtained at a lower flowrate. The effect of the continuous phase viscosity appears less pronounced than for W/O nanoemulsions. It could be explained by the lower flowrate used, resulting in lower shear stress, which can affect the influence of the continuous phase viscosity. Also, the droplet sizes showed a broader distribution, and therefore it is more difficult to observe a real effect on the droplet size.

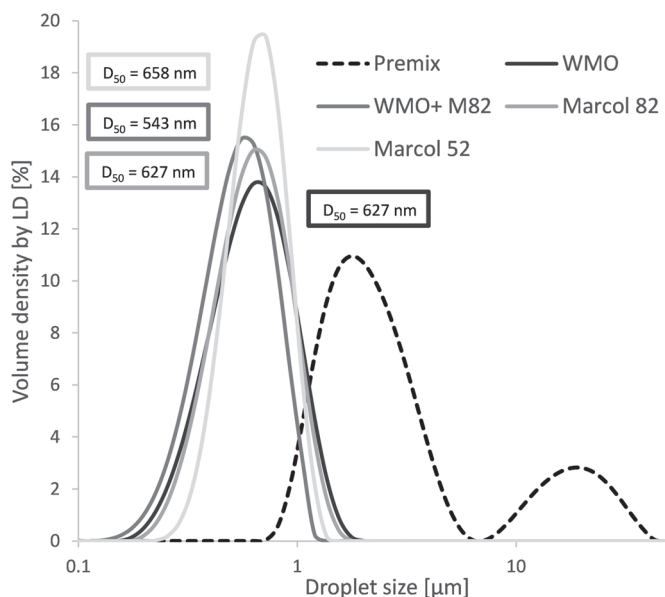


Figure 4.15: Droplet size distribution of W/O nanoemulsions with different oils obtained at 50 mL/min except for WMO at 40 mL/min

## 4.5 Conclusion

In this study, O/W and W/O nanoemulsions were prepared successfully by PME and SPG membranes. For that, a controlled set-up including a high pressure syringe and a membrane module in PME mode, developed in our previous study, was used [124]. As the pressure through the membrane must be lower than 65 bar, we investigated the effect of viscosities of the continuous phase, dispersed phase, and dispersed phase content to be able to produce viscous O/W and W/O nanoemulsions successfully.

The resulting pressure is a key parameter which governs the production of nanoemulsions in PME and is due to three main resistances: the resistance of flow through the pipe connecting the pump to the membrane module  $\Delta P_{pipe}$ , the resistance of flow through the membrane pores  $\Delta P_{flow}$  and the resistance due to the disruption of the premix droplets into nanodroplets in the membrane pores  $\Delta P_{dis}$ .

First, the pressure drop through the pipe connecting the pump to the membrane module was measured and shown to be proportional to the emulsion viscosity as predicted by Poiseuille's equation, for both O/W or W/O nanoemulsions. Then, the effect of viscosity on the pressure through the membrane and droplet size was investigated for O/W nanoemulsions. It was found that the membrane pressure was highly dependent on the emulsion viscosity especially at higher

viscosities. The continuous phase viscosity had a great impact on the pressure as it increased the overall emulsion viscosity and on the droplet size distribution with a significant decrease due to the increase of the shear stress within the membrane pores. The dispersed phase viscosity had a lower impact on the membrane pressure, which can be explained by the viscosity difference between the dispersed and continuous phases, and no significant influence on the droplet size distribution.

W/O nanoemulsions were produced with mean droplets size around 600 nm at 50 mL/min. W/O nanoemulsions were more difficult to produce and to characterize, but the different viscosities had the same influence on the membrane pressure as for O/W nanoemulsions.

These results suggest that in PME the pressure needed to break up the droplets from the premix  $\Delta P_{dis}$  does not depend on viscosity. At low flowrates and low viscosities, the resulting pressure is nearly equal to  $\Delta P_{dis}$ . However, at high flowrates and high viscosities, the two other pressures  $\Delta P_{flow}$  and  $\Delta P_{pipe}$  have an important effect as they are proportional to the viscosity of the overall emulsion.

## Acknowledgment

This work was supported by PeptiCaps project. This project has received funding from the European Union's Horizon 2020 Research and Innovation program under Grant Agreement n°686141.



## **Chapter 5**

### **Production of O/W and W/O PeptiCaps nanoemulsions**

## 5.1 Introduction

The aim of this study was to produce O/W and W/O nanoemulsions within the frame of the european project PeptiCaps (Figure 5.1). A consortium of 9 partners worked on this 3-years project starting in October 2015. The final objective of the projet is to develop and validate a new family of safe stimuli-responsive nanoemulsions designed to encapsulate fragile active ingredients, either hydrophilic or hydrophobic, as cosmetic ingredients. Within this project, a specific part is dedicated to the production of nanoemulsions using industrially relevant manufacturing processes, in our case membrane processes. These nanoemulsions are produced using the macroemulsifiers developed within the project. The major requirement are their long term stability, submicron size and narrow size distribution.

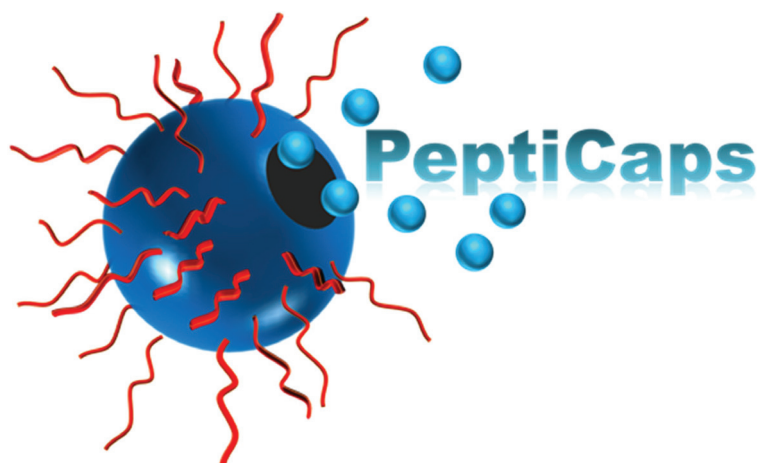


Figure 5.1: PeptiCaps logo

First, preliminary essays were performed in order to evaluate the possibility to produce with PME nanemulsions stabilized by PP1. Essays were performed with the proof of concept set-up and results are presented in Appendix A.1. Once the final set-up developed, we first tested a model composition with the oil chosen by the European partners in order to understand the effect of process and composition parameters, and then produce O/W and W/O nanoemulsions with PP1 and PP2 respectively.

First, the production of O/W nanoemulsions required a development phase presented in Chapter 3. Then, PP1 was used and results are presented focusing on the influence of surfactant concentration and flowrate on the emulsion properties. For W/O nanoemulsions, as the MCT as oil had not been investigated previously, the results with PGPR as model surfactant are presented in a first section. In a second part, production of W/O nanoemulsions with PP2 is reported.

## 5.2 Materials and methods

Compositions and procedures for formulations with polypeptides are presented in Chapter 2. Additionally, products used for W/O model composition emulsions are PGPR (Palsgaard DMG 0295) kindly provided by Palsgaard, Medium Chain Triglyceride (MCT) oil purchased at Gattefossé (commercial name Labrafac Lipophile WL 1349) and demineralized water. The proportions were 10% water, 10% PGPR and 80% MCT unless mentioned otherwise.

For O/W emulsions, membranes of 20 mm length were used and for W/O emulsions membranes of 125 mm length. Membranes of smaller length were first used in order to minimize the amount of surfactant but for W/O as their viscosity was higher it was more convenient to work with longer membranes to produce nanoemulsions at higher flowrate.

## 5.3 Results for O/W emulsions production

### 5.3.1 Influence of copolypeptide percentage

All the following results in this section were obtained with the final set-up with the high pressure syringe pump, the microkit module and a 20 mm long membrane, as presented in Chapter 2.

As shown previously, the surfactant percentage has an important effect on the resulting pressure and size reduction. On Figure 5.2, we see clearly that surfactant concentration of 1% was not sufficient to get monodispersed nanoemulsions with the 0.8  $\mu\text{m}$  pore size membrane. However, 2% allowed to get a monodispersed emulsion with  $D_{50} = 837$  nm (Figure 5.2).

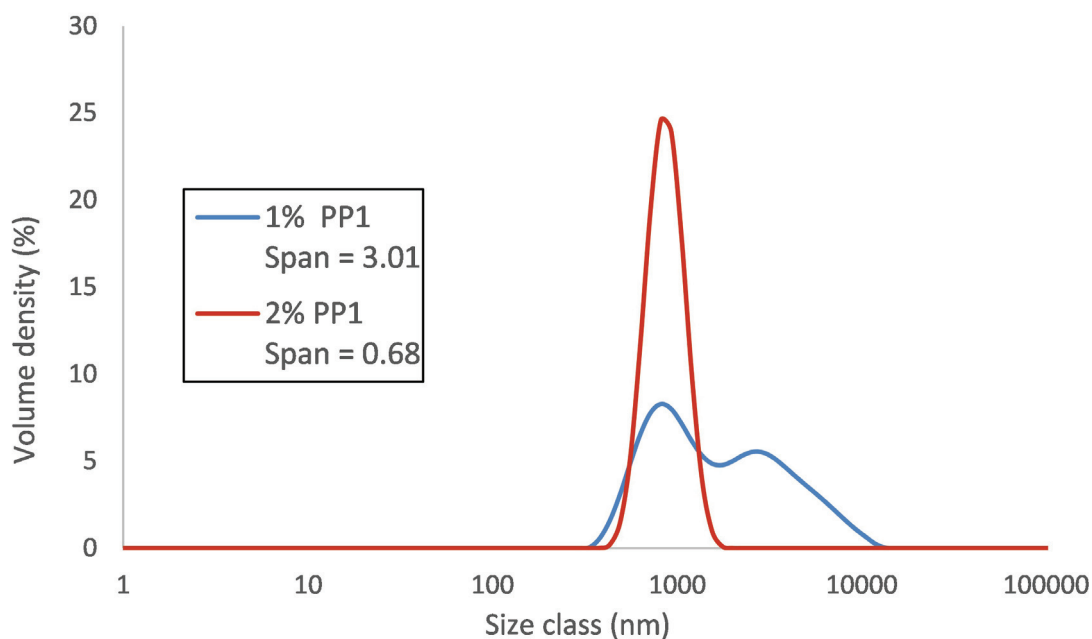


Figure 5.2: Size distribution in volume at different polypeptide concentrations and 10% oil with the 0.8  $\mu\text{m}$  membrane

The smallest droplet size obtained at different PP1 concentrations are presented in Figure 5.3: at 2% PP1 concentration and with the 0.8  $\mu\text{m}$  pore size membrane and at 1% PP1 with the 1.1  $\mu\text{m}$  pore size membrane.

Monodispersed emulsions with 1% PP1 was only achievable with a 1.1  $\mu\text{m}$  pore size membrane and with these conditions, 74 bars were needed to pass through the membrane pores at 200 mL/min.

For 2% PP1, the premix was able to pass through the pores of a 0.8  $\mu\text{m}$  pore size membrane but 110 bars were needed for a flowrate of 50 mL/min. Higher flowrates were not achievable with these conditions.

### 5.3.2 Influence of flowrate

The influence of flowrate was studied and the results were similar to the ones obtained with other compositions studied in Chapter 3. The droplet size decreased at higher flowrate (Figure 5.4). However, the effect of flowrate was less important than with the model formulation. At low flowrates, 10 mL/min and 50 mL/min, the mean drop size was higher and the distribution wider than the ones obtained at 75 mL/min to 200 mL/min which gave droplet size close to each other.

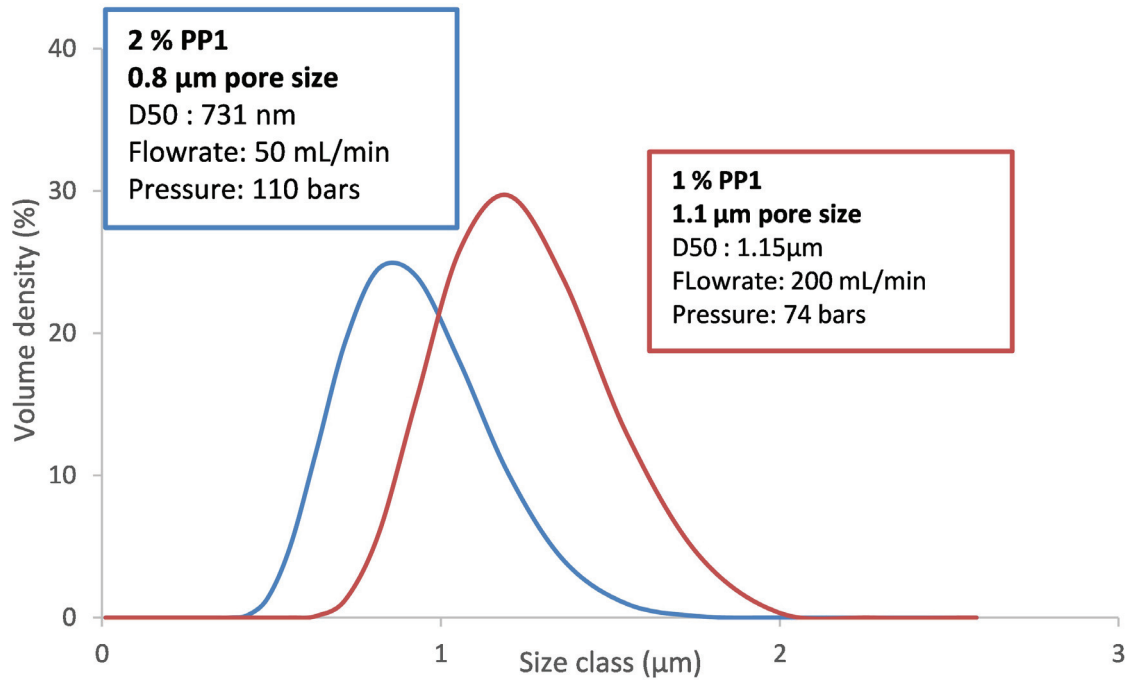


Figure 5.3: Size distribution in volume of emulsion with the smallest droplet size at two polypeptide concentrations and two different pore sizes

The fact that the formulation based on the polypeptide was not optimized might explain this difference.

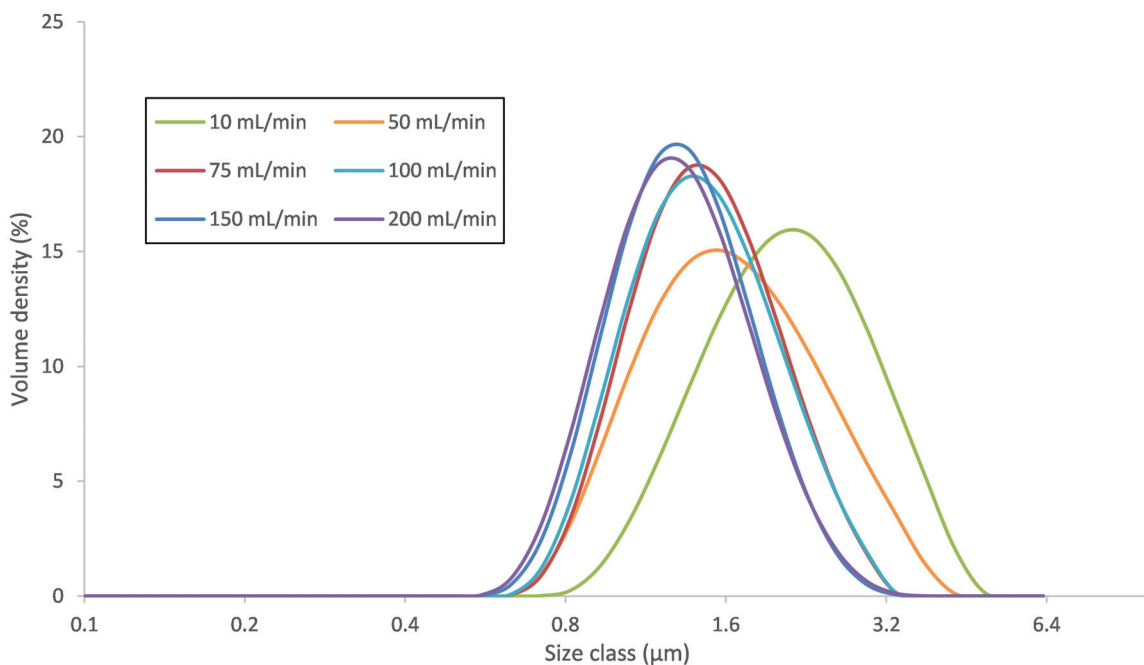


Figure 5.4: Size distribution in volume for different flowrates with the 1.1  $\mu\text{m}$  membrane at 10% oil and 2% PP1

Emulsion with the smallest droplet size was obtained with the 2% copolypeptide and the 0.8  $\mu\text{m}$  membrane at 50 mL/min. The droplet size distribution is shown on Figure 5.5.

### 5.3.3 Stability

As can be seen on Figure 5.5, nanoemulsions produced with 2% PP1 were very stable over time up to 9 months minimum. We observe that even at low concentration, PP1 was able to stabilize nanoemulsions and that PME produced stable nanoemulsions.

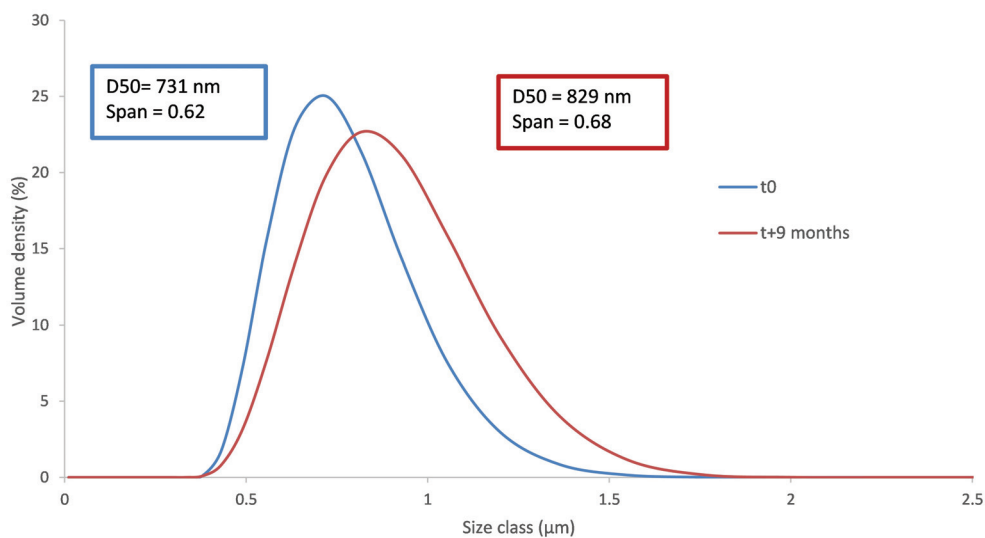


Figure 5.5: Size distributions for the smallest emulsion obtained with PP2 at 2% , 0.8  $\mu\text{m}$  membrane and 10% oil just after production, (t0) and after 9 months at room temperature (t+9 months)

## 5.4 Results for W/O emulsions production

Contrary to O/W, W/O nanoemulsion production by PME with the MCT oil has not been reported in previous chapters. In order to optimize first the production of W/O emulsions with PME, nanoemulsions with MCT oil and a classical hydrophobic surfactant, PGPR were prepared. PGPR was chosen because Span 80 was not soluble in MCT. Also PGPR is commonly used for the production of W/O emulsions [62, 90, 108, 109].

### 5.4.1 Model composition with PGPR

In this section, we first prepared emulsions by PME using a commercial emulsifier, namely PGPR. We investigated:

- The effect of flowrate on resulting pressure
- The effect of water content on resulting pressure at various flowrates

Figure 5.6 shows the influence of flowrate on the resulting pressure for emulsions with different water content. The resulting pressure drastically increased when the aqueous phase content increased, in particular for the emulsion with 20% water content. These results have already been reported and the effect of viscosity studied in Chapter 4. Same observations were made for different oils and different surfactants.

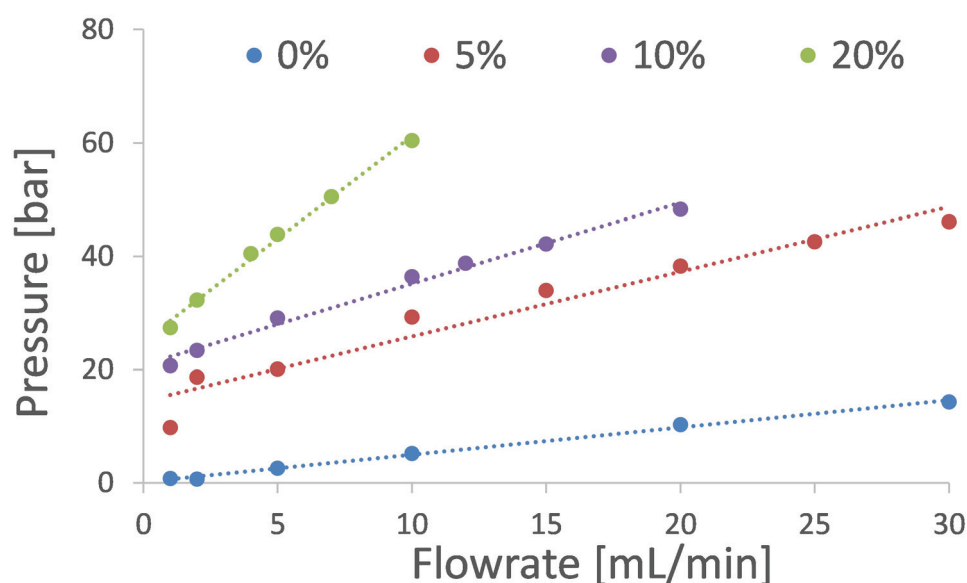


Figure 5.6: Variation of the resulting pressure as function of flowrate for W/O emulsions with different water contents

In Figure 5.7, the resulting pressure is plotted versus water content for three flowrates. Pressure and flowrate were proportional for all formulations tested with different water contents.

The resulting emulsions were then characterized in terms of droplet size.

In Table 5.1, the droplet sizes measured by DLS of the emulsions obtained by PME are reported for each flowrate. The size range of the emulsions varied between 640 and 740 nm. Size distributions were relatively homogeneous with PDI varying from 0.1 to 0.25. Furthermore, there seems to be no clear influence of the flowrate on droplet size.

In this section, W/O emulsions with various water contents were prepared by PME with a good control of flowrate and pressure. Among all formulations, the maximum flowrate which could be

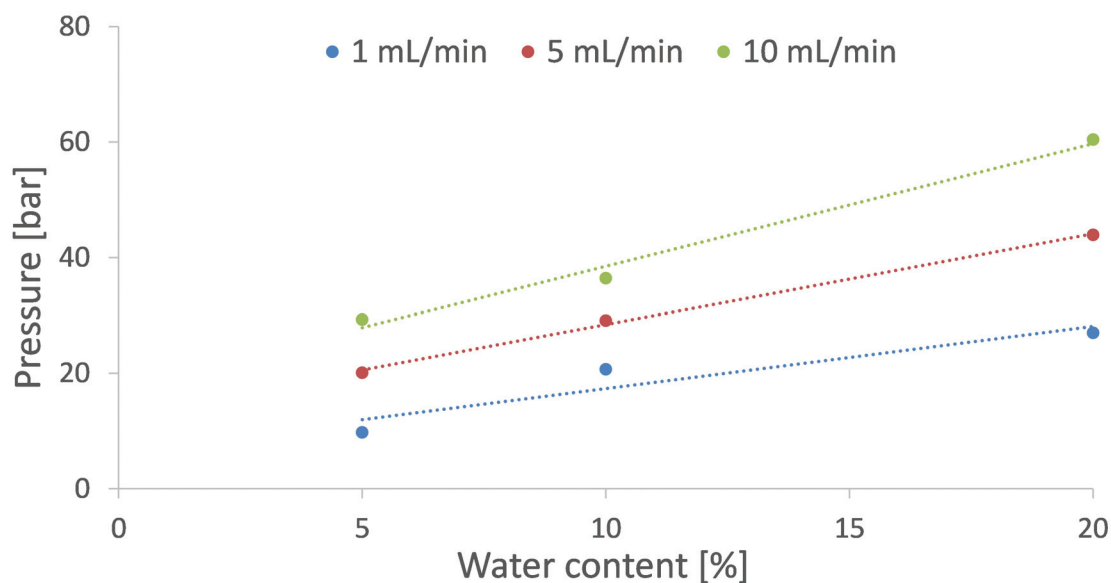


Figure 5.7: Variation of the resulting pressure with water phase content at various flowrates

Flow rate (mL/min)	Z average (nm)	PDI	Peak mean value (nm)
1	743	0.2	970
2	751	0.22	1019
5	671	0.25	989
10	658	0.2	838
12	647	0.19	808
15	640	0.24	883

Table 5.1: Variation of the Z-average, PDI and mean value at various flowrates from 1 to 15 mL/min

achieved with the 0.5  $\mu\text{m}$  membrane was 30 mL/min. However, size measurements are limited by the emulsion overall viscosity.

#### 5.4.2 PeptiCaps composition with PP2

In this section, W/O emulsions stabilized with the copolypeptide PP2 were prepared by PME. The formulation was optimized by the European partners. As described in Chapter 2, these conditions are the following: Ewocream was used as an oil soluble surfactant and PeptiCaps surfactant PP2 as a water soluble one. Furthermore, the aqueous phase was either a mixture of 30/70 buffer / glycerol or pure glycerol.

The copolypeptide was first dissolved at 10 % in a mixture of 30/70 citrate buffer / glycerol. We observed that while the copolypeptide solution in 30/70 buffer/glycerol was slightly viscous, the one in pure glycerol yielded to the formation of a gel. Therefore, emulsions were prepared with a

30/70 buffer/glycerol solution as dispersed phase. Two types of formulations were prepared: one with and one without PP2 as water soluble surfactant.

We investigated the influence of the injection flowrate on resulting pressure and droplet size for each formulation. The resulting pressure increased with flowrate for both formulations, with a maximum flowrate of 50 mL/min. Droplet sizes of the resulting emulsions were then measured by DLS. Figure 5.8 shows typical size distribution for both formulations in comparison with the premix emulsion. The emulsions containing PP2 were nearly transparent while the one without were turbid (Figure 5.9). However, both formulations displayed the same size distribution, at around 600 nm with PDI between 0.13 and 0.19. This was further confirmed in Figure 5.10, where it can be seen that the average size of both formulations ranged from 400 nm at low flowrates, probably due membrane filtration instead of emulsification, to 600 nm at high flowrates.

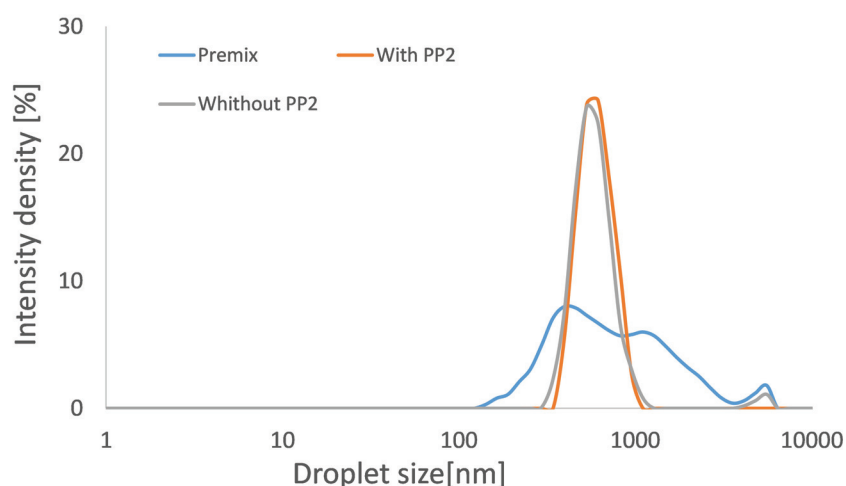


Figure 5.8: Size distribution comparison of the emulsions obtained with or without PP2 after passing through a 0.5  $\mu\text{m}$  pore size membrane at a flowrate of 30 mL/min. Composition: dispersed phase 10 % of a 30/70 citrate buffer /glycerol mixture with or without 1 % PP2; continuous phase: 90 % of 20 % Ewocream in MCT oil

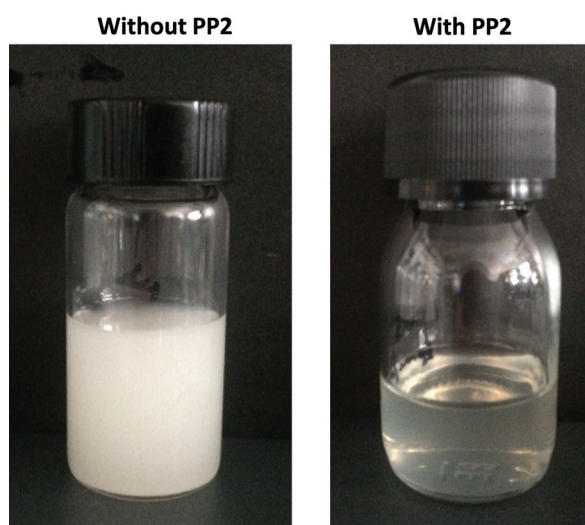


Figure 5.9: Composition: dispersed phase 10 % of a 30/70 citrate buffer /glycerol mixture with or without 1 % PP2; continuous phase: 90 % of 20 % Ewocream in MCT oil

The difference in transparency between both formulations was explained by the modification of the refractive index due to PP2 addition. Indeed, the refractive indexes were measured with a PAL-1 Pocket refractometer (ATAGO, Japan), with water phase containing 30% citrate buffer and 70% glycerol. The following results were obtained:

- Without PP2:  $1.42935 \pm 0.00012$
- With 1 % PP2:  $1.43832 \pm 0.00000$

And for the oil phase (20 % Ewocream + 80 % MCT) :  $1.45184 \pm 0.00000$

With the addition of 1% PP2 to the dispersed phase composed of 30% citrate buffer and 70% glycerol, the refractive index increased and became closer to the refractive index of the continuous phase. Visually, the emulsion became more transparent.

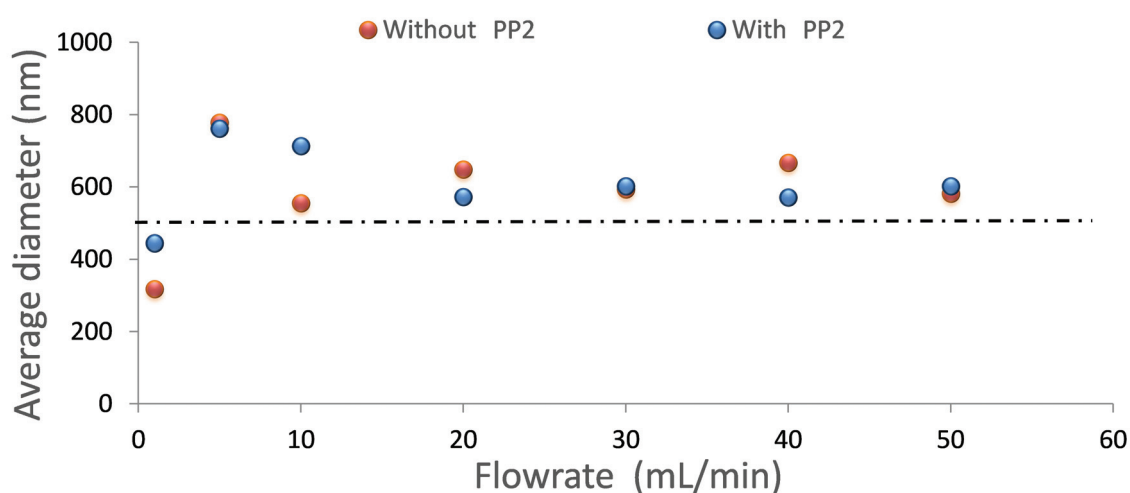


Figure 5.10: Variation of the average droplet diameter as a function of flowrate for emulsions with or without PP2. Emulsification conditions: membrane pore size  $0.5 \mu\text{m}$

## 5.5 Conclusion

In this study, O/W and W/O nanoemulsions of specific composition were produced by PME. These compositions were specified by our European partners from PeptiCaps project.

First, parameters were optimized with model compositions of commercially available surfactants. For O/W nanoemulsions, results are presented in Chapter 3 and for W/O nanoemulsions with PGPR in this chapter. Finally O/W and W/O nanoemulsions with polypeptidic surfactants, respectively PP1 and PP2 were produced by PME .

These results show that the process developed allows the production of nanoemulsions of different compositions and different requirements. Indeed it can be used for different applications with the advantages of high monodispersity, easy scalability, lower energy consumption and better compatibility to sensitive actives compared to other processes.



# Chapter 6

## Comparison of three processes for parenteral nanoemulsion production: ultrasounds, microfluidizer and premix membrane emulsification

### Contents

---

<b>5.1 Introduction</b> . . . . .	<b>112</b>
<b>5.2 Materials and methods</b> . . . . .	<b>112</b>
<b>5.3 Results for O/W emulsions production</b> . . . . .	<b>113</b>
5.3.1 Influence of copolypeptide percentage . . . . .	113
5.3.2 Influence of flowrate . . . . .	113
5.3.3 Stability . . . . .	115
<b>5.4 Results for W/O emulsions production</b> . . . . .	<b>116</b>
5.4.1 Model composition with PGPR . . . . .	116
5.4.2 PeptiCaps composition with PP2 . . . . .	117
<b>5.5 Conclusion</b> . . . . .	<b>119</b>

---

## Preamble

As seen in previous chapters, a new process, PME, has been developed for nanoemulsions production with encouraging results. This motivated us to compare PME with traditional processes. Two high energy processes were chosen and investigated for exactly the same composition.

The first one, microfluidizer is considered as the best industrial option for nanoemulsion production in the market. Moreover, it is available in our laboratory and influence of numerous parameters has already been studied in a preliminary study and found in agreement with what was reported in the literature. For this reason these results are not presented here.

The second one, ultrasounds is extensively used in laboratory research for its good performance. However, it is known to be not scalable to large scale.

The idea was to find a model composition to be able to compare droplet sizes and preservation of a sensitive active. As PME requires less energy, it is expected to preserve better the active ingredients. Pharmacy is one field where droplet size and active preservation are of prime importance for effectiveness and safety reasons. Among pharmaceutical applications, parenteral route of administration is the most sensible to these parameters.

All-trans retinoic acid (AtRA) was chosen because of its promising results in influencing tumor progression by affecting cancer cell proliferation rates and their state of differentiation and because of the laboratory expertise with this active ingredient. Moreover, even if different formulations with atRA have already been studied, atRA has never been loaded in nanoemulsion to our knowledge.

# Comparison of three processes for parenteral nanoemulsion production: ultrasounds, microfluidizer and premix membrane emulsification

*O. Alliod, E. Almouazen, G. Nemer H. Fessi, C. Charcosset*

**Journal of Pharmaceutical Sciences (submitted, 2018)**

## 6.1 Abstract

Nanoemulsions are of great interest for pharmaceutical applications, including parenteral dosage forms. However, their production is still limited and requires more efficient and adaptive technologies. The more common systems are high-shear homogenization like microfluidizers (MF) at industrial scale and ultrasounds at research scale, both based on high energy limiting their application for sensitive drugs. Recently, a process based on premix membrane emulsification (PME) was developed to produce nanoemulsions. These three processes have been compared for the production of a model parenteral nanoemulsion containing all-trans-retinoic acid, a thermolabile molecule which is used in the treatment of acute promyelocytic leukemia in a parenteral form. Droplet size and active integrity were studied because of their major interest for efficacy and safety assessment. Regarding droplet size, PME produced monodispersed droplets of 335 nm compared to the other processes which produced nanoemulsions of around 150 nm but with the presence of micron size droplets detected by laser diffraction and optical microscopy. No real difference between the three processes was observed on active degradation during emulsification process. However, regarding stability, especially at 40°C nanoemulsions obtained with the microfluidizer showed a greater molecule degradation and unstable nanoemulsion with a 4 times droplet size increase under stress conditions compared to those produced with the other processes.

## 6.2 Introduction

Nanoemulsions are dispersed systems of droplets with nanometric diameter (< 500 nm) which are used in several pharmaceutical dosage forms and cosmetic formulations. The small droplet size enhances emulsion kinetic stability, allows to solubilize and protect hydrophobic drug molecules and contributes to drug bioavailability enhancement. Their versatility, biocompatibility and biodegradability make these systems valuable pharmaceutical asset in different marketed dosage forms for oral, nasal, parenteral, dermal, transdermal, ocular and pulmonary administration routes [130, 131, 132].

Nanoemulsions are the unique choice for intravenous emulsion-based formulations which require specific and strict criteria including controlled droplet sizes (less than 1 or 2  $\mu\text{m}$ ) [45], restricted composition, physico-chemical and biological stability and sterilized requirement. Parenteral nanoemulsions have been presented in numerous studies [133, 134, 135, 136] and included in several clinical trials such as treatment of leukemia [137] and diabetic dyslipidemia [138]. Parenteral nanoemulsions are interesting formulations for the delivery of many drugs [45]. They can avoid the use of conventional co-solvent systems and the associated undesirable effects caused by precipitation of the drug at the injection site, as well as protein binding and hydrolytic degradation of drugs. Another advantage of parenteral emulsions is their potential to achieve a sustained release and to target concerned tissue [135].

Manufacturing of nanoemulsions is usually classified into low and high energy emulsification methods. Low-energy emulsification methods are based on physico-chemical principles such as phase inversion temperature, phase inversion composition or nanoprecipitation [25]. However, the specific composition requirement inherent in these methods gives high energy methods an advantage. Indeed, high energy processes are suitable for a larger range of formulations as nanoemulsions are generated using mechanical devices with intensive disruptive forces that breakup the oil and water phases [44]. Among these high energy methods, the most used are high pressure homogenizers, microfluidizers (MF) and ultrasounds (US). The two first techniques are based on similar technologies, a high pressure flux in a microchannel creating high shear stress with cavitation and impact. The main difference is that MF presents an interaction chamber of fixed geometry whereas in traditional high pressure homogenizers the valve moves to create the pressure. MF and high pressure homogenizers [37] require high energy input (pressure applied up to around 2000 bars). Unfortunately, only 0.1 % of the energy input is actually used for emulsification, while the remaining energy (99.9%) is dissipated as heat [8]. Moreover, monodispersed droplets are obtained only after several cycles, as all droplets do not undergo the same shear stress depending on their position in the interaction chamber. US is based on cavitation mechanism and requires also high energy input. This process can generate nanoemulsions with very small droplet size, but usually broad size distributions are obtained and is limited to laboratory scale. The drawback of these technologies is their energy consumption but also the additional cost for scaling up, which is known as one of the biggest challenges for nanoemulsions production in the pharmaceutical industry [139]. Moreover, high thermal energy produced during emulsification limits their application for thermolabile drugs.

More recently, membrane emulsification has gained significant attention because of the low energy required leading to low shear stress and temperature increase and its good scalability. Membranes can be used either to generate an emulsion, the process is then called direct membrane emulsification or to modify it and is then called premix membrane emulsification (PME). In direct membrane emulsification a dispersed phase is injected through membrane pores in a continuous phase. In PME, a coarse emulsion called premix is injected directly through the microporous membrane in order to form smaller droplets. Advantages of PME over DME are that the flowrate of the product emulsion is generally much higher, higher droplet concentrations are obtained and the mean droplet sizes are smaller [87, 62]. For the production of nanoemulsions, PME is of great interest. Bunjes et al. prepared nanoemulsions by PME with droplet sizes lower or around 200 nm with a narrow size distribution [110, 92, 111]). This result was explained by the high pore tortuosity and thickness of the Shirasu Porous Glass (SPG) membranes which are the most commonly used membranes for emulsification. Using these SPG membranes and PME, Bunjes and Joseph produced a few milliliters of nanoemulsion [110, 92, 59]. The production of nanoemulsions by membrane emulsification remains a challenging undertaking [110] especially for large volumes at high flowrates. Hitherto, this process has been used to homogenize small amounts of emulsion, but a recent publication by Alliod et al. [124] proposed a novel approach which allowed the homogenization of 500 mL of coarse emulsion into a nanoemulsion by running it through membranes with average pore sizes at a minimum of 0.2  $\mu\text{m}$  whilst keeping pressure under 60 bars. Thus, PME can be used to create nanoemulsions that carry sensitive active pharmaceutical ingredients prone to isomerization or degradation. Also, this process present additional industrial interest because it can work in a continuous way. Moreover, SPG membranes can be sterilized and to ensure aseptic production for injectable nanoemulsions.

The aim of this study is to evaluate the potential of these three different processes on production of nanoemulsions within the specific requirements of parenteral formulation. The first process, MF, is a commercially and industrially available process. The second, US is a process used mostly at laboratory scale for the production of nanoemulsions. The last process, PME, is a process under investigation for micron size for some decades but new at nano-scale. These three processes have never been investigated in the same study, however a study compared a traditional membrane process (micron size) and a microfluidizer for emulsion production [56] and several compared ultrasounds and microfluidizer for nanoemulsion production [140, 141]. The first study showed interesting results for both processes but no size under one micron were reached with the membrane process [56]. Concerning comparison of US and MF, similar results in size were often

obtained.

In order to evaluate the effect of each process on possible active degradation, a model active was chosen, all-trans-retinoic acid (atRA). This active has a great potential for injection but is very light and temperature sensitive. This active form of vitamin A, atRA, has been marketed for oral and topical administrations. Its therapeutic potential is thus far limited to the treatment of acne [142] and other superficial skin ailments and to the treatment of acute promyelocytic leukemia [143, 144], among other cancer types [145]. Modern research posits that atRA influences tumor progression by affecting cancer cell proliferation rates and their state of differentiation [146]. Numerous research efforts were dedicated to the development of parenterally administrable forms in order to overcome the limitations of the existing prominent cancer-treating oral forms such as variable atRA bioavailability among patients and decrease its plasmatic level after long-term treatment [142]. Therefore, it has been the subject of thorough investigation to propose adaptable parenteral forms using cyclodextrins [147], liposomes [148], or lipid core nanocapsules [149, 150, 151]. To our knowledge, no atRA-loaded nanoemulsion for parenteral administration has been developed.

The objective of this study is to compare the three processes for the production of atRA parenteral nanoemulsions regarding the droplet size and drug stability. Firstly, the emulsion composition was selected after HLB determination, solubility and osmometry measurements. Then, nanoemulsions production was optimized regarding droplet size and dispersity. For that pressure and cycle number were investigated for MF, number of cycle coupled with pore size for PME and intensity and processing time for US. Following this optimization, the more interesting conditions for each process were selected and the active preservation was determined over 3 month with four storage conditions, ie: dark conditions temperature of 4°C, ambient temperature and 40°C and in light conditions at ambient temperature.

## 6.3 Experimental Section

### 6.3.1 Materials

AtRA, 13-cis-retinoic acid, 9-cis-retinoic acid, Tween 20 (Polysorbate 20), Span 80 (Polysorbate 80) were purchased from Sigma Aldrich (France). Derquim+ was purchased from Derquim (Spain), Labrafac wl1349 (MCT oil) was purchased from Gattefossé (France). Glycerol was purchased from Carl Roth (France). Ultrapure water was obtained using a Millipore (France) Synergy Unit system.

### 6.3.2 Preparation of the premix

In order to determine the final quantity of atRA to be added to the emulsion to avoid crystallization after manufacturing, the solubility in MCT was determined. Tween 20 and Span 80 were chosen because both emulsifiers are FDA approved for intravenous administration and are relatively innocuous in low quantities. Moreover, to ensure optimal stability of the nanoemulsion, the emulsifier mix was added at a mass percentage of 5% [124]. Finally, the osmolarity was adjusted by adding glycerol and was measured using an OSMOMAT 030 cryoscopic osmometer

Preparations were all performed at room temperature. Both phases were first prepared separately. The oil phase was prepared by adding 10% MCT, 2.7% Span 80 and 0.2% atRA and stirring magnetically at 600 rpm until a homogeneous consistency was obtained. In the aqueous phase, 1.88% glycerol and 2.3% Tween 20 were dissolved in water. Once a homogeneous consistency was obtained for the aqueous phase, the oil phase was poured while magnetic stirring was set at 600 rpm. The mixture was stirred until a homogeneous and consistent white color was obtained. During all the process, exposition to day light was avoided.

### 6.3.3 Production of nanoemulsions

#### 6.3.3.1 PME

The experimental set-up and method used for the preparation of nanoemulsions by PME are adapted from the approach detailed by Alliod et al. [124] (Figure 6.1). The set-up comprised a high pressure benchtop single cylinder pump BTSP 500-5 (Floxlabs, Nanterre, France). The pump is made of high grade stainless steel and equipped with a pressure sensor ( $\pm 0.1$  bar), two pneumatic valves for tank feeding and outlet delivery, a control panel and a storage tank of 500 mL. Pressurization was obtained by way of an electric motor-driven piston. A maximum flowrate of 200 mL/min can be obtained with this pump. The membrane module was connected to the pump with high pressure fittings (Swagelock, France).

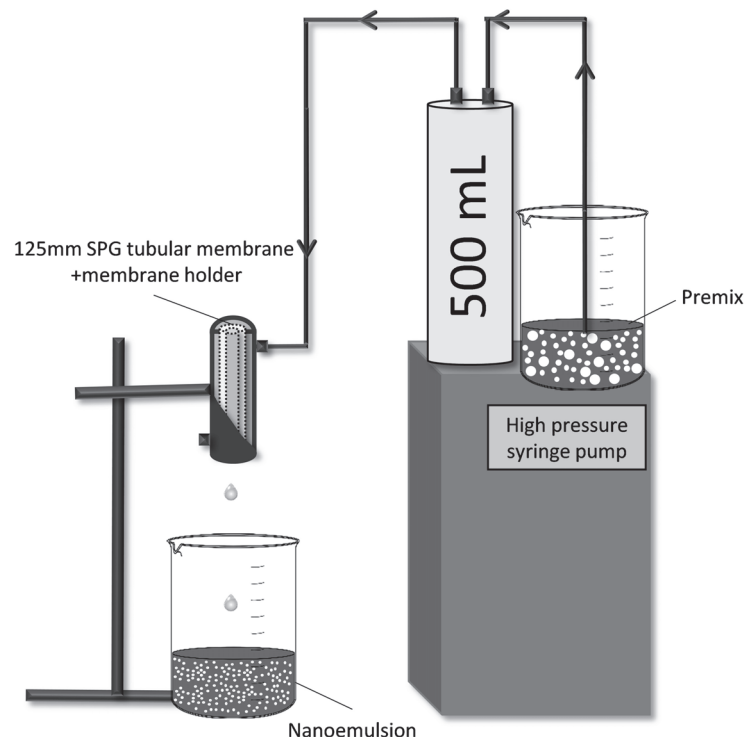


Figure 6.1: Experimental set-up of the high syringe pump with membrane holder and SPG membrane

Hydrophilic SPG membranes were provided by SPG Technology Co.Ltd (Miyazaki, Japan). These membranes are of a tubular design with an inner diameter of 8.5 mm and a uniform thickness of 0.8 mm. 20 mm membranes were used throughout the experimentation. Membranes with mean pore size of 0.2, 0.3, 0.4, 0.5  $\mu\text{m}$  were investigated and their mean pore size data was provided by the manufacturer. The membrane module used was an external pressure microkit module for membranes with a length of 20 mm (SPG Technology). The cleaning procedure consisted in three injections through the membrane of 500 mL of a 1 % Derquim + solution [57] at 70°C and 200 mL/min, and then three injections of 500 mL of pure water at room temperature and 200 mL/min. The membrane resistance to water was recovered after this treatment.

To produce nanoemulsions, the premix was placed in the feed tank and pumped in the syringe pump. First 20 mL premix was injected in order to remove air from the experimental set-up and fill it with premix. Most of the experiments were then carried out with volumes of injection from 40 to 200 mL to perform all cycles with sufficient material. The transmembrane pressure never exceeded 60 bars. The nanoemulsion produced flew from the membrane tube under gravity and was collected in a beaker placed beneath the module.

The membrane used for production at each cycle was the following: Cycle 1 : 0.5  $\mu\text{m}$  pore size; Cycle 2 : 0.4  $\mu\text{m}$  pore size; Cycle 3 : 0.3  $\mu\text{m}$  pore size; Cycle 4 : 0.2  $\mu\text{m}$  pore size. After each cycle the emulsion was collected and analyzed. All emulsions were investigated in a stability study.

### **6.3.3.2 MF**

An LM20 series Microfluidizer processor (Microfluidics, Massachusetts, USA) was used. Its reservoir capacity is 300 mL and it can be operated at pressures up to 2068 bars.

The effects of several parameters were investigated: pressure values from 500 to 2000 bars; number of cycles : 1, 2, 3, 4, and 5 cycles. After each cycle, the emulsion was collected and analyzed. For the stability study, the preparations investigated were obtained after cycle 1, 3 and 5 at a pressure of 1000 bars.

### **6.3.3.3 US**

A UP400S Ultrasonic Processor (Hielscher, Teltow, Germany) was used to create nanoemulsions. It is equipped with a 100 mm titanium cylindrical sonotrode (radius = 7 mm) and a sound protection box. Its operating frequency is 24 kHz and its amplitude can be modulated using a simple knob fitted onto the device. To obtain homogeneous size reduction, the emulsion was magnetically stirred throughout the homogenization process. The preparations were placed in an ice bath to limit temperature increase.

Two variables were taken into account when evaluating US as an homogenization method: amplitude which was modulated at 30% and 60% and time of exposure which lasted 1, 2 or 5 min. For the stability study, the essay investigated was obtained at 60% intensity for a duration of 5 min.

## **6.3.4 Particle size distribution measurements**

For droplet size experiments and measurements were all done in triplicate. Average droplet size distributions and average results with standard deviations are presented.

### **6.3.4.1 Dynamic light scattering**

The droplet size was measured by means of dynamic light scattering (DLS) using a Zetasizer Nano Z (Malvern Instruments, France). Data processing of the DLS measurements were done with the Zetasizer software by both cumulants and distribution analysis. Results were z-average, which is the mean size, and the size distribution in intensity. Before measurement, the nanoemulsions were diluted in ultrapure water (the dilution factor was adjusted to obtain an attenuation factor between 7 and 9). The measurements were realized at 25°C.

### **6.3.4.2 Laser diffraction**

The droplet sizes of optimized nanoemulsions were measured by Laser Diffraction (LD) particle size analysis with a Mastersizer 3000 (Malvern Instruments, France). The technique is based on measurement of the intensity of light scattered as a laser beam passes through a dispersed particulate sample. The Mie scattering theory was used, with a refractive index and an absorption index set at 1.55 and 0.005 for the dispersed phase, respectively. The continuous phase was ultrapure water with a refractive index 1.33. The results were expressed by  $D_{50}$  the mean droplet diameter for which 50 % of droplets in volume are below this size and the dispersity of the sample is given by the span value.

## **6.3.5 Optical microscopy**

A Leica DM2000 LED optical microscope fitted with a high definition camera was used to observe droplets without dilution. The images were captured remotely and analyzed via the LAS EZ software developed by Leica. Droplet sizes were determined using the software integrated features.

### 6.3.6 High Performance Liquid Chromatography

atRA quantification in nanoemulsion was monitored using a RP-HPLC method (Agilent 1200 series) as previously described by Almouazen et al.[152]. Briefly, C18 column with 2.6  $\mu\text{m}$  particle size (Phenomenex, Kinetex) was used as a stationary phase. Mobile phase composed of 30% methanol, 35% acetonitrile, 35% of deionized water with 0.5% acetic acid was injected at a flowrate of 1.4 mL/min. All samples were diluted in acetonitrile and the injected volume was 10 $\mu\text{l}$ . Finally the UV-detector was used at  $\lambda = 356 \text{ nm}$ .

### 6.3.7 Stability

Samples of interest were kept in stability in four different conditions: protected from light at temperature of 4°C, ambient temperature and 40°C and exposed to day light at ambient temperature.

## 6.4 Results

### 6.4.1 Determination of optimal formulation

O/W emulsions with HLB values of 9, 10 and 11 were observed by optical microscopy and the preparation corresponding to the HLB value of 10 was determined to give the smallest droplet size. The total mass of emulsifier (5 g per 100 g of emulsion) was comprised of 46% Tween 20 and 54% Span 80, or 2.3 g and 2.7 g per 100 g of emulsion, respectively. The solubility of atRA per gram of MCT was determined to be 2.24 mg in average thus a concentration of 0.02% was used, 1.88% of glycerol was added to adjust emulsion osmolality to 0.300 osmol/kg and be isotonic with plasma. All experiments were performed at a composition described in Table 6.1. The premix was obtained by the same procedure for all experiments as described in Materials and Methods. The droplet size distribution of the premixes were similar for all experiments and determined by LD at  $D_{50} = 10.3 \mu\text{m}$  and Span = 2.77.

	Component	Mass percentage [%]
Oil	atRA	0.20
	Span 80	2.70
	MCT	10.00
Water	Glycerol	1.88
	Tween 20	2.30
	Water	82.92

Table 6.1: Composition of the atRA emulsions formulation

### 6.4.2 Effect of the process on the resulting droplet size of the nanoemulsions

Using the predefined premix formulation, nanoemulsions were prepared by the three procedures described in details in Material and Methods. For each procedure, we evaluated and optimized experimental conditions regarding the nanoemulsion size distribution determined by DLS.

### 6.4.2.1 Effect of PME parameters on resulting droplet size by DLS

In PME, four cycles were performed using decreasing pores sizes. The influence of cycle number on particle size distribution, Z-average and PDI are presented in Figure 6.2. Considering size distribution presented in Fig 6.2a, the droplet size was reduced with the number of cycles which is explained by the fact that pore sizes were smaller and smaller after each cycle. All droplets were below 2  $\mu\text{m}$  after cycle 1 and 2, and only cycle 3 and 4 ensured size distribution below 1  $\mu\text{m}$ . Also, the size distribution width was smaller for cycles 3 and 4 than for cycles 1 and 2.

Regarding Z-average and PDI (Fig. 6.2b), which were measured by the same apparatus but estimated by different calculation methods, observations were similar. Z-average decreased from 615 nm at cycle 1 to 335 nm at cycle 4. PDI of the nanoemulsions obtained after the first two cycles were slightly above 0.10, for cycle 1 and 2, 0.10 and 0.13 respectively. For cycle 3 and 4, there were below 0.1: 0.03 and 0.09 respectively. Cycle 1 and 2 produced quite monodispersed nanoemulsions and cycle 3 and 4 very monodispersed ones. Standard deviations for the different tests and measurements were low from 4 nm and 0.02 for the last two cycles; to 18 nm and 0.06 for the first two cycles for Z-average and PDI, respectively.

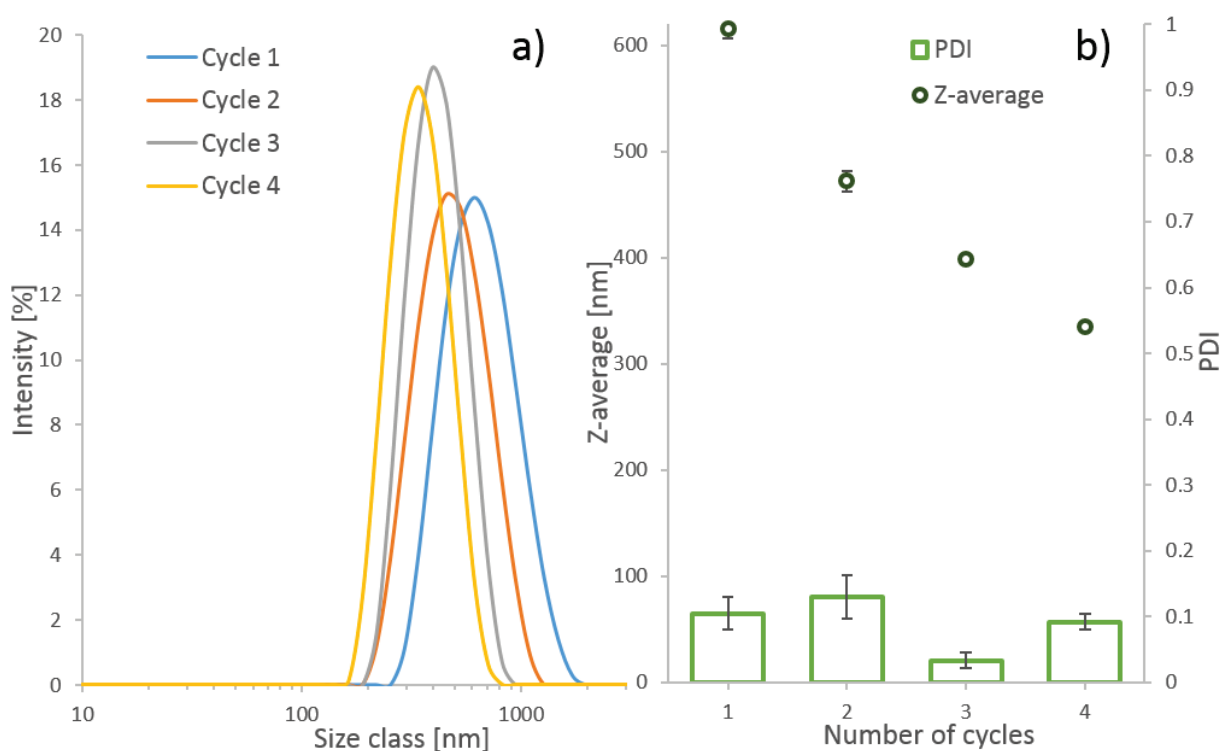


Figure 6.2: Effect of cycles number on particle size distribution in intensity a); Z-average and PDI b) by DLS for PME at cycles 1 to 4

### 6.4.2.2 Effect of MF parameters on resulting droplet size by DLS

Nanoemulsions were prepared at different pressures 1000 bars was selected as the optimized one. (data not shown). MF results regarding the influence of cycle number on particle size distribution, Z-average and PDI at a pressure of 1000 bars are presented in Figure 6.3. Size distributions (Fig. 6.3a) were significantly different between cycle 1 and all other cycles from 2 to 5. Indeed, cycle 1 presented a larger distribution and particles above 1  $\mu\text{m}$ , contrary to all other cycles that showed similar size distribution in terms of droplet sizes and distributions.

Z-average (Fig. 6.3b) varied from 162 nm for cycle 1 to 110 nm for cycle 5. Z-average decreased with cycle number, however the decrease from cycle 1 to cycle 2 was the more significant with a

value of 38 nm. From cycle 2, Z-average values were quite stable. Moreover, standard deviation was high for cycle 1, S.D. = 40 nm, and negligible for other cycles. PDI values were stable with cycle number and set between 0.11 and 0.17 for cycle 4 and 1 respectively, which indicated quite monodispersed emulsion. As seen on Fig 6.3a, size distribution was larger for cycle 1.

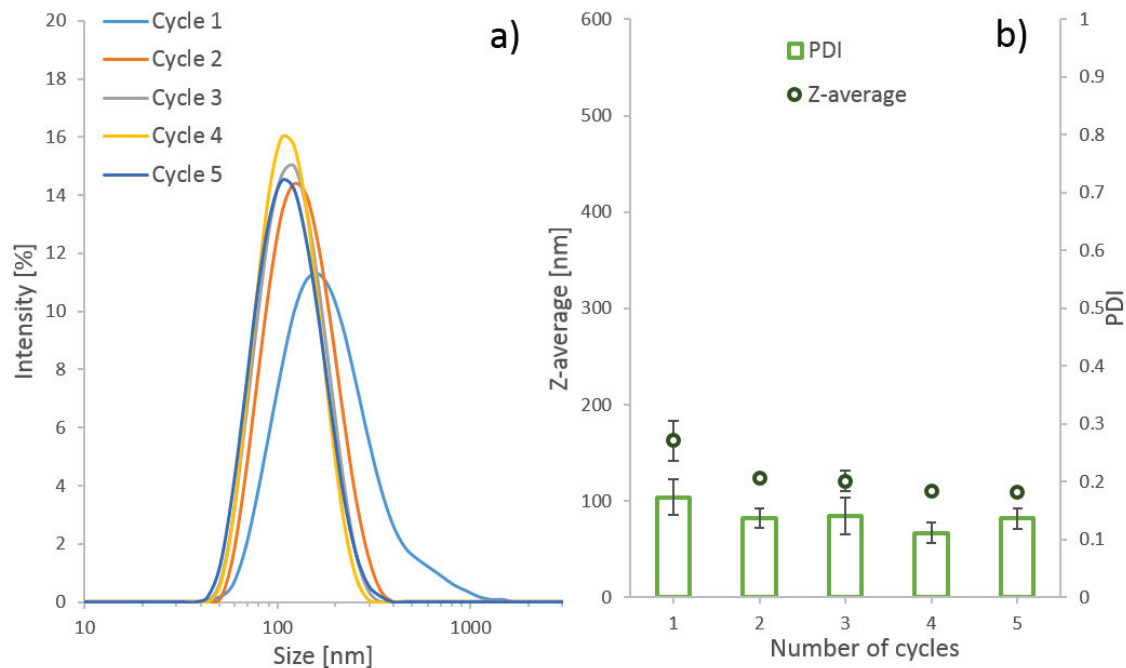


Figure 6.3: Effect of cycle numbers on particle size distribution in intensity a); Z-average and PDI b) by DLS for MF at a pressure of 1000 bars and cycles 1 to 5

### 6.4.2.3 Effect of US parameters on resulting droplet size by DLS

Figure 6.4 presents optimization of droplet sizes of nanoemulsions produced by US. Droplet size distributions at processing time of 1, 2 and 5 min are shown in Fig.6.4a and Z-average and PDI for US intensities of 30% and 60% and processing time of 1, 2 and 5 min in Fig 6.4b. Regarding droplet size distribution (Fig 6.4a), 1 min processing time led to polydispersed and bigger droplets, a part of the distribution being above 1  $\mu\text{m}$  compared to longer processing times. At 2 and 5 min, the distributions were similar and all of the distribution was below 1  $\mu\text{m}$ .

In addition, Z-average (Fig 6.4b), decreased with processing time, from 334 nm to 173 nm at 1 min and 5 min at 30% US intensity and from 195 nm to 173 nm at 1 min and 5 min at 60% US intensity. Also, at 1 and 2 min processing time, nanoemulsions obtained at 60% US intensity were smaller than the ones obtained at 30%. However, at 5 min, nanoemulsions obtained at 30% and 60% US intensities had the same Z-average. Finally, PDIs, (Fig 6.4b) were high at 1 min processing time, 0.26 and 0.61 at 30% US intensity and 60% US intensity, respectively, with high standard deviation. They both decreased with processing time to finally reached 0.19 and 0.21 at 30% US intensity and 60% US intensity, respectively, after 5 min. Even if the PDI values decreased with increasing processing time and US intensity, they were still quite high and DLS may not be the ideal apparatus to measure the mean droplet size, as DLS is aimed at measuring monodispersed emulsions.

### 6.4.2.4 Comparison of the processes regarding droplet size by DLS, LD and optical microscopy

From previous sections, optimal conditions were determined for each process in order to compare droplets size. For PME, the condition selected was cycle 4, for MF, 1000 bars and cycle 5, for US, 5

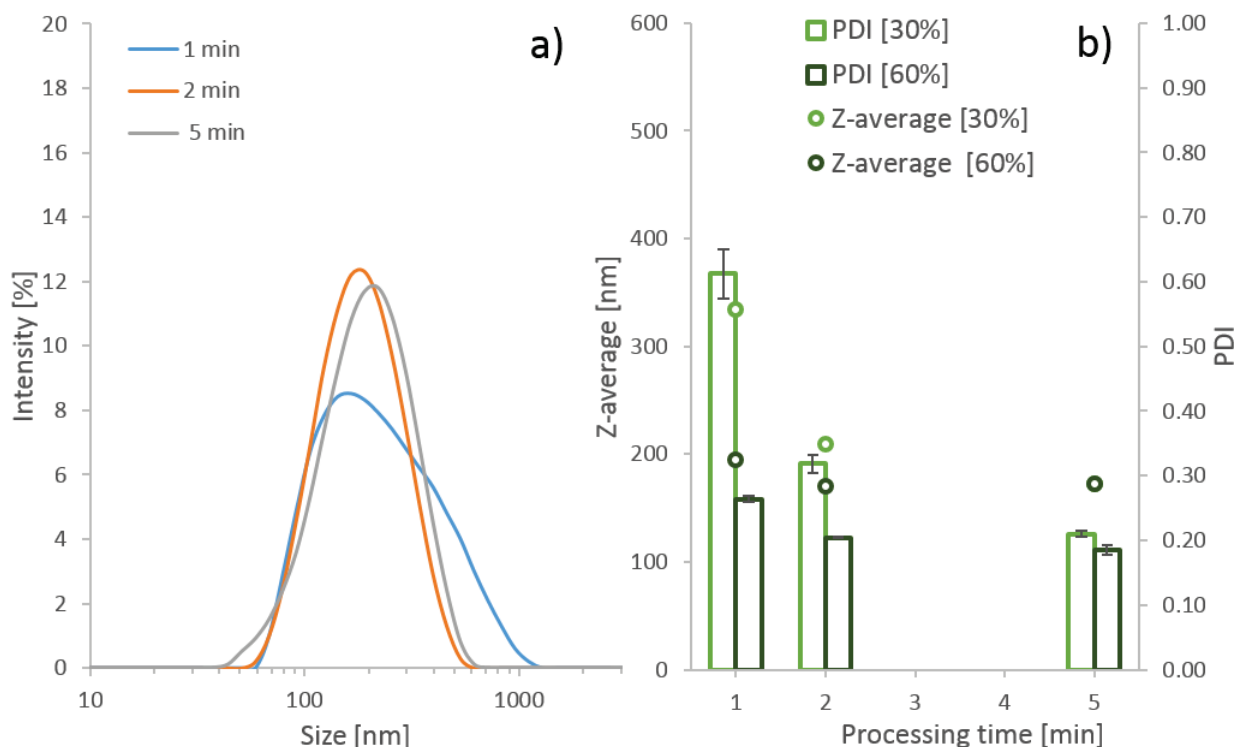


Figure 6.4: Effect of US duration from 1 min to 5 min on particle size distribution in intensity by DLS a) and effect of US duration and intensity on Z-average and PDI b)

min at 60% US intensity. In this section, only results obtained at these conditions are presented. Size distributions in intensity obtained by DLS and in volume obtained by LD are presented on Figure 6.4 a) and b) respectively. With DLS (Fig 6.5a), the three size distributions were strictly below 1  $\mu\text{m}$ . PME presented the bigger droplet size but narrower size distribution; US a large size distribution and intermediate mean size; and MF, the smallest size and medium dispersity.

With LD (Fig 6.5b), the volume size distribution for nanoemulsions prepared by PME was similar to the one obtained by DLS. However, for the two other processes, LD and DLS gave very different size distributions. Indeed, bimodal distributions instead of monomodal were obtained with a first peak between 50 nm and 300 nm corresponding to DLS measurements and a second peak between 300 nm and 1  $\mu\text{m}$ . Moreover, nanoemulsions produced with US showed two small peaks at around 1.5  $\mu\text{m}$  and 2.5  $\mu\text{m}$ .

These observations are confirmed by the mean size and dispersity by DLS and LD presented on Table 6.2. The nanoemulsions obtained by PME presented a mean droplet size value of 335 nm and 333 nm by DLS and LD respectively, a PDI of 0.09 and Span of 0.56. This corroborates the results shown on Figure 6.5, both analytic methods confirmed a monodisperse nanoemulsion with a mean size value of around 330 nm. On the contrary, nanoemulsions obtained by MF presented different mean size and dispersity by DLS and LD. The mean droplet size was 40 nm bigger with LD than with DLS. But more importantly LD and DLS gave different dispersities. Indeed, nanoemulsion produced by MF presented a Span of 2.75 and could be considered as polydispersed whereas a PDI of 0.14 by DLS indicated a monodispersed sample. Same observation can be made for the nanoemulsions obtained by US, the difference in mean size obtained by DLS and LD was small, 14 nm smaller by LD, but the dispersities were much different. PDI was measured at 0.19 with DLS, which was considered as quite monodispersed and Span at 2.04 indicating a polydispersed distribution.

A third observation method, optical microscopy, was used to confirm the presence of microscopic droplets (> 1  $\mu\text{m}$ ).

On Figure 6.6, four photographs are presented, two of nanoemulsions obtained with MF at 1000

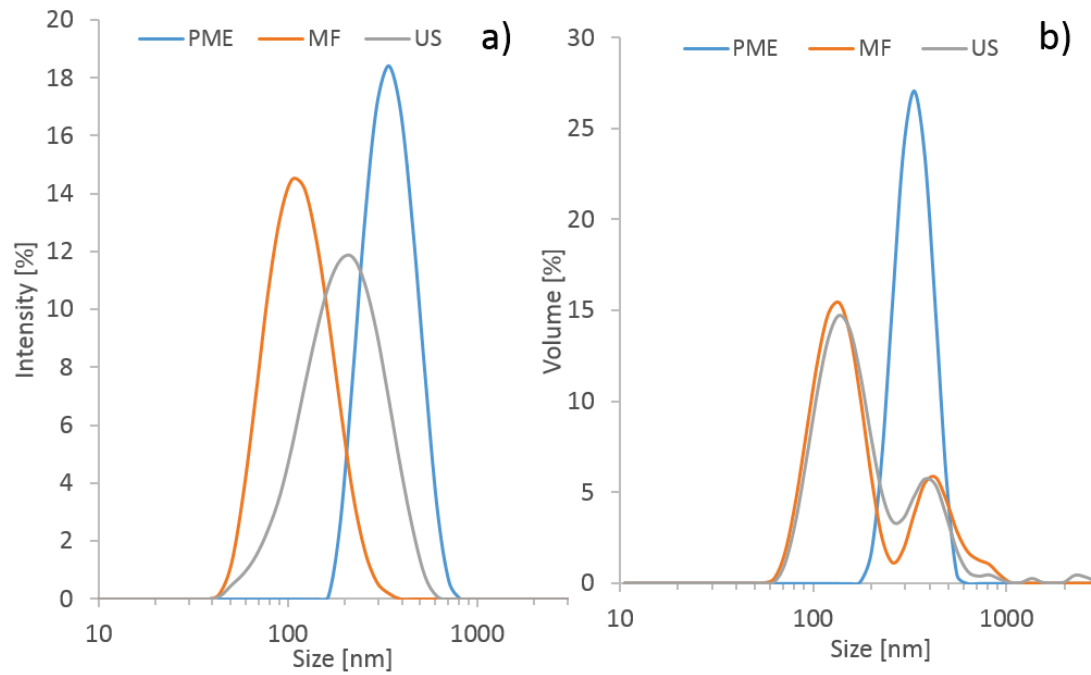


Figure 6.5: Comparison of size distribution in intensity by DLS a) and in volume by LD b) for the three different processes PME, MF and US for selected conditions

	DLS		LD	
	Z-average	PDI	D <sub>50</sub>	Span
US	173±2 nm	0.19±0.01	159±1 nm	2.04±0.05
MF	110±6 nm	0.14±0.03	152±4 nm	2.75±0.39
PME	335±4 nm	0.09±0.02	333±3 nm	0.55±0.04

Table 6.2: Summary of size results for the three different processes PME, MF and US for selected conditions

bars, at cycle 1: Figure 6.6a) and at cycle 5: Figure 6.6b). Figure 6.6c) shows an emulsion produced with US at 60% intensity during 5 min and finally Figure 6.6d) an emulsion produced by PME at cycle 4. On Figure 6.6a), we observe several droplets bigger than 1 μm and droplets up to 5.6 μm were measured. Figure 6.6b) shows that most micron size droplets disappeared after 5 cycles but some were still present with size between 1 and 3 μm, in agreement with what was observed on Figure 6.5 by LD. Figure 6.6c) shows the nanoemulsion produced by US, with also micron size droplets. Droplets between 1 and 5 μm were observed which is in agreement with the size distribution by LD presented on Figure 6.5. On the contrary, for nanoemulsions prepared by PME (Figure 6.6d), no droplets can be seen even if the magnification factor was 100 instead of 40 for the other photographs. This is also in agreement with the droplet size distribution obtained with LD.

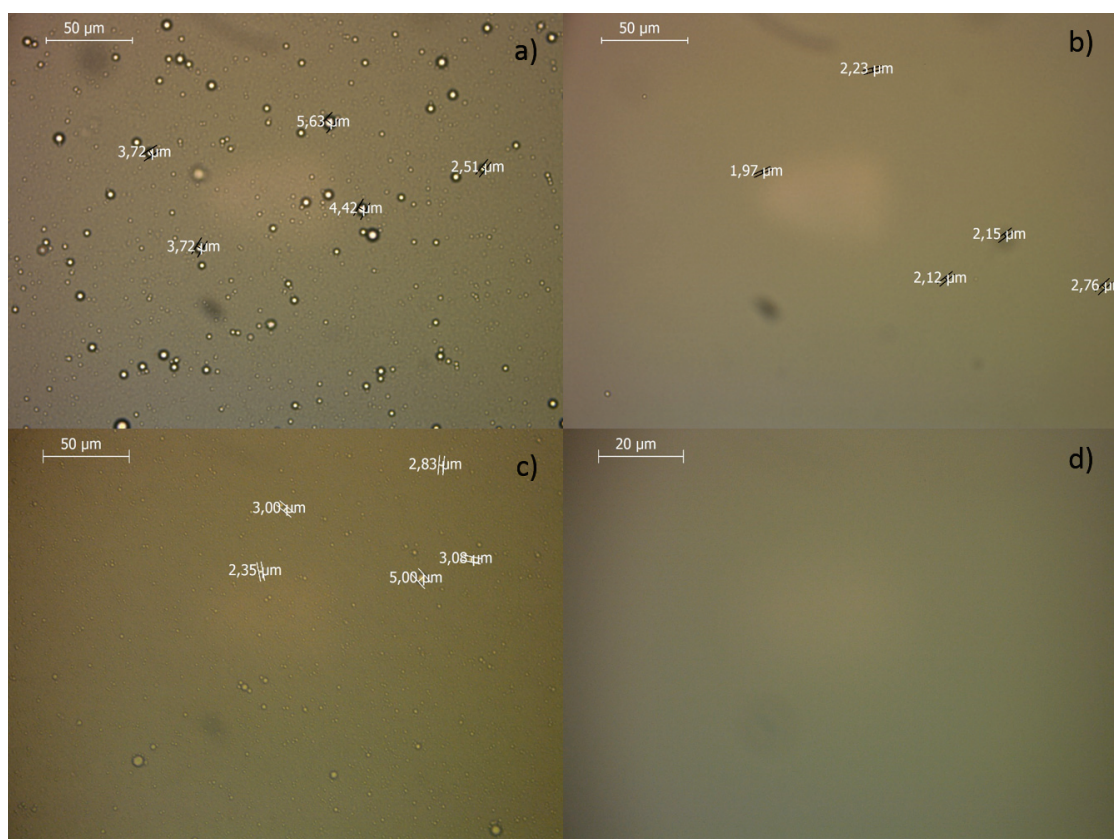


Figure 6.6: Optical microscopy photographs at x40 of three emulsions a) first cycle of MF at 1000 bars; b) fifth cycle of MF at 1000 bars; c) 5 min at 60% intensity US; and one at x 100, d) fourth cycle of PME

Stability assessment was made by DLS and presented on Figure 6.7. Droplet size distributions at each selected condition for each process are presented at t0, just after production, at t+2 weeks and at t+3 months measured 15 days and 3 months after preparation, respectively, for samples kept at 40°C. Regarding nanoemulsion produced by PME, no difference in droplet size distribution was observed between post production and t+3 months. For US, the size distribution changed slightly but not significantly. Then for MF, the distribution became larger and mean droplet size increased from 110 to 150 nm at 2 weeks and to 607 nm at 3 months. These results were confirmed by LD and optical microscopy (data not shown).

### 6.4.3 Effect of the process on API degradation

Results presented in this section were obtained at the optimal conditions determined previously for each process. AtRA degradation was negligible for each process and approximately 100% of atRA was recovered at the end of the production (data not shown). AtRA stability was investigated under accelerated and normal stability conditions including light and temperature over 2 weeks (Figure 6.8).

The stability conditions investigated were ambient temperature in day light and protected from day light, at 4°C protected from day light and at 40°C protected from day light. At 4°C, no degradation of atRA occurred regardless of the process used, the lowest percentage being 97% after 2 weeks for PME and MF. At ambient temperature, in dark conditions, degradation started slowly with the lowest percentage of 84% obtained for MF. No real difference was seen between the different processes. To evaluate the process impact on atRA degradation and predict long term stability, stressed stability at 40°C was done over 2 weeks. After 1 week, MF showed the lowest percentage at 18% followed by PME at 67% and finally US seemed to present no degradation but a very high

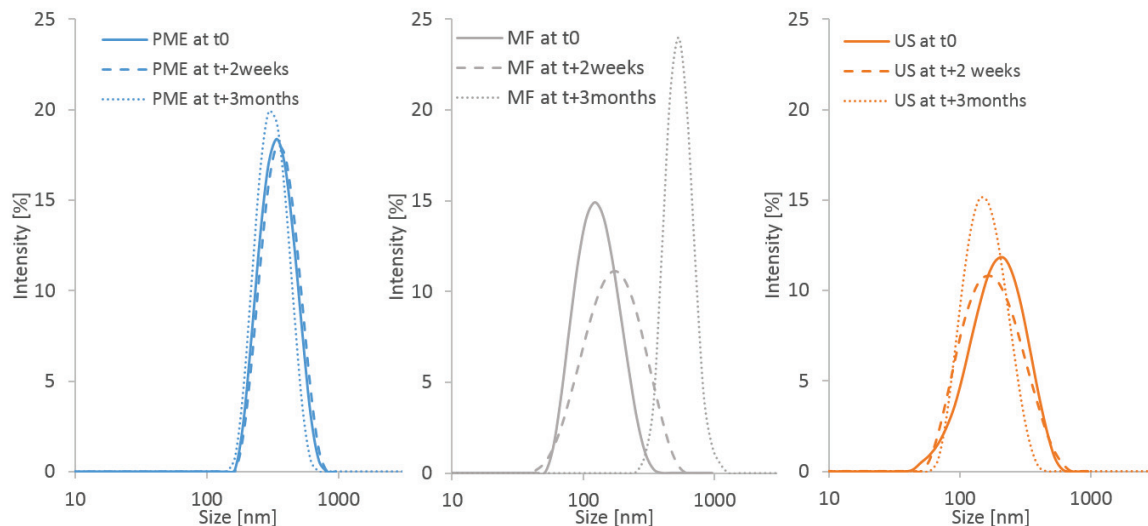


Figure 6.7: Comparison of size distributions in intensity (DLS) at t0, t+2 weeks and t+3 months under accelerated stability at (40°C) for nanoemulsions prepared by PME, MF and US with selected conditions

standard deviation compared to the other processes. At 2 weeks, atRA completely disappeared for MF whereas for PME and US it was still present at 35% and 54%, respectively. The chromatography analysis showed a decrease of atRA within the nanoemulsion without any isomeration as the principal isomers (13 cis, 9 cis and 11 cis) were not detected (Figure 6.9). In order to study the process impact on atRA isomeration, stability under day light exposure was also performed over 2 weeks. After one week, like with other conditions, MF was the most degraded down to 21%, followed by PME, 35% and finally US with 41%. After two weeks the percentages became very low: 17% for MF, 22% for PME and 25% for US. This reduced atRA quantity under light was mainly due to isomeration as the three isomers can be seen, peaks at 15.5 min for 9-cis-atRA, at 14 min for 13-cis-atRA and at 12.5 for 11-cis-atRA by chromatography analysis (Figure 6.9) and no difference was observed between the three processes.

These data were completed by long term stability measurements at 3 months at 4°C and percentage were found to be 77%, 76% and 63% for nanoemulsions produced by US, PME and MF respectively (data not shown), which is in accordance with accelerated stability.

Overall, the process which seems to degrade less atRA was US, followed closely by PME but nanoemulsions produced by MF were significantly more degraded at the more extreme conditions regarding temperature and light exposure.

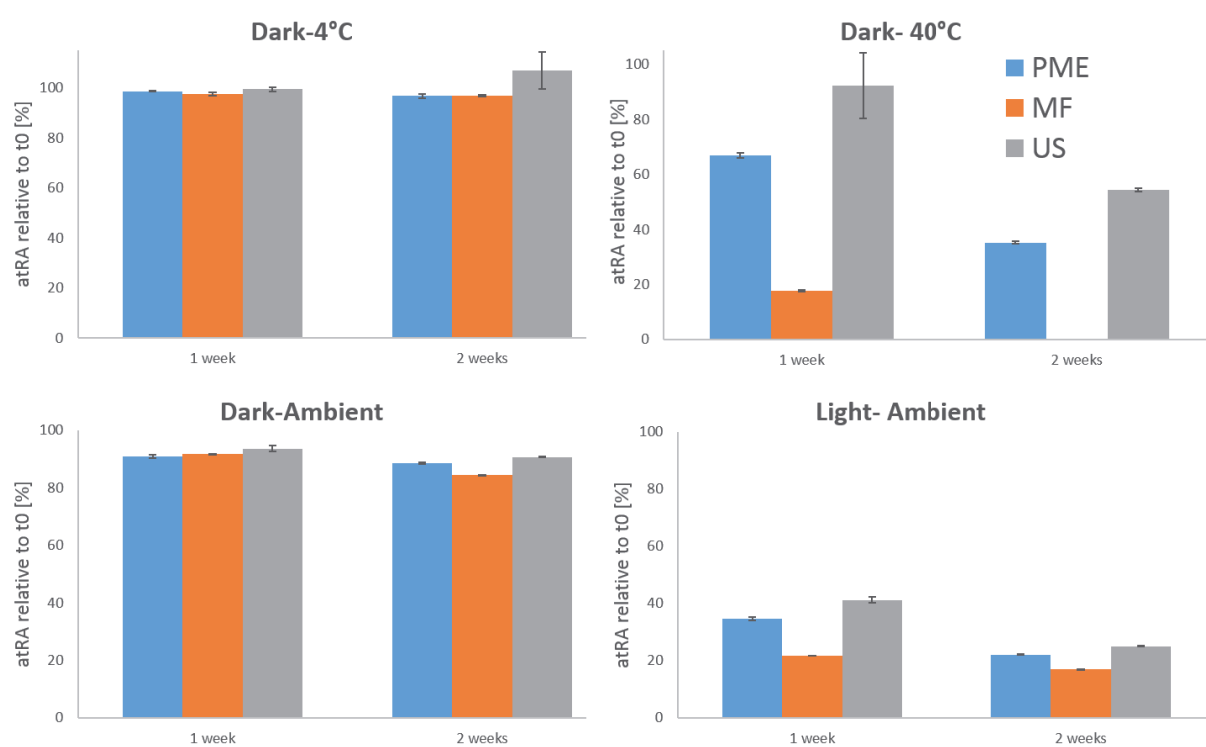


Figure 6.8: Stability of atRA nanoemulsions during 2 weeks: remained atRA was determined and expressed as percentage of post-production content

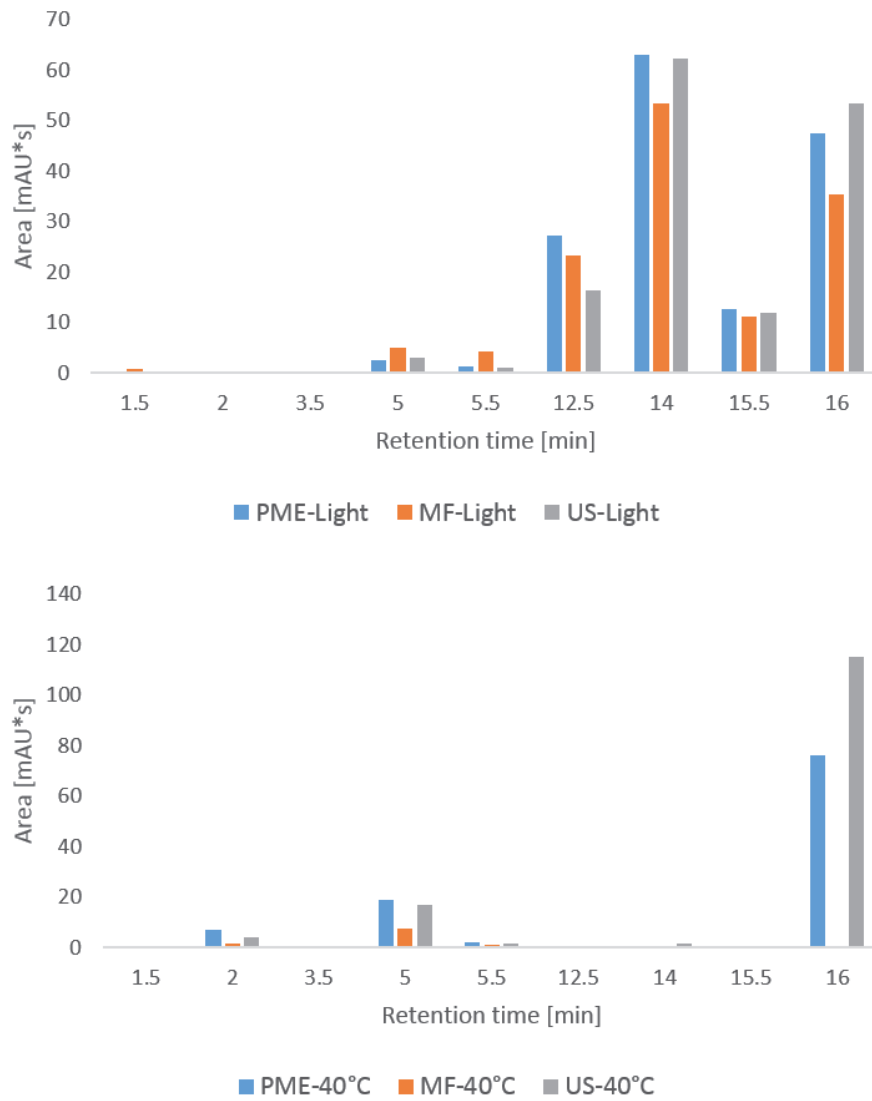


Figure 6.9: Peak areas at different retention times after 2 weeks in stability at day light exposure and 40°C

## 6.5 Discussion

Emulsions produced by US and MF at optimal conditions presented similar characteristics, with very fine droplets below 200 nm but large size distribution. This large size distribution was not seen by DLS which is not adapted to polydispersed samples. However, it was observed by two other techniques, LD and optical microscopy. US is known to produce polydispersed samples as only the suspension near the sonifier probe is affected by ultrasonic waves [153]. In MF, all droplets need to experience the peak shear rate generated by a flow-producing device otherwise the resulting emulsions are polydispersed [154]. This explains why several cycles are needed, and this study shows that even after 5 cycles, micron size droplets were present in the sample. PME presented a different droplet size distribution profile, the optimized sample had a mean value of 335 nm and a good monodispersity confirmed by DLS, LD and optical microscopy showing no micron sized droplets. These results were similar to the ones obtained previously with this set-up and the same surfactant system [124].

In terms of stability, nanoemulsions produced by PME and US did not present any destabilization over 3 months under stressed stability at 40°C. On the contrary, MF showed emulsion droplets 36% bigger after 2 weeks and 452% after 3 months. These nanoemulsions can be considered unstable.

The three processes produced nanoemulsions that can be used in intravenous applications. However, MF and US will lose expensive active ingredients during the filtration/sterilization step where micron droplets would be removed. On the contrary, a sterile nanoemulsion can be obtained by PME, if the membrane is sterilized as the final pore size used is 0.2 µm [59]. Thus PME could be a one step process of emulsification/sterilization with no active ingredient loss and presenting advantages regarding economical aspects.

The three processes had a small impact on at-RA degradation during emulsification and no difference was observed. For this reason and considering the variation of input energy between the three processes, the impact of emulsification process on atRA was evaluated in stability study. After 2 weeks, no significant degradation was seen at 4°C and at ambient temperature protected from light. However, at 40°C and day light conditions, nanoemulsions produced by MF were more degraded than the ones obtained by other processes. US and PME showed similar behavior but US produced nanoemulsions even less sensible to degradation.

Similar degradation profile was previously observed on other colloidal formulation of atRA. For solid lipid nanoparticles of atRA, prepared also for parenteral administration, rapid degradation was observed by light (in 10 h) and also by the storage at 4°C (about of 50% after 1 month) [155]. This degradation could be due to the use of high-pressure homogenizer during SLN preparation and the authors proposed lyophilization or adding anti-oxidant agent to enhance the storage. In our study, storage at 4°C will be recommended as the nanoemulsions prepared by US and PME showed slow degradation over 3 months. In a final formulation for a parenteral application, an antioxidant can be added to improve atRA stability. However, accelerated stability (40°C) indicated rapid degradation for nanoemulsion prepared by MF together with greater long term instability at 4°C than the other processes.

This difference in degradation rate between processes might be explained by the temperature increase in MF which was up to 73°C at 2000 bars and fifth pass. Indeed, MF requires a high energy input per unit volume (E/V),  $E/V = 10^8 \text{ J} \cdot \text{m}^{-3}$  with a lot of heat loss by viscous dissipation. US requires nearly the same E/V as MF [156], however in our study, an ice bath was used preventing a high temperature increase. This can explain why the lowest degradation was seen with this process. PME, working at around 50 bars, requires nearly 3 orders of magnitude lower energy  $E/V = 5 \times 10^5 \text{ J} \cdot \text{m}^{-3}$  compared to US or MF, which can explain the lower degradation observed.

## 6.6 Conclusion

In this study, O/W nanoemulsions for parenteral administration of at-RA were prepared successfully by MF, US and PME. First, the composition parameters were investigated in order to fulfill

the requirement of a parenteral nanoemulsion.

Three processes were studied regarding the influence of the production parameters on droplet size by DLS, LD and optical microscopy. It was found that for PME, droplet size distributions were all monodispersed and except for cycle 1, all below 500 nm, reaching 335 nm at cycle 4. DLS and LD measurements were similar and no micron size droplet was seen by optical microscopy. For MF, after cycle 1, the nanoemulsions presented all low PDI and a mean droplet size below 200 nm by DSL. However, by LD and optical microscopy, bigger droplets above 500 nm and a very large dispersity were measured. By US, after 5 min, all nanoemulsions were below 200 nm but with quite high PDI. By LD and optical microscopy, some bigger droplets were seen above 1  $\mu\text{m}$ . Moreover, nanoemulsions produced by US appeared to be more polydispersed. In stressed stability, nanoemulsions produced by US and PME did not change over 3 months. Those produced by MF, on the contrary showed a drastic increase in droplet size of 426% after 3 months. Nanoemulsions produced by MF were found unstable under stress conditions.

Also, the three processes were evaluated for their impact of drug degradation and no difference was seen. In stability, no significant difference was observed of atRA degradation at  $t_0$  and after 2 weeks of storage at 4°C and dark ambient temperature. However, atRA nanoemulsion exposed to 40°C or day light showed rapid atRA degradation with significant differences between the three processes. Nanoemulsions prepared by US showed the best overall resistance to degradation, followed by the one produced by PME and finally by MF which was totally degraded after 2 weeks at 40°C and showed the higher degradation under light exposure.

In conclusion, all processes are suitable to produce injectable nanoemulsions but only PME was adapted to thermosensitive actives with the potential of large scale production. Moreover, in terms of droplet size, PME produced monodispersed droplets of 330 nm compared to the other processes which produced nanoemulsions of around 150 nm but with the presence of micron size droplets combined with droplet instability over 3 months for MF. Therefore, PME could be an alternative industrial process for parenteral emulsions manufacturing with no additional sterilization step and a lower energy requirement.

## Complementary datas

Complementary measurements on effect of processes on stability of the final nanoemulsions have been performed.

On Figure 6.10, size distributions measured by LD for the nanoemulsions produced by the three processes at  $t_0$  after production and kept in stability for 3 months at  $40^\circ\text{C}$  are presented. We observed the same evolution as presented in Figure 6.7 by DLS. Nanoemulsions produced by PME and US did not destabilize over 3 months in stress conditions, droplet size distributions were exactly the same. However, nanoemulsions produced by MF presented a severe degradation with a drastic increase of the size distribution. The emulsion produced by MF was found unstable in stressed conditions with LD measurement.

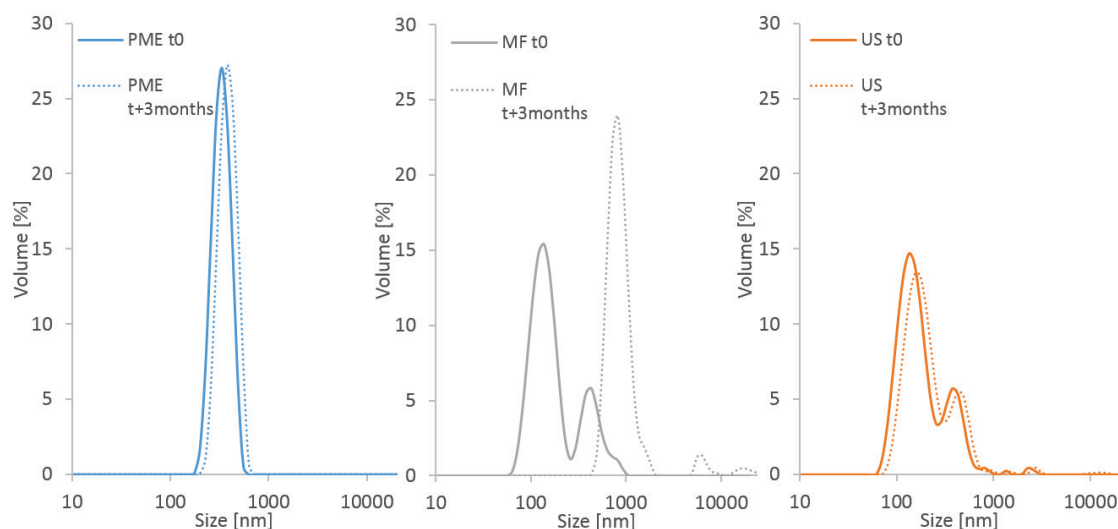


Figure 6.10: Comparison of size distributions in volume (LD) at  $t_0$ ,  $t+2$  weeks and  $t+3$ months accelerated stability at  $40^\circ\text{C}$  for the three different processes PME, MF and US for selected conditions

The effect of MF cycle on destabilization at  $40^\circ\text{C}$  at 3 months has also been investigated and size distribution results for cycle 1, cycle 3 and cycle 5 are presented on Figure 6.11. We observe that the nanoemulsion produced at cycle 5 was more destabilized than the one at cycle 3, their mean size value increased from around 110 nm to 295 nm and 607 nm for cycle 3 and cycle 5 respectively. Finally, the emulsion that underwent less destabilization was the one obtained at cycle 1 for which the mean size varied from 167 nm to 230 nm.

These results showed that by increasing cycle number in MF, polydispersity and mean size were reduced but this may not be a good choice for stability issues.

The stability was observed at accelerated conditions at  $40^\circ\text{C}$ . Comparison of results at ambient temperature at 2 weeks and 3 months are presented on Figure 6.12 to verify if the same phenomena were observed. For samples kept at ambient temperature, mean droplet size and dispersity increased with time but slower than in stress conditions at  $40^\circ\text{C}$ . Nanoemulsions produced with MF showed nearly the same size distribution when kept 2 weeks at  $40^\circ\text{C}$  or 3 months at ambient temperature. Higher temperature led to faster destabilization which also occurred at ambient temperature. Keeping samples at  $40^\circ\text{C}$  was confirmed to be a good way to accelerate destabilization of a sample and thus anticipate it.

With these complementary results we confirm by LD the results observed by DLS with similar size distributions and similar mean values. Moreover, we showed that destabilization was a function of the number of cycles with MF so a function of the energy given to the system. Increasing the

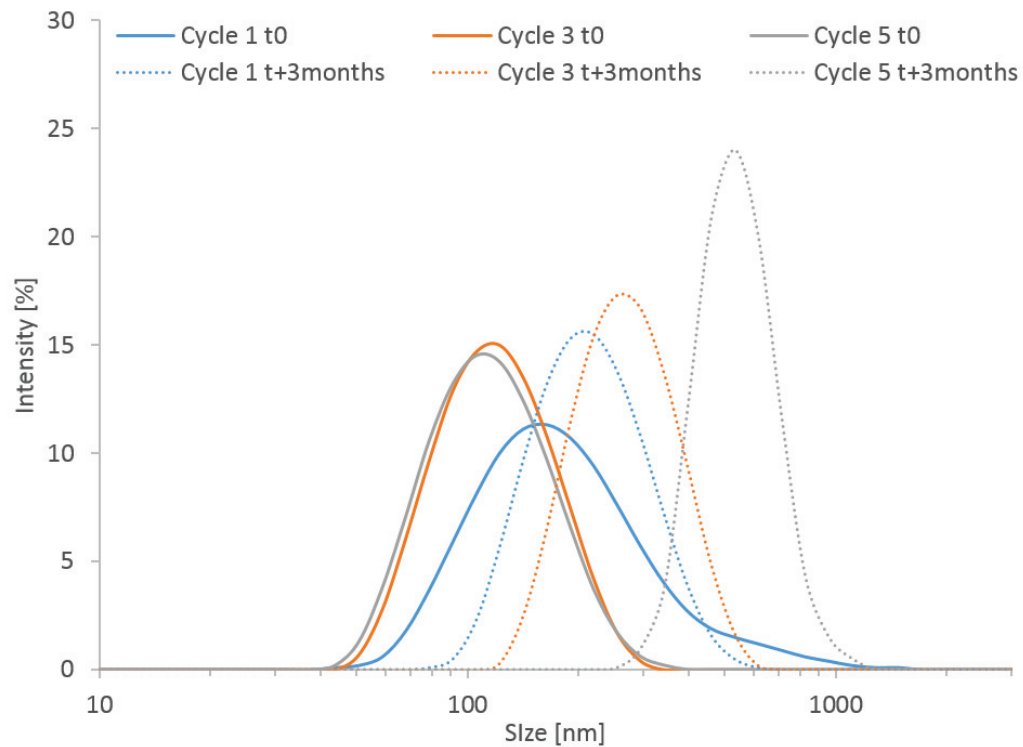


Figure 6.11: Comparison of size distributions in intensity (DLS) at t0 and t+3months accelerated stability at 40°C for the different cycle number in MF

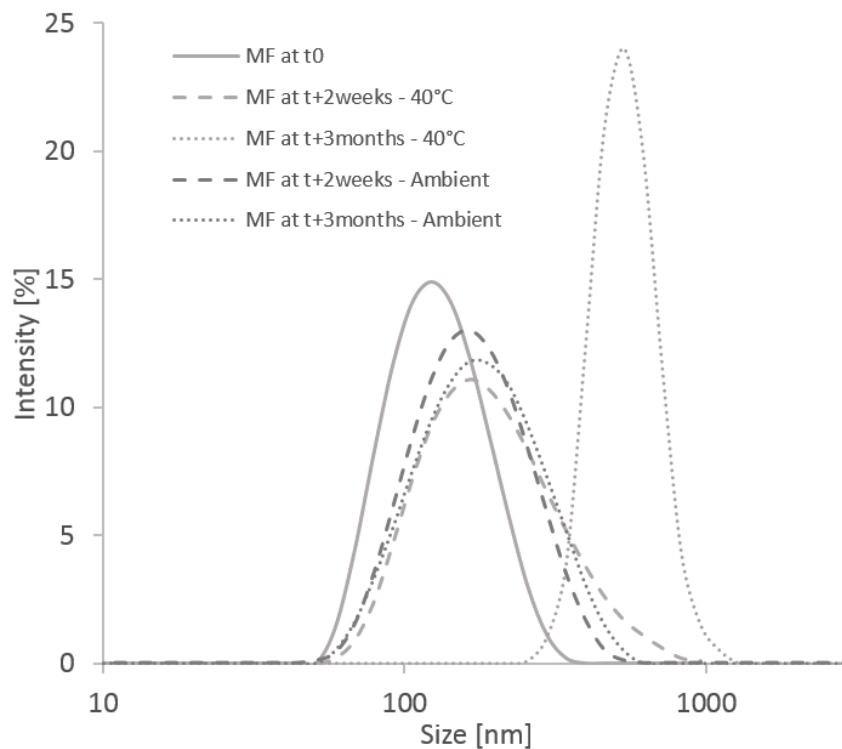


Figure 6.12: Comparison of size distributions in intensity (DLS) at t0, t+2 weeks and t+3months for different stability conditions, ambient temperature and 40°C for MF sample at cycle 5

number of cycles to get smaller and less polydispersed samples may have negative impact on stability. Then, we confirmed that destabilization which occurred rapidly at 40°C also occurred at ambient temperature but slower.



# Conclusion

## General conclusions of the work

The general aim of the work was to develop a PME process to produce nanoemulsions at large scale with specific compositions related to the European project, PeptiCaps.

First, the production of O/W nanoemulsions down to 260 nm was shown to be possible with a special set-up composed of a high pressure pump and a 125 mm long membrane. With this set-up, batches up to 500 mL were produced with no change in droplet size and no pressure increase. These nanoemulsions were stable for 9 months at room temperature.

This study was made with a model composition and the influence of oil and surfactant concentrations are important parameters which affect the resulting pressure and droplet size. Oil content and viscosity were pointed out to have a great influence on the pressure generated through the membrane and so on the feasibility of the process.

Moreover, process parameters were also investigated, related to larger scale production (flowrate and membrane length) and to the final droplet size of the emulsion (pore size and number of cycles).

The results were either in agreement with what was observed at micron size and already reported in the literature or new observations. Droplet size decreased with flowrate increase. The increase of membrane surface by a certain factor led to an increase in flowrate with the same factor with no change in pressure or droplet size. The droplet size varied linearly with membrane pore size, offering a great tunability of resulting droplet size. Moreover, one single cycle appeared to be sufficient to achieve monodispersity contrary to what was observed with polymeric membranes [53, 94, 110, 111].

Then, we focused on the production of W/O nanoemulsions and understanding the influence of viscosities on nanoemulsion production by PME in terms of pressure and droplet sizes. In order to investigate viscosity effect, the water phase viscosity was modified by adding glycerol at different concentrations, the oil phase viscosity by using mineral oils of different viscosities and the overall emulsion viscosity by increasing the dispersed phase content of the emulsion.

The resulting pressure was shown to be the addition of three pressures: the pressure required to break up the droplets inside the membrane pores,  $\Delta P_{dis}$ , which did not depend on viscosities, contrary to the pressures generated by the flows through the pipe  $\Delta P_{pipe}$  and the membrane  $\Delta P_{flow}$ , that were proportional to the viscosity of the overall emulsion.

W/O nanoemulsions were more difficult to produce and to characterize but thanks to the original set-up which allows working at pressures up to 65 bar and high flowrates, W/O mineral oil nanoemulsions were produced with mean droplets size around 600 nm and flow rate of 50 mL/min.

In a following part, the results obtained showed that the process developed allows the production of nanoemulsions of different composition and different requirements, in particular, the compositions specified by our European partners from PeptiCaps project. Their originality is that the surfactants used, PP1 for O/W emulsions and PP2 for W/O emulsions are amphiphilic polypeptides. Thus, O/W nanoemulsion of droplet size of  $D_{50} = 837$  nm were produced with a composition of 10% EHP and 2% PP1. Also W/O nanoemulsions of around 600 nm were produced with a composition of 10% 30/70 citrate buffer/glycerol mixture, 1% PP2, 18% Ewocream and 72% MCT. Both O/W and W/O nanoemulsions were produced at a maximum flowrate of 50 mL/min.

Finally, the set-up developed was compared to Microfluidizer and ultrasounds, the more common processes for nanoemulsions production. These processes were evaluated for the production of all-trans retinoic acid nanoemulsions because of the interest of this molecule and its route of administration for pharmaceutical applications. In terms of droplet size, PME produced a stable monodispersed droplets of 335 nm compared to the other processes which produced nanoemulsions of around 150 nm but with the presence of micron size droplets combine with droplet instability over 3 months for MF.

Thus, PME could be an interesting alternative to other processes for nanoemulsion production,

for example nanoemulsions suitable for injection, with no need of adding a filtration step in order to remove bigger droplets, creating API loss.

To conclude, the high pressure PME developed can be used for different applications with the advantages of high monodispersity, improved stability, easy scalability, good tunability of final droplet size and lower energy consumption.

## Perspectives

Perspectives of future studies and applications are the following:

- Other formulations could be produced with the set-up developed such as SLN (with addition of an heating system to the set-up), double emulsions (first to form W/O emulsions and then W/O/W) or nanocapsules if the process is coupled with an encapsulation technique.
- Other membrane types can be tested to see if their pressure resistance is better in order to work at higher pressure and to be able to reach smaller droplet sizes.
- Further investigation of the effect of microfluidizer on destabilization processes with other formulations to gain a better understanding of the phenomena involved.
- Lastly, going to larger scale is a challenging perspective. Longer membrane and two pumps in parallel can be used to improve flowrate and to work continuously.



# Appendix A

## Appendixes

### A.1 "Proof of concept" set-up results

#### A.1.1 Model composition

As presented in Chapter 2, the process was first developed on a "proof of concept" set-up to be able to increase the pressure safely. The idea was first to test the ability of the SPG membrane to resist to higher pressures and thus to produce nanoemulsions. The first concluding results are presented in Figure A.1. With this set-up we were able to produce monodispersed nanoemulsions of  $D_{50} = 855$  nm with a  $0.5 \mu\text{m}$  membrane and  $D_{50} = 261$  nm with a  $0.2 \mu\text{m}$  pore size membrane. These nanoemulsions were produced at moderate pressure, under 50 bars with no issues regarding membrane resistance to pressure.

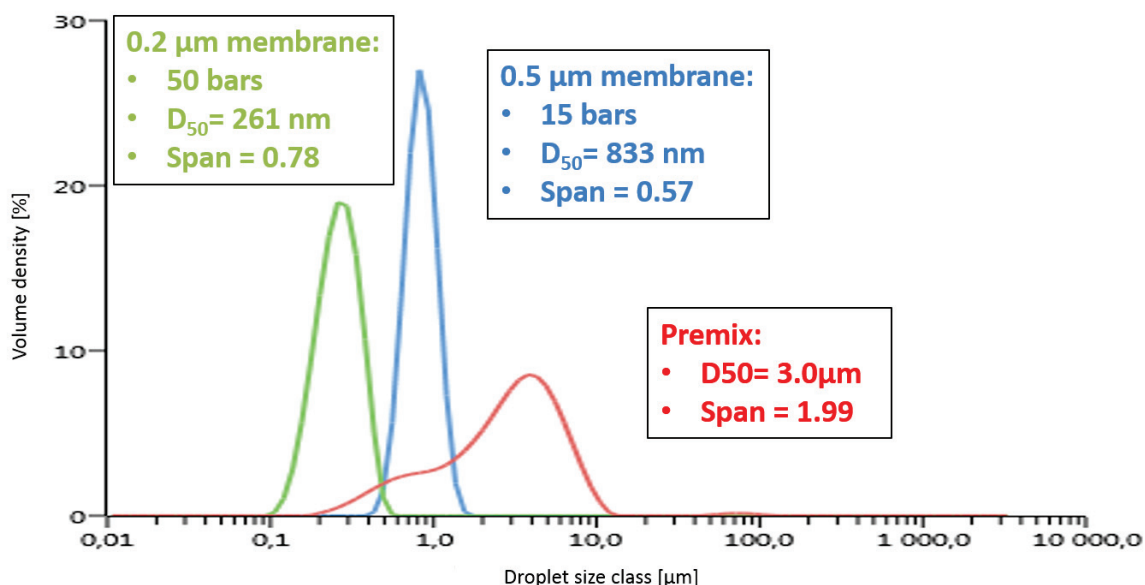


Figure A.1: Size distribution in volume with different membranes with a composition of 10% EHP and 5% Span 80 and Tween 20 mix

These first results confirmed that nanoemulsions could be produced by PME and encourage us to develop a pilot scale set-up which allows a production in a controllable way.

### A.1.2 PeptiCaps composition

The final aim of this study being to produce nanoemulsions with polypeptidic surfactant, the "proof of concept" set-up was also tested with PP1. These first results are presented on Figure A.2 at 1% PP1 and on Figure A.3 with 5% PP1. On these figures, only membrane pore sizes were changed. The composition was kept constant at 10% EHP and 1% PP1.

On Figure A.2, we see that droplet size was reduced by passing through the membrane but the process did not produced monodispersed emulsions of controlled size, moreover nanoemulsions could not be reached with this composition.

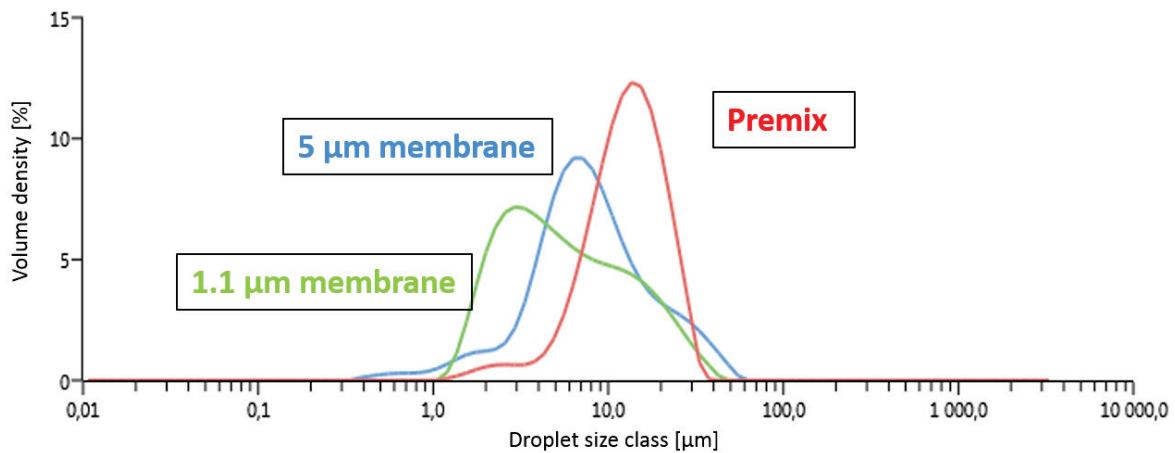


Figure A.2: Size distribution in volume with membranes of different pore size with 10% EHP and 1% PP1 in citrate buffer at pH 5.5

On Figure A.3, PP1 concentration was increased to 5% in order to produced smaller emulsions. With the 1.1 µm membraen, monodispersed emulsions of  $D_{50} = 1,2 \mu\text{m}$  were produced containing a small amount of bigger droplets, certainly due to the variation of the pressure in this set-up. With this composition, 70 bars was already required instead of 15 bars required to go through a 0.5 µm membrane with the model composition. Then, in order to produce nanoemulsions, this emulsion of  $D_{50} = 1,2 \mu\text{m}$  was passed through a 0.5 µm membrane. A sub-micron emulsion was successfully produced at 80 bars with a  $D_{50} = 838 \text{ nm}$ , however still some bigger droplets were obtained due to the variation in pressure.

These results confirmed that sub-micron emulsions of specific composition could be produced by PME at moderate pressure. They also suggest that a pilot scale set-up to produce nanoemulsions in a controllable way could be developed.

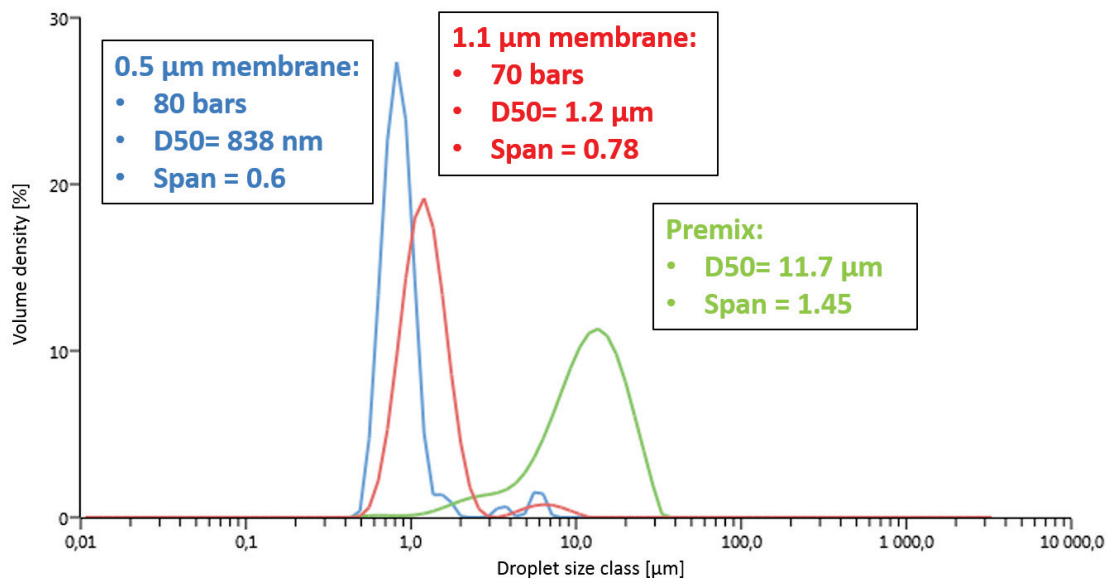


Figure A.3: Size distribution in volume for 10% EHP and 5% PP1 concentration and with the 0.8  $\mu\text{m}$  membrane in citrate buffer at pH 5.5

## A.2 Preliminary results with a 1.1 $\mu\text{m}$ pore size membrane

First the set-up was used to produce emulsions droplets at microscale with a 1.1  $\mu\text{m}$  membrane. The aim of this study was to handle the set-up and verify that the phenomenon observed were the same as the ones described in the literature for PME.

On Figure A.4, droplet size distribution for the premix emulsion obtained by magnetic stirring, emulsion obtained with a rotor-stator at 10 000 rpm during 3 min, and emulsions obtained with PME with membrane of 1.1, 2 and 5  $\mu\text{m}$  pore size are presented. We observed that membranes led to more monodispersed emulsions than rotor-stator or stirrer, and that a precise size control was achievable by choosing the membrane pore size.

Figure A.5 presents the influence of membrane length on resulting pressure and mean droplet size with a 1.1  $\mu\text{m}$  pore size membrane. Resulting pressures and droplets sizes were proportional disregarding of membrane length. Moreover, the longer membrane was able to work at higher flowrate for the same resulting pressure.

The influence of flowrate on droplet size distribution for a 1.1  $\mu\text{m}$  pore size membrane is presented on Figure A.6. We observe that droplet size decreased with increasing flowrate. Additionally, at high flowrate the droplets became smaller than the pore size, this is due to the oil jet phenomenon and is described in the literature review in section 1.2.3.3.

On Figure A.7, the influence of oil concentration at a constant surfactant to oil ratio on resulting pressure for a 1.1  $\mu\text{m}$  membrane is presented. It was observed that the resulting pressure was highly dependent on oil droplets concentration and was proportional to it, from pure water to 40% oil.

These results confirms that the set-up developed and the procedure used allow to obtain the same observations as reported in the literature and detailed in chapter 1 for membranes with pore sizes of some microns.

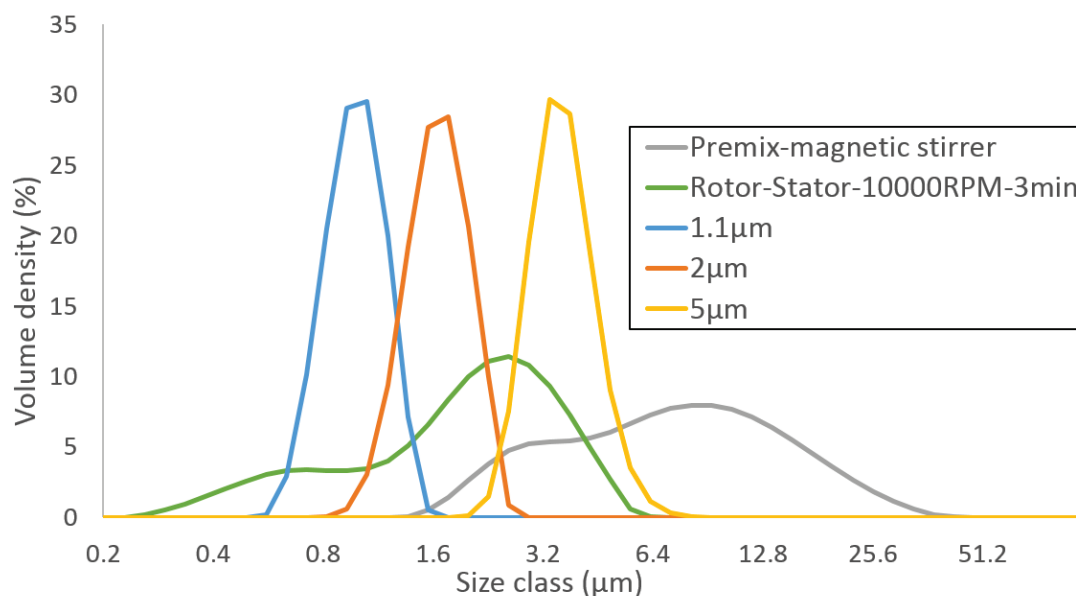


Figure A.4: Size distribution in volume for different membrane pore sizes at 200 mL/min, 10% EHP and 5% surfactants

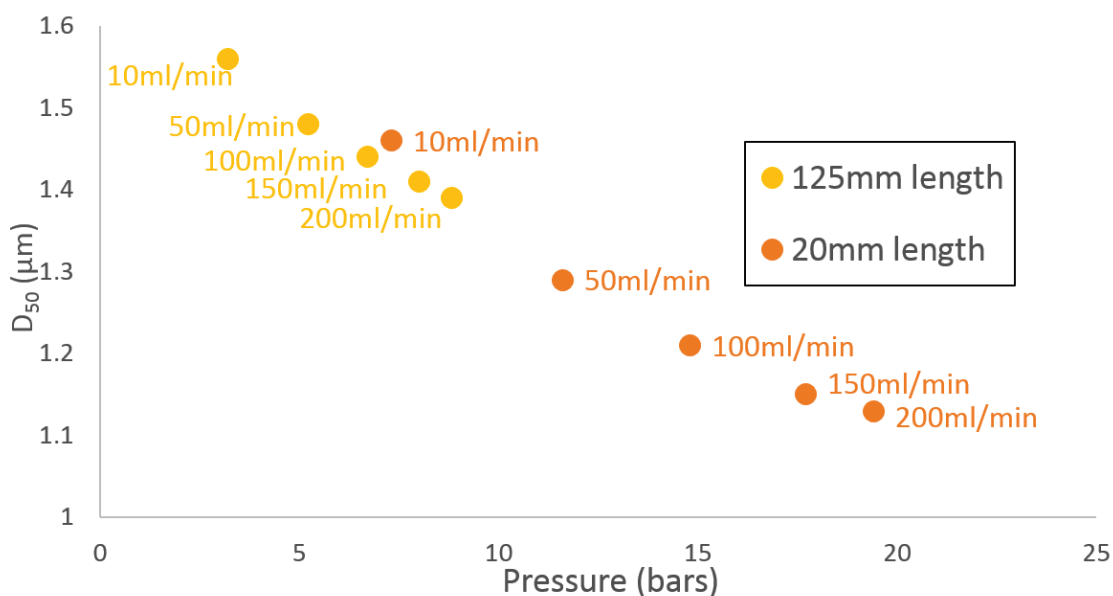


Figure A.5: Influence of membrane length on resulting pressure and size with 1.1 µm membrane at 10% EHP and 5% surfactants

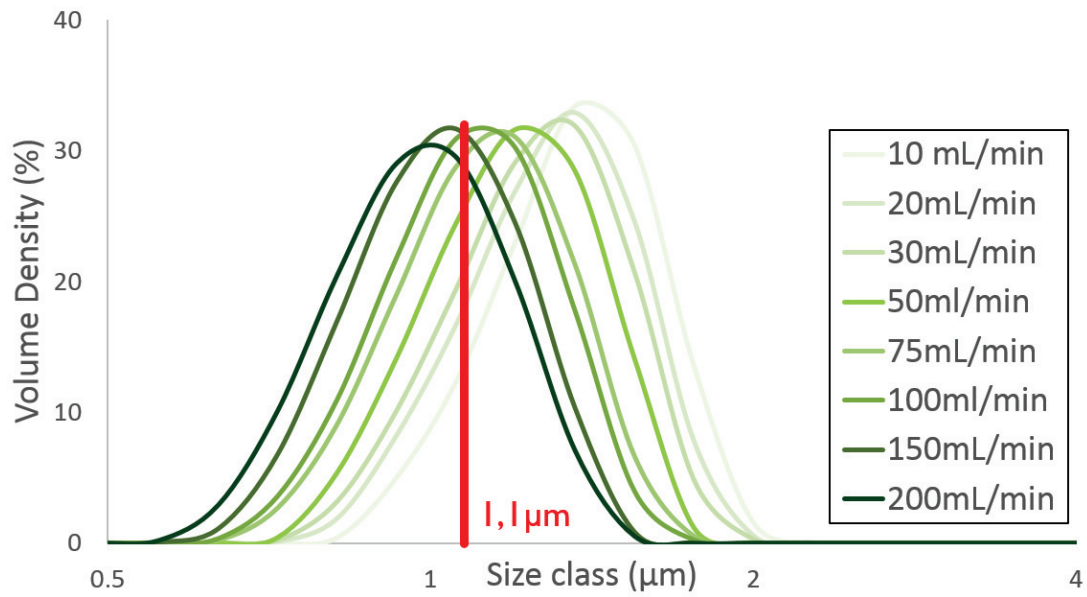


Figure A.6: Size distribution in volume for different flowrates with 1.1 μm membrane 10% EHP and 5% surfactant

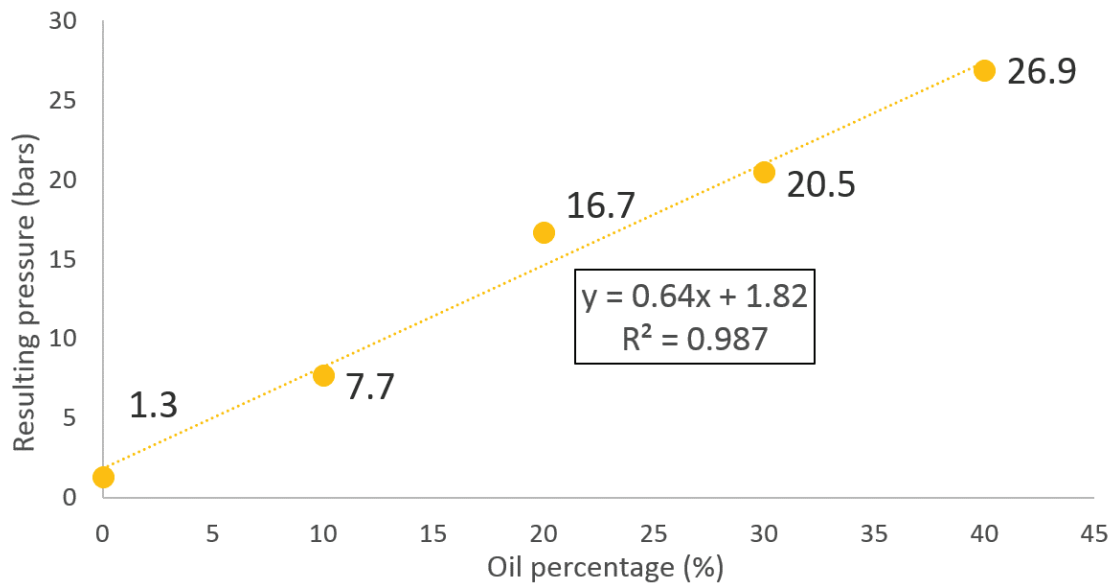


Figure A.7: Resulting pressure variation with oil concentration at a surfactant/oil ratio of 10% with 1.1 μm membrane



# Bibliography

- [1] T. F. Tadros, *Emulsion formation and stability*, John Wiley & Sons, 2013.
- [2] A. Mihranyan, N. Ferraz, M. Strømme, Current status and future prospects of nanotechnology in cosmetics, *Progress in Materials Science* 57 (5) (2012) 875–910. doi:10.1016/j.pmatsci.2011.10.001.  
URL <http://linkinghub.elsevier.com/retrieve/pii/S0079642511001046>
- [3] H. D. Silva, M. A. Cerqueira, A. A. Vicente, Nanoemulsions for Food Applications: Development and Characterization, *Food and Bioprocess Technology* 5 (3) (2012) 854–867. doi:10.1007/s11947-011-0683-7.  
URL <http://link.springer.com/10.1007/s11947-011-0683-7>
- [4] M. Nomura, H. Tobita, K. Suzuki, *Emulsion Polymerization: Kinetic and Mechanistic Aspects*, Springer Berlin Heidelberg, Berlin, Heidelberg, 2005, pp. 1–128. doi:10.1007/b100116.  
URL <https://doi.org/10.1007/b100116>
- [5] M. Rondón, P. Bouriart, J. Lachaise, J.-L. Salager, Breaking of water-in-crude oil emulsions. 1. physicochemical phenomenology of demulsifier action, *Energy & Fuels* 20 (4) (2006) 1600–1604. arXiv:<https://doi.org/10.1021/ef060017o>, doi:10.1021/ef060017o.  
URL <https://doi.org/10.1021/ef060017o>
- [6] S. van der Graaf, C. G. P. H. Schroën, R. M. Boom, Preparation of double emulsions by membrane emulsification a review, *Journal of Membrane Science* 251 (1-2) (2005) 7–15. doi:10.1016/j.memsci.2004.12.013.  
URL <http://linkinghub.elsevier.com/retrieve/pii/S0376738804008312>
- [7] J. W. Gibbs, On the equilibrium of heterogeneous substances, *American Journal of Science Series 3 Vol. 16 (96) (1878) 441–458*. arXiv:<http://www.ajsonline.org/content/s3-16/96/441.full.pdf+html>, doi:10.2475/ajs.s3-16.96.441.  
URL <http://www.ajsonline.org/content/s3-16/96/441.short>
- [8] T. Tadros, P. Izquierdo, J. Esquena, C. Solans, Formation and stability of nano-emulsions, *Advances in Colloid and Interface Science* 108-109 (2004) 303–318. doi:10.1016/j.cis.2003.10.023.  
URL <http://linkinghub.elsevier.com/retrieve/pii/S000186860300157X>
- [9] P. Brochette, *Emulsification – élaboration et études des émulsions*, no. J 2150, Ed. Techniques Ingénieur, 1999.
- [10] M. E. Helgeson, Colloidal behavior of nanoemulsions: Interactions, structure, and rheology, *Current Opinion in Colloid & Interface Science* 25 (2016) 39–50. doi:10.1016/j.cocis.2016.06.006.  
URL <http://linkinghub.elsevier.com/retrieve/pii/S1359029416300644>

- [11] D. Evans, H. Wennerström, *The Colloidal Domain: Where Physics, Chemistry, Biology, and Technology Meet*, Advances in Interfacial Engineering, Wiley, 1999.  
URL <https://books.google.fr/books?id=XPjvAAAAMAAJ>
- [12] T. Delmas, H. Piraux, A.-C. Couffin, I. Texier, F. Vinet, P. Poulin, M. E. Cates, J. Bibette, How To Prepare and Stabilize Very Small Nanoemulsions, *Langmuir* 27 (5) (2011) 1683–1692. doi: 10.1021/la104221q.  
URL <http://pubs.acs.org/doi/abs/10.1021/la104221q>
- [13] A. Kabalnov, A. Pertzov, E. Shchukin, Ostwald ripening in emulsions: I. direct observations of ostwald ripening in emulsions, *Journal of Colloid and Interface Science* 118 (2) (1987) 590–597.
- [14] M. J. Rosen, J. T. Kunjappu, *Surfactants and interfacial phenomena*, John Wiley & Sons, 2012.
- [15] G. W. C., Calculation of hlb values of non-ionic surfactants, *Journal of the Society of Cosmetic Chemists* (5) (1954) 249–256.
- [16] J. T. Davies, A quantitative kinetic theory of emulsion type. I. Physical chemistry of the emulsifying agent, Proc. 2nd Intern. Congr. Surface Activity, Butterworths Scientific Publication, London 426.
- [17] R. Pons, Polymeric surfactants as emulsion stabilizers, *Amphiphilic Block Copolymers: Self-Assembly and Applications*. (2000) 409–22.
- [18] R. S. Lam, M. T. Nickerson, Food proteins: a review on their emulsifying properties using a structure–function approach, *Food Chemistry* 141 (2) (2013) 975–984.
- [19] T. M. Allen, P. R. Cullis, Liposomal drug delivery systems: From concept to clinical applications, *Advanced Drug Delivery Reviews* 65 (1) (2013) 36–48. doi: 10.1016/j.addr.2012.09.037.  
URL <http://linkinghub.elsevier.com/retrieve/pii/S0169409X12002980>
- [20] S. U. Pickering, Cxvi.-Emulsions, *Journal of the Chemical Society, Transactions* 91 (1907) 2001–2021. doi: 10.1039/CT9079102001.  
URL <http://dx.doi.org/10.1039/CT9079102001>
- [21] X.-B. Xiong, Z. Binkhathlan, O. Molavi, A. Lavasanifar, Amphiphilic block co-polymers: Preparation and application in nanodrug and gene delivery, *Acta Biomaterialia* 8 (6) (2012) 2017–2033. doi: 10.1016/j.actbio.2012.03.006.  
URL <http://linkinghub.elsevier.com/retrieve/pii/S174270611200092X>
- [22] L. Zhao, N. Li, K. Wang, C. Shi, L. Zhang, Y. Luan, A review of polypeptide-based polymerosomes, *Biomaterials* 35 (4) (2014) 1284–1301. doi: 10.1016/j.biomaterials.2013.10.063.  
URL <http://linkinghub.elsevier.com/retrieve/pii/S0142961213013070>
- [23] M. Nagasawa, A. Holtzer, The helix-coil transition in solutions of polyglutamic acid, *Journal of the American Chemical Society* 86 (4) (1964) 538–543.  
URL <http://pubs.acs.org/doi/abs/10.1021/ja01058a002>
- [24] J. A. Hanson, C. B. Chang, S. M. Graves, Z. Li, T. G. Mason, T. J. Deming, Nanoscale double emulsions stabilized by single-component block copolypeptides, *Nature* 455 (7209) (2008) 85–88. doi: 10.1038/nature07197.  
URL <http://www.nature.com/doi/abs/10.1038/nature07197>

- [25] C. Solans, I. Solé, Nano-emulsions: Formation by low-energy methods, *Current Opinion in Colloid & Interface Science* 17 (5) (2012) 246–254. doi:10.1016/j.cocis.2012.07.003. URL <http://linkinghub.elsevier.com/retrieve/pii/S1359029412000787>
- [26] K. Shinoda, H. Saito, The effect of temperature on the phase equilibria and the types of dispersions of the ternary system composed of water, cyclohexane, and nonionic surfactant, *Journal of Colloid and Interface Science* 26 (1) (1968) 70–74.
- [27] C. Solans, D. Morales, M. Homs, Spontaneous emulsification, *Current Opinion in Colloid & Interface Science* 22 (2016) 88–93. doi:10.1016/j.cocis.2016.03.002. URL <http://linkinghub.elsevier.com/retrieve/pii/S1359029416300309>
- [28] K. Bouchemal, S. Briançon, E. Perrier, H. Fessi, Nano-emulsion formulation using spontaneous emulsification: solvent, oil and surfactant optimisation, *International Journal of Pharmaceutics* 280 (1-2) (2004) 241–251. doi:10.1016/j.ijpharm.2004.05.016. URL <http://linkinghub.elsevier.com/retrieve/pii/S0378517304003072>
- [29] S. Gibaud, D. Attivi, Microemulsions for oral administration and their therapeutic applications, *Expert Opinion on Drug Delivery* 9 (8) (2012) 937–951, PMID: 22663249. arXiv:<https://doi.org/10.1517/17425247.2012.694865>, doi:10.1517/17425247.2012.694865. URL <https://doi.org/10.1517/17425247.2012.694865>
- [30] M. A. Malik, M. Wani, M. Hashim, Microemulsion method: A novel route to synthesize organic and inorganic nanomaterials., *Arabian Journal of Chemistry* 5.
- [31] J.-P. Canselier, M. Poux, *Procédés d'émulsification*, Ed. Techniques Ingénieur, 2004.
- [32] E. L. Paul, V. A. Atiemo-Obeng, S. M. Kresta, *Handbook of industrial mixing: science and practice*, John Wiley & Sons, 2004.
- [33] Y.-F. Maa, C. Hsu, Liquid-liquid emulsification by rotor/stator homogenization, *Journal of Controlled Release* 38 (2-3) (1996) 219–228.
- [34] S. L. Anna, Droplets and bubbles in microfluidic devices, *Annual Review of Fluid Mechanics* 48 (1) (2016) 285–309. arXiv:<https://doi.org/10.1146/annurev-fluid-122414-034425>, doi:10.1146/annurev-fluid-122414-034425. URL <https://doi.org/10.1146/annurev-fluid-122414-034425>
- [35] P. Zhu, L. Wang, Passive and active droplet generation with microfluidics: a review, *Lab Chip* 17 (2017) 34–75. doi:10.1039/C6LC01018K. URL <http://dx.doi.org/10.1039/C6LC01018K>
- [36] M. Manea, A. Chemtob, M. Paulis, J. C. de la Cal, M. J. Barandiaran, J. M. Asua, Miniemulsification in high-pressure homogenizers, *AIChE Journal* 54 (1) (2008) 289–297. doi:10.1002/aic.11367. URL <http://doi.wiley.com/10.1002/aic.11367>
- [37] S. Schultz, G. Wagner, K. Urban, J. Ulrich, High-Pressure Homogenization as a Process for Emulsion Formation, *Chemical Engineering & Technology* 27 (4) (2004) 361–368. doi:10.1002/ceat.200406111. URL <http://doi.wiley.com/10.1002/ceat.200406111>
- [38] J. Floury, J. Legrand, A. Desrumaux, Analysis of a new type of high pressure homogeniser. Part B. study of droplet break-up and re-coalescence phenomena, *Chemical Engineering Science* 59 (6) (2004) 1285–1294. doi:10.1016/j.ces.2003.11.025. URL <http://linkinghub.elsevier.com/retrieve/pii/S0009250904000363>

- [39] L. Lee, I. T. Norton, Comparing droplet breakup for a high-pressure valve homogeniser and a Microfluidizer for the potential production of food-grade nanoemulsions, *Journal of Food Engineering* 114 (2) (2013) 158–163. doi:10.1016/j.jfoodeng.2012.08.009.  
URL <http://linkinghub.elsevier.com/retrieve/pii/S0260877412003925>
- [40] V. Ghosh, A. Mukherjee, N. Chandrasekaran, Ultrasonic emulsification of food-grade nanoemulsion formulation and evaluation of its bactericidal activity, *Ultrasonics Sonochemistry* 20 (1) (2013) 338–344. doi:10.1016/j.ultsonch.2012.08.010.  
URL <http://linkinghub.elsevier.com/retrieve/pii/S1350417712001782>
- [41] M. Y. Koroleva, E. V. Yurtov, Nanoemulsions: the properties, methods of preparation and promising applications, *Russian Chemical Reviews* 81 (1) (2012) 21–43.
- [42] A. Maali, M. T. H. Mosavian, Preparation and application of nanoemulsions in the last decade (2000–2010), *Journal of Dispersion Science and Technology* 34 (1) (2013) 92–105. arXiv:<https://doi.org/10.1080/01932691.2011.648498>, doi:10.1080/01932691.2011.648498.  
URL <https://doi.org/10.1080/01932691.2011.648498>
- [43] O. G. Jepps, Y. Dancik, Y. G. Anissimov, M. S. Roberts, Modeling the human skin barrier — towards a better understanding of dermal absorption, *Advanced Drug Delivery Reviews* 65 (2) (2013) 152 – 168. doi:<https://doi.org/10.1016/j.addr.2012.04.003>.  
URL <http://www.sciencedirect.com/science/article/pii/S0169409X12001226>
- [44] M. N. Yukuyama, D. D. M. Ghisleni, T. J. A. Pinto, N. A. Bou-Chacra, Nanoemulsion: process selection and application in cosmetics - a review, *International Journal of Cosmetic Science* doi:10.1111/ics.12260.  
URL <http://doi.wiley.com/10.1111/ics.12260>
- [45] A. G. Floyd, Top ten considerations in the development of parenteral emulsions, *Pharmaceutical Science & Technology Today* 2 (4) (1999) 134–143.
- [46] G. T. Vladislavljević, *Integrated Membrane Processes for the Preparation of Emulsions, Particles and Bubbles*, Wiley-Blackwell, 2016, Ch. 5, pp. 79–140. arXiv:<https://onlinelibrary.wiley.com/doi/pdf/10.1002/9781118739167.ch5>, doi:10.1002/9781118739167.ch5.  
URL <https://onlinelibrary.wiley.com/doi/abs/10.1002/9781118739167.ch5>
- [47] G. Vladislavljević, M. Shimizu, T. Nakashima, Permeability of hydrophilic and hydrophobic Shirasu-porous-glass (SPG) membranes to pure liquids and its microstructure, *Journal of Membrane Science* 250 (1-2) (2005) 69–77. doi:10.1016/j.memsci.2004.10.017.  
URL <http://linkinghub.elsevier.com/retrieve/pii/S0376738804007112>
- [48] T. Nakashima, M. Shimizu, M. Kukizaki, Mechanical strength and thermal resistance of porous glass, *Journal of the Ceramic Society of Japan* 100 (1168) (1992) 1411–1415.
- [49] M. Kukizaki, Relation between salt rejection and electrokinetic properties on shirasu porous glass (spg) membranes with nano-order uniform pores, *Separation and Purification Technology* 69 (1) (2009) 87–96.
- [50] T. Nakashima, Porous glass material and its recent applications, paper presented at 38th International SPG Forum on Membrane and Particle Science and Technology in Food and Medical Care in Sadowara, Japan 2002.
- [51] M. Kukizaki, T. Wada, Effect of the membrane wettability on the size and size distribution of microbubbles formed from shirasu-porous-glass (spg) membranes, *Colloids and Surfaces A: Physicochemical and Engineering Aspects* 317 (1-3) (2008) 146–154.

- [52] M. Kukizaki, M. Goto, Preparation and characterization of a new asymmetric type of shirasu porous glass (spg) membrane used for membrane emulsification, *Journal of Membrane Science* 299 (1) (2007) 190–199. doi:<https://doi.org/10.1016/j.memsci.2007.04.040>. URL <http://www.sciencedirect.com/science/article/pii/S0376738807003092>
- [53] S. Gehrman, H. Bunjes, Influence of membrane material on the production of colloidal emulsions by premix membrane emulsification, *European Journal of Pharmaceutics and Biopharmaceutics* 126 (2018) 140–148, innovative Processes for Bio-Pharmaceuticals and Poorly Water-Soluble API. doi:<https://doi.org/10.1016/j.ejpb.2016.11.006>. URL <http://www.sciencedirect.com/science/article/pii/S0939641116304301>
- [54] M. T. Stillwell, R. G. Holdich, S. R. Kosvintsev, G. Gasparini, I. W. Cumming, Stirred cell membrane emulsification and factors influencing dispersion drop size and uniformity, *Industrial & Engineering Chemistry Research* 46 (3) (2007) 965–972. arXiv:<https://doi.org/10.1021/ie0611094>, doi:10.1021/ie0611094. URL <https://doi.org/10.1021/ie0611094>
- [55] N. A. Wagdare, A. T. Marcelis, O. B. Ho, R. M. Boom, C. J. van Rijn, High throughput vegetable oil-in-water emulsification with a high porosity micro-engineered membrane, *Journal of Membrane Science* 347 (1-2) (2010) 1–7. doi:10.1016/j.memsci.2009.09.057. URL <http://linkinghub.elsevier.com/retrieve/pii/S0376738809007145>
- [56] G. T. Vladislavljević, U. Lambrich, M. Nakajima, H. Schubert, Production of O/W emulsions using SPG membranes, ceramic  $\alpha$ -aluminium oxide membranes, microfluidizer and a silicon microchannel plate a comparative study, *Colloids and Surfaces A: Physicochemical and Engineering Aspects* 232 (2-3) (2004) 199–207. doi:10.1016/j.colsurfa.2003.10.026. URL <http://linkinghub.elsevier.com/retrieve/pii/S0927775703006137>
- [57] S. H. Silalahi, T. Leiknes, Cleaning strategies in ceramic microfiltration membranes fouled by oil and particulate matter in produced water, *Desalination* 236 (1-3) (2009) 160–169. doi:10.1016/j.desal.2007.10.063. URL <http://linkinghub.elsevier.com/retrieve/pii/S0011916408006395>
- [58] A. Trentin, C. Güell, T. Gelaw, S. de Lamo, M. Ferrando, Cleaning protocols for organic microfiltration membranes used in premix membrane emulsification, *Separation and Purification Technology* 88 (2012) 70–78. doi:10.1016/j.seppur.2011.12.003. URL <http://linkinghub.elsevier.com/retrieve/pii/S138358661100709X>
- [59] S. Joseph, H. Bunjes, Preparation of nanoemulsions and solid lipid nanoparticles by premix membrane emulsification, *Journal of Pharmaceutical Sciences* 101 (7) (2012) 2479–2489. doi:10.1002/jps.23163. URL <http://doi.wiley.com/10.1002/jps.23163>
- [60] Q.-Z. Zhou, G.-H. Ma, Z.-G. Su, Effect of membrane parameters on the size and uniformity in preparing agarose beads by premix membrane emulsification, *Journal of Membrane Science* 326 (2) (2009) 694–700. doi:10.1016/j.memsci.2008.11.012. URL <http://linkinghub.elsevier.com/retrieve/pii/S0376738808009629>
- [61] Q.-Z. Zhou, L.-Y. Wang, G.-H. Ma, Z.-G. Su, Multi-stage premix membrane emulsification for preparation of agarose microbeads with uniform size, *Journal of Membrane Science* 322 (1) (2008) 98–104. doi:10.1016/j.memsci.2008.05.025. URL <http://linkinghub.elsevier.com/retrieve/pii/S0376738808004638>
- [62] G. Vladislavljević, M. Shimizu, T. Nakashima, Preparation of monodisperse multiple emulsions at high production rates by multi-stage premix membrane emulsification, *Journal of Membrane Science* 244 (1-2) (2004) 97–106. doi:10.1016/j.memsci.2004.07.008. URL <http://linkinghub.elsevier.com/retrieve/pii/S0376738804005058>

- [63] K. Suzuki, I. Shuto, Y. Hagura, Characteristics of the membrane emulsification method combined with preliminary emulsification for preparing corn oil-in-water emulsions, *Food Science and Technology International*, Tokyo 2 (1) (1996) 43–47. doi:10.3136/fsti9596t9798.2.43.
- [64] C. Charcosset, Membranes for the preparation of emulsions and particles, in: *Membrane Processes in Biotechnology and Pharmaceuticals*, Elsevier, Ed. C. Charcosset, 2012, pp. 213–251.  
URL <http://linkinghub.elsevier.com/retrieve/pii/B978044456334700006X>
- [65] M. M. Dragosavac, M. N. Sovilj, S. R. Kosvintsev, R. G. Holdich, G. T. Vladislavljević, Controlled production of oil-in-water emulsions containing unrefined pumpkin seed oil using stirred cell membrane emulsification, *Journal of Membrane Science* 322 (1) (2008) 178–188.  
URL <http://www.sciencedirect.com/science/article/pii/S0376738808004742>
- [66] R. Hancocks, F. Spyropoulos, I. Norton, The effects of membrane composition and morphology on the rotating membrane emulsification technique for food grade emulsions, *Journal of Membrane Science* 497 (2016) 29–35. doi:10.1016/j.memsci.2015.09.033.  
URL <http://linkinghub.elsevier.com/retrieve/pii/S0376738815301964>
- [67] A. K. Pawlik, I. T. Norton, SPG rotating membrane technique for production of food grade emulsions, *Journal of Food Engineering* 114 (4) (2013) 530–537. doi:10.1016/j.jfoodeng.2012.09.008.  
URL <http://linkinghub.elsevier.com/retrieve/pii/S0260877412004426>
- [68] N. Aryanti, R. Hou, R. A. Williams, Performance of a rotating membrane emulsifier for production of coarse droplets, *Journal of Membrane Science* 326 (1) (2009) 9–18. doi:10.1016/j.memsci.2008.08.052.  
URL <http://linkinghub.elsevier.com/retrieve/pii/S0376738808008090>
- [69] O. Akoum, M. Y. Jaffrin, L. Ding, P. Paullier, C. Vanhoutte, An hydrodynamic investigation of microfiltration and ultrafiltration in a vibrating membrane module, *Journal of Membrane Science* 197 (1) (2002) 37 – 52. doi:[https://doi.org/10.1016/S0376-7388\(01\)00602-0](https://doi.org/10.1016/S0376-7388(01)00602-0).  
URL <http://www.sciencedirect.com/science/article/pii/S0376738801006020>
- [70] J. Zhu, D. Barrow, Analysis of droplet size during crossflow membrane emulsification using stationary and vibrating micromachined silicon nitride membranes, *Journal of Membrane Science* 261 (1) (2005) 136 – 144. doi:<https://doi.org/10.1016/j.memsci.2005.02.038>.  
URL <http://www.sciencedirect.com/science/article/pii/S0376738805002693>
- [71] C. Sebaaly, H. Greige-Gerges, G. Agusti, H. Fessi, C. Charcosset, Large-scale preparation of clove essential oil and eugenol-loaded liposomes using a membrane contactor and a pilot plant, *Journal of Liposome Research* 26:2 (2015) 126–138. doi:10.3109/08982104.2015.1057849.  
URL <http://informahealthcare.com/doi/abs/10.3109/08982104.2015.1057849>
- [72] S. R. Kosvintsev, G. Gasparini, R. G. Holdich, I. W. Cumming, M. T. Stillwell, Liquid- liquid membrane dispersion in a stirred cell with and without controlled shear, *Industrial & Engineering Chemistry Research* 44 (24) (2005) 9323–9330.
- [73] M. Kukizaki, Shirasu porous glass (spg) membrane emulsification in the absence of shear flow at the membrane surface: Influence of surfactant type and concentration, viscosities of dispersed and continuous phases, and transmembrane pressure, *Journal of Membrane Science* 327 (1) (2009) 234 – 243. doi:<https://doi.org/10.1016/j.memsci.2008.11>.

026.  
URL <http://www.sciencedirect.com/science/article/pii/S0376738808009903>
- [74] S. Sugiura, M. Nakajima, N. Kumazawa, S. Iwamoto, M. Seki, Characterization of Spontaneous Transformation-Based Droplet Formation during Microchannel Emulsification, *The Journal of Physical Chemistry B* 106 (36) (2002) 9405–9409. doi:10.1021/jp0259871.  
URL <http://pubs.acs.org/doi/abs/10.1021/jp0259871>
- [75] T. Nakashima, M. Shimizu, M. Kukizaki, Particle control of emulsion by membrane emulsification and its applications, *Advanced Drug Delivery Reviews* 45 (1) (2000) 47–56.
- [76] A. Abrahamse, R. Van Lierop, R. Van der Sman, A. Van der Padt, R. Boom, Analysis of droplet formation and interactions during cross-flow membrane emulsification, *Journal of Membrane Science* 204 (1-2) (2002) 125–137.
- [77] G. T. Vladislavljević, H. Schubert, Influence of process parameters on droplet size distribution in spg membrane emulsification and stability of prepared emulsion droplets, *Journal of Membrane Science* 225 (1-2) (2003) 15–23.
- [78] E. Egidi, G. Gasparini, R. G. Holdich, G. T. Vladislavljević, S. R. Kosvintsev, Membrane emulsification using membranes of regular pore spacing: Droplet size and uniformity in the presence of surface shear, *Journal of Membrane Science* 323 (2) (2008) 414–420.
- [79] S. van der Graaf, C. Schroën, R. van der Sman, R. Boom, Influence of dynamic interfacial tension on droplet formation during membrane emulsification, *Journal of Colloid and Interface Science* 277 (2) (2004) 456–463. doi:10.1016/j.jcis.2004.04.033.  
URL <http://linkinghub.elsevier.com/retrieve/pii/S0021979704003972>
- [80] V. Schröder, O. Behrend, H. Schubert, Effect of dynamic interfacial tension on the emulsification process using microporous, ceramic membranes, *Journal of Colloid and Interface Science* 202 (2) (1998) 334–340.
- [81] M. Rayner, G. Trägårdh, C. Trägårdh, The impact of mass transfer and interfacial expansion rate on droplet size in membrane emulsification processes, *Colloids and Surfaces A: Physicochemical and Engineering Aspects* 266 (1-3) (2005) 1–17. doi:10.1016/j.colsurfa.2005.05.025.  
URL <http://linkinghub.elsevier.com/retrieve/pii/S0927775705003675>
- [82] R. Hancocks, F. Spyropoulos, I. Norton, Comparisons between membranes for use in cross flow membrane emulsification, *Journal of Food Engineering* 116 (2) (2013) 382–389. doi:10.1016/j.jfoodeng.2012.11.032.  
URL <http://linkinghub.elsevier.com/retrieve/pii/S026087741200605X>
- [83] Y. Mine, M. Shimizu, T. Nakashima, Preparation and stabilization of simple and multiple emulsions using a microporous glass membrane, *Colloids and Surfaces B: Biointerfaces* 6 (4-5) (1996) 261–268.
- [84] A. Abrahamse, R. van Lierop, R. van der Sman, A. van der Padt, R. Boom, Analysis of droplet formation and interactions during cross-flow membrane emulsification, *Journal of Membrane Science* 204 (1) (2002) 125 – 137. doi:[https://doi.org/10.1016/S0376-7388\(02\)00028-5](https://doi.org/10.1016/S0376-7388(02)00028-5).  
URL <http://www.sciencedirect.com/science/article/pii/S0376738802000285>
- [85] S. van der Graaf, T. Nisisako, C. G. P. H. Schroën, R. G. M. van der Sman, R. M. Boom, Lattice Boltzmann Simulations of Droplet Formation in a T-Shaped Microchannel, *Langmuir* 22 (9) (2006) 4144–4152. doi:10.1021/la052682f.  
URL <http://pubs.acs.org/doi/abs/10.1021/la052682f>

- [86] E. Lepercq-Bost, M.-L. Giorgi, A. Isambert, C. Arnaud, Use of the capillary number for the prediction of droplet size in membrane emulsification, *Journal of Membrane Science* 314 (1-2) (2008) 76–89. doi:10.1016/j.memsci.2008.01.023.  
URL <http://linkinghub.elsevier.com/retrieve/pii/S0376738808000719>
- [87] A. Nazir, K. Schroën, R. Boom, Premix emulsification: A review, *Journal of Membrane Science* 362 (1-2) (2010) 1–11. doi:10.1016/j.memsci.2010.06.044.  
URL <http://linkinghub.elsevier.com/retrieve/pii/S0376738810005119>
- [88] E. van der Zwan, K. Schroën, K. van Dijke, R. Boom, Visualization of droplet break-up in premix membrane emulsification using microfluidic devices, *Colloids and Surfaces A: Physicochemical and Engineering Aspects* 277 (1–3) (2006) 223–229. doi:10.1016/j.colsurfa.2005.11.064.  
URL <http://www.sciencedirect.com/science/article/pii/S092777570500912X>
- [89] D. R. Link, S. L. Anna, D. A. Weitz, H. A. Stone, Geometrically Mediated Breakup of Drops in Microfluidic Devices, *Physical Review Letters* 92 (5). doi:10.1103/PhysRevLett.92.054503.  
URL <https://link.aps.org/doi/10.1103/PhysRevLett.92.054503>
- [90] G. T. Vladislavljević, M. Shimizu, T. Nakashima, Production of multiple emulsions for drug delivery systems by repeated SPG membrane homogenization: Influence of mean pore size, interfacial tension and continuous phase viscosity, *Journal of Membrane Science* 284 (1-2) (2006) 373–383. doi:10.1016/j.memsci.2006.08.003.  
URL <http://linkinghub.elsevier.com/retrieve/pii/S0376738806005370>
- [91] G. Vladislavljevic, I. Kobayashi, M. Nakajima, R. Williams, M. Shimizu, T. Nakashima, Shirasu Porous Glass membrane emulsification: Characterisation of membrane structure by high-resolution X-ray microtomography and microscopic observation of droplet formation in real time, *Journal of Membrane Science* 302 (1-2) (2007) 243–253. doi:10.1016/j.memsci.2007.06.067.  
URL <http://linkinghub.elsevier.com/retrieve/pii/S0376738807004553>
- [92] S. Joseph, H. Bunjes, Evaluation of Shirasu Porous Glass (SPG) membrane emulsification for the preparation of colloidal lipid drug carrier dispersions, *European Journal of Pharmaceutics and Biopharmaceutics* 87 (1) (2014) 178–186. doi:10.1016/j.ejpb.2013.11.010.  
URL <http://linkinghub.elsevier.com/retrieve/pii/S0939641113003822>
- [93] S. Brösel, H. Schubert, Investigations on the role of surfactants in mechanical emulsification using a high-pressure homogenizer with an orifice valve, *Chemical Engineering and Processing: Process Intensification* 38 (4-6) (1999) 533–540.
- [94] S. Gehrman, H. Bunjes, Preparation of nanoemulsions by premix membrane emulsification: which parameters have a significant influence on the resulting particle size?, *Journal of Pharmaceutical Sciences* 106 (8) (2017) 2068–2076. doi:10.1016/j.xphs.2017.04.066.  
URL <http://linkinghub.elsevier.com/retrieve/pii/S0022354917303374>
- [95] K. Suzuki, I. Fujiki, Y. Hagura, Preparation of corn oil/water and water/corn oil emulsions using PTFE membranes, *Food Science and Technology International, Tokyo* 4 (2) (1998) 164–167.
- [96] S.-H. Park, T. Yamaguchi, S. ichi Nakao, Transport mechanism of deformable droplets in microfiltration of emulsions, *Chemical Engineering Science* 56 (11) (2001) 3539–3548. doi: [https://doi.org/10.1016/S0009-2509\(01\)00047-1](https://doi.org/10.1016/S0009-2509(01)00047-1).  
URL <http://www.sciencedirect.com/science/article/pii/S0009250901000471>

- [97] J. Altenbach-Rehm, K. Suzuki, H. Schubert, Production of o/w-emulsions with narrow droplet size distribution by repeated premix membrane emulsification, Paper presented at the 3rd World Congress on Emulsions, Lyon 2002.
- [98] E. Toorisaka, Hypoglycemic effect of surfactant-coated insulin solubilized in a novel solid-in-oil-in-water (S/O/W) emulsion, *International Journal of Pharmaceutics* 252 (1-2) (2003) 271–274. doi:10.1016/S0378-5173(02)00674-9.  
URL <http://linkinghub.elsevier.com/retrieve/pii/S0378517302006749>
- [99] W. Jing, J. Wu, W. Xing, W. Jin, N. Xu, Emulsions prepared by two-stage ceramic membrane jet-flow emulsification, *AIChE Journal* 51 (5) (2005) 1339–1345. doi:10.1002/aic.10405.  
URL <http://doi.wiley.com/10.1002/aic.10405>
- [100] G. T. Vladislavljević, J. Surh, J. D. McClements, Effect of emulsifier type on droplet disruption in repeated Shirasu porous glass membrane homogenization, *Langmuir* 22 (10) (2006) 4526–4533.
- [101] A. Trentin, M. Ferrando, F. López, C. Güell, Premix membrane O/W emulsification: Effect of fouling when using BSA as emulsifier, *Desalination* 245 (1-3) (2009) 388–395. doi:10.1016/j.desal.2009.02.002.  
URL <http://linkinghub.elsevier.com/retrieve/pii/S001191640900352X>
- [102] A. Trentin, S. De Lamo, C. Güell, F. López, M. Ferrando, Protein-stabilized emulsions containing beta-carotene produced by premix membrane emulsification, *Journal of Food Engineering* 106 (4) (2011) 267–274. doi:10.1016/j.jfoodeng.2011.03.013.  
URL <http://linkinghub.elsevier.com/retrieve/pii/S0260877411001385>
- [103] R. Berendsen, C. Güell, O. Henry, M. Ferrando, Premix membrane emulsification to produce oil-in-water emulsions stabilized with various interfacial structures of whey protein and carboxymethyl cellulose, *Food Hydrocolloids* 38 (2014) 1–10. doi:10.1016/j.foodhyd.2013.11.005.  
URL <http://linkinghub.elsevier.com/retrieve/pii/S0268005X13003664>
- [104] J. Santos, G. T. Vladislavljević, R. G. Holdich, M. M. Dragosavac, J. Muñoz, Controlled production of eco-friendly emulsions using direct and premix membrane emulsification, *Chemical Engineering Research and Design* 98 (2015) 59–69. doi:10.1016/j.cherd.2015.04.009.  
URL <http://linkinghub.elsevier.com/retrieve/pii/S0263876215001136>
- [105] N. Hornig, U. Fritsching, Liquid dispersion in premix emulsification within porous membrane structures, *Journal of Membrane Science* 514 (2016) 574–585. doi:10.1016/j.memsci.2016.04.051.  
URL <http://linkinghub.elsevier.com/retrieve/pii/S0376738816302794>
- [106] Y. Liu, L. Wang, Y. Zhang, W. Zhang, X. Chen, T. Yang, Z. Wang, G. Ma, Uniform-sized water-in-oil vaccine formulations enhance immune response against Newcastle disease and avian influenza in chickens, *International Immunopharmacology* 23 (2) (2014) 603–608. doi:10.1016/j.intimp.2014.10.011.  
URL <http://linkinghub.elsevier.com/retrieve/pii/S1567576914003932>
- [107] M. Shima, Y. Kobayashi, T. Fujii, M. Tanaka, Y. Kimura, S. Adachi, R. Matsuno, Preparation of fine W/O/W emulsion through membrane filtration of coarse W/O/W emulsion and disappearance of the inclusion of outer phase solution, *Food Hydrocolloids* 18 (1) (2004) 61–70. doi:10.1016/S0268-005X(03)00042-0.  
URL <http://linkinghub.elsevier.com/retrieve/pii/S0268005X03000420>

- [108] V. Eisinaite, D. Juraite, K. Schroën, D. Leskauskaite, Preparation of stable food-grade double emulsions with a hybrid premix membrane emulsification system, *Food Chemistry* 206 (2016) 59–66. doi:10.1016/j.foodchem.2016.03.046.  
URL <http://linkinghub.elsevier.com/retrieve/pii/S0308814616303995>
- [109] V. Eisinaite, D. Juraite, K. Schroën, D. Leskauskaite, Food-grade double emulsions as effective fat replacers in meat systems, *Journal of Food Engineering* 213 (2017) 54–59. doi:10.1016/j.jfoodeng.2017.05.022.  
URL <http://linkinghub.elsevier.com/retrieve/pii/S0260877417302340>
- [110] S. Gehrman, H. Bunjes, Instrumented small scale extruder to investigate the influence of process parameters during premix membrane emulsification, *Chemical Engineering Journal* 284 (2016) 716–723. doi:10.1016/j.cej.2015.09.022.  
URL <http://linkinghub.elsevier.com/retrieve/pii/S1385894715012796>
- [111] S. Gehrman, H. Bunjes, Preparation of lipid nanoemulsions by premix membrane emulsification with disposable materials, *International Journal of Pharmaceutics* 511 (2) (2016) 741–744. doi:10.1016/j.ijpharm.2016.07.067.  
URL <http://linkinghub.elsevier.com/retrieve/pii/S0378517316307177>
- [112] H. Sawalha, N. Purwanti, A. Rinzema, K. Schroën, R. Boom, Polylactide microspheres prepared by premix membrane emulsification—Effects of solvent removal rate, *Journal of Membrane Science* 310 (1-2) (2008) 484–493. doi:10.1016/j.memsci.2007.11.029.  
URL <http://linkinghub.elsevier.com/retrieve/pii/S0376738807008253>
- [113] Y.-Q. Wang, Q.-Z. Fan, Y. Liu, H. Yue, X.-W. Ma, J. Wu, G.-H. Ma, Z.-G. Su, Improving adjuvanticity of quaternized chitosan-based microgels for H5n1 split vaccine by tailoring the particle properties to achieve antigen dose sparing effect, *International Journal of Pharmaceutics* 515 (1-2) (2016) 84–93. doi:10.1016/j.ijpharm.2016.09.082.  
URL <http://linkinghub.elsevier.com/retrieve/pii/S0378517316309280>
- [114] G. T. Vladislavljević, Structured microparticles with tailored properties produced by membrane emulsification, *Advances in Colloid and Interface Science* 225 (2015) 53–87. doi:10.1016/j.cis.2015.07.013.  
URL <http://linkinghub.elsevier.com/retrieve/pii/S000186861500144X>
- [115] D. H. Oh, P. Balakrishnan, Y.-K. Oh, D.-D. Kim, C. S. Yong, H.-G. Choi, Effect of process parameters on nanoemulsion droplet size and distribution in SPG membrane emulsification, *International Journal of Pharmaceutics* 404 (1-2) (2011) 191–197. doi:10.1016/j.ijpharm.2010.10.045.  
URL <http://linkinghub.elsevier.com/retrieve/pii/S0378517310008215>
- [116] M. S. Muthu, B. Wilson, Challenges posed by the scale-up of nanomedicines, *Nanomedicine* 7 (3) (2012) 307–309. doi:10.2217/nnm.12.3.  
URL <http://www.futuremedicine.com/doi/abs/10.2217/nnm.12.3>
- [117] C. Charcosset, A. Juban, J.-P. Valour, S. Urbaniak, H. Fessi, Preparation of liposomes at large scale using the ethanol injection method: Effect of scale-up and injection devices, *Chemical Engineering Research and Design* 94 (2015) 508–515. doi:10.1016/j.cherd.2014.09.008.  
URL <http://linkinghub.elsevier.com/retrieve/pii/S0263876214004092>
- [118] L. D. Mayer, M. J. Hope, P. R. Cullis, Vesicles of variable sizes produced by a rapid extrusion procedure, *Biochimica et Biophysica Acta (BBA)-Biomembranes* 858 (1) (1986) 161–168.

- [119] N. Berger, A. Sachse, J. Bender, R. Schubert, M. Brandl, Filter extrusion of liposomes using different devices: comparison of liposome size, encapsulation efficiency, and process characteristics, *International Journal of Pharmaceutics* 223 (1-2) (2001) 55–68.
- [120] F. Shakeel, W. Ramadan, Transdermal delivery of anticancer drug caffeine from water-in-oil nanoemulsions, *Colloids and Surfaces B: Biointerfaces* 75 (1) (2010) 356–362. doi:10.1016/j.colsurfb.2009.09.010.  
URL <http://linkinghub.elsevier.com/retrieve/pii/S0927776509004202>
- [121] H. Wu, C. Ramachandran, N. D. Weiner, B. J. Roessler, Topical transport of hydrophilic compounds using water-in-oil nanoemulsions, *International Journal of Pharmaceutics* 220 (1-2) (2001) 63–75.
- [122] M. Iqbal, N. Zafar, H. Fessi, A. Elaissari, Double emulsion solvent evaporation techniques used for drug encapsulation, *International Journal of Pharmaceutics* 496 (2) (2015) 173–190. doi:10.1016/j.ijpharm.2015.10.057.  
URL <http://linkinghub.elsevier.com/retrieve/pii/S0378517315303264>
- [123] C. Solans, P. Izquierdo, J. Nolla, N. Azemar, M. Garciacelma, Nano-emulsions, *Current Opinion in Colloid & Interface Science* 10 (3-4) (2005) 102–110. doi:10.1016/j.cocis.2005.06.004.  
URL <http://linkinghub.elsevier.com/retrieve/pii/S1359029405000348>
- [124] O. Alliod, J.-P. Valour, S. Urbaniak, H. Fessi, D. Dupin, C. Charcosset, Preparation of oil-in-water nanoemulsions at large-scale using premix membrane emulsification and Shirasu Porous Glass (SPG) membranes, *Colloids and Surfaces A: Physicochemical and Engineering Aspects* doi:10.1016/j.colsurfa.2018.04.045.  
URL <http://linkinghub.elsevier.com/retrieve/pii/S0927775718303212>
- [125] P. S. Silva, V. M. Starov, R. G. Holdich, Membrane emulsification: Formation of water in oil emulsions using a hydrophilic membrane, *Colloids and Surfaces A: Physicochemical and Engineering Aspects* 532 (2017) 297–304. doi:10.1016/j.colsurfa.2017.04.077.  
URL <http://linkinghub.elsevier.com/retrieve/pii/S0927775717304181>
- [126] P. S. Silva, S. Morelli, M. M. Dragosavac, V. M. Starov, R. G. Holdich, Water in oil emulsions from hydrophobized metal membranes and characterization of dynamic interfacial tension in membrane emulsification, *Colloids and Surfaces A: Physicochemical and Engineering Aspects* 532 (2017) 77–86. doi:10.1016/j.colsurfa.2017.06.051.  
URL <http://linkinghub.elsevier.com/retrieve/pii/S0927775717306131>
- [127] C.-J. Cheng, L.-Y. Chu, R. Xie, Preparation of highly monodisperse W/O emulsions with hydrophobically modified SPG membranes, *Journal of Colloid and Interface Science* 300 (1) (2006) 375–382. doi:10.1016/j.jcis.2006.03.056.  
URL <http://linkinghub.elsevier.com/retrieve/pii/S0021979706002451>
- [128] K. Kandori, K. Kishi, T. Ishikawa, Preparation of monodispersed W/O emulsions by Shirasuporous-glass filter emulsification technique, *Colloids and surfaces* 55 (1991) 73–78.
- [129] G. T. Vladislavljević, S. Tesch, H. Schubert, Preparation of water-in-oil emulsions using microporous polypropylene hollow fibers: influence of some operating parameters on droplet size distribution, *Chemical Engineering and Processing: Process Intensification* 41 (3) (2002) 231–238.
- [130] C. Lovelyn, A. A. Attama, Current State of Nanoemulsions in Drug Delivery, *Journal of Biomaterials and Nanobiotechnology* 02 (05) (2011) 626–639. doi:10.4236/jbmb.2011.225075.  
URL <http://www.scirp.org/journal/doi.aspx?DOI=10.4236/jbmb.2011.225075>

- [131] D. Mou, H. Chen, D. Du, C. Mao, J. Wan, H. Xu, X. Yang, Hydrogel-thickened nanoemulsion system for topical delivery of lipophilic drugs, *International Journal of Pharmaceutics* 353 (1-2) (2008) 270–276.
- [132] S. Setya, S. Talegaonkar, B. K. Razdan, Nanoemulsions: formulation methods and stability aspects, *World Journal of Pharmaceutical Sciences* 3 (2) (2014) 2214–2228.
- [133] X. Yang, D. Wang, Y. Ma, Q. Zhao, J. K. Fallon, D. Liu, X. E. Xu, Y. Wang, Z. He, F. Liu, Theranostic nanoemulsions: codelivery of hydrophobic drug and hydrophilic imaging probe for cancer therapy and imaging, *Nanomedicine* 9 (18) (2014) 2773–2785, pMID: 25000945. arXiv:<https://doi.org/10.2217/nnm.14.50>, doi:10.2217/nnm.14.50. URL <https://doi.org/10.2217/nnm.14.50>
- [134] A. Desai, T. Vyas, M. Amiji, Cytotoxicity and apoptosis enhancement in brain tumor cells upon coadministration of paclitaxel and ceramide in nanoemulsion formulations, *Journal of Pharmaceutical Sciences* 97 (7) (2008) 2745 – 2756. doi:<https://doi.org/10.1002/jps.21182>. URL <http://www.sciencedirect.com/science/article/pii/S0022354916326284>
- [135] I. Venkateshwarlu, K. Prabhakar, M. Ali, V. Kishan, Development and in vitro cytotoxic evaluation of parenteral docetaxel lipid nanoemulsions for application in cancer treatment, *PDA Journal of Pharmaceutical Science and Technology* 64 (3) (2010) 233–241, cited By 8. URL <https://www.scopus.com/inward/record.uri?eid=2-s2.0-78149352110&partnerID=40&md5=7d51fef7a38566d82248c4ab44bbc281>
- [136] K. K. Singh, S. K. Vingkar, Formulation, antimalarial activity and biodistribution of oral lipid nanoemulsion of primaquine, *International Journal of Pharmaceutics* 347 (1) (2008) 136 – 143. doi:<https://doi.org/10.1016/j.ijpharm.2007.06.035>. URL <http://www.sciencedirect.com/science/article/pii/S0378517307005522>
- [137] ClinicalTrials.gov Bethesda (md): National Library of Medicine (US). February 29, 2000 . Identifier NCT01326078. Use of Lipid Emulsion or Nanoemulsion of Propofol on Children Undergoing Ambulatory Invasive Procedures, March 30, 2011; Available at: <https://clinicaltrials.gov/ct2/show/nct01326078>. Accessed September 26, 2018.
- [138] ClinicalTrials.gov Bethesda (md): National Library of Medicine (US). February 29, 2000 . Identifier NCT01010035. Cholesterol Metabolism and Lipid Transfer in Diabetes; Nov 9, 2009 Available at: <https://clinicaltrials.gov/ct2/show/nct01010035>. Accessed September 26, 2018.
- [139] Y. Singh, J. G. Meher, K. Raval, F. A. Khan, M. Chaurasia, N. K. Jain, M. K. Chourasia, Nanoemulsion: Concepts, development and applications in drug delivery, *Journal of Controlled Release* 252 (2017) 28–49. doi:10.1016/j.jconrel.2017.03.008. URL <http://linkinghub.elsevier.com/retrieve/pii/S0168365917301128>
- [140] S. Mahdi Jafari, Y. He, B. Bhandari, Nano-Emulsion Production by Sonication and Microfluidization-A Comparison, *International Journal of Food Properties* 9 (3) (2006) 475–485. doi:10.1080/10942910600596464. URL <http://www.tandfonline.com/doi/abs/10.1080/10942910600596464>
- [141] S. Y. Tang, P. Shridharan, M. Sivakumar, Impact of process parameters in the generation of novel aspirin nanoemulsions – comparative studies between ultrasound cavitation and microfluidizer, *Ultrasonics Sonochemistry* 20 (1) (2013) 485 – 497. doi:<https://doi.org/10.1016/j.ultsonch.2012.04.005>. URL <http://www.sciencedirect.com/science/article/pii/S1350417712000806>

- [142] E. Trapasso, D. Cosco, C. Celia, M. Fresta, D. Paolino, Retinoids: new use by innovative drug-delivery systems, *Expert Opinion on Drug Delivery* 6 (5) (2009) 465–483. doi:10.1517/17425240902832827.  
URL <http://www.tandfonline.com/doi/full/10.1517/17425240902832827>
- [143] M. Huang, Y.-C. Ye, S. Chen, J.-R. Chai, J.-X. Lu, L. Zhao, L. Gu, Z.-Y. Wang, Use of all-trans retinoic acid in the treatment of acute promyelocytic leukemia, *Blood* 72 (2) (1988) 567–572.
- [144] S. Castaigne, C. Chomienne, M. T. Daniel, P. Ballerini, R. Berger, P. Fenaux, L. Degos, All-trans retinoic acid as a differentiation therapy for acute promyelocytic leukemia. I. Clinical results [see comments], *Blood* 76 (9) (1990) 1704–1709.
- [145] D. K. Singh, S. M. Lippman, Cancer Chemoprevention-Part 1: Retinoids and Carotenoids and Other Classic Antioxidants, *Physicians Practice* 12 (1998) 1643–1658.
- [146] M. Bryan, E. D. Pulte, K. C. Toomey, L. Pliner, A. C. Pavlick, T. Saunders, R. Wieder, A pilot phase II trial of all-trans retinoic acid (Vesanoïd) and paclitaxel (Taxol) in patients with recurrent or metastatic breast cancer, *Investigational New Drugs* 29 (6) (2011) 1482–1487. doi:10.1007/s10637-010-9478-3.  
URL <http://link.springer.com/10.1007/s10637-010-9478-3>
- [147] L. Coelho, I. Almeida, J. Sousa Lobo, J. Sousa e Silva, Photostabilization strategies of photosensitive drugs, *International Journal of Pharmaceutics* 541 (1-2) (2018) 19–25. doi:10.1016/j.ijpharm.2018.02.012.  
URL <https://linkinghub.elsevier.com/retrieve/pii/S0378517318300930>
- [148] B. Ozpolat, G. Lopez-Berestein, P. Adamson, C. J. Fu, A. H. Williams, Pharmacokinetics of intravenously administered liposomal all-trans-retinoic acid (ATRA) and orally administered ATRA in healthy volunteers, *Journal of Pharmacy and Pharmaceutical Sciences* 6 (2) (2003) 292–301.
- [149] A. Ourique, S. Azoubel, C. Ferreira, C. Silva, M. Marchiori, A. Pohlmann, S. S. Guterres, R. Beck, Lipid-core nanocapsules as a nanomedicine for parenteral administration of tretinoin: development and in vitro antitumor activity on human myeloid leukaemia cells, *Journal of Biomedical Nanotechnology* 6 (3) (2010) 214–223.
- [150] A. Chinsriwongkul, P. Chareanputtakhun, T. Ngawhirunpat, T. Rojanarata, W. Sila-on, U. Ruktanonchai, P. Opanasopit, Nanostructured Lipid Carriers (NLC) for Parenteral Delivery of an Anticancer Drug, *AAPS PharmSciTech* 13 (1) (2012) 150–158. doi:10.1208/s12249-011-9733-8.  
URL <http://www.springerlink.com/index/10.1208/s12249-011-9733-8>
- [151] E. Schultze, J. Buss, K. Coradini, K. R. Begnini, S. S. Guterres, T. Collares, R. C. R. Beck, A. R. Pohlmann, F. K. Seixas, Tretinoin-loaded lipid-core nanocapsules overcome the triple-negative breast cancer cell resistance to tretinoin and show synergistic effect on cytotoxicity induced by doxorubicin and 5-fluorouracil, *Biomedicine & Pharmacotherapy* 96 (2017) 404–409. doi:10.1016/j.biopha.2017.10.020.  
URL <https://linkinghub.elsevier.com/retrieve/pii/S0753332217330925>
- [152] E. Almouazen, S. Bourgeois, A. Boussaïd, P. Valot, C. Malleval, H. Fessi, S. Nataf, S. Briancon, Development of a nanoparticle-based system for the delivery of retinoic acid into macrophages, *International Journal of Pharmaceutics* 430 (1) (2012) 207–215. doi:https://doi.org/10.1016/j.ijpharm.2012.03.025.  
URL <http://www.sciencedirect.com/science/article/pii/S0378517312002669>

- [153] N. Anton, J.-P. Benoit, P. Saulnier, Design and production of nanoparticles formulated from nano-emulsion templates-a review, *Journal of Controlled Release* 128 (3) (2008) 185 – 199. doi:<https://doi.org/10.1016/j.jconrel.2008.02.007>. URL <http://www.sciencedirect.com/science/article/pii/S0168365908001016>
- [154] M. M. Fryd, T. G. Mason, Advanced nanoemulsions, *Annual Review of Physical Chemistry* 63 (1) (2012) 493–518, PMID: 22475339. arXiv:<https://doi.org/10.1146/annurev-physchem-032210-103436>, doi:10.1146/annurev-physchem-032210-103436. URL <https://doi.org/10.1146/annurev-physchem-032210-103436>
- [155] S.-J. Lim, M.-K. Lee, C.-K. Kim, Altered chemical and biological activities of all-trans retinoic acid incorporated in solid lipid nanoparticle powders, *Journal of Controlled Release* 100 (1) (2004) 53 – 61. doi:<https://doi.org/10.1016/j.jconrel.2004.07.032>. URL <http://www.sciencedirect.com/science/article/pii/S0168365904003773>
- [156] W. Li, T. S. H. Leong, M. Ashokkumar, G. J. O. Martin, A study of the effectiveness and energy efficiency of ultrasonic emulsification, *Physical Chemistry Chemical Physics* 20 (1) (2018) 86–96. doi:10.1039/C7CP07133G. URL <http://xlink.rsc.org/?DOI=C7CP07133G>

# French abstract (Résumé en Français)

## Contexte du travail de thèse

Ce travail s'inscrit dans le cadre de projet européen PeptiCaps, au sein duquel le laboratoire (LAGEPP) a pour objectif de développer un procédé membranaire à l'échelle pilote pour produire des nanoémulsions H/E et eau-dans-huile E/H avec les tensioactifs polypeptidiques du projet.

Les nanoémulsions sont des systèmes dispersés de deux liquides non miscibles ayant une taille de gouttelettes inférieure à 1000 nm. Elles présentent un grand intérêt industriel car leur petite taille de gouttelettes leur confère une grande stabilité.

De plus, cette taille nanométrique engendre d'autres propriétés intéressantes telles qu'une amélioration de la pénétration à travers les différentes barrières du corps humain, une amélioration de la biodisponibilité de médicaments, mais aussi, pour des applications cosmétiques, un meilleur profil sensoriel. Les nanoémulsions constituent également la première étape de techniques de nanoencapsulation qui permettent la production de systèmes d'administration de médicaments stables et fonctionnalisables.

Les nanoémulsions sont plus difficiles à produire que les macroémulsions. Une énergie élevée doit être fournie au système afin de dépasser la tension interfaciale. Les nanoémulsions sont produites par deux principaux types de procédés, les procédés à basse et à haute énergie. Les procédés à basse énergie reposent sur les propriétés physico-chimiques des composants et nécessitent donc l'utilisation de tensioactifs et/ou de co-tensioactifs spécifiques en forte concentration. Leurs principes reposent sur une formation dite spontanée de gouttelettes d'huile donc sans apport d'énergie mécanique. Des techniques telles que l'inversion de phase en composition ou en température, l'émulsification dans le domaine de la microémulsification et la nanoprécipitation sont utilisées.

Les procédés à haute énergie sont plus courants, notamment au niveau industriel. En effet, ils permettent une plus grande liberté dans le choix de la composition. Les nanoémulsions sont obtenues à l'aide d'énergie mécanique générant d'intenses forces de division. A l'échelle industrielle, les homogénéisateurs haute pression sont majoritairement utilisés et à l'échelle du laboratoire c'est la sonication. Ces techniques génèrent des nanoémulsions avec une taille de gouttelettes très petites, mais on obtient habituellement des distributions de taille larges avec la sonication et plusieurs cycles sont nécessaires avec l'homogénéisateur haute pression pour obtenir des distributions de tailles monodisperses.

L'émulsification membranaire nécessitant moins d'énergie, a été mise au point pour la production d'émulsions. Les avantages de l'émulsification membranaire sont: un faible taux de cisaillement, un contrôle précis de la taille finale des gouttelettes et une distribution granulométrique étroite.

Les deux configurations principales sont l'émulsification membranaire directe et celle par prémix. En émulsification directe, la phase dispersée est poussée à travers les pores de la membrane dans une phase continue agitée ou en circulation. L'un des principaux inconvénients pour la préparation de nanoméulsions est que l'émulsification directe nécessite des débits très faibles de la phase dispersée et donc ne peut pas convenir à d'importants volumes de production ou à des émulsions concentrées.

En émulsification par prémix, une émulsion grossière appelée prémix est poussée à travers les

pores de la membrane, réduisant ainsi la taille des gouttelettes et la distribution de taille. Le débit de l'émulsion produite est généralement beaucoup plus élevé et des concentrations plus élevées en gouttelettes sont obtenues.

Dans ces procédés, les membranes SPG, polymériques ou micro-usinées sont les plus couramment utilisées. Généralement, les membranes SPG sont choisies pour l'émulsification directe et les membranes polymériques pour l'émulsification par prémix. De nombreuses configurations de membranes existent en fonction de la forme de la membrane, plane ou tubulaire, du type de membranes et de l'échelle de production requise.

L'émulsification par prémix est décrite dans la littérature pour un grand nombre de compositions différentes pour des applications alimentaires ou pharmaceutiques. Des émulsions H/E ou doubles sont principalement produites, mais aussi quelques émulsions E/H. La taille des gouttelettes est généralement supérieure à 1  $\mu\text{m}$ . C'est seulement il y a 6 ans, qu'une équipe a commencé à décrire la production de nanoémulsions H/E à petite échelle avec un procédé membranaire utilisant principalement des membranes polymériques.

## Questions de recherche

À partir de ces observations, nous constatons qu'aucune installation ne permet la production de nanoémulsion H/E et E/H avec un procédé membranaire à l'échelle pilote. Ainsi, certaines questions se sont posées:

- Est-il possible de développer un procédé à membrane à l'échelle pilote pour produire des nanoémulsions H/E et E/H?
- Quels paramètres ont un impact sur la faisabilité du procédé et la taille finale des gouttelettes de nanoémulsions?
- Est-il possible de produire des nanoémulsions avec des compositions spécifiques (émulsions visqueuses, tensioactifs polypeptidiques ou l'injectables)?
- Quels sont les avantages et les inconvénients du procédé membranaire par rapport à un procédé industriel traditionnel pour la production de nanoémulsions?

## Organisation du travail

La première étape a consisté à développer un procédé membranaire capable de produire des nanoémulsions H/E et E/H à l'échelle pilote et de comprendre les paramètres de composition et de procédé ayant une influence sur la faisabilité de l'émulsification et la taille des gouttelettes obtenues.

Tout d'abord, les montages expérimentaux "preuve de concept" et la configuration finale développée sont présentées dans Matériel et Méthodes, ainsi que les méthodes de caractérisation, en particulier les méthodes de mesure de taille, qui est un paramètre important dans notre étude.

La première partie des résultats se concentre sur la production de nanoémulsions H/E avec le montage développé. Une émulsion grossière (prémix) a été injectée à travers la membrane avec une taille de pores comprise entre 0,2 et 0,8  $\mu\text{m}$  pour réduire et homogénéiser la taille des gouttelettes.

L'effet de plusieurs paramètres a été étudié: paramètres du procédé (possibilité de changement d'échelle, nombre de cycles, taille des pores de la membrane, débit) et de formulation (concentrations en huile et en tensioactif). Les nanoémulsions ont été préparées pour un volume de 500 mL, à un débit de production allant jusqu'à 200 mL/min en maintenant une pression inférieure à 60-65 bar. La taille des gouttelettes a varié linéairement avec la taille des pores de la membrane. Ainsi, avec la plus petite membrane de taille de pore (0,2  $\mu\text{m}$ ), des nanoémulsions monodisperses d'environ 260 nm de diamètre, stables pendant 9 mois à température ambiante ont été obtenues.

Dans la deuxième partie, nous avons décrit la production de nanoémulsion E/H avec le montage mis au point et une membrane SPG avec une taille de pores de 0,5  $\mu\text{m}$ .

L'effet des viscosités sur la pression et la taille des gouttelettes a été étudié dans un premier temps sur des émulsions H/E: la viscosité de la phase aqueuse en augmentant la concentration de glycérol, la viscosité de la phase huileuse avec des huiles minérales de viscosités différentes et la viscosité globale de l'émulsion en augmentant la teneur en phase dispersée de l'émulsion.

La pression requise pour diviser les gouttelettes à l'intérieur des pores de la membrane  $\Delta P_{dis}$  ne dépend pas des viscosités, tandis que les pressions générées par le tuyau connectant la pompe à la membrane  $\Delta P_{pipe}$  et la membrane  $\Delta P_{flow}$  ont été trouvées proportionnelles à la viscosité de l'émulsion globale.

Les nanoémulsions E/H ont été plus difficiles à produire et à caractériser, mais grâce à notre installation fonctionnant à des pressions atteignant 60-65 bar et à des débits élevés, des nanoémulsions d'huile minérale E/H ont été produites avec une taille moyenne de gouttelettes de 600 nm et un débit de 50 mL/min. De plus, les observations faites pour les nanoémulsions H/E ont été confirmées pour les nanoémulsions E/H.

Nous avons ensuite préparé des nanoémulsions H/E et E/H dans le cadre du projet européen. Les émulsions H/E et E/H ont été produites avec succès avec le polypeptide dibloc optimisé par nos partenaires du projet et avec le montage développé dans notre laboratoire.

Tout d'abord, les paramètres ont été optimisés avec des compositions modèles de tensioactifs disponibles dans le commerce. Pour les nanoémulsions H/E, les résultats ont été présentés dans un chapitre précédent, pour les nanoémulsions E/H avec du PGPR, ils sont présentés dans ce chapitre. Enfin, des nanoémulsions H/E et E/H avec des tensioactifs polypeptidiques, respectivement PP1 et PP2, ont été produites par émulsification membranaire par prémix.

Ces résultats montrent que le procédé développé permet la production de nanoémulsions de compositions différentes. Ainsi, il peut être utilisé pour différentes applications avec certains avantages: sa faible consommation d'énergie, ses conditions douces qui peuvent être meilleures pour les actifs sensibles, sa sélectivité et la monodispersité des émulsions produites.

La dernière partie compare la production de nanoémulsion par plusieurs procédés. Pour cela, une étude comparative a été réalisée entre un microfluidizer, les ultrasons et l'émulsification par prémix pour la production de nanoémulsions injectables d'acide all-trans-rétinoïque. Les différentes techniques ont été évaluées principalement en termes de caractérisation de la distribution en taille des nanoémulsions, de la conservation de l'actif et de la stabilité. Cette étude permet de répondre à la dernière question, en comprenant si le procédé développé présente des avantages significatifs par rapport aux procédés conventionnels. En ce qui concerne la taille des gouttelettes, l'émulsification par prémix a produit des gouttelettes monodisperses de 335 nm par rapport aux autres procédés qui ont produit des nanoémulsions d'environ 150 nm mais avec des gouttelettes de taille micronique détectées par diffraction laser et microscopie optique. Par conséquent, les nanoémulsions PME conviennent également aux applications parentérales sans étape de filtration supplémentaire requise. Aucune différence entre les trois procédés n'a été observée en ce qui concerne la dégradation de l'actif. Cependant, en stabilité, en particulier à 40°C, le microfluidizer a provoqué une dégradation plus importante que les autres procédés et produit une nanoémulsion instable, la taille des gouttelettes augmentant de 426% dans des conditions de stress.

## Conclusion générale

En conclusion, nous avons développé un procédé d'émulsification membranaire par pré-mix à haute pression qui peut être utilisé pour différentes applications des nanoémulsions. Ces principaux avantages sont: un contrôle précis de la taille finale de l'émulsion et une consommation d'énergie réduite.

Ces caractéristiques en font un procédé potentiellement intéressant pour différentes industries comme les cosmétiques, la pharmacie et l'agroalimentaire.

En particulier le contrôle de la taille, qui est primordial pour des applications injectables, par exemple. En effet, la présence de gouttelettes de taille importantes peut provoquer des embolies.

## Perspectives

Les perspectives qui concernent le développement du procédé et les applications potentielles sont les suivantes:

- D'autres formulations pourraient être produites avec le montage développé telles que des particules lipidiques solides (avec l'ajout d'un système de chauffage), des émulsions doubles (pour la première émulsification puis la deuxième) ou des nano-capsules si le procédé est couplé à une technique d'encapsulation.
- D'autres types de membranes pourraient être testées pour voir si leur résistance à la pression permet de travailler à des pressions plus élevées afin d'atteindre des tailles de gouttelettes plus petites.
- Etude approfondie de l'effet du microfluidiseur sur les processus de déstabilisation avec d'autres formulations pour mieux comprendre les phénomènes impliqués.
- Enfin, il paraît important d'augmenter le volume produit afin de tester le réel potentiel d'industrialisation du procédé. Une membrane plus longue et deux pompes en parallèle pourraient être utilisées pour augmenter le débit et travailler en continu.